

IAEA TECDOC SERIES

IAEA-TECDOC-1967

Status and Trends in Pyroprocessing of Spent Nuclear Fuels



IAEA

International Atomic Energy Agency

STATUS AND TRENDS IN
PYROPROCESSING OF
SPENT NUCLEAR FUELS

The following States are Members of the International Atomic Energy Agency:

AFGHANISTAN	GEORGIA	OMAN
ALBANIA	GERMANY	PAKISTAN
ALGERIA	GHANA	PALAU
ANGOLA	GREECE	PANAMA
ANTIGUA AND BARBUDA	GRENADA	PAPUA NEW GUINEA
ARGENTINA	GUATEMALA	PARAGUAY
ARMENIA	GUYANA	PERU
AUSTRALIA	HAITI	PHILIPPINES
AUSTRIA	HOLY SEE	POLAND
AZERBAIJAN	HONDURAS	PORTUGAL
BAHAMAS	HUNGARY	QATAR
BAHRAIN	ICELAND	REPUBLIC OF MOLDOVA
BANGLADESH	INDIA	ROMANIA
BARBADOS	INDONESIA	RUSSIAN FEDERATION
BELARUS	IRAN, ISLAMIC REPUBLIC OF	RWANDA
BELGIUM	IRAQ	SAINT LUCIA
BELIZE	IRELAND	SAINT VINCENT AND THE GRENADINES
BENIN	ISRAEL	SAMOA
BOLIVIA, PLURINATIONAL STATE OF	ITALY	SAN MARINO
BOSNIA AND HERZEGOVINA	JAMAICA	SAUDI ARABIA
BOTSWANA	JAPAN	SENEGAL
BRAZIL	JORDAN	SERBIA
BRUNEI DARUSSALAM	KAZAKHSTAN	SEYCHELLES
BULGARIA	KENYA	SIERRA LEONE
BURKINA FASO	KOREA, REPUBLIC OF	SINGAPORE
BURUNDI	KUWAIT	SLOVAKIA
CAMBODIA	KYRGYZSTAN	SLOVENIA
CAMEROON	LAO PEOPLE'S DEMOCRATIC REPUBLIC	SOUTH AFRICA
CANADA	LATVIA	SPAIN
CENTRAL AFRICAN REPUBLIC	LEBANON	SRI LANKA
CHAD	LESOTHO	SUDAN
CHILE	LIBERIA	SWEDEN
CHINA	LIBYA	SWITZERLAND
COLOMBIA	LIECHTENSTEIN	SYRIAN ARAB REPUBLIC
COMOROS	LITHUANIA	TAJIKISTAN
CONGO	LUXEMBOURG	THAILAND
COSTA RICA	MADAGASCAR	TOGO
CÔTE D'IVOIRE	MALAWI	TRINIDAD AND TOBAGO
CROATIA	MALAYSIA	TUNISIA
CUBA	MALI	TURKEY
CYPRUS	MALTA	TURKMENISTAN
CZECH REPUBLIC	MARSHALL ISLANDS	UGANDA
DEMOCRATIC REPUBLIC OF THE CONGO	MAURITANIA	UKRAINE
DENMARK	MAURITIUS	UNITED ARAB EMIRATES
DJIBOUTI	MEXICO	UNITED KINGDOM OF GREAT BRITAIN AND NORTHERN IRELAND
DOMINICA	MONACO	UNITED REPUBLIC OF TANZANIA
DOMINICAN REPUBLIC	MONGOLIA	UNITED STATES OF AMERICA
ECUADOR	MONTENEGRO	URUGUAY
EGYPT	MOROCCO	UZBEKISTAN
EL SALVADOR	MOZAMBIQUE	VANUATU
ERITREA	MYANMAR	VENEZUELA, BOLIVARIAN REPUBLIC OF
ESTONIA	NAMIBIA	VIET NAM
ESWATINI	NEPAL	YEMEN
ETHIOPIA	NETHERLANDS	ZAMBIA
FIJI	NEW ZEALAND	ZIMBABWE
FINLAND	NICARAGUA	
FRANCE	NIGER	
GABON	NIGERIA	
	NORTH MACEDONIA	
	NORWAY	

The Agency's Statute was approved on 23 October 1956 by the Conference on the Statute of the IAEA held at United Nations Headquarters, New York; it entered into force on 29 July 1957. The Headquarters of the Agency are situated in Vienna. Its principal objective is "to accelerate and enlarge the contribution of atomic energy to peace, health and prosperity throughout the world".

IAEA-TECDOC-1967

STATUS AND TRENDS IN
PYROPROCESSING OF
SPENT NUCLEAR FUELS

INTERNATIONAL ATOMIC ENERGY AGENCY
VIENNA, 2021

COPYRIGHT NOTICE

All IAEA scientific and technical publications are protected by the terms of the Universal Copyright Convention as adopted in 1952 (Berne) and as revised in 1972 (Paris). The copyright has since been extended by the World Intellectual Property Organization (Geneva) to include electronic and virtual intellectual property. Permission to use whole or parts of texts contained in IAEA publications in printed or electronic form must be obtained and is usually subject to royalty agreements. Proposals for non-commercial reproductions and translations are welcomed and considered on a case-by-case basis. Enquiries should be addressed to the IAEA Publishing Section at:

Marketing and Sales Unit, Publishing Section
International Atomic Energy Agency
Vienna International Centre
PO Box 100
1400 Vienna, Austria
fax: +43 1 26007 22529
tel.: +43 1 2600 22417
email: sales.publications@iaea.org
www.iaea.org/publications

For further information on this publication, please contact:

Nuclear Fuel Cycle and Materials Section
International Atomic Energy Agency
Vienna International Centre
PO Box 100
1400 Vienna, Austria
Email: Official.Mail@iaea.org

© IAEA, 2021
Printed by the IAEA in Austria
August 2021

IAEA Library Cataloguing in Publication Data

Names: International Atomic Energy Agency.
Title: Status and trends in pyroprocessing of spent nuclear fuels / International Atomic Energy Agency.
Description: Vienna : International Atomic Energy Agency, 2021. | Series: IAEA TECDOC series, ISSN 1011-4289 ; no. 1967 | Includes bibliographical references.
Identifiers: IAEAL 21-01431 | ISBN 978-92-0-122921-2 (paperback : alk. paper) | ISBN 978-92-0-122821-5 (pdf)
Subjects: LCSH: Spent reactor fuels. | Reactor fuel reprocessing. | Nuclear fuels — Recycling.

FOREWORD

Reprocessing of spent nuclear fuel and recycling of separated usable materials are essential to reduce the environmental impact of nuclear power by reducing the volume and radiotoxicity of the final waste. There is growing interest in effective utilization of uranium and in partitioning and transmutation of transuranic elements. Both aqueous and pyrochemical processes are being studied, with the common goal of ensuring proliferation resistance by avoiding a separated fissile material stream during partitioning.

Partitioning processes involve the separation of actinides — including minor actinides — from the spent nuclear fuel or the high level waste from reprocessing, with the objective of burning them in fast reactors or accelerator driven systems. Recycling of minor actinides enables the efficient use of resources and reduces the volume, heat load and radiotoxicity of the waste. The importance of partitioning processes for increasing and sustaining nuclear energy growth has been realized worldwide. Accordingly, advanced partitioning processes are being developed for separation of plutonium and minor actinides, with the objective of burning them, mainly in fast reactors, in order to reduce the long term radiotoxicity of spent nuclear fuels. This publication reviews the status of and trends in the development of pyro processes for processing spent nuclear fuel in various Member States and identifies areas for further development.

On the recommendation of the Technical Working Group on Nuclear Fuel Cycle Options and Spent Nuclear Fuel Management (TWG-NFCO), the IAEA initiated several consultancy and technical meetings on developments in fuel recycling technologies between 2011 and 2015. Some of the technical content of this publication has been recently updated to reflect new R&D results and developments. This report has been prepared on the basis of inputs from leading experts in this area. The IAEA thanks all the experts who contributed to the drafting and review of this publication. The IAEA officers responsible for this publication were A. González-Espartero and U. Basak of the Division of Nuclear Fuel Cycle and Waste Technology.

EDITORIAL NOTE

This publication has been prepared from the original material as submitted by the contributors and has not been edited by the editorial staff of the IAEA. The views expressed remain the responsibility of the contributors and do not necessarily represent the views of the IAEA or its Member States.

Neither the IAEA nor its Member States assume any responsibility for consequences which may arise from the use of this publication. This publication does not address questions of responsibility, legal or otherwise, for acts or omissions on the part of any person.

The use of particular designations of countries or territories does not imply any judgement by the publisher, the IAEA, as to the legal status of such countries or territories, of their authorities and institutions or of the delimitation of their boundaries.

The mention of names of specific companies or products (whether or not indicated as registered) does not imply any intention to infringe proprietary rights, nor should it be construed as an endorsement or recommendation on the part of the IAEA.

The authors are responsible for having obtained the necessary permission for the IAEA to reproduce, translate or use material from sources already protected by copyrights.

The IAEA has no responsibility for the persistence or accuracy of URLs for external or third party Internet web sites referred to in this publication and does not guarantee that any content on such web sites is, or will remain, accurate or appropriate.

CONTENTS

1.	INTRODUCTION.....	1
1.1.	OVERVIEW OF ADVANCED SEPARATION TECHNOLOGY DEVELOPMENT	1
1.2.	OVERVIEW OF PYROCHEMICAL PROCESSES.....	2
1.2.1.	Advantages of pyroprocessing	3
1.2.2.	Disadvantages of pyroprocessing.....	3
1.3.	OBJECTIVE OF THE REPORT	4
2.	NATIONAL STRATEGIES FOR FUEL RECYCLING.....	5
2.1.	FRANCE	5
2.2.	INDIA.....	7
2.2.1.	Thermal reactor fuel reprocessing	7
2.2.2.	Fast reactor fuel reprocessing.....	8
2.2.3.	Pyrochemical reprocessing of metal fuels.....	8
2.2.4.	Thorium fuel reprocessing.....	9
2.2.5.	Waste management.....	9
2.3.	JAPAN	10
2.4.	REPUBLIC OF KOREA.....	11
2.5.	RUSSIAN FEDERATION.....	12
2.5.1.	RT-1 plant at ‘PO Mayak’	13
2.5.2.	The Mining and Chemical Complex SNF management integrated complex	14
2.5.3.	Recycling technologies development.....	15
2.5.4.	REMIX conception.....	15
2.5.5.	PRORYV project.....	15
2.5.6.	Research programme on the pyrochemical process	17
2.5.7.	High level waste partitioning technologies development.....	18
2.5.8.	The technologies for minor actinides transmutation	18
2.6.	UNITED STATES OF AMERICA.....	19
3.	PYROPROCESSING DEVELOPMENTS	22
3.1.	PYROPROCESSING DEVELOPMENT IN FRANCE	22
3.1.1.	Liquid metallic solvents classification for actinides/lanthanides separation.....	22
3.1.2.	Liquid-liquid reductive extraction process in molten fluoride/liquid aluminium.....	24
3.1.3.	Salt decontamination for recycling.....	29
3.1.4.	Direct electrochemical reduction of oxides in molten fluoride...30	
3.2.	OVERVIEW OF PYROCHEMICAL REPROCESSING IN INDIA.....	33
3.2.1.	Introduction	33
3.2.2.	Pyrochemical reprocessing.....	33
3.2.3.	Molten salt electrorefining process for metallic fuels	33
3.2.4.	Electrorefining process	36
3.2.5.	R&D needs for pyroprocessing technology	36
3.2.6.	Conversion of actinide oxides to metals.....	37
3.2.7.	Electroreduction of uranium oxides	37
3.2.8.	R&D needs for the Indian programme	38

3.3.	PYROPROCESSING IN JAPAN	38
	3.3.1. Metal fuel cycle integrated the spent oxide fuel treatment and the separation of actinides	38
	3.3.2. Metal fuel cycle with electrorefining	39
	3.3.3. Engineering scale electrorefiner	40
	3.3.4. High temperature melt transport technology	42
	3.3.5. Electrochemical reduction of oxides guiding to electrorefining	45
	3.3.6. Reductive extraction and verification of actinides recovery from HLLW.....	48
3.4.	PYROPROCESSING PROGRESS IN REPUBLIC OF KOREA	51
	3.4.1. Official plan and R&D	51
	3.4.2. Overview	52
	3.4.3. Disassembling, rod extraction and cutting technologies	52
	3.4.4. Decladding technology	53
	3.4.5. Advanced voloxidation technology	53
	3.4.6. Off-gas treatment technology	54
	3.4.7. Solid waste treatment technology.....	55
	3.4.8. Oxide reduction to metal electrorefining.....	55
	3.4.9. Metal electrorefining	57
	3.4.10. Salt decontamination for recycling.....	59
	3.4.11. Waste form processing	62
	3.4.12. Metal waste processing.....	63
3.5.	DEVELOPMENTS OF SPENT NUCLEAR FUEL PYROPROCESSING TECHNOLOGY AT IDAHO NATIONAL LABORATORY.....	64
	3.5.1. Introduction	64
	3.5.2. Initial focus on EBR-II metal fuel treatment.....	64
	3.5.3. Conditioning oxide fuel for pyroprocessing treatment.....	72
	3.5.4. Technology development to support commercialization of pyroprocessing.....	75
	3.5.5. Conclusions	78
3.6.	ELECTROREFINING IN MOLTEN LiCl-KCl USING SOLID ALUMINIUM CATHODES AT JRC-KARLSRUHE	78
3.7.	DEVELOPMENT OF PYROCHEMICAL TECHNOLOGIES FOR SNF REPROCESSING IN RUSSIAN FEDERATION.....	79
	3.7.1. Introduction	79
	3.7.2. Fuel cycle of lead-cooled fast reactors	80
	3.7.3. Fuel cycle of sodium-cooled fast reactors	81
	3.7.4. Conclusion.....	82
3.8.	PYROCHEMICAL TECHNOLOGY BASED ON FLUORIDE VOLATILITY PROCESS IN CZECH REPUBLIC.....	83
4.	OUTSTANDING ISSUES FOR INDUSTRIAL APPLICATION	85
4.1.	ENGINEERING SCALE DEVELOPMENT.....	85
	4.1.1. Head-end process.....	86
	4.1.2. Electrolytic reduction	86
	4.1.3. Electrorefiner	86
	4.1.4. Salt transport.....	87
	4.1.5. Electrowinning	87
	4.1.6. Remote handling and automation.....	88

4.1.7.	Safeguard technology development in Republic of Korea.....	88
4.2.	PRODUCT PURITY IN PYROPROCESSING WITH METAL ELECTROREFINING	91
4.2.1.	Benefit of increased product purity	91
4.2.2.	Material flow and product purity.....	92
4.2.3.	Characterization of the product	93
4.2.4.	Reduction of process losses.....	94
4.3.	PROCESS MODELLING.....	95
4.3.1.	Overview of process modelling development	95
4.3.2.	Process modelling at KAERI.....	96
4.3.3.	Modelling of electrorefining process.....	96
4.3.4.	Anodic dissolution model of metallic fuel	99
4.3.5.	Computational model for the Mark-IV electrorefiner	105
5.	ECONOMIC ASPECTS OF PYROPROCESSING	112
5.1.	BACKGROUND.....	112
5.2.	MATERIAL FLOW OF NUCLEAR FUEL CYCLE OPTIONS.....	112
5.3.	ECONOMICS OF NUCLEAR FUEL CYCLE OPTIONS	114
6.	SUMMARY AND CONCLUSIONS.....	116
	REFERENCES	119
	LIST OF ABBREVIATIONS.....	133
	CONTRIBUTORS TO DRAFTING AND REVIEW	137

1. INTRODUCTION

1.1. OVERVIEW OF ADVANCED SEPARATION TECHNOLOGY DEVELOPMENT

With the advent of a global nuclear renaissance, spent nuclear fuels (SNF) from nuclear power plants (NPPs) became a major impediment to the expansion of the nuclear share in the global electricity market. In some countries spent nuclear fuels were considered as waste to be disposed of in permanent repositories. However, the long period of safety management time that is required for all viable repository options is one of the challenges in gaining acceptance, especially in countries with small territory and/or high population density. In the 1990s, partitioning and transmutation (P&T) of SNF received increasing attention under the Generation IV International Forum, as it can greatly reduce the radiological toxicity and the amount of final wastes to be disposed of by incinerating the majority of separated long-lived radioactive isotopes. The Obama Presidential Administration of the US formed a Blue Ribbon Commission (BRC) in 2010 to review the issue of long term spent nuclear fuel disposal and make a recommendation for a path forward. The final report of the BRC made seven key recommendations including:

- The necessities for continued research and development (R&D) in nuclear energy technology;
- The development of consolidated interim storage facilities;
- US leadership in international efforts to address safety, waste management, non-proliferation, and safety concerns.

Meanwhile, emerging Asian countries that are projecting a large increase in the use of nuclear energy are viewed as major players in the development and future implementation of advanced fuel cycle technologies.

Thus, many countries with large nuclear installations are exploring advanced separation technologies for the next generation fuel cycle. Both aqueous and pyrochemical processes have been investigated to strengthen the proliferation resistance and mitigate the environmental burden by managing transuranic (TRU) elements. China envisages a large nuclear installation of 250 GW(e) by 2050 and is investigating aqueous process technology for the next two decades with pyrochemical process development planned post-2030 to recycle metallic SNF in fast reactors (FRs). France is focused on the study of advanced aqueous separation with recovery of most of the minor actinides (MA), while retaining a smaller ongoing interest in the area of pyrochemical processing. India expects a remarkable increase of nuclear energy up to as high as 250 GW(e) by 2050. They are very active in the study of pyrochemical recycle of actinides in metallic fuel, which is planned to be used in their fast breeder reactor (FBR) after 2020. Japan is focused on the advanced aqueous process with MA management under the framework of the Fast Reactor Fuel Cycle Technology (FACT) programme. Pyrochemical process development was explored in parallel step by step before the accident at the Fukushima Daiichi NPP as a result of the earthquake and following tsunami on 11 March, 2011. After the accident, the Japanese strategy of nuclear utilization is being re-evaluated. The Republic of Korea has the most ambitious programme, with a steady investigation of pyrochemical technology since 1990 and plans to demonstrate the technology in collaboration with the US via the Joint Fuel Cycle Study Programme. In the long-term, construction of an engineering scale hot cell facility is planned. The Russian Federation has a long history of study of the separation of several species such as Cs, Sr, Am, and Cm by aqueous processes, but they are currently applying pyrochemical

technology for UO_2 and PuO_2 recovery from spent oxide fuel. They have performed a feasibility study to pyrochemically separate MA based on direct electrorefining of oxide fuel. In recent years, the US announced initiatives such as the Advanced Fuel Cycle Initiative (AFCI) and Global Nuclear Energy Partnership (GNEP) with an intention of installing a pilot facility to explore both aqueous and pyrochemical processes. However, at this time the U.S. Department of Energy is focused on continuing basic research to support a future decision on implementing aqueous or pyrochemical technology to close the nuclear fuel cycle with a focus on safety and safeguards. Meanwhile, pyrochemical technology continues to be applied at Idaho National Laboratory (INL) to stabilize SNF arisings from Fast Flux Test Facility (FFTF)¹ and Experimental Breeder Reactor II (EBR-II)².

In addition to aqueous and pyrochemical processes with electrorefining, a fluoride process has been investigated to recover uranium and plutonium from spent oxide fuel in some countries, including the Czech Republic and Japan. Research at the European Commission's Joint Research Centre (JRC) Karlsruhe focuses on the fundamentals of actinide separation with aqueous and pyro technology based on the long-historical expertise on TRU elements.

This publication focuses on the development of pyrochemical process technology with brief description of the aqueous processes.

1.2. OVERVIEW OF PYROCHEMICAL PROCESSES

Pyrochemical processes are defined as a set of partitioning technologies that utilize high temperature oxidation and reduction reactions involving inorganic molten salts, gases, and liquid metals for process media, either in electrolytic or electrorefining steps. One of the earliest examples of a pyrochemical process involving molten salts is the electrochemical smelting of aluminium using the Hall-Heroult Process. Now several billion tonnes of aluminium are produced annually by the process at a cost that modestly exceeds the price of electricity.

Existing partitioning technology for spent nuclear fuel is based on aqueous media including nitric acid and organic extractant such as tri-butyl phosphate (TBP). While the aqueous reprocessing of SNF has been matured on an industrial scale, its use is limited on non-proliferation grounds. In addition, organic extractants are susceptible to radiolysis-induced breakdown, increasing both the cost and the amount of secondary wastes produced.

In order to overcome the drawbacks of the aqueous processes, pyrochemical processes have been explored during the past fifty years, mainly in the Russian Federation and the USA. Recently, pyroprocessing has been recognized to have higher proliferation resistance to make it a better choice for use as a partitioning technology for SNF for future FRs and accelerator driven transmutation systems (ADS). In this report, the characteristics, the status of process

¹ The Fast Flux Test Facility (FFTF) is a 400 MW thermal, liquid sodium cooled, nuclear test reactor owned by the U.S. Department of Energy. It does not generate electricity and is a facility for investigation into the behavior of fuels and structural materials subjected to high, fast neutron flux. It is situated in the 400 Area of the Hanford Site, which is located in the state of Washington, U.S.

² Experimental Breeder Reactor-II (EBR-II) is a sodium-cooled fast reactor designed, built, and operated by Argonne National Laboratory at the National Reactor Testing Station in Idaho, U.S. It was shut down in 1994. Custody of the reactor was transferred to Idaho National Laboratory after its founding in 2005. The tests and experiments that have been conducted in EBR-II have contributed heavily to national and international reactor technology, especially FBR (Fast Breeder Reactor) technology.

developments, impact on reducing the final waste management load, and the approaches to strengthen the proliferation-resistance are summarized.

1.2.1. Advantages of pyroprocessing

The scientific principles of pyroprocessing involving chloride salts are relatively well established, and the technical viability has been demonstrated on an industrial scale in aluminium smelting over the past one hundred years. For both chloride and fluoride processes, it has been demonstrated that there are no critical technical barriers in their application to nuclear fuel processing. Unlike the aqueous process, where the susceptibility of organic and aqueous media to radiolysis-induced degradation is a factor affecting the SNF cooling time required, pyroprocessing can be readily applied to high burnup SNF without requiring excessive cooling time. The process medium consists of inorganic chemicals with very high operating temperatures. This enables short-cooled SNF with an intense radiation level to be accepted, which is advantageous in the prevention of illicit and/or unauthorized operation to remove sensitive materials from the process facility. Therefore, pyroprocessing provides an important technical barrier to proliferation.

Pyroprocessing with metal electrorefining is not capable of separating pure plutonium, as other actinides are recovered with the plutonium. There is also typically a contamination of the actinide product by lanthanide fission products. This situation leads to not only a strong proliferation resistance, but also a high barrier of physical protection due to an extremely high level of heat and radiation.

Pyroprocessing uses a process medium that does not contain hydrogen and carbon; both of these elements are neutron moderators (a risk factor in criticality accidents) and can absorb the fission product tritium and the activation product carbon-14, leading to dilute solutions that cannot be separated later. Furthermore, the head-end process of voloxidation can remove over 90% of long lived radioisotopes including iodine, technetium, and tritium from oxide SNF and recover it in the form of a target that can be transmuted in appropriate reactor environments. Due to the high neutron absorption cross section of chloride salts, pyroprocessing equipment is designed to handle much greater quantities of SNF in comparison to aqueous. Therefore, the facility is more compact than in the case of aqueous methods, allowing on-site reprocessing in the proximity of a reactor, which avoids transportation of SNF and hence reduces nuclear security issues. With much smaller amounts of secondary wastes, the final waste volume can also be drastically reduced. For this reason, many reactors designs dedicated to the transmutation of SNF, including the integral FR and the molten salt reactor (MSR), have adopted pyroprocessing for on-site recycling.

1.2.2. Disadvantages of pyroprocessing

Unlike aqueous process technology, pyroprocessing is not yet fully industrialized. There have been substantial implementations however, including that of the Research Institute of Atomic Reactor (RIAR) of the Russian Federation. RIAR has successfully applied the technology to fabricate mixed oxide particle based fuel from UO_2 and PuO_2 dissolved in molten salt. These particles are converted into fuel via vibro compaction and destined for irradiation in their BN-600 sodium cooled FR. This reprocessing of spent oxide fuels has been demonstrated at kilogram scale in hot cell operations, but an industrial scale installation has not been fully implemented. Pyroprocessing with metal electrorefining has been successfully applied since the 1980s to treat spent metal fuels used in FFTF and EBR-II reactors for demonstrating a co-located reactor/recycle system at semi-industrial scale. This demonstration has been focused mostly on uranium recovery on a solid cathode, but the separation of TRU elements into a liquid

metal cathode has also been investigated via both laboratory and engineering scale experiments in a hot cell. Although the industrial application requires minimizing process losses, it has proven to be difficult to quantify these losses. In the aqueous process, more than 99.5% of the uranium and plutonium have been shown to be recoverable via the combined extraction processes. However, the inhomogeneous nature of pyroprocessing makes it difficult to evaluate the loss of process material. Given this situation, the material accounting system is not clearly defined, which is essential for the purpose of safeguards.

In order to complete a fully industrial installation, the remote- and automatic-operation of molten salt/metal transfer equipment should be developed. Pyroprocessing consists of a batch-wise operation, which makes it difficult to scale up to over several hundreds of tonnes throughput per year. All in all, the process should be well cultivated for co-location with a FR, which is considered to be an ideal system for a FR fleet. However, this industrialization is currently delayed by the fact that the technology is not economically viable in any country.

1.3. OBJECTIVE OF THE REPORT

In the 1990s, attention worldwide was directed towards the development of enhanced environmentally friendly nuclear energy systems together with economically viable partitioning processes. Accordingly, the Generation IV systems with environmentally less burdened systems and economic advantages were initiated in the late 1980s and 1990s in the nuclear R&D community. The centre of the investigation was the development of innovative reprocessing processes to recover MA³, together with uranium and plutonium, and recycle them in FRs. The possibility of using pyroprocessing to recover MA is being explored in parallel with advanced aqueous processes, in which MA separation is mainly undertaken following uranium and plutonium separation. Meanwhile, it is difficult to achieve the separation of plutonium from MA using pyroprocessing due to their electrochemical potential differences in molten salt.

The objectives of this publication are to review the current state of the art on pyroprocessing under exploration worldwide, such as in France, India, Japan, Republic of Korea, the Russian Federation and the USA. In addition, the report examines the existing barriers from technological viewpoints for implementation of this technology and the importance of minimizing radioactive and radiotoxic waste to be disposed of. Moreover, comprehending the characterization of pyroprocessing is essential in directing the fuel cycle policy of a country amongst other innovative technologies for the next generation. Additionally, it leads to boost the number of fuel cycle options for SNF management.

This publication provides an introduction to the fuel recycling strategy and the process technology developed or under development in each of the countries above mentioned. Following these sections, this report focuses on the outstanding issues in which the product purity, non-proliferation, and process and computational modelling are discussed. The final section summarizes the R&D needs for industrial deployment.

³ The minor actinides are the actinide elements in SNF other than uranium and plutonium, which are termed the major actinides. The minor actinides include neptunium, americium, curium, berkelium, californium, einsteinium, and fermium.

2. NATIONAL STRATEGIES FOR FUEL RECYCLING

2.1. FRANCE

In 2019 France had 58 nuclear reactors in operation by Electricité de France (EdF), with a total capacity of over 63 GW(e), deriving about 75% of its electricity from nuclear energy [1]. France chose a closed fuel cycle at the very beginning of its nuclear programme, involving the reprocessing of SNF to recover uranium and plutonium for reuse and to reduce the volume of high level waste for disposal. Recycling allows 30% more energy to be extracted from the original uranium and leads to a great reduction in both the amount and the radiotoxicity of waste to be disposed of (Fig. 1).

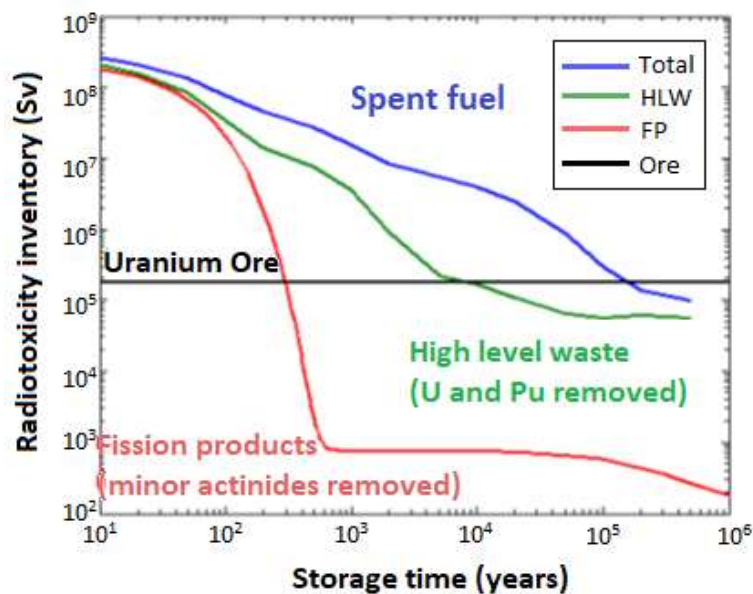


FIG. 1. Nuclear waste radiotoxicity inventory versus storage time (ingestion dose coefficient from ICRP 72) [2].

The La Hague plant has the capacity to reprocess up to 1700 tonnes per year of SNF in the UP2 and UP3 facilities. The PUREX process extracts 99.9% of the plutonium and uranium for recycling, leaving 3% of the SNF material as high level wastes that are vitrified and stored at the site for later disposal [1]. Some 10.5 tonnes of plutonium and 1000 tonnes of reprocessed uranium (RepU) are recovered each year from the 1050 tonnes treated annually since 2010. The plutonium is immediately shipped to the Melox plant at Marcoule (South of France) for prompt fabrication into about 120 tonnes of mixed oxide (MOX) fuel, which is used in 24 of EdF's 900 MW(e) reactors. Four more are being licensed to use MOX fuel.

France's backend strategy and industrial developments are evolving progressively in line with future needs and technological developments. In order to prepare for this future, the French R&D programme on the back end is carried out under Parliamentary Acts. The first one, voted in 1991, gave research tracks spanning 15 years. The second was voted in June 2006 to apply for a further 15 years and orients the current R&D on nuclear waste. Since 2012, the R&D acknowledged more the role of advanced technologies to capitalize on the value of plutonium in FRs, as well as transmuting long-lived actinides. ASTRID (Advanced Sodium Technological Reactor for Industrial Demonstration) became a high priority in R&D on account of its actinide-

burning potential. All of the French studies on reprocessing, interim storage, and geological repository are performed under the umbrella of these Acts since 1991.

For reprocessing, the development of advanced separation processes, either for the heterogeneous strategy (uranium and plutonium in MOX fuel, and MA in blanket fuel or transmutation targets) or for the homogeneous strategy (recycling of all the actinides together in FR fuel), is pursued. The recycling of the MA would allow for a significant reduction of the heat load and the radiotoxicity of the waste to be disposed of (Fig. 1, from the blue or the green lines to the red line). Both aqueous and pyro-reprocessing are studied by the French Alternative Energy and Atomic Energy Commission (CEA).

Aqueous reprocessing based on PUREX, as implemented in the La Hague plant, remains the reference route. In this respect, four main R&D areas (Fig. 2) for the next decade include [1]:

- The COEX process based on co-extraction and co-precipitation of uranium and plutonium together, as well as a pure uranium stream (eliminating any separation of plutonium on its own). This is designed for MOX fuel fabrication;
- Selective separation of long lived radionuclides (with a focus on americium and curium separation) from short-lived fission products (the two cycle DIAMEX and SANEX, the one cycle DIAMEX-SANEX or SANEX TODGA processes) for their recycling in Generation IV FR with uranium as blanket fuel;
- Group extraction of actinides (GANEX process) as a long term R&D goal for homogeneous recycling of actinides (i.e. U-Pu plus MA together) in Generation IV FR as driver fuel;
- The sole extraction of americium (AmEX) from a PUREX or COEX raffinate to enable its recycling in Generation IV reactor blanket fuels, leaving curium in the waste stream.

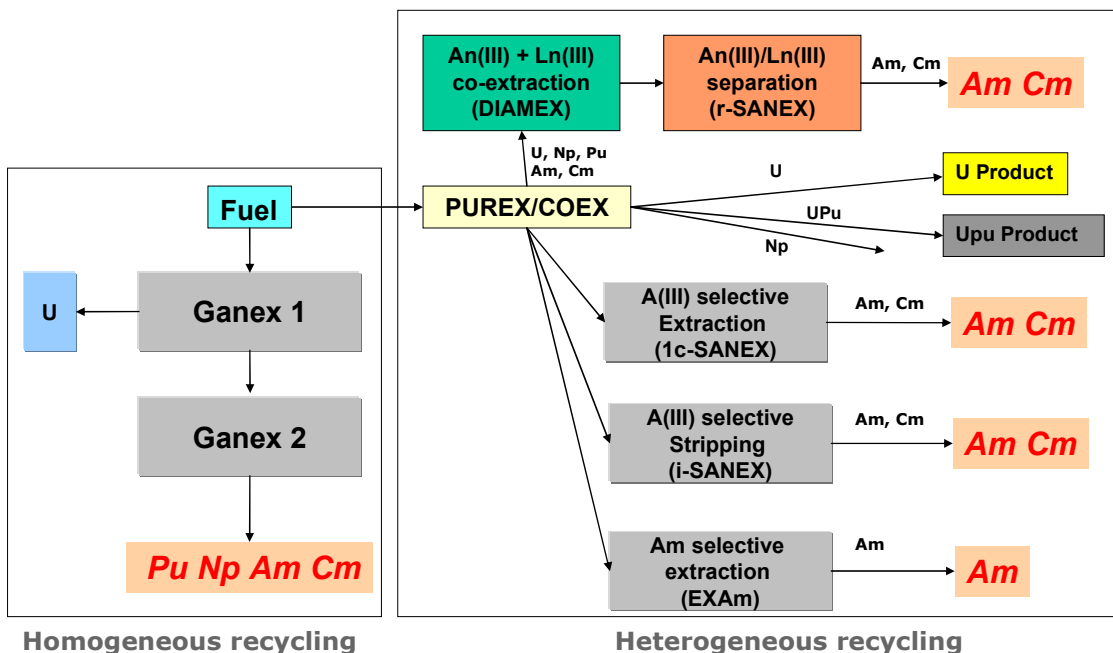


FIG. 2. The different separation process concepts.

Alternative options to DIAMEX-SANEX and GANEX have been developed within European research projects for more than 25 years. These processes are based on different organic extractants than those developed at CEA.

Pyroprocesses could be one alternative in P&T strategy in the longer term to treat specific fuels or targets from Generation IV reactors or from ADS that are difficult to reprocess by aqueous means. The research programme implemented at CEA since the end of 1990s is closely linked to the work performed within European research projects. During the last 20 years, two reference cores of pyroprocessing have been selected:

- The electrorefining in molten chloride on solid aluminium cathode, developed at the Joint Research Centre (JRC) Karlsruhe in Germany;
- The liquid-liquid reductive extraction in molten fluoride/liquid aluminium, developed at CEA.

The electrorefining process is more suitable for metallic fuel, whereas the liquid–liquid reductive extraction process is more suitable for oxide fuel. However, an appropriate head-end treatment can allow each process to be applied to very different kinds of fuel. In addition, a liquid–liquid reductive extraction process has been developed in molten chloride to be applied on a PUREX raffinate to selectively recover the MAs (CRIEPI, Japan). Today, most of the work has been performed at laboratory scale in order to validate all of the identified technological stages.

2.2. INDIA

2.2.1. Thermal reactor fuel reprocessing

2.2.1.1. *Current status*

Thermal reactor fuel reprocessing was started in India with the commissioning of the plutonium plant at Bhabha Atomic Research Centre (BARC), Mumbai in 1964. The plant reprocessed fuel with a typical burnup of 1000 MWd/tHM from the 40 MW(th) research reactor CIRUS. The PUREX process, the common technology choice for reprocessing, was used in the plant. Based on the experience gained in the operation of the BARC plant, the design and construction of a second plant located at Tarapur — called Power Reactor Fuel Reprocessing (PREFRE) — was completed in 1975 for the reprocessing of zircaloy clad oxide SNF from the power reactors at Tarapur and Rajasthan. Several campaigns of reprocessing were carried out under international safeguards at this facility, which provided valuable experience in material accounting practices to meet the international standards [3].

The BARC plant was decommissioned, refurbished with the introduction of innovations as developed in PREFRE, and restarted in 1983. Based on the successful operation of PREFRE and the experience gained during the decommissioning operation of the BARC plant, Kalpakkam reprocessing plant (KARP) was designed and commissioned in 1996.

2.2.2. Fast reactor fuel reprocessing

2.2.2.1. Current status

With the experience gained in thermal reactor fuel reprocessing, R&D efforts were initiated during the early 1970s towards development of reprocessing technology for FR fuel. It is envisaged to achieve the goal of development of aqueous reprocessing technology for FR fuels at Indira Gandhi Centre for Atomic Research (IGCAR), Kalpakkam, using four overlapping stages; continuous feedback from one stage to another is necessary for successful development of the technology:

- Stage I: To understand and provide solutions for the challenges of FR fuel reprocessing;
- Stage II: Construction and operation of a pilot plant — called a ‘compact facility for reprocessing of advanced fuels in lead cells’ (CORAL) — to demonstrate the process flow sheet and optimize the process parameters;
- Stage III: Construction and operation of the demonstration FR fuel reprocessing plant (DFRP) to gain experience in reprocessing of FR fuel with high availability factors and plant throughput;
- Stage IV: Construction and operation of the large scale reprocessing plant for prototype fast breeder reactor (PFBR) as part of the FR fuel cycle facility (FRFCF).

CORAL has been used to reprocess the spent carbide fuels from the fast breeder test reactor (FBTR) after various burnups, namely, 25, 50, 100 and 155 GWd/tHM. The demonstration fuel reprocessing plant is presently in the advanced stage of construction and will be commissioned shortly. The FRFCF is in the design stage.

2.2.2.2. Future plans

The FRFCF can cater to the needs of PFBR and two more FBRs. Based on the experience gained through the construction and operation of FRFCF, it is envisaged to build fuel cycle parks in which a fuel reprocessing plant, having capacity to cater to multiple units of FBRs, will be co-located with the reactors.

The SNF from the metallic FBRs with relatively higher burnup will be reprocessed through the pyrochemical reprocessing technology after shorter cooling periods as compared to aqueous reprocessing technology. The salient features of pyrochemical reprocessing technology are described in section 3.2.

2.2.3. Pyrochemical reprocessing of metal fuels

Metallic fuels will be introduced in the Indian FRs after 2020. Pyrochemical reprocesses based on molten salt electrorefining offer several advantages over the aqueous processes for the reprocessing of spent metallic fuels, development of pyrochemical methods are underway. The current status and future plans are discussed in detail in section 3.2.

2.2.4. Thorium fuel reprocessing

For India, the building up of a fissile material inventory at a fast pace is a prerequisite for the early introduction of thorium in the fuel cycle, as natural thorium does not contain any fissile component. In tune with the increase in fissile inventory with advancement in the nuclear energy programme, various steps towards implementation of thorium fuel cycle were also initiated. To meet the challenges of thorium based fuel cycle, R&D efforts were directed towards extractive metallurgy of thorium, fuel fabrication and utilization in reactors, reprocessing of irradiated thorium for ^{233}U recovery and studies on ^{233}U based reactor systems [3]. Irradiation studies with thoria started in the blanket region of the CIRUS research reactor. Reactor physics studies led to the use of thoria in the flux flattening during the initial start-up of the pressurized heavy water reactor (PHWR). With the introduction of the advanced heavy water reactor (AHWR) into the power programme in the beginning of the next decade and utilizing Th–Pu MOX fuel, an altogether new dimension will be added to reprocessing, requiring three component separations. In addition to this, the radiological aspects of a thorium fuel cycle also need to be addressed. Irradiated thorium reprocessing campaigns have been successfully carried out both in BARC and IGCAR for separation of ^{233}U , which has given valuable inputs for development of this technology.

2.2.5. Waste management

The safe and effective management of radioactive waste has been given utmost importance from the very inception of nuclear industry in India, and it covers the entire range of activities from handling, treatment, conditioning, transport, storage and finally disposal [4, 5]. Waste management facilities at various nuclear installation sites in India have been safely and successfully operating for more than four decades.

2.2.5.1. Technology and status

Currently, there are three industrially operating vitrification plants located at Trombay, Tarapur, and Kalpakkam. An interim storage facility has been operational for the storage of vitrified high level waste (HLW) overpacks for more than 35 years. The near surface disposal facilities are co-located with power/research reactors in various parts of the country for disposal of low and intermediate level solid and solidified wastes.

2.2.5.2. Future plans

Since all future reprocessing plants are envisaged to be designed as integrated plants, they will have both reprocessing and vitrification plants, including interim storage for vitrified waste canisters. There is constant endeavour for waste volume reduction as part of the sustainable development of waste management. The adoption of partitioning technology helps to achieve this as it not only addresses the reduction in radiotoxicity, but also the reduction in waste volume. The strategy for the management of high level liquid waste is in partitioning of MA, and the recovery and reuse of useful fission products [4]. It is planned to induct a partitioning step in future integrated reprocessing plants.

2.3. JAPAN

Prior to the Fukushima Daiichi accident, 51.5 GW(e) of electricity in Japan was generated by nuclear power, equating to around 28% of the total electricity demand. This electricity was generated by the light water reactor (LWR) fleet of boiling water reactors (BWR) and pressurized water reactors (PWR). After the accident, the Nuclear Regulation Authority (NRA) announced that to restart NPPs, there was a requirement to clear an NRA safety assessment based on the safety guidelines in the NRA's New Regulatory Requirements of July 2013 [6].

As of March 2019, nine PWR units were operating. The Ministry of Economy, Trade and Industry (METI) reported that there were 14 730 tonnes of SNF in wet and dry storage at Japan's power plants, filling about 71% of the existing storage capacity, as of September 2015 [7]. Around 2900 tonnes of SNF is stored in the Japan Nuclear Fuel Ltd (JNFL) reprocessing plant [8]. Most of Japan's utilities use plutonium as mixed oxide (MOX) fuel under the 'pluthermal' programme. MOX was initially planned to be used in 16–18 reactors in 2015, but currently there are only a couple of MOX fuelled PWRs in operation. The circumstances imposed by the Fukushima Daiichi NPP accident led to a review of the nuclear energy policy. In April 2012, the Government announced that this review was to commence and would consider economic and other criteria in a range of different scenarios: direct disposal of SNF, and reprocessing and recycling. The Strategic Energy Plan [9] of July 2018 outlines the basic policy of a closed nuclear fuel cycle where SNF is reprocessed and the recovered plutonium utilized to maximize the use of resources and reduce the volume of high level waste.

Operation of the Japan Nuclear Fuel Limited (JNFL) reprocessing plant in Rokkasho-mura (800 tonnes/year capacity) is anticipated to commence in 2022 [8]. Eventually it will produce about 4 tonnes of plutonium per year, equivalent to around 80 tonnes of MOX fuel to be used in the current LWR fleet. The operation of the MOX fabrication, plant 'J-MOX' located at Rokkasho-mura is expected to start in 2022 and has a capacity of 140 tHM/year [8].

A decision was taken to decommission the prototype FR 'Monju' in 2016. Despite this, the future implementation of FRs remains in consideration as a means to reduce waste burden and provide resource security. The technological feasibility of MOX fuelled FRs with aqueous processing and metal fuelled FRs with pyroprocessing are being studied and benefit from international cooperation.

Once the FBR fuel cycle technology with respect to U and Pu recycling is matured, an innovative fuel cycle incorporating MA recycling can be achieved. The pyroprocessing development programme includes metal electrorefining/reductive extraction technology for the FR metal fuel cycle and the nitride fuel cycle of accelerator driven systems for transmutation of MAs. As the metal electrorefining requires no additional process to separate MAs, which accumulate in the Pu recovery electrode, it is a potential recycle technology for U, Pu and MAs.

The pyroprocessing technology investigated in Japan is shown in Fig. 3. The oxide electrorefining programme is based on the Russian proposal, where oxide SNF is directly electrorefined to recycle UO_2 and PuO_2 to FBR fuel. The feasibility of the scheme has been examined, in addition to the identification of potential improvements to the original process.

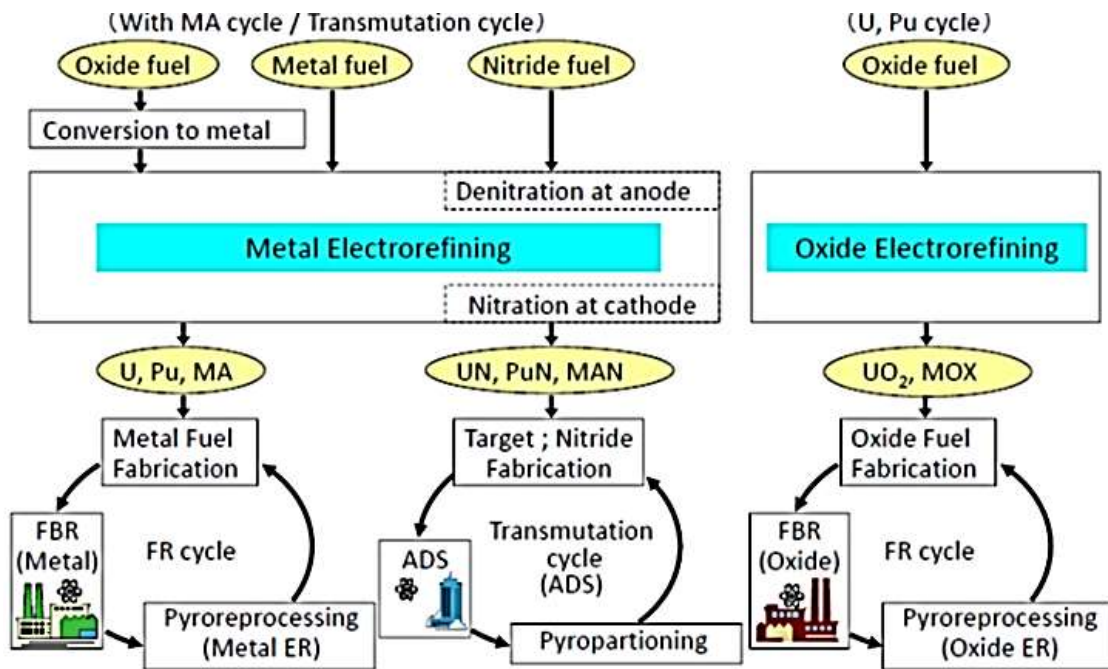


FIG. 3. Pyroprocessing technology in Japan (reproduced courtesy of CRIEPI).

2.4. REPUBLIC OF KOREA

In 2016, electricity production in Republic of Korea was 162 TWh (29%) from the 23 operational reactors.

South Korea has adopted an open fuel cycle. The SNF is stored on each reactor site pending the construction of a centralized interim storage facility, which is planned to be operational by 2035, eventually having a capacity of 20 000 tonnes. About 14 000 tonnes were stored at the end of 2015, with 12 000 tonnes of that in on-site pools, and, with about half of both figures corresponding to CANDU fuel at Wolsong [10].

There are two options in general to treat SNF: one based on the solvent extraction method for the separation of actinides and the other based on pyroprocessing involving the processing of molten salts. One of the advantages of pyroprocessing is that it is able to handle the relatively fresh SNF with high radioactivity and heat and hence the facility does not necessarily need a large capacity storage pool at the plant for long term cooling of the SNF; thus reducing the capacity required for interim storage of SNF.

Based on these practical demands and comparisons, the Korean government set an R&D programme for pyroprocessing technology development as a potential option for SNF treatment.

The basic research on pyroprocessing technology development has been done for decades.

To demonstrate the engineering scale pyroprocessing and to evaluate the technical feasibility of pyroprocessing, the design work of the PyRoProcess Integrated inactive DEMonstration (PRIDE) facility started in 2007, aiming to integrate all existing R&D and engineering technologies at the Korea Atomic Energy Research Institute (KAERI). The facility has been under commissioning since 2014 and unit process tests have been ongoing since 2014. The full spectrum of the engineering-scale pyroprocessing demonstration will be evaluated in PRIDE

using depleted uranium and surrogate materials [11]. The purposes of PRIDE are as a scale-up test of unit equipment, and as a test of integrity between equipment.

In parallel, KAERI is conducting a joint study with US laboratories, in which real SNF is handled. This will provide the information on real SNF and will be combined with the scaling-up information from PRIDE, providing integrated information on pyroprocessing.

2.5. RUSSIAN FEDERATION

At present, the Russian Federation's nuclear power industry continues its development and increases its contribution to the overall energy mix, reaching 18.4% in 2018. The basis of nuclear power generation is formed by LWRs⁴, with an additional two industrial scale FRs — BN-600 and BN-800, and a floating small modular reactor (SMR) unit that was commissioned in 2019. The planned layout of future NPPs in the Russian Federation (as outlined in the Government Order of the Russian Federation No. 1634-r of August 1, 2016) includes 11 new power units scheduled for construction before 2030. In addition to the LWR power reactor designs, various advanced reactor designs such as FRs with lead, lead-bismuth, and sodium coolant are being developed. It is anticipated that from 2030 there will be a large-scale implementation of fast neutron power reactors and a transition to a two-component nuclear system with a unified fuel cycle, linking the needs of both existing thermal reactors and FRs. Solving the problems associated with the accumulation of SNF and radioactive waste, in this context, is becoming a priority.

The BN-600 Sodium-cooled Fast Reactor (SFR), operating since 1980, is a commercial power unit that was upgraded to give a 15-year operating lifetime extension until 2025. The Beloyarsk 4 BN-800 FR commenced operations in 2014 and began with the use of MOX fuel obtained from separated plutonium. The unit is intended to demonstrate the use of MOX fuel at industrial scale in a closed fuel cycle strategy. BN-800 is a major step towards the design of BN-1200.

The PRORYV⁵ project has the aim of developing new generation nuclear power technologies based on the closed nuclear fuel cycle with FR. The basic provisions include exclusion of severe accidents with population evacuation, closing of the nuclear fuel cycle for the full utilization of the uranium energy potential, radiation neutral management of radioactive waste disposal, development of technology supporting non-proliferation (no uranium enrichment and no plutonium separation, breeding ratio about 1), and bringing the capital expenditures FR construction to at least to the level of the thermal NPPs. The PRORYV project has entered the implementation phase, and the results achieved by 2019 are published in Ref. [12].

⁴ The LWR fleet comprises 15 WWER-1000/1200, 10 RBMK, 5 WWER-440, 3 EGP-6 (graphite moderated BWR for combined heat and power).

⁵ The PRORYV (in Russian: Прорыв, “Breakthrough”) Project is a main innovative project in the global nuclear power industry implemented in the Russian Federation by the State Atomic Energy Corporation Rosatom. It envisages the development of a new nuclear industry technology platform based on a closed nuclear fuel cycle with FR. The purpose of activities under the Proryv Project is the creation of nuclear-energy complexes that include NPPs, SNF reprocessing plant and fuel refabrication plant, preparation of all types of radioactive waste to the final disposal into geological formations for development of large-scale nuclear power.

NIKIET⁶ designed BREST-OD 300 is a prototype power unit with lead-cooled FR with an enhanced proliferation resistance. The reactor design and construction of the on-site closed fuel cycle facilities, including dense uranium-plutonium mixed nitride (MNUP) fuel fabrication for the reactor, as a demonstration for closed fuel cycle technologies are expected to be completed by 2026.

As a basic approach to the SNF management in the Russian Federation, the concept of reprocessing and recycling of the nuclear materials in a two-component nuclear power energy system (with thermal and FRs) has been adopted. This is to ensure the efficient use of natural uranium resources, avoid accumulation of SNF, recycle nuclear materials, and reduce the radiotoxicity and volume of the generated radioactive waste.

The task of ensuring the safe management of radioactive waste is considered to be, on the one hand, a key element of the national security and safety, and, on the other hand, an essential precondition for present and future use of nuclear energy. The Russian SNF management facilities are illustrated in Fig. 4.

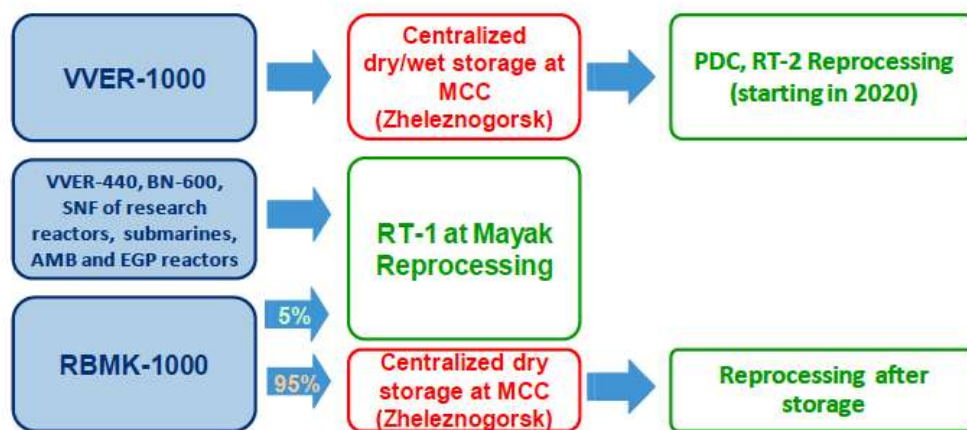


FIG. 4. Spent nuclear fuel management facilities in Russian Federation [13].

2.5.1. RT-1 plant at ‘PO Mayak’

Industrial-scale SNF reprocessing is performed at RT-1 at ‘PO Mayak’, which has been in operation since 1977 and has a design capacity of 400 tonnes/year. Approximately 6000 tonnes of SNF have been processed, with the processed SNF inventory including almost all existing uranium and plutonium compositions and covering all of the potential fuel assembly dimensions. The design capacity is 400 tonnes per year⁷.

⁶ NIKIET is one of Russia’s major nuclear design and research centres with a primary focus on reactor technologies. The Institute develops designs of advanced and innovative power reactors, including those for regional power supplies, research and isotope production reactors, and neutronic systems for the international fusion reactor (ITER), carries out the scientific and technological support for the RBMK NPPs operation, as well as develops and supplies integrated computer-aided reactor instrumentation, control, protection, diagnostic and other systems.

⁷ At present, the SNF from WWER-440, BN-600, and research reactors, as well as defect RBMK fuel (which cannot be accommodated in dry storage) is reprocessed at the RT-1 plant; reprocessing of WWER-1000

The RT-1 process is based on the PUREX-process ('modified PUREX'), involving the extraction of uranium and plutonium as target reprocessing products with a possibility of extracting neptunium, as well as a broad range of other isotopes (^{137}Cs , ^{85}Kr , ^{241}Am , ^{238}Pu , ^{90}Sr , ^{147}Pm). Alumophosphate glass is produced from intermediate and high level wastes using direct evaporation-calcination-vitrification technology. Vitrified wastes are placed in steel canisters and are stored in a dry vault-type storage facility. Borosilicate glass will be also used in the near future.

The first in the world pilot plant for partitioning of high level waste was put in operation at RT-1 in August 1996.

2.5.2. The Mining and Chemical Complex SNF management integrated complex

An integrated complex for SNF management is being established at the site of the Mining and Chemical Complex (MCC), which includes:

- centralized water cooled ('wet') SNF storage;
- centralized air-cooled ('dry') SNF storage;
- a pilot-demonstration centre for the reprocessing of SNF based on innovative technologies;
- MOX fuel fabrication for FRs (BN-800 type).

An underground research laboratory will be established at MCC to develop technologies for the disposal of HLW.

2.5.2.1. MOX fuel fabrication for fast neutron reactors

The facility is currently in operation and produces fuel for BN-800 located at Beloyarsk NPP. The production provides the possibility of fuel assembly fabrication with the separated Pu from SNF coming from nuclear power reactors.

2.5.2.2. The Pilot Demonstration Center on SNF reprocessing based on innovative technologies

The Pilot Demonstration Center (PDC) is an integral component of the MCC. The key goal of the innovative technology development at PDC is to achieve ecological acceptance and economic efficiency of the reprocessing technologies.

The PDC is being constructed in two stages. The first stage includes hot research cells, analytical facilities, and other necessary infrastructure; it was granted license to operate in 2016. The R&D programme aimed at elaborating innovative SNF reprocessing technologies was launched in 2016 with the purpose of confirming the design parameters of the new technological scheme, to further improve technologies for reprocessing SNF, and to develop HLW partitioning technologies for reducing the radiotoxicity of the final radioactive waste to be disposed of.

Construction of the second PDC stage is underway and is scheduled to be commissioned in 2021. It has a design capacity of 250 tonnes/year and the reprocessing technologies have been developed (based on the simplified PUREX process) to exclude liquid radioactive waste effluents. The main products of PDC are the mixed oxides of plutonium, neptunium, and

commenced in 2016. The necessary infrastructure is being installed to enable AMB (early version of RBMK) and EGP-6 SNF reprocessing. BN-600 spent MOX fuel was reprocessed at RT-1 plant in 2012 and 2014.

uranium that will be used in the manufacture of FR fuel and REMIX fuel (see 2.5.4), and RepU. PDC is also ready to deliver fuel products for REMIX. HLW produced are vitrified in borosilicate glass for final disposal.

2.5.3. Recycling technologies development

Regenerated nuclear materials (RepU and Pu) have been traditionally used in Russia separately. RepU has been used in Russian commercial nuclear reactors (RBMK type, WWER-440 and WWER-1000) since 1996. At present, the Russian fuel fabrication plant TVEL-MSZ has a license to fabricate fuel based on RepU, with U-232 content up to $5 \times 10^{-7}\%$.

Separated plutonium from LWR SNF is to be used in FR MOX fuel for initial loading and feeding during their first 10 years of operation.

The concept of a two-component nuclear energy system has been approved in the Russian Federation and includes both reactor types (WWER and BN). The transition period may include the reuse of reprocessed nuclear materials as mixed fuel for LWRs (like WWERs) in terms of more effective utilization than MOX fuel with partial core loading.

2.5.4. REMIX conception

The Russian Federation has been developing multi-recycling technology for plutonium and RepU recovered from LWR SNF in the form of fuel for the existing and future fleet of WWER-1000 reactors. REMIX fuel is the mixture of regenerated RepU and Pu, with the addition of enriched uranium (natural or RepU). REMIX fuel enables up to seven recycles of the full quantity of U and Pu from SNF, with 100% core charge and saving of natural uranium in each cycle. The main advantage of REMIX is that it enables multiple recycling of uranium and plutonium in thermal reactors.

Rosatom has developed a programme for REMIX fuel implementation. In the framework of this programme, three experimental fuel assemblies containing 18 REMIX-fuel elements have been manufactured and irradiated at Balakovo NPP, starting in 2016. In parallel, samples have been irradiated in the MIR research reactor — they have been removed for post irradiation examination.

The safety case development programme for REMIX fuel use in WWER-1000 and 1200 reactors started in 2018. It includes the development and validation of computer codes for nuclear and radiation safety demonstration. The development of investment justification for the REMIX fuel fabrication facility was initiated in 2018.

2.5.5. PRORYV project

An Experimental and Demonstration Energy Complex (EDEC) is under construction at the Siberian Chemical Combine (SCC) in Seversk. It will be a part of the BREST-OD-300 reactor power unit and will close the nuclear fuel cycle of the plant, which includes a reprocessing module of irradiated MNUP fuel and a fabrication/refabrication module (FRM) for producing reactor fuel for the starting loads from imported materials, and nuclear fuel for trans-shipment from recycled materials. The EDEC FRM is planned to be commissioned in 2022 and will utilize the MNUP fuel carbothermal synthesis technology. The construction of the SNF reprocessing module at the EDEC is expected to begin in 2024 and it is planned to utilize combined (pyrochemical + hydrometallurgical) MNUP fuel reprocessing technology, which is also suitable for reprocessing spent FR MOX fuel. The development of an alternative pure

hydrometallurgical technology for FR SNF reprocessing is also being completed. EDEC should demonstrate for the first time in the world the sustainable operation of the full range of nuclear fuel cycle closure facilities.

When implemented at reactor sites, this process will allow the site to demonstrate an onsite closed fuel cycle.

Competitive FRs are expected to be introduced from the mid-2030s with a transition to a two-component nuclear power structure and a closed nuclear fuel cycle [14].

A combined reprocessing technology — PH-process — has been developed for reprocessing MNUP and MOX FR SNF with short residence times. This technology involves the joint separation of uranium and plutonium, taking into account the requirements for technological support for the non-proliferation regime as well as its purely hydrometallurgical version. Both options also provide for the separation of americium and curium, and the production of a mixture of uranium oxides, plutonium, and neptunium, as well as mixtures of uranium and americium oxides, and uranium and curium oxides as the target product. Alternatively, mixtures of uranium oxides, plutonium, neptunium, and americium oxides can be obtained.

The pyrochemical conversion of the combined technology is under development, while research on the hydrometallurgical conversion of the combined technology (Fig. 5) is under completion [15].

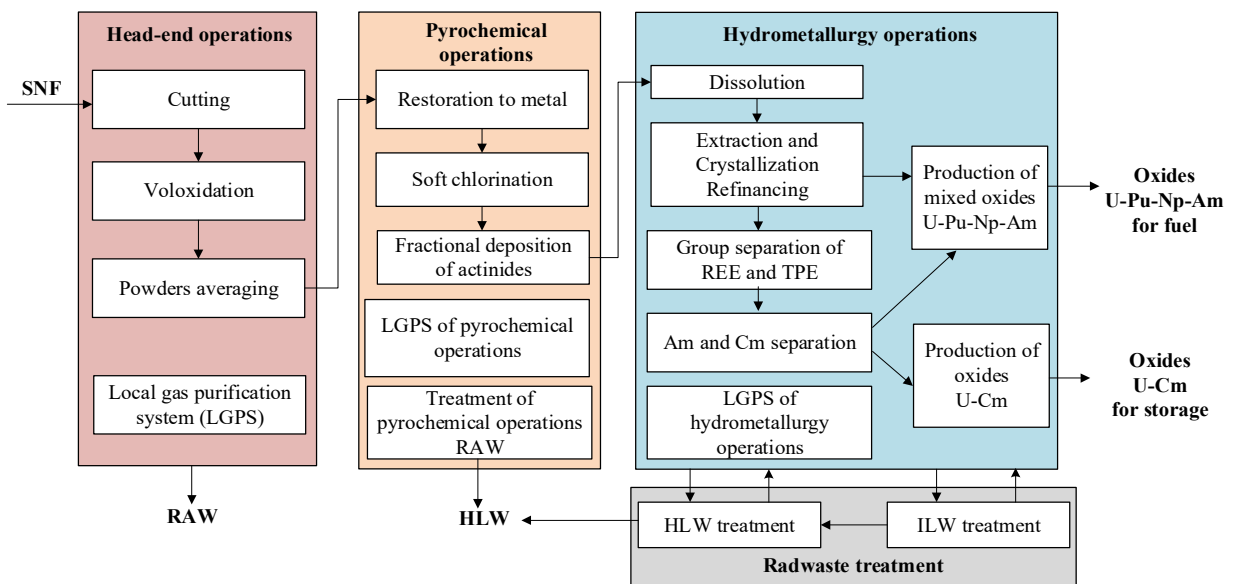


FIG. 5. Flow sheet scheme of combined reprocessing (PH-process) of mixed U-Pu nitride and mixed U-Pu oxide SNF; LGPS – local gas purification system; RAW – radioactive waste; REE - rare earth elements; TPE – trans-plutonium elements; ILW – intermediate-level waste; HLW – high-level waste.

2.5.6. Research programme on the pyrochemical process

The research programme on pyrochemical process includes the partitioning and transmutation of TRU elements in the framework of the PRORYV project.

At the end of 2013, a demonstration experiment on pyrochemical conversion of irradiated MNUP SNF in the air chamber of JSC SSC NIIAR was conducted in Russian Federation. However, this experiment did not take into account the passivation of MNUP SNF tablets due to the formation of UNCl film on their surface, which has low solubility in the salt electrolyte, and the possibility of UN/U₂N₃ recharge which leads to uranium losses. Research and development of the MOX and MNUP SNF pyrochemical technology processing is currently underway at The Institute of High Temperature Electrochemistry of the Ural Branch of the Russian Academy of Sciences. The work is based on the proposed technological scheme (Fig. 6), which includes the separation of target components (U-Pu-Np-Am) and their purification from fission products to a level that meets the requirements of nuclear fuel reprocessing [12].

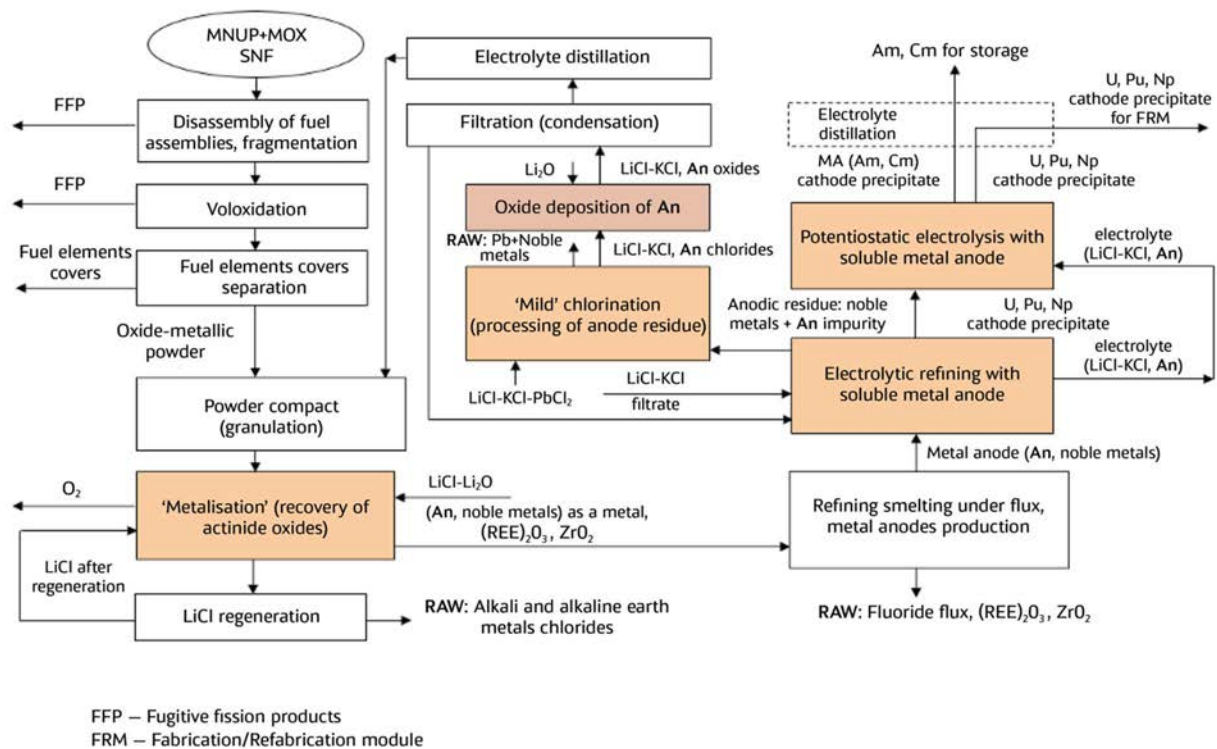


FIG. 6. Technological scheme for pure pyrochemical processing of MNUP and MOX SNF of FRs.

The proposed technological scheme could enable fissile materials in the form of metal powder to be obtained and to reduce the activity to a level that makes it possible to use this product in the hydrometallurgical conversion of the combined scheme. It could also drastically reduce material flows of technological media at the initial stage of processing and simplify the hardware design of subsequent operations.

The knowledge of physical chemistry and electrochemistry of basic fission products is sufficient for process understanding and modelling. Research into Pu, Np, Am and Cm and Tc chemistry in molten salt is required.

2.5.7. High level waste partitioning technologies development

To reduce radiotoxicity and the volume of ultimate waste to be disposed of, HLW partitioning technologies are being developed for recovery of MA and heat-generating fission products. The Russian Federation has already industrial experience in HLW partitioning.

Since 1996, the Mayak RT-1 plant has operated a pilot plant for HLW partitioning. During the operation more than 1200 m³ of HLW were processed with Cs-Sr recovering.

As part of the PRORYV project, technologies for group separation of TRU and transplutonium elements (TPE) have been developed and tested, and the extraction system N,N,N',N'-tetra-octyldiglycolamide-methanitrobenzotrifluoride is currently under consideration [16]. In 2017–2018, 'hot' dynamic tests were carried out to separate americium and curium from high level waste by a system based on N,N,N',N'-tetra-octyldiglycolamide-methanitrobenzotrifluoride and more than 99.9% americium recovery was achieved.

At the Bochvar institute, Am-Cm separation was tested by high pressure displacement complex-forming chromatography using REE and TPE concentrate obtained from WWER-1000 SNF reprocessed at the 'PO Mayak' plant. As a result, 1.39 g of Am (96% of the original) with a purity of more than 99.9% was obtained. The combined Am-Cm fraction contained 36.4 mg Am (about 2.6% of the original). The amount of Am in the Am-Eu and Am-Cm fractions did not exceed 4% of its initial amount. Thus, with regard to the reprocessing of spent nuclear fuel from both PWRs and FRs, the technology for the separation of americium and curium has been developed and tested, enabling justification of americium in FR fuel [16].

The Rosatom programme for partitioning HLW technologies development includes:

- Maturing of HLW partitioning technology (with recovery of Am, Cm, REEs, Cs-Sr from HLW and their separation) including modernization of the RT-1 partitioning facility;
- Development of Am and Cm separation;
- Development and deployment of a HLW partitioning facility at the MCC;
- Development of the technologies for preparation of Am, Cm oxides and mixed U-TPE oxides;
- Development and maturation of the technologies for MA-bearing fuel fabrication, irradiation, post irradiation examination, recycling experimental Am- and Np-bearing fuel;
- Development of a complex database for fuel characteristics and codes for MA recycling.

2.5.8. The technologies for minor actinides transmutation

Both solid-fuel FRs (like BN-800 type) and MSR will both be studied in regard to MA transmutation. The following scenarios are considered when analysing the concept of MA management in FRs:

- Homogeneous transmutation of MA in the fuel;
- Heterogeneous transmutation of MA in special assemblies.

Both the homogeneous and heterogeneous approaches are capable of achieving the required efficiency and are researched within the framework of the Proryv Project.

The development programme for the MA transmutation technologies in FRs includes:

- Justification of core neutron-physical characteristics with MA, the efficiency of MA transmutation in FRs, the development of requirements for MA fuel (including experiments with MA-bearing fuel assemblies in BFS⁸, BOR-60 and BN-800);
- Development of Np homogeneous recycling technologies (design, fabrication, irradiation, and post-irradiation examination of MOX and MNUP containing 0.1–1% Np);
- Development of Am homogeneous recycling technologies (with an Am content of 0.4–1.2%), mixed nitride and oxide fuel, uranium nitride and oxide fuel; and heterogeneous recycling (with an Am content of 10–12%), mixed nitride and oxide fuel, uranium nitride and oxide fuel (design, fabrication, irradiation, and post-irradiation examination).

As an alternative option for MA burning, the Russian Federation is developing the approach of burning MA in molten salt reactors (MSRs).

The advantages of an MSR as a TRU elements burner are primarily due to their being no requirement to manufacture a fuel pellet and the possibility of widely varying the content of long-lived actinides in the fuel salt without core modification.

The construction of a large power MSR is proposed to be preceded by the construction of 5–10 MWt Demo MSR unit to demonstrate control of the reactor and fuel salt management, investigating volatile and fission product management with different TRU elements, loadings for start-up, transition to equilibrium, drain-out, shut down etc. The development of the proposed technology on an industrial scale will require a number of technical issues to be solved.

2.6. UNITED STATES OF AMERICA

The United States of America anticipate the expanded use of nuclear energy worldwide and countries will need to face the very important issues of effectively dealing with SNF and high level liquid waste. Former US administrations promoted the Advanced Fuel Cycle Initiative (AFCI) and Global Nuclear Energy Partnership (GNEP) initiatives for managing TRU elements via advanced fuel cycle technology. The GNEP programme included plans to implement a pilot plant fuel cycle facility and a large scale reprocessing plant. However, these initiatives were later terminated. To focus on the SNF problem, a BRC was launched in 2010 to evaluate existing fuel cycle technologies and R&D programmes in terms of multiple criteria, which included cost, safety, resource utilization and sustainability, and the promotion of nuclear non-proliferation and counter-terrorism goals. The BRC recommended pursuing advances in nuclear energy technology with potential to deliver an array of benefits. Effort is needed to improve the safety and performance of existing LWRs, and SNF and HLW storage, transport, and disposal systems. It called for innovations with potentially large advantages over current technologies for the long term. The current advanced nuclear energy development programme funded by the U.S. Department of Energy is the ‘Fuel Cycle Research and Development’ (FCR&D) programme and targets to address the BRC recommendations. The FCR&D programme is currently focused on long term, science-based research and development of technologies with

⁸ The Bystrye Fisicheskie Stendy (BFS) facility at the Institute of Physics and Power Engineering (IPPE) enables scientists to perform research on fast breeder reactors using the two critical assemblies BFS-1 and BFS-2.

the potential to produce transformational changes to the way in which the nuclear fuel cycle, and particularly nuclear waste, is managed.

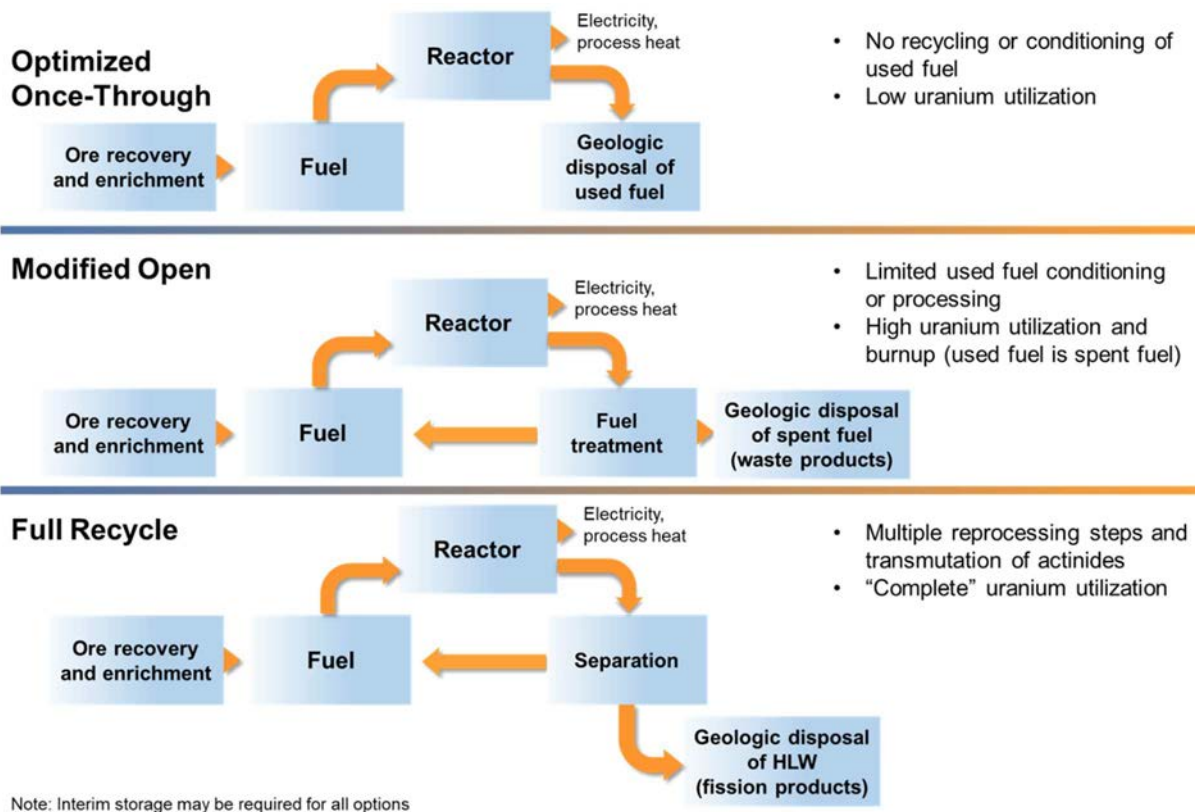


FIG. 7. Three fuel cycle options (courtesy of Idaho National Laboratory, USA).

Three options are envisaged, as seen in Fig. 7. The first is the optimized once-through, meaning no recycling or conditioning, which leads to a low uranium utilization. The second is the modified option with limited SNF conditioning or processing. The third is the full recycle with complete uranium utilization. For recycling fuel in the next generation fuel cycle, development is needed for the separation and waste management technologies that enable a sustainable fuel cycle with minimal processing, waste generation, and potential for material diversion.

The FCR&D programme is currently developing options to support possible future selection of sustainable fuel cycles, for which a broad range of separation technologies are being investigated, including both modified open and full recycle options. This programme is also focused on understanding the scientific fundamentals of separation methods. Within the FCR&D programme, there are separations, fuels, safeguards, and waste disposal campaigns. These efforts are carefully coordinated to achieve optimal programme performance and accomplishment of overall goals. Demonstrations of PUREX, COEX or UREX type flow sheets have not been conducted.

Meanwhile, much effort has been focused on finding processes that could be simpler and more economic. This includes options that support the modified open fuel cycle and transformational approaches. Two collaborative efforts labelled as Sigma Teams were established for focused and collaborative research into separations grand challenges. One such collaboration is the MA sigma team for Am or Am and Cm separations. The other is the off-gas Sigma Team for capture and immobilization of fission gases. In addition, much funding and effort is being spent to

develop the capabilities, tools, and methods to understand fundamental properties of separation processes (thermodynamics, kinetics, non-ideal behaviour, bond covalency, etc.) to enable the future design of efficient and robust separation technologies. Figure 8 shows six fuel cycle separations focus areas with activities.

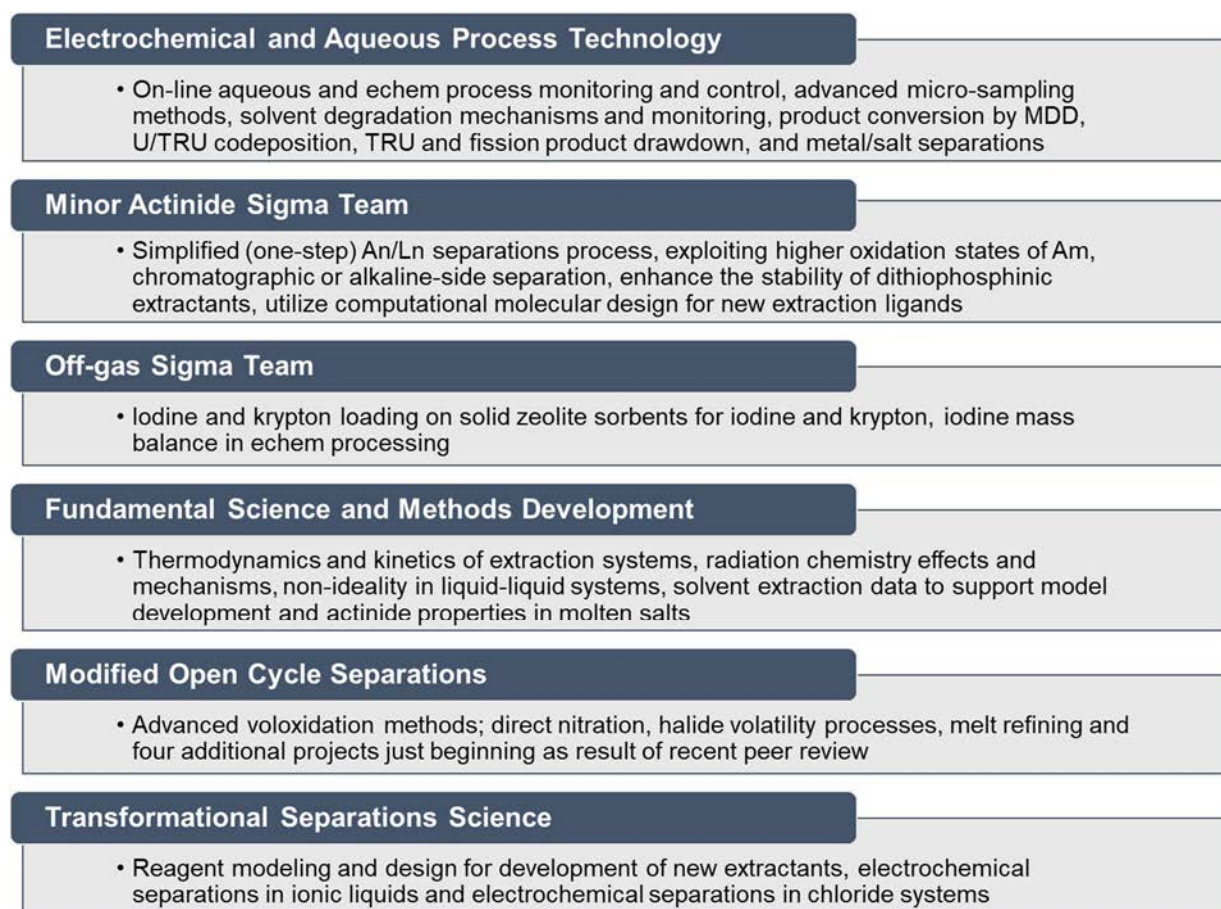


FIG. 8. Fuel cycle separation areas with activities (courtesy of Idaho National Laboratory, USA).

3. PYROPROCESSING DEVELOPMENTS

3.1. PYROPROCESSING DEVELOPMENT IN FRANCE

3.1.1. Liquid metallic solvents classification for actinides/lanthanides separation

3.1.1.1. Thermodynamic aspects for actinides-lanthanides separation

Within the suite of pyrochemical technologies, liquid–liquid reductive extraction in a metallic solvent and electro deposition on a liquid metallic cathode from either a molten chloride or fluoride salt is very similar from a thermodynamic point of view. They consist in reducing cationic species (oxidation state ‘n’) dissolved in the molten salt to the metallic state in a metallic phase. Both actinides and lanthanides are considered to be at the same oxidation state in the molten salt in order to simplify the different equations.

Electrolytic separation on a liquid metallic cathode (metal ‘Me’) is controlled by the equilibrium potential difference between the redox couple An^{n+}/An and Ln^{n+}/Ln written as follows:

$$\Delta E_{An/Ln} = \Delta E_{An/Ln}^o + \frac{2.3RT}{nF} \log \left(\frac{x_{An^{n+}} \cdot x_{Ln(Me)}}{x_{Ln^{n+}} \cdot x_{An(Me)}} \right) + \frac{2.3RT}{nF} \log \left(\frac{\gamma_{An^{n+}}}{\gamma_{Ln^{n+}}} \right) + \frac{2.3R}{nF} \log \left(\frac{\gamma_{Ln(Me)}}{\gamma_{An(Me)}} \right) \quad (1)$$

where ΔE^o is the standard potentials difference (V), R is the ideal gas constant, T is the temperature (K), n is the number of exchanged electrons, F is the Faraday constant, x is the mole fraction of in the salt or in the metallic solvent Me when specified. In the case of liquid-liquid extraction in the metallic solvent Me (being the reducing agent or not), the expression of the separation factor (mole fraction scale) is quite similar:

$$\log S F_{An/Ln} = \log \left(\frac{K_{An}^o}{K_{Ln}^o} \right) + \log \left(\frac{\gamma_{An^{n+}}}{\gamma_{Ln^{n+}}} \right) + \log \left(\frac{\gamma_{Ln(Me)}}{\gamma_{An(Me)}} \right) \quad (2)$$

The first term in equations (1) and (2) is driven by thermodynamic constants. An important parameter is the ratio of activity coefficients, which can vary a lot from one metal to another. On the contrary, the ratio in the salt does not vary much when the nature of the salt is changed. Hence, the choice of the metallic solvent for those two techniques is crucial for the process.

3.1.1.2. Classification of metallic solvents

Plutonium and cerium were chosen as representatives for actinides and lanthanides respectively. Al, Bi, Ga, Cd and Zn were selected as metallic solvents because of their low melting temperature and the high Pu solubility in Al, Bi, Ga, Cd [17–19]. Despite a low Pu solubility in Zn, this metal was also considered because its low boiling temperature enables distillation, as for Cd. Some activity coefficient data for the selected metals have been published in the literature, mostly by Lebedev [17]. Some data concerning gallium [20] shows the potentiality of this metal. Additional activity coefficients were measured here (particularly Pu in Ga) in order to classify the different selected solvents for the Pu/Ce separation methodology for activity coefficient determination.

3.1.1.3. Methodology for activity coefficients determination

The activity coefficient (of the actinide element in the metallic phase Me) determination consists in measuring the electromotive force (e.m.f) between the pure metallic actinide (An) element at an inert electrode and the metallic actinide element dissolved in the metallic phase. The activity coefficients (γ) expressed through (mole fraction scale, pure solid as reference state):

$$\log(\gamma_{An(Me)}) = \frac{-nF \cdot e.m.f}{2.3RT} - \log(x_{An(Me)}) \quad (3)$$

where $x_{An(Me)}$ is the mole fraction of An in the metallic solvent and n is the number of moles. F , R and T are the Faraday constant, gas constant, and temperature (K) respectively.

If the activity coefficient is constant in the studied concentration range, the curve $e.m.f = f(\log(x_{An(Me)}))$ exhibits a linear variation. It gives access to $\gamma_{An(Me)}$ and its slope is related to the exchanged number of electrons. As the molten salt electrolyte containing An^{n+} is an intermediate it was chosen to work with molten chlorides, with electrochemistry measurements being easier in this media. As no pure metallic actinides were available, the electromotive force is determined indirectly in two steps (Fig. 9) [21, 22]:

- (i) The e.m.f measurement of the galvanic cell: $An \mid \text{molten salt, } AnCl_3 \mid Ag/AgCl$, between the pure metallic deposit and the reference electrode. An^{n+} was reduced in metallic An at the electrode;
- (ii) The e.m.f measurement of the galvanic cell: $An_{(Me)} \mid \text{molten salt, } AnCl_3 \mid Ag/AgCl$, between the An-Me alloy and the reference electrode. The mole fraction of An in the metal is progressively increased by coulometry at controlled potential. ICP and alpha analysis allow the faradic yield and the molar fraction $x_{An(Me)}$ to be determined precisely. For gallium, a Pu-Ga alloy was directly used.

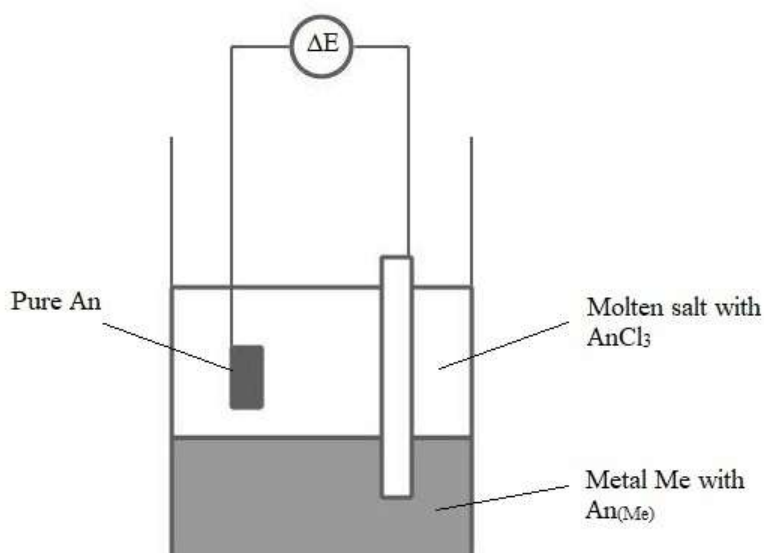


FIG. 9. Electrochemical cell — Schematic figure for $\gamma_{An(Me)}$ determination.

3.1.1.4. Comparison of the different metallic solvents

It is established that for a given molten salt and at a given temperature, the metallic solvent showing the highest separation factor is the one for which $\gamma_{Ce(Me)}/\gamma_{Pu(Me)}$ is the highest [17]. The evolution of $\log(\gamma_{Ce(Me)}/\gamma_{Pu(Me)})$ as a function of the temperature in the different metallic solvents is shown in Fig. 10 [23]. Aluminium exhibits the less negative value.

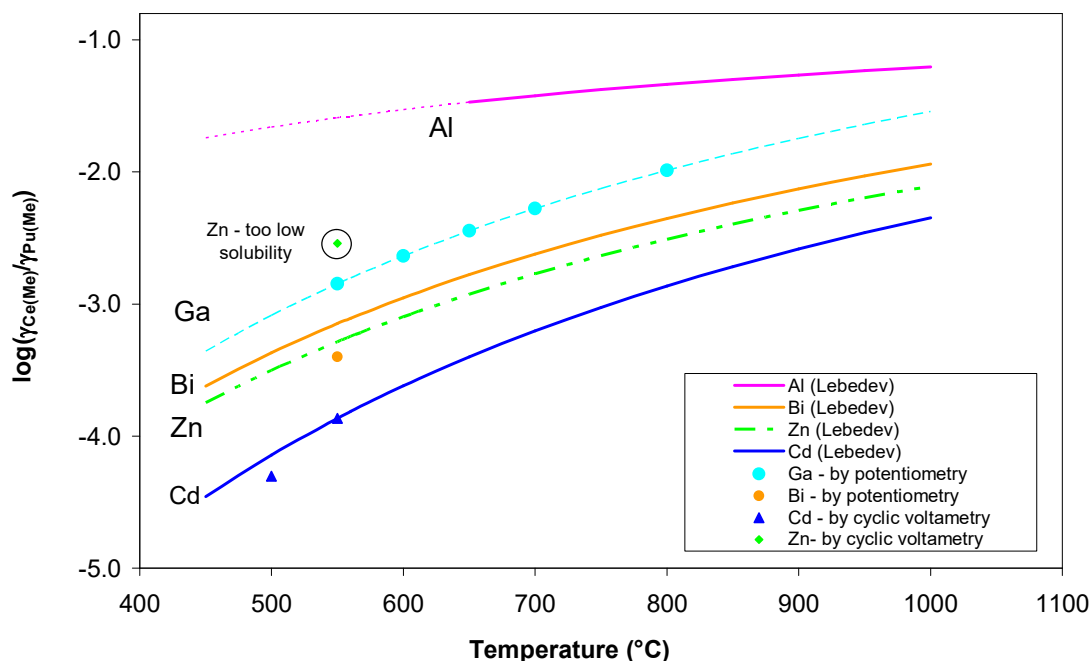


FIG. 10. Comparison of the ratio $\gamma_{Ce(Me)}/\gamma_{Pu(Me)}$ in various metallic solvents as a function of temperature [23].

Under this consideration, at a given temperature, aluminium appears as the best metallic solvent for the Pu/Ce separation. The aluminium melting point is 660°C. In order to work at a lower temperature, this metal can be alloyed with another metal. For example, aluminium alloyed with copper (at 17 wt.%) has a melting point around 550°C and its solvation properties are not changed [24].

The considered solvents were ranked from the most selective to the least selective as: Al>Ga>Bi>Zn>Cd at a given temperature. This classification was established for plutonium and cerium, but this should remain valid for actinides and lanthanides. As it is not possible to separate the aluminium solvent from the metallic actinides by distillation, actinide back-extraction processes are currently under study.

3.1.2. Liquid-liquid reductive extraction process in molten fluoride/liquid aluminium

Launched at the CEA Marcoule in the late 1990s, the pyrochemical R&D programme aims to provide experimental data for the demonstration of a grouped management of the actinides with sufficient fission products decontamination. The sustainability of the programme depends on how the process fulfils the following key points:

- (a) Recovering all of the actinides (>99.9%) present in the process input stream to recycle them;
- (b) Ensuring sufficient decontamination between actinides and fission products;
- (c) Generating the minimum of quantity of final waste streams;
- (d) Having a suitable confinement method for process waste.

Preliminary studies showed that the fluoride medium was very attractive in terms of confinement [25]. The processes currently assessed, and considered as the reference route at CEA, for actinides/fission products separation are based on a two-step liquid/liquid extraction. The complete process flowsheet is presented in Fig. 11 [25]. Most of the work already achieved was focused on the core of process, namely on the actinide reductive extraction and oxidative stripping. As the salt distillation — one of the head-end steps — is a key point for the sustainability of the process (mainly for the minimisation of the wastes), a study into the distillation of fluorides salts was also undertaken.

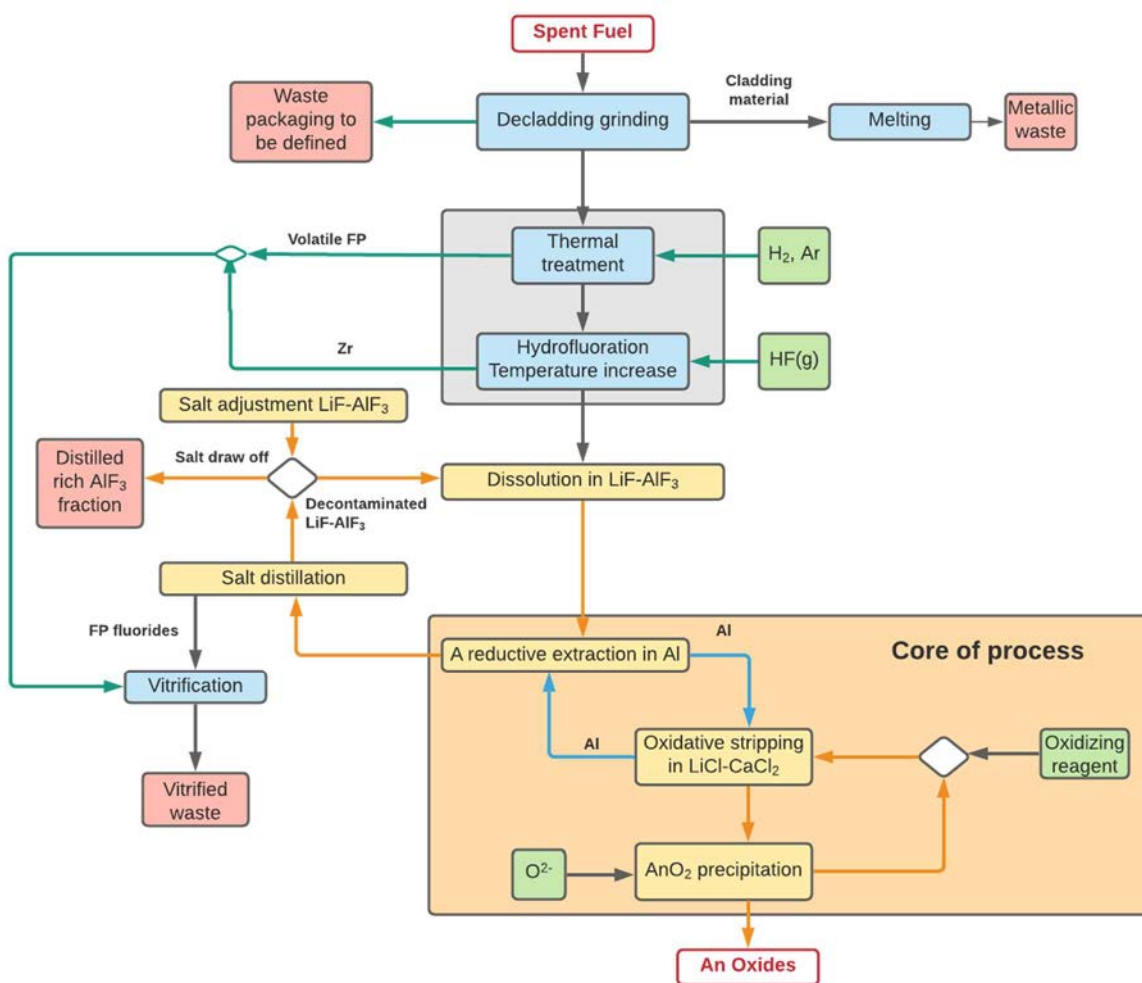
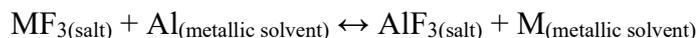


FIG. 11. Flowsheet of the pyrochemical reprocessing of spent nuclear fuel developed by CEA Marcoule [25].

3.1.2.1. Reductive liquid/liquid extraction

The first step consists in a chemical reductive extraction of the actinides from a molten fluoride phase (LiF-AlF₃ mixture) to a liquid aluminium phase [26] and can be described by the following equilibrium:



For a given element M and temperature T , two important factors must be taken into account: the distribution coefficient and the separation factor.

The distribution coefficient D_M is calculated as:

$$D_M = \frac{X_M}{X_{MF_3}} \quad (4)$$

where X_M is the fraction of the element M present inside the metallic solvent and X_{MF_3} is the fraction of the element remaining inside the salt phase once the thermodynamic equilibrium is reached. The higher the D_M value is, the better the extraction of the element M will be.

The separation factor is calculated as:

$$SF_{M_1/M_2} = \frac{D_{M_1}}{D_{M_2}} \quad (5)$$

The distribution coefficients of actinides and rare earth elements (REEs) were measured in LiF–AlF₃ (85–15 mol%)/Al system at 830°C (Table 1). According to Table 1, actinides and REEs (Ce, Nd, Sm, and La) are distributed in two separated groups. First, plutonium, americium, and curium, having similar distribution coefficients, could be co-extracted. Second, their separation from REEs should be easily reached thanks to their high separation factors ($SF > 1000$). As a consequence, a grouped actinide recovery can be expected.

TABLE 1. WEIGHT DISTRIBUTION COEFFICIENT (D_M) AND SEPARATION FACTOR ($SF_{Am/M}$) in LiF–AlF₃ (85–15 mol%)/Al at 830°C [27].

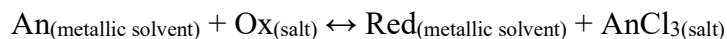
Element	D_M	$SF_{Am/M}$
Pu	273±126	0.78±0.47
Am	213±30	1
Cm	185±31	1.15±0.35
Ce	0.162±0.02	1315±289
Sm	0.044±0.004	4954±1139
Eu	<0.03	>7100
La	0.03	7100

More recently, additional experiments were performed on the extraction of U, Pu, Am, and Nd by liquid Al in molten LiF–AlF₃, using three different salt compositions. These experiments

confirmed the first results obtained and the extraction of 85% of U and 98% of Pu and Am could be achieved in a single step, while 10% of Nd was extracted by Al.

3.1.2.2. Oxidative liquid/liquid back-extraction of actinides

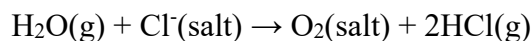
The second step of the process, i.e. the actinide back-extraction from the Al matrix, is also based on a liquid/liquid extraction method. This extraction is provided by a chloride melt containing an oxidizing agent. The occurring reaction is described by the following equilibrium:



Some experiments were carried out on the back-extraction of U (known from thermodynamic studies to be the most difficult actinide to be recovered) from the Al matrix, using different salt compositions and different concentrations of the oxidizing agent. Recently, this study led to the back extraction of 96% of U, from the liquid Al, in a LiCl-CaCl₂ molten salt (at 700°C), in a single stage.

3.1.2.3. Actinides conversion into oxides by precipitation

After back extraction step, actinides (III) dissolved in the molten chloride have to be converted into an oxide form in order to recycle them in a new nuclear fuel. The investigated process of conversion is precipitation using wet argon sparging in LiCl-CaCl₂ (30–70 mol%, 700°C). The use of a gaseous reagent for the precipitation is interesting from a process point of view because it does not increase the salt volume and does not change the solvent composition.



In order to investigate this conversion process, precipitation was first studied with cerium and neodymium as actinides surrogates [28]. Then, the method was applied to uranium and plutonium.

(a) Plutonium precipitation

Precipitation in molten LiCl-CaCl₂ (30–70 mol%) using wet argon sparging was performed on plutonium (III). Alpha spectrometry analysis of salt samples collected after the end of precipitation indicated a precipitation yield over 99%. XRD analysis of the resulting powder showed a PuO₂ oxide precipitate.



The formation of an intermediate PuOCl, which is a compound susceptibly formed in such media, remains to be clarified.

(b) Uranium precipitation

The uranium (III) precipitation study is the most difficult because of the high oxidation sensitivity of this element. Indeed, after experimental parameters optimization, uranium precipitation led to brown red oxide UO₂ as single compound (Fig. 12). Nevertheless, when wet argon is polluted by oxygen traces, uranium precipitation leads to higher oxide compounds as U₄O₉ or calcium uranate as CaUO₄. Moreover, despite a reaction of precipitation in the salt over 99%, some uranium is lost by volatilization. This is caused by UCl₃ partial oxidation to

UCl₄ during the precipitation reaction, which is volatile at the working temperature ($T_{\text{vap}}(\text{UCl}_4) = 689^\circ\text{C}$).

Uranium precipitation was well followed using oxide ions O²⁻ specific electrodes. The free oxide ions concentration O²⁻ in the molten chloride can be described by the pO²⁻ (Eq. 6).

$$p\text{O}^{2-} = -\log[\text{O}^{2-}] \quad (6)$$

Before the precipitation beginning by wet argon introduction, solubilized U(III) consumes O²⁻ leading to a low concentration of free O²⁻ and, in consequence, a high pO²⁻. Then, despite O²⁻ input by water reaction, pO²⁻ during the precipitation is roughly stable because of the O²⁻ consumption. Finally, end of precipitation is characterized by sharp drop of pO²⁻ demonstrating the increase of free O²⁻ in the molten salt.

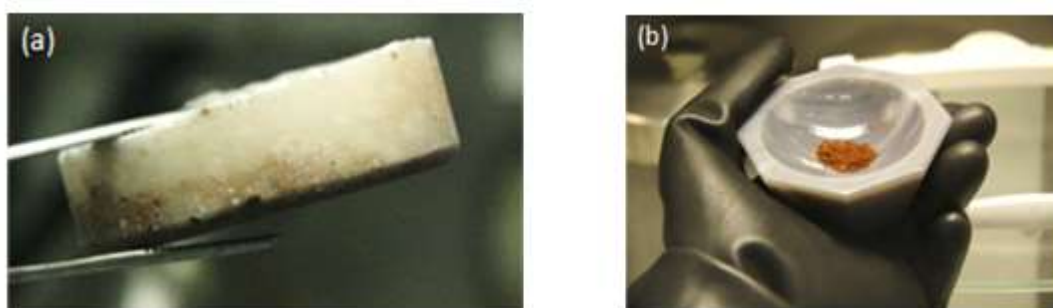


FIG. 12. (a) LiCl-CaCl₂ (30–70 mol%) after solidification at room temperature with UO₂ precipitate at the bottom. (b) Uranium precipitate isolated after salt dissolution (reprinted from [28] with permission. Copyright (2012) American Chemical Society).

(c) U-Pu co-precipitation

Co-precipitation of uranium (III) and plutonium (III) in the 50/50 molar ratio in molten LiCl-CaCl₂ (30–70 mol%, 700°C) using wet argon sparging formed a mixture of UO₂ and PuO₂. Therefore, this method of actinide conversion is oxidative enough to obtain PuO₂ and moderated enough not to oxidize uranium oxide beyond UO₂. In contrast with lanthanides (Ce and Nd), this process directly leads to the oxide form in the case of uranium and plutonium, which is a positive point for new fuel fabrication. However, co-precipitation does not give a U-Pu solid solution that would allow homogenous repartition of the two elements at the atomic scale. This separation between UO₂ and PuO₂ is caused by the uranium high sensitivity to precipitation. In consequence, uranium reacts first and then plutonium.

3.1.2.4. Conclusion

The R&D programme launched by CEA/DEN on pyrochemistry proves that fluoride melts are very promising for the selective An/Ln separation. High An/Ln separation factors could be obtained during the reductive liquid-liquid extraction in LiF-AlF₃/Al. The feasibility of the oxidative back extraction was successfully demonstrated on the most difficult actinide to be recovered from Al, i.e. uranium. Such a separation technique also offers an important advantage from technological point of view: it may lead to continuous counter-current separation

processes. Wet argon sparging in molten chloride is an interesting way of uranium (III) and plutonium (III) quantitative conversion to oxides in order to refabricate nuclear fuel and leads to the desired oxides forms UO_2 and PuO_2 formation in a single step. However, the partial volatilization of uranium needs to be decreased by optimization of the experimental conditions.

3.1.3. Salt decontamination for recycling

3.1.3.1. Fluoride salt distillation

Prior to recycling, the salt must be decontaminated towards FPs. In a second step, the salt composition (LiF/AlF_3 ratio) has to be readjusted as the LiF/AlF_3 ratio decreases during the extraction step. Among the different techniques potentially available to decontaminate the bath, the $\text{LiF}-\text{AlF}_3$ distillation was considered. The feasibility of the distillation of a salt containing remaining FPs was first assessed by thermodynamic calculations (Fig. 13). This theoretical study highlighted two important points:

- (a) The $\text{LiF}-\text{AlF}_3$ salt is distilled before LnF_3 and $(\text{FP})\text{F}_x$ remaining in the salt;
- (b) Zirconium and Caesium have to be removed before the extraction.

Several distillation experiments were performed first on a pure $\text{LiF}-\text{AlF}_3$ salt and then on contaminated fluoride salts (i.e. either with BaF_2 as a single contaminant or with a representative fission products mixture of Nd, Ce, Sm, Sr, Zr and Ba). All laboratory scale studies on the distillation of the pure or contaminated $\text{LiF}-\text{AlF}_3$ solvent demonstrated the feasibility and the efficiency towards the decontamination in FPs. One point of interest is the very substantial reduction of the volume of FP containing waste, as the solvent can be recovered at 95% and recycled in the extraction process.

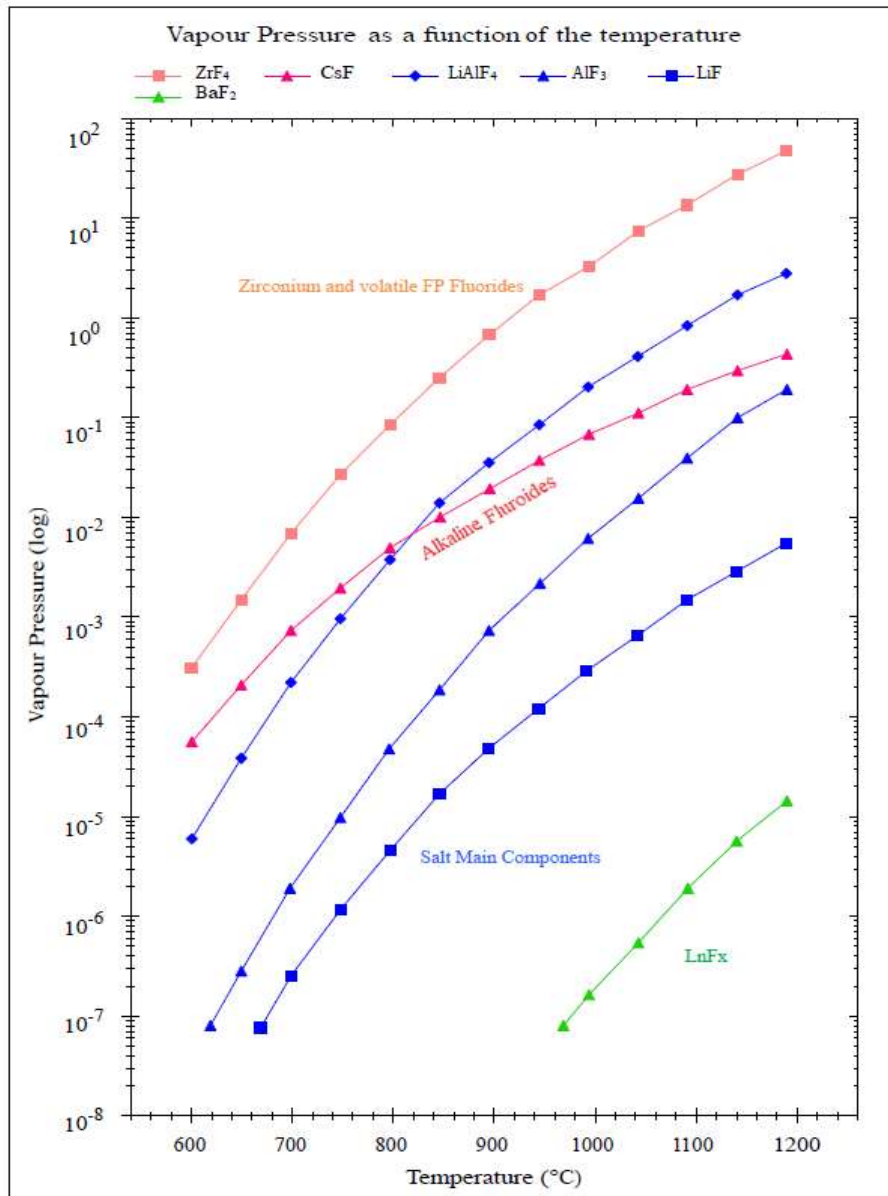


FIG. 13. Vapor pressure as a function of the temperature.

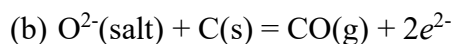
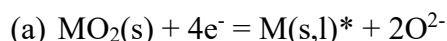
3.1.4. Direct electrochemical reduction of oxides in molten fluoride

SNF recycling using pyrochemical treatment presents several options, with most based on an electrorefining process with a metallic fuel as starting material. The process consists of an anodic dissolution of the SNF that is then selectively recovered on a cathode. Oxide fuels are not suitable for the electrorefining process, as ceramic materials are mostly insoluble in molten salts. Therefore, a preliminary step is required to convert oxide into metal.

Many studies have been dedicated to oxide reduction by metallic Li [29–32], and the reduction process has been demonstrated on AmO_2 , UO_2 , U_3O_8 , PuO_2 . But the process is limited by the need to handle active lithium metal and requires a precise control of Li_2O concentration.

A more efficient process has been elaborated based on a direct electrochemical reduction of oxide. The overall reaction is on one side the electroreduction of a solid oxide MO_2 into metal

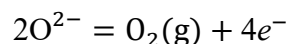
M at the cathode (*a*) and on the other side the evolution of CO and CO₂ at the anode (*b* & *c*). The oxide ions released at the cathode are transported through the support electrolyte and oxidised at a carbon anode:



Where s refers to solid phase, l refers to liquid phase and g refers to gaseous phase.

The electroreduction of UO₂, MOX (UO₂-PuO₂) and SNF has been performed with success in molten LiCl and CaCl₂ solvents [33–36]. One of the major issues is the use of a reactive carbon anode where CO₂ gas is released; the final product can be polluted by carbides, due to the reduction of carbonates (CO₃²⁻), and carbon dust is often detected at the surface of the melt, causing a short-circuit [37–39].

In the frame of the European ACSEPT programme, a different category of electrolyte composed of molten fluorides was tested, with the advantage of using an inert gold anode on which oxygen ions are oxidised into O₂ [40], preventing the carbides formation and carbon deposition at the cathode:



This exploratory research has been realised in the Laboratoire de Génie Chimique in a molten fluoride mixture. The direct electrochemical reduction of UO₂ samples, contained in a Mo basket, was studied in LiF-CaF₂-Li₂O (2 mass %) at 850°C. For the first time in such electrolyte, an electrochemical characterisation of UO₂ sample by linear sweep voltammetry has been realised and is presented in Fig. 14. The reduction peak at $E = +150$ mV/solvent is attributed to UO₂ direct electrochemical reduction.

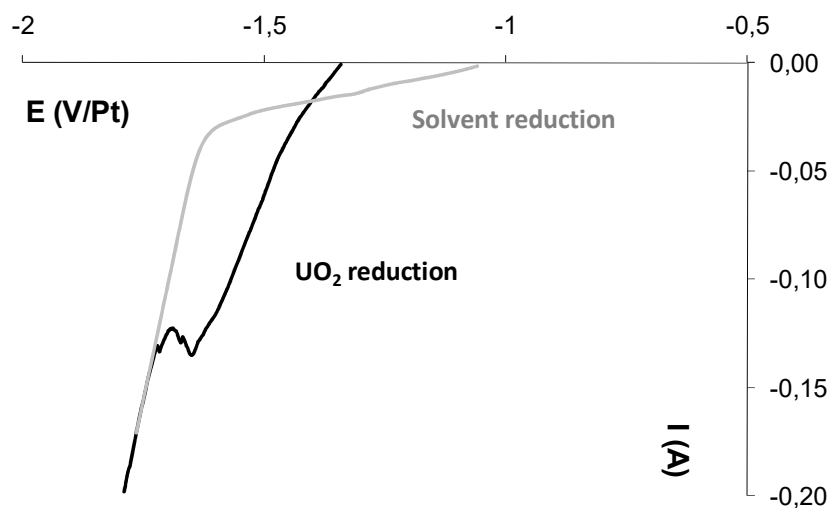


FIG. 14. Linear sweep voltammograms in $LiF-CaF_2-Li_2O$ (2 mass % Li_2O) at $10mV/s$ and $850^\circ C$ on UO_2 sample and in the solvent [41].

Galvanostatic electrolysis has been performed on single pellets of about 200–300 mg and a fully reduced sample is presented in Fig. 15.

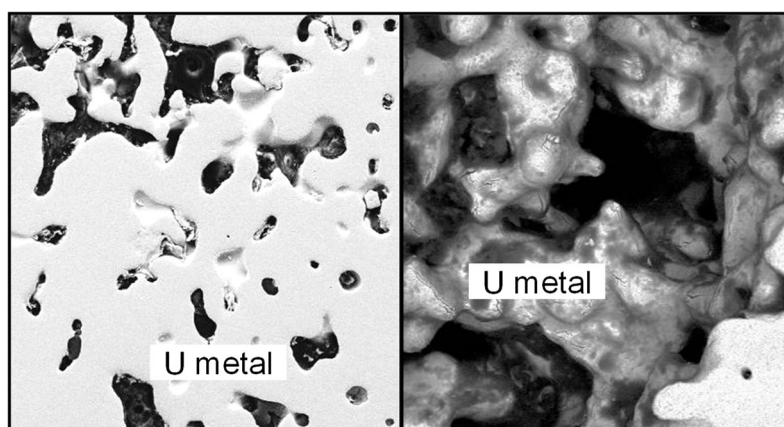


FIG. 15. SEM observations of UO_2 pellet cross section after electrolysis at $850^\circ C$ in $LiF-CaF_2-Li_2O$ (2 mass. % Li_2O).

Uranium metal has been analysed by SEM-EDX and by XRD. The observed sponge-like structure is characteristic of the direct electrochemical reduction process and has been already mentioned in chloride melts.

A complete conversion into metal was achieved at $850^\circ C$ and XRD analysis did not reveal the presence of any carbide phase, confirming the use of a gold anode for dioxygen evolution.

3.2. OVERVIEW OF PYROCHEMICAL REPROCESSING IN INDIA

3.2.1. Introduction

An assessment of the energy needs of India has projected an energy demand of 1300 GW(e) by 2050. In order to meet this demand, an increased contribution from nuclear energy has been identified one of the sources with a many-fold increase over the next four decades [42, 43]. As the availability of natural uranium is only sufficient to meet the demand of the PHWR fleet, the high growth rate envisaged can be achieved only by the effective utilization of uranium in FRs and increasing the breeding ratio with suitable fuel cycle technology choices. Reducing the doubling time by reducing the cooling period, and the introduction of metallic fuels are some of the options available for increasing the breeding ratio. Accordingly, it has been proposed that metallic fuels will be introduced into FRs by the next decade. Pyrochemical reprocessing becomes imperative for such a scenario, and efforts have been taken to develop pyrochemical reprocessing methods for FR fuels. A well-defined road map for the development of all aspects of the metal fuel cycle based on pyroprocessing has been drawn up and supporting activities have commenced.

3.2.2. Pyrochemical reprocessing

Molten salt electrorefining is a pyrochemical process ideally suited for reprocessing metallic fuels. The advantages of the molten salt electrorefining process over the aqueous process for metallic fuels are:

- A reduced number of steps, as the fuel is in the metallic state throughout the process;
- Compatibility with short cooled, high burnup fuels due to the ability of the inorganic solvents to withstand higher amounts of radiation compared to the organic reagents, leading to shorter doubling time;
- Ability to handle higher amounts of SNF in a given volume than the aqueous processes, leading to more compact plants;
- Reduced criticality problems due to the absence of moderating agents;
- Almost no high level liquid waste;
- Inherent recycle potential for minor actinides, which follow uranium and plutonium during the separation that makes the processes more proliferation resistant.

The challenges are:

- High temperatures of operation and the employment of corrosive salts, which pose technological challenges in the selection of materials;
- As the salts are hygroscopic and the metals are pyrophoric in nature, the process demands an inert atmosphere having very low levels of moisture and oxygen;
- Separation factors for fission products are about 1000 times lower compared to the aqueous processes;
- Limited experience, mostly at laboratory scale.

3.2.3. Molten salt electrorefining process for metallic fuels

The process was developed by ANL (USA) for reprocessing the U-19Pu-10Zr alloy fuels of Integral FR (IFR). It is based on the thermodynamic stabilities of the chlorides of fuel materials and fission products. The schematic diagram of the molten salt electrorefining process is shown in Fig. 16. In this process carried out at 773 K, LiCl-KCl eutectic salt is used as the electrolyte

salt. The chopped pieces of SNF pins are loaded into the anode basket of the electrorefining cell. A solid metal rod or molten cadmium serves as the cathodes. A layer of molten cadmium is maintained at the bottom of the electrorefiner to collect any deposit falling off the cathode.

During the electrorefining process, the elements whose chlorides are highly stable are easily oxidized and are transferred to the electrolyte phase as their chlorides. They are not easily reduced and so they remain in the electrolyte phase. Noble metals whose chlorides are the least stable do not get oxidized and so they remain in the anode basket. Fuel materials, uranium and plutonium and the minor actinides whose chlorides are of intermediate stability are transported to the anode through the electrolyte, are reduced and then deposited on the cathode.

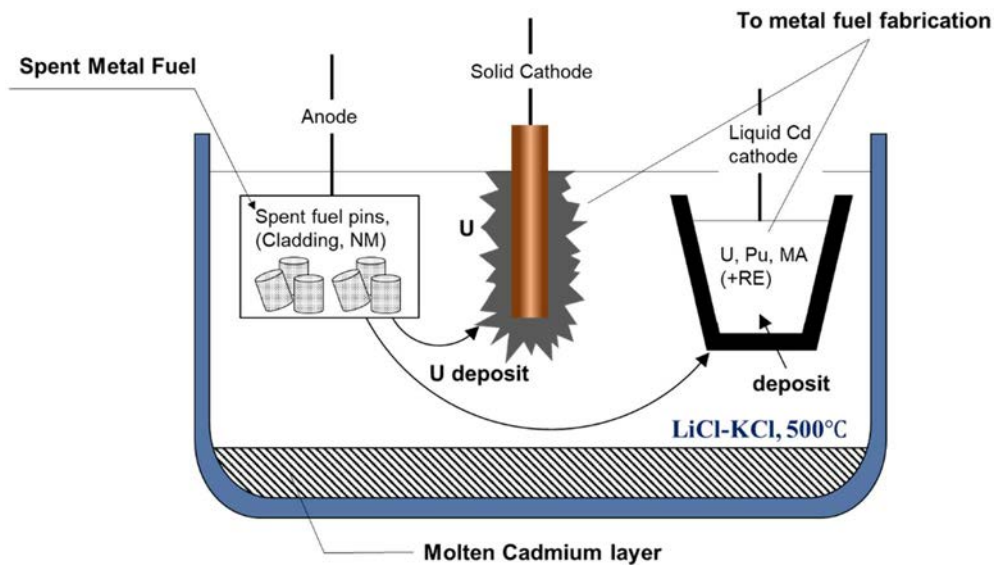
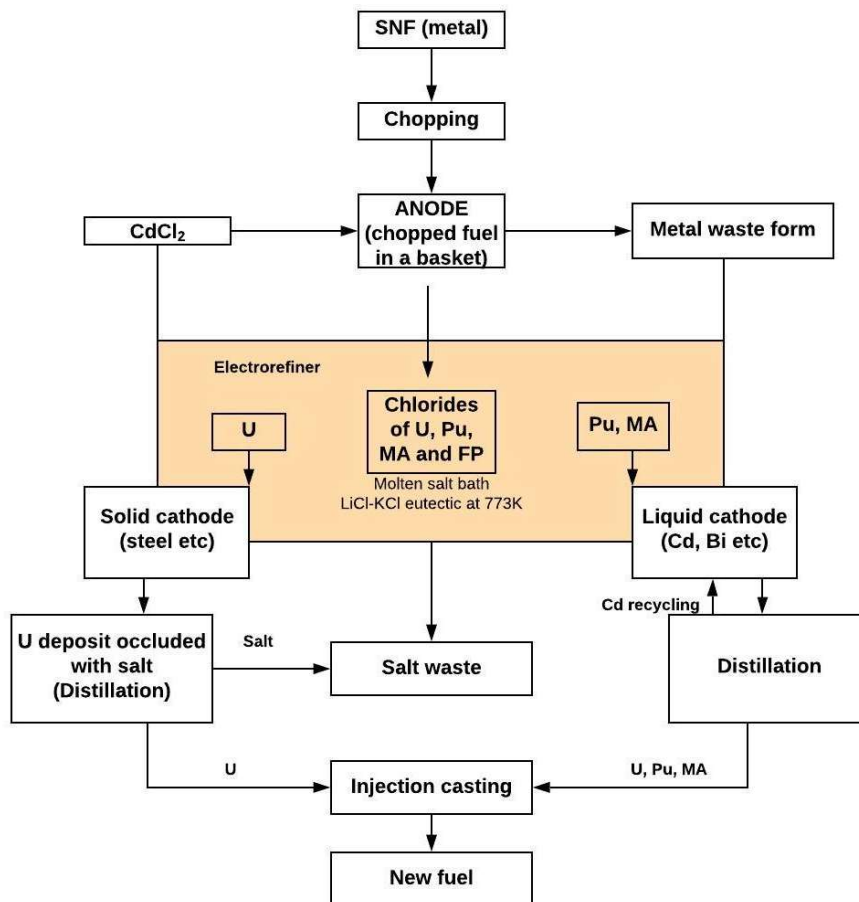


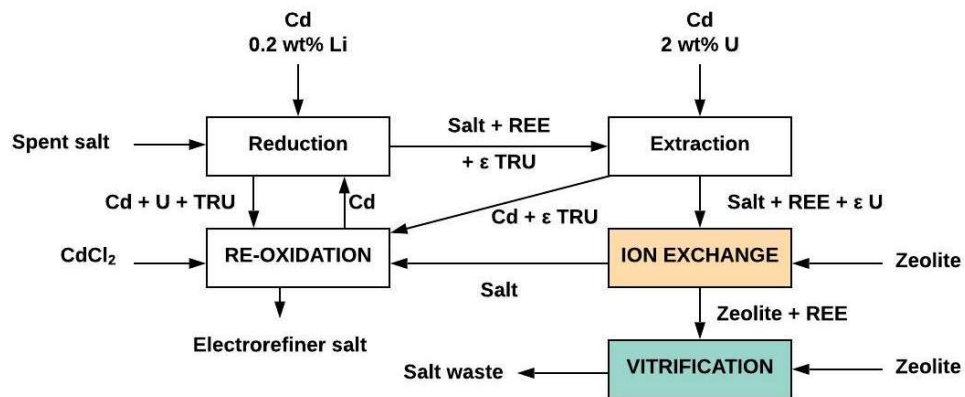
FIG. 16. Schematic diagram of the molten salt electrorefining process.

When a solid rod is used as the cathode, uranium alone is deposited, whereas when liquid cadmium is used as the cathode, uranium and plutonium are co-deposited along with MAs.

The complete pyroprocess flowsheet is shown in Fig. 17.



(a)



(b)

FIG. 17. The complete pyroprocess flowsheet (a) Pyroprocess flowsheet-I (b) Pyroprocess flowsheet-II.

Uranium metal deposited on the solid cathode is occluded with salt, which is then distilled to recover the metallic uranium; this step is known as the ‘consolidation step’. Similarly, the consolidation step for the cadmium cathode is the distillation of cadmium to recover uranium, plutonium, and MAs.

The LiCl-KCl electrolyte salt is purified from the FPs by passing it through a zeolite column and then recycled. The zeolite containing the salt and fission products are heated with boron aluminium silicate glass to form a glass bonded ceramic waste form for the salt.

Prior to the removal of salt for purification using zeolite, the actinides in the salt (6 wt%) must be removed and added to the next batch. It is done by an 'actinide draw down' step involving equilibration between the salt containing actinides and Li-Cd alloy at 773 K. This is an essential step for achieving a recovery of >98% for actinides.

The noble metal fission products along with the cladding hulls are left behind in the anode in the electrorefining process. These are melted and cast with 15% Zr to form a metal waste form. Thus there are two waste forms in the pyroprocess, namely ceramic and metal waste forms.

3.2.4. Electrorefining process

A laboratory scale argon atmosphere facility for carrying out studies on molten salt electrorefining has been operating at the Indira Gandhi Centre for Atomic Research (IGCAR) centre for more than ten years. The facility is a train of five interconnected glove boxes maintained under high purity argon atmosphere with less than 20 ppm each of moisture and oxygen. Studies have been carried out on all the unit operations of the uranium alloys electrorefining process. Separation factors of typical fission products (Ce, Pd and Zr) have been determined using U-10 wt% Zr and U-Ce-Pd alloys as the anodes. Studies are now in progress with Pu based alloys.

A code based on thermochemistry, 'PRAGAMAN', has been developed for the numerical simulation of the electro transport behaviour of U and Pu in the electrorefining cell.

Based on the experience gained with laboratory scale studies, a demonstration facility has been set up and commissioned. Electrorefining studies of uranium have been carried out at 1 kg level. The laboratory scale facility will continue to be used for studies on plutonium bearing alloys. The experience gained in the operations of these facilities will give vital inputs for the design of a pyrochemical reprocessing plant that can be used for the trial reprocessing of metallic fuel pins to be irradiated in FBTR, as well as the metallic SNFs of FBTR.

It is proposed to start the design of a pyrochemical reprocessing plant for the SNFs from FBTR based on the laboratory scale experience with Pu alloys and engineering scale experience with U alloys.

3.2.5. R&D needs for pyroprocessing technology

For the development of pyroprocessing technology, the following R&D is required:

- Engineering scale processing of U alloys in the demonstration facility;
- Laboratory scale studies on Pu alloys with simulated fission products using different cathode materials, such as Cd and Bi;
- Development of advanced electrorefiners and an advanced consolidation set up for the recovery of actinides from cathode deposits;
- Development of actinide drawdown processes, scaling from laboratory scale studies to plant scale studies — both salt/ Li-Cd alloy equilibration process are included, as well as alternate processes;
- Development of ceramic and metal waste forms, with characterization and leachability studies using simulated fission products;

- Development of electro kinetic model for electro transport properties;
- Thermodynamics studies on alloy and salt systems.

3.2.6. Conversion of actinide oxides to metals

The technology for the conversion of actinide oxides to the respective metals in tonnage quantities is essential to transition from a thermal reactor fuel cycle to a metal fuelled FBR fuel cycle. Currently, the conversion is carried out by calciothermic reduction of the actinide fluorides. In recent years a simpler electrochemical reduction process has been reported, which is being developed in many countries.

A schematic diagram of the process is shown in Fig. 18. In this process, the actinide oxide (in the form of a pellet) is used as the cathode of an electrolytic cell using LiCl or CaCl₂ as the electrolyte. When LiCl is used as the electrolyte, 2–3% Li₂O is added to the salt. Platinum is used as the anode. When a potential of ~3V is applied, the actinide oxide cathode is converted to the metal and oxygen evolves at the anode. The exact mechanism is still being debated.

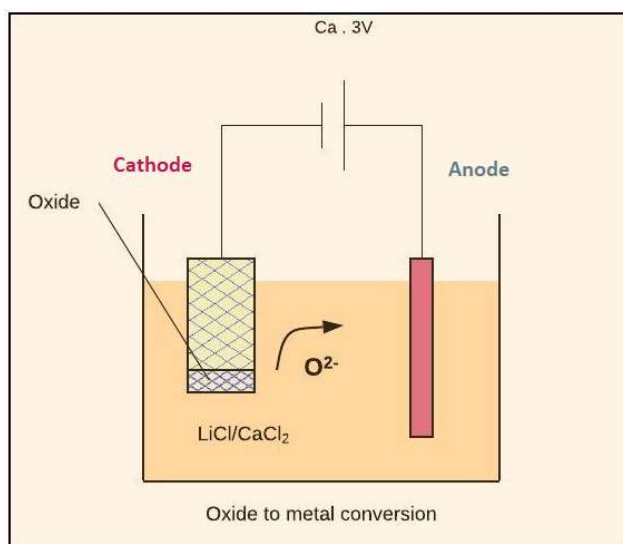


FIG. 18. Schematic diagram of the electrochemical reduction process.

3.2.7. Electroreduction of uranium oxides

Studies have been initiated to investigate the electroreduction of uranium oxide in molten LiCl-Li₂O electrolyte at 923 K. The solid oxide served as the cathode, and platinum as the anode in the electro-reduction cell. Cyclic voltammetric (CV) experiments were carried out to test the electrochemical stability of different electrode materials like glassy carbon, platinum, stainless steel, molybdenum, and tantalum in the molten salt system. These experiments were also used to obtain the safe electrochemical window for electro-reduction work with the platinum anode. The CV experiments were carried out in molten LiCl containing 1–3 wt% Li₂O, and the results showed that melt compositions with 2–3 wt% Li₂O are ideal for the electro-reduction work. Preliminary electro-reduction experiments carried out with solid UO₂ and U₃O₈ powder electrodes, in both controlled potential and controlled current conditions, yielded partially reduced uranium oxides as well as uranium metal in different experiments. The experiments revealed that a moisture free electrolyte melt is a pre-requisite for the successful reduction of

the oxide to the metal and it is necessary to control the anodic potentials below platinum dissolution to avoid the damage of the electrode. Few experiments were carried out with graphite anode, but the electrolysis product was found to be uranium carbide.

3.2.8. R&D needs for the Indian programme

- Laboratory scale studies on direct electrochemical reduction of uranium oxides to optimize the concentration of Li_2O in LiCl , to arrive at the best cathode material and the density and form of the oxide material best suited for 100% conversion;
- Studies on PuO_2 reduction at laboratory scale;
- Scaling up the process.

3.3. PYROPROCESSING IN JAPAN

3.3.1. Metal fuel cycle integrated the spent oxide fuel treatment and the separation of actinides

The integrated actinides recycle system for LWR oxide fuel and for FR metal fuel using pyrochemical technology is shown in Fig. 19 [44]. This system also envisages the P&T of TRU elements contained within the high level liquid waste (HLLW) stream arising from aqueous reprocessing. The pyrochemical reprocessing consists of electrorefining with a solid cathode for uranium recovery and a liquid cadmium cathode for actinides collection in a LiCl-KCl salt bath, reductive extraction for recovering TRU elements in LiCl-KCl/Cd or LiCl-KCl/Bi using lithium as the reductant, and fuel fabrication by casting after removing salt and cadmium by distillation of the actinide products. The electrochemical reduction is applied to convert spent oxide fuels to metals in LiCl-KCl salt with the addition of Li_2O . To recover TRU elements, HLLW is converted to chloride for reductive-extraction. To facilitate chlorination, HLLW has to first be denitrated to obtain the oxides. The chlorination of oxides occurs in a LiCl-KCl bath. The MAs used in the preparation of FR U-Pu-Zr metal fuels resulted from electrorefining and reductive extraction and contain a small quantity of lanthanides that were separated along with the actinides. This is because there is only a small difference between the free energy of formation for the chlorides of lanthanides and actinides.

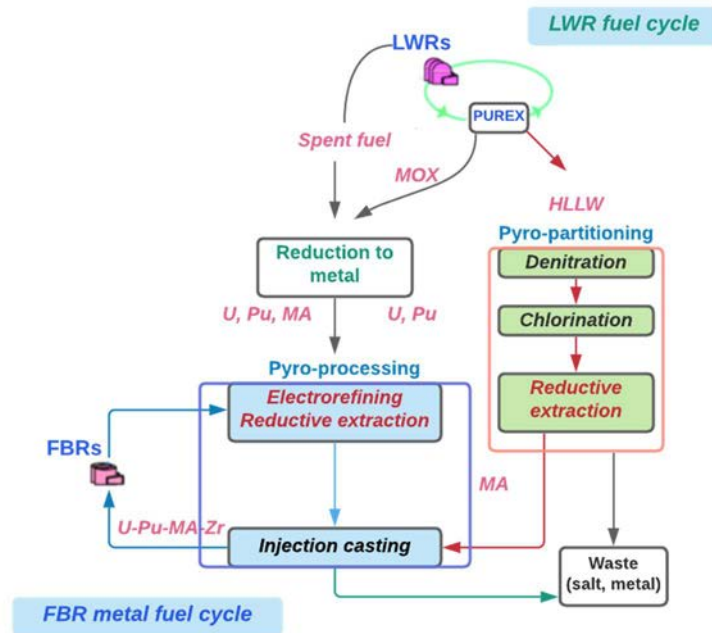


FIG. 19. Integrated actinide recycle system [44].

3.3.2. Metal fuel cycle with electrorefining

The reprocessing of metal fuel consists of two stages of electrorefining, with a solid cathode for uranium, and a liquid, and for uranium and TRU elements at each stage. The actinides separated from the salt and cadmium by distillation, are transferred to fuel fabrication by the casting method. The LiCl-KCl salt, containing a small quantity of actinides and fission products, used for electrorefining is purified by a multistage counter-current extraction and zeolite column before recycling to the electrorefining stage. The zeolite containing absorbed fission products is solidified at high temperature under high pressure to make a stable sodalite for disposal [45]. The process diagram is given in Fig. 20.

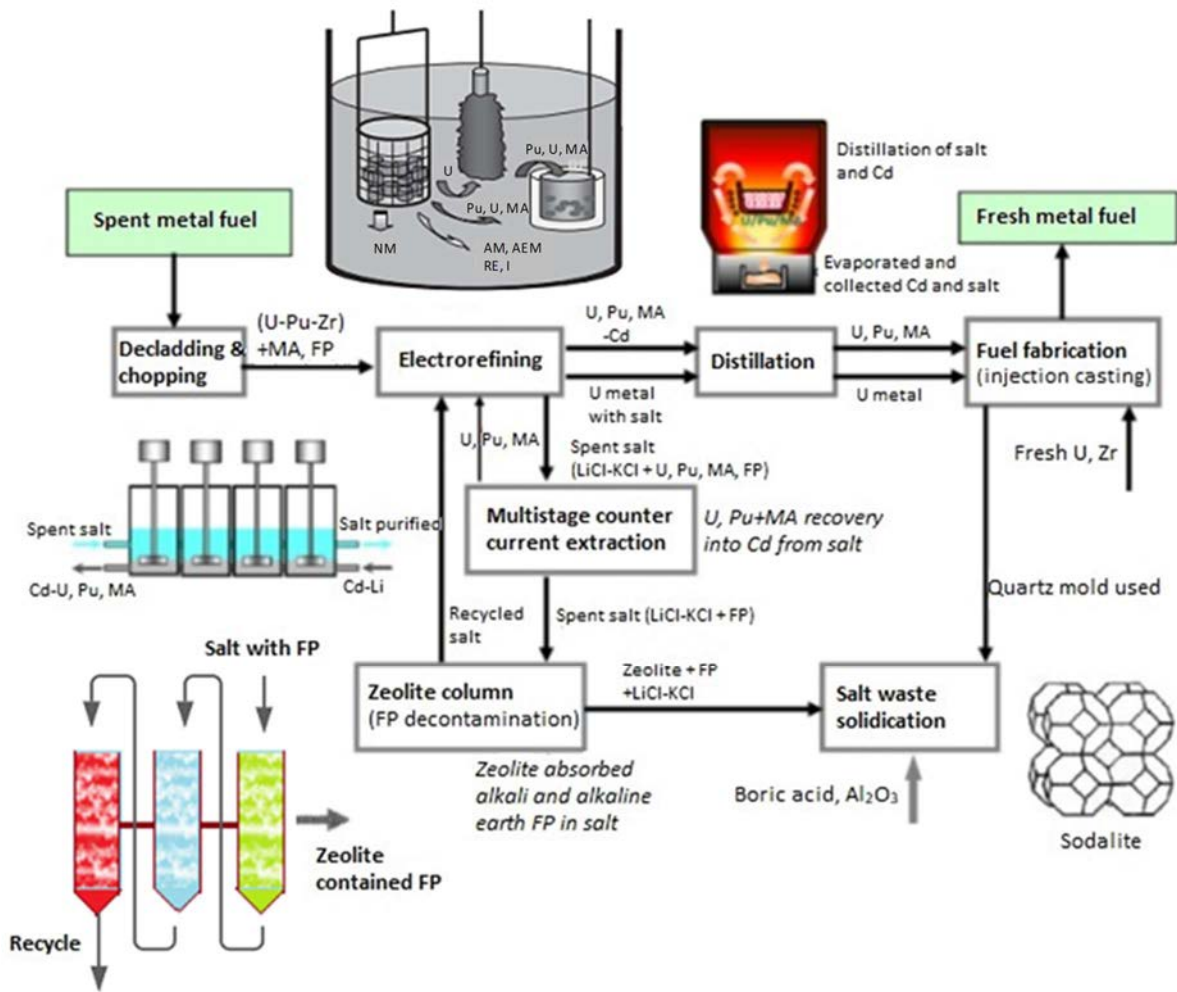


FIG. 20. Process flow diagram of metal fuel cycle with salt purification and waste solidification.

3.3.3. Engineering scale electrorefiner

Two types of electrorefining apparatus with different dimensions were examined [46, 47]. One was a laboratory scale electrorefiner, with 3.5 kg of LiCl-KCl electrolyte and a maximum batch size of 500 g of uranium. The other was an engineering-scale electrorefiner with around 60 kg of electrolyte and a maximum batch size of about 7 kg of U. Figure 21 gives the concept of electrorefiner with cathode deposit scraper mechanism. The simulated metal SNF was charged in an anode basket. The composition of the U-Zr rod containing fission products is given in Table 2. The operational function of each component was examined in a laboratory-scale apparatus prior to application with the engineering scale electrorefiner. The total electric charge was 330.8 Ah for 29 h, with 70.7 % of the uranium initially loaded in the anode successfully electro transported to the cathode with the cathode current of 27.1%.

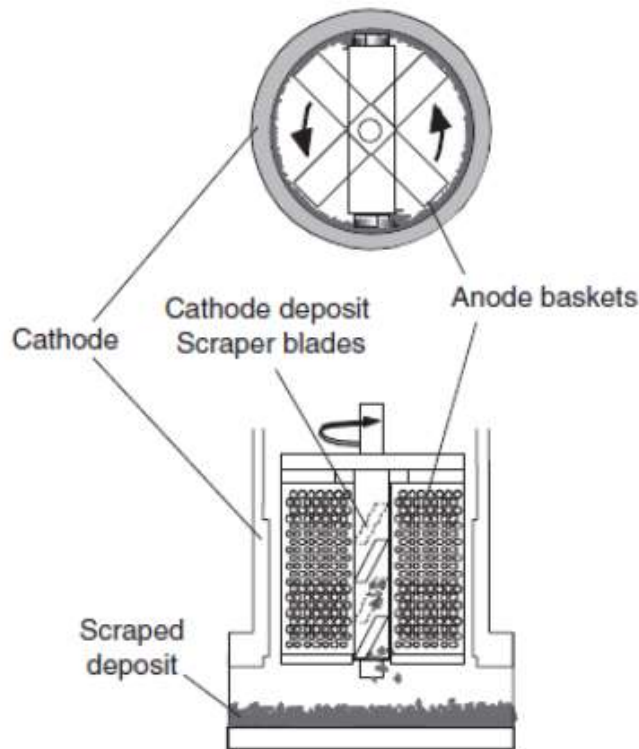


FIG. 21. Concept of electrorefiner with cathode deposit scraper mechanisms ([47], reprinted by permission of Taylor & Francis Ltd, on behalf of Atomic Energy Society of Japan).

TABLE 2. COMPOSITION OF U-ZR ROD CONTAINING FP ELEMENTS MANUFACTURED BY INJECTION CASTING ([47], reprinted by permission of Taylor & Francis Ltd, on behalf of Atomic Energy Society of Japan).

	Zr (wt%)	Mo (wt%)	Pd (wt%)	Ce (wt%)	Nd (wt%)	O (ppm)	N (ppm)	C (ppm)
Injection casting loading	10	1.10	0.8	0.06	0.10			
Sample-1	8.61	1.02	0.5	0.03	0.04	85	<20	49
Sample-2	9.38	1.09	0.68	0.04	0.04	72	<20	12
Average	8.99	1.06	0.59	0.04	0.04			

The engineering scale electrorefiner with a high electrorefining current was equipped to maximize the uranium recovery rate by allowing the simultaneous dissolution of zirconium and uranium. The current was experimentally determined by current-potential curve measurement just prior to the electrorefining as the highest value at which no indication of anodic dissolution of stainless steel parts was found. A large electrorefining current (400–450 A) was maintained until 82% of the loaded uranium was collected. The uranium recovery rate for this period reached 789 gU/h, which corresponds to 32.9 gU/h/L per unit volume of the electrode assembly. The total electric charge allowed to pass throughout the test was 3510 Ah, which is equivalent to 10.4 kg of U, assuming a current efficiency of 100%. This amount is 1.65 times as large as that of uranium in the alloy initially loaded to the anode baskets. The total weights of the

collected products and the residues on the cathode after each scraper operation are shown in Table 3. By comparison with the amount of the initial loading to the anode, approximately 90% of uranium in the anode was transported to the product. The cathodic current efficiency was evaluated to be 57.1% [47].

TABLE 3. WEIGHT AND CHEMICAL COMPOSITION OF COLLECTED PRODUCTS AND RESIDUES ON CATHODE ([47], *reprinted by permission of Taylor & Francis Ltd, on behalf of Atomic Energy Society of Japan*).

Sample	Total weight (g)	Composition (wt%)					
		U	Zr	Mo	Pd	Nd	Ce
Scraper operation-1 Collected product	3570	99.5	0.314	0.000	0.068	0.078	0.063
Scraper operation-2 Collected product	1884	87.4	12.3	0.000	0.059	0.069	0.161
Scraper operation-2 Residue on cathode	59.4	81.7	18.2	0.000	0.047	0.060	0.052
Scraper operation-3 Collected product	308	83.6	16.3	0.005	0.047	0.052	0.044
Scraper operation-3 Residue on cathode	214	86.8	13.0	0.009	0.063	0.080	0.073
Scraper operation-4 Collected product	72.7	95.0	4.81	0.007	0.076	0.057	0.070
Scraper operation-4 Residue on cathode	345	94.5	5.32	0.007	0.050	0.066	0.039
Residue on cathode after 4th scraper operation	260	93.9	5.84	0.016	0.081	0.065	0.079

The microstructure observation and chemical analysis indicated that anodic dissolution progressed axially from radial surfaces of chopped U-Zr alloy pins, and a Zr-rich region grew from all directions toward the centre of the pins, and chemical and wave length dispersive spectrometry (WDS) analysis for anode residue samples predicted that noble elements would remain in the anode residue together with zirconium even after the dissolution of most of the uranium. A comparison of analytical results on noble element behaviour in simulated material and irradiated EBR-II driver fuels indicated no large difference between them. Moreover, decontamination factors of uranium from molybdenum and palladium defined as the ratios of their concentrations in the initial alloy loaded to the anode to those in the cathode products was estimated to be around 70 for molybdenum and 10 for palladium.

3.3.4. High temperature melt transport technology

A large amount of molten salt and liquid cadmium, more than 150 kg, has to be transferred without temperature loss at an engineering scale or a commercial scale system, for example the transfer from the electrorefiner to a distillation device.

The development of high-temperature transport technology for molten salt and liquid cadmium is a crucial prerequisite for effectively designed pyroprocessing installation. Few transport studies have been reported on high-temperature fluids [48–52]. CRIEPI have reported the successful transport of molten LiCl-KCl eutectic salt at approximately 773 K using gravity and a centrifugal pump [53]. The transport of pure liquid Cd by several methods were also examined [54]. On the basis of these high-temperature fluid transport experiments, an engineering-scale electrorefiner was designed and installed in an argon-atmosphere glove box [53]. The schematic presentation is given in Fig. 22.

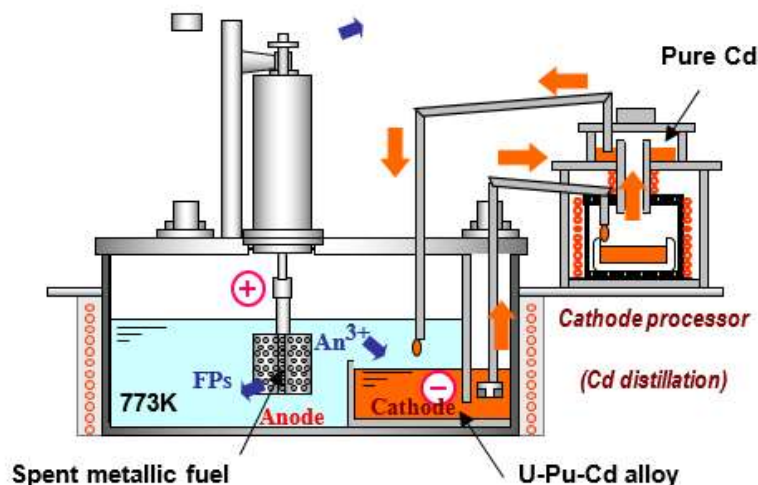


FIG. 22. Schematic presentation of melt transfer equipment (reproduced courtesy of CRIEPI).

This electrorefiner has a high-temperature fluid transport system for the liquid Cd cathode. After electrorefining, the liquid Cd-actinide alloy is transported to the distillation crucible of the cathode processor. The Cd is collected at the condenser by the distillation of the Cd-actinide alloy. The distilled Cd is then transported back to the cathode crucible. Using a Cd-Gd alloy, operations using the engineering-scale electrorefiner were demonstrated. Gadolinium was used to simulate the actinides. Based on that expertise, an electrorefiner with high-temperature fluid transport system was designed and installed, as illustrated in Fig. 23(a). This electrorefiner had a 780 mm diameter and was 800 mm deep and was loaded with approximately 150 kg of LiCl-KCl eutectic salt. The concentration of Gd in the molten salt was between 1 and 4 wt% and the amount of Gd metal in the anode was about 2 kg. The crucible of the Cd cathode had a 300 mm diameter and was 160 mm deep and held approximately 30 kg of Cd. The Gd was transported from the Gd metal anode to the Cd cathode by electrowinning. Afterwards, the liquid Cd-Gd alloy was transported from the Cd cathode to the cathode processor [55]. Pure Cd was supplied from the Cd supply tank to the cathode crucible by gravitation (Trans. 1). After electrorefining, the Cd cathode deposit was transported to the vacuum tank from the Cd cathode crucible by a suction pump (Trans. 2). Since the suction pump cannot directly transport the Cd-Gd alloy to the cathode processor, which is located at a high position (1.6 m), it was transported from the vacuum tank to the Cd alloy buffer tank by gravitation (Trans. 3) and then was transported to the distillation crucible from the Cd alloy buffer tank by the centrifugal pump (Trans. 4). At the cathode processor, the Cd-Gd alloy was distilled to separate the actinides and Cd, with Cd vapor condensed at the condenser. The pure Cd was then transported from the condenser to the Cd supply tank by gravitation (Trans. 5). This electrorefiner with a high-temperature fluid transport system was equipped in a large argon glove box, as shown in Fig. 23(b) [55, 56].

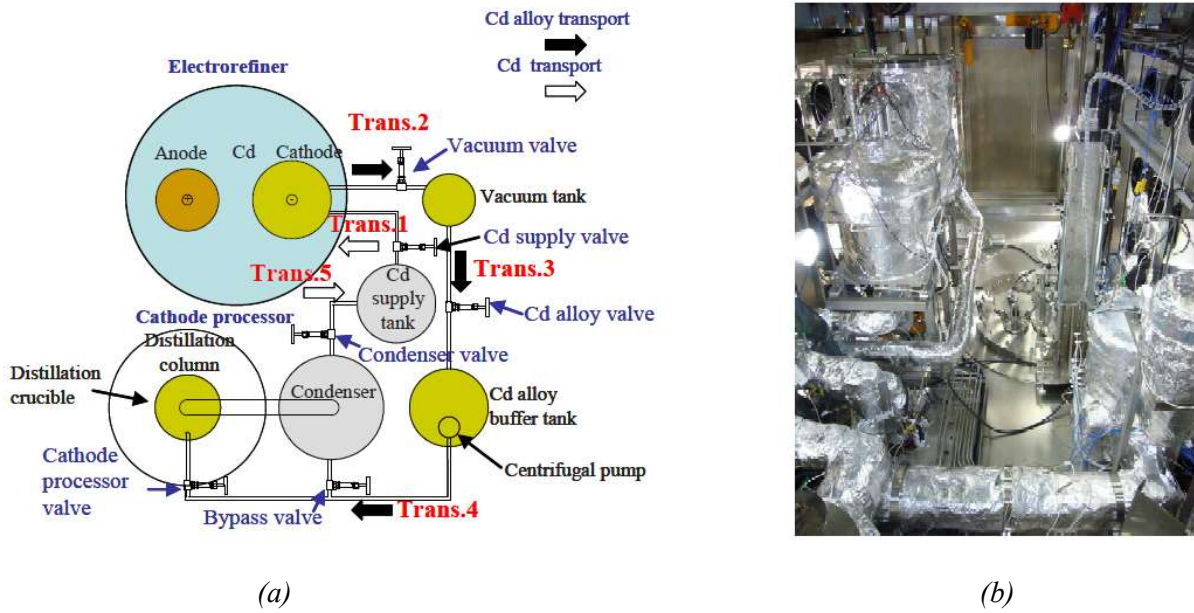


FIG. 23. Electrorefiner with high temperature fluid transport system (a) Diagram of the electrorefiner (b) Photograph of the electrorefiner ([55, 56], reprinted with permission).

The performance of the electrorefiner for the pyroprocessing of the SNF over 24 hours was calculated using the processing rate and transportation rate in Table 4. The operation time involving the handling of electrorefiner was defined as the total sum of processing time of Trans. 1 and Trans. 2, and the operation time of the cathode process was the processing time of Trans. 3 and Trans. 5. The achievable quantity of actinides collected in the Cd cathode of the electrorefiner was determined to be 4.8 kgHM, as shown in Table 4. The amount of Cd required to produce this mass would be 235.2 kg, assuming the concentration of the actinides in Cd to be 2 wt%, given the saturation limit of U in Cd of 2.35 wt% [57] and that of Pu in Cd of 3.62 wt% at 773 K [58]. With a recovery of 4.8 kgHM at the Cd cathode over 24 h, 48.5 kg of U would be recovered at the solid cathode over the same period. An electrorefiner with a newly designed solid cathode, which was reported to have a performance of 789 gU/h [46], would be able to recover 17 kg of U, thus 3 modules in the solid cathode would be required to recover 48.5 kg of U. Consequently, the electrorefiner was estimated to be able to refine 53 kgHM of SNF in 24 h. The distillation capacity of the cathode processor was estimated to be 0.5 kgHM/day. Assuming the diameter of the distillation crucible to be 400 mm, each module of the cathode processor could distil 240 kg of Cd alloy.

TABLE 4. PERFORMANCE OF THE LIQUID CD CATHODE ELECTROFINER WITH TRANSPORT SYSTEM IN FIG. 23 (reproduced courtesy of CRIEPI).

Process	Electrorefining (liquid Cd cathode)			Cathode processing (Cd distillation)			
	Trans. 1	Electrorefining	Trans. 2	Trans. 3	Trans. 4	Distillation	Trans. 5
Processing / Transportation rate	0.3 dm ³ Cd/min	0.24 kgHM/h	1.1 dm ³ -Cd alloy/min	1.3 dm ³ -Cd alloy/min	0.3 dm ³ -Cd alloy/min	0.07 kgHM/h	2.5 dm ³ Cd/min
Performance	4.8 kgHM/day			0.5 kgHM/day			

3.3.5. Electrochemical reduction of oxides guiding to electrorefining

The electrochemical reduction of oxides is the key technological step for oxide fuel treatment prior to electrorefining for a FR cycle. The schematic presentation of this series of processes is given in Fig. 24 [59].

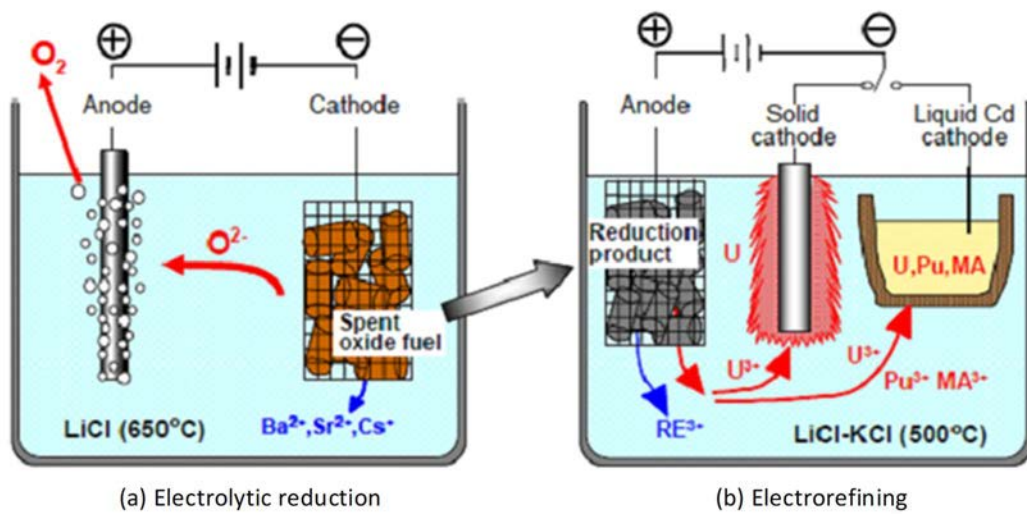
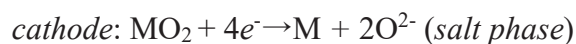
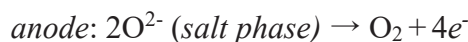


FIG. 24. Schematic diagram of pyrochemical reprocessing for oxide fuel, consisting of (a) electrolytic reduction of oxide fuel and (b) electrorefining of reduced product [59].

In the electrochemical reduction process, oxide fuels are loaded at the cathode in a molten chloride bath dissolving oxide ion. The reactions at the cathode and anode occur according to the following reactions:



and



where, M denotes actinides such as uranium and plutonium. The oxygen is electrochemically ionized, and the actinide metal remains at the cathode. The ionized O_2^- is transported through the salt and discharges at the anode to form O_2 gas. When a carbon anode is employed, CO_2 or CO is evolved instead of O_2 . The advantages of the electrochemical are that no reductants needed, and the by-product is only oxygen or carbon oxide gas. The concentration of oxide ion in the salt is almost constant and can be maintained at a low value, which is effective for reducing TRU oxides [32]. The amount of salt used in the process could be small as the oxide ion does not accumulate in the salt bath. The reduction behaviour of UO_2 at the cathode was clarified in both the LiCl and CaCl_2 salt baths and indicated that the LiCl salt bath was more suitable for UO_2 . The reduction study with $(\text{U-40Pu-5Np})\text{O}_2$ conducted by Iizuka et al. indicated that plutonium and neptunium oxides could be easily reduced to metals in a LiCl salt bath [60]. Herrmann et al. [36, 61] reported that the reduction of spent LWR oxide fuel was successfully demonstrated at bench-scale in a hot cell. More than 98% of uranium oxide was reduced to metal, and the distribution of fission products between the salt and fuel phases was quantified. A unique cathode assembly was attempted for U_3O_8 reduction by Jeong et al. [62] in which U_3O_8 powder was contained by a porous magnesia membrane and a stainless steel rod conductor was placed in the U_3O_8 powder. Conversion of U_3O_8 to metallic uranium was successfully achieved in a 20 kg U_3O_8 batch cell. From an engineering perspective, the high throughput of electrolyzer and the knowledge of FPs behaviour, material balance and material measures are required. CRIEPI have proposed a novel pre-treatment process for preparing porous oxide pellets from spent oxide fuels [59, 63]. Regarding the rate of oxide reduction, the porous pellets have a large advantage over powders. Pre-treatment process for porous oxide preparation is given in Fig. 25.

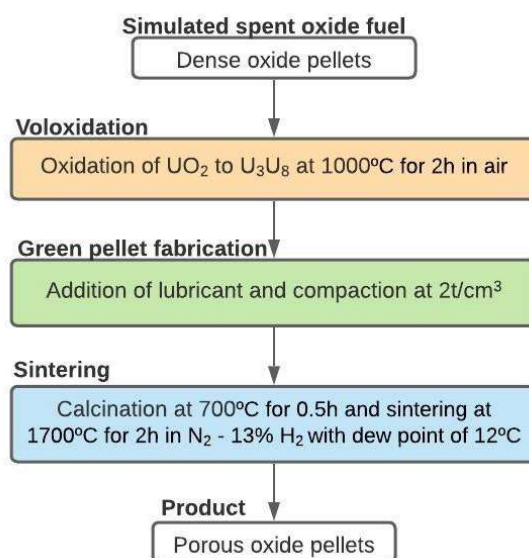


FIG. 25. Flow chart of pre-treatment process.

Following the 100 g scale UO_2 study [63], the electrolytic reduction was applied on the porous pellet simulated oxide SNF with a composition of 93 wt% U and 1 wt% each of Ce, Sr, Nd, Sm, Zr, Mo, and Pd [59]. Approximately 100 g oxides divided into 34 pellets were loaded into a cathode basket immersed in $\text{LiCl-Li}_2\text{O}$ melt with ca. 880 g at a temperature of 650°C . The reduction was conducted under the current-controlled condition.

Figure 26 shows the reduction product in the cathode basket. Most of the pellets were fully reduced, as shown in Fig. 26(c). Five out of the 34 pellets were partially reduced, as shown in Fig. 26(d). The centre region had not been reduced. The volume of the non-reduced region was 0.8% of the total volume of the 34 pellets, and, thus, the overall reduction yield and current efficiency for a 7.6 h reaction time was estimated to be 99.2% and 74%, respectively. Hence, the preparation of porous oxide pellets was highly advantageous in increasing the rate of oxide reduction. After the analysis of reduced pellet by scanning electron microscopy-energy dispersive X-ray (SEM-EDX), U metal yielded by electrolytic reduction was observed to form a ‘coral like’ structure, with the oxide phase in the reduction product consisting of the REEs and Zr. Some of the REEs were deposited at locations where Pd existed, indicating that a small part of the REEs were reduced to form an intermetallic compound with Pd [64]. Table 5 shows the mass balance of the elements. The reduction product contained about 18 wt% of the salt. All the Sr dissolved in the salt as expected. Most of the REEs remained in the reduction product, mainly as an oxide and partly as an alloy with Pd. In addition, some quantity of REEs was detected in the salt. The solubility of REE sesquioxide, which dissolves in the form of complex oxide species such as CeO^{2-} , increases with increasing Li_2O concentration in LiCl melt [65, 66]. U, Zr, Pd and Mo remain in the reduction product.

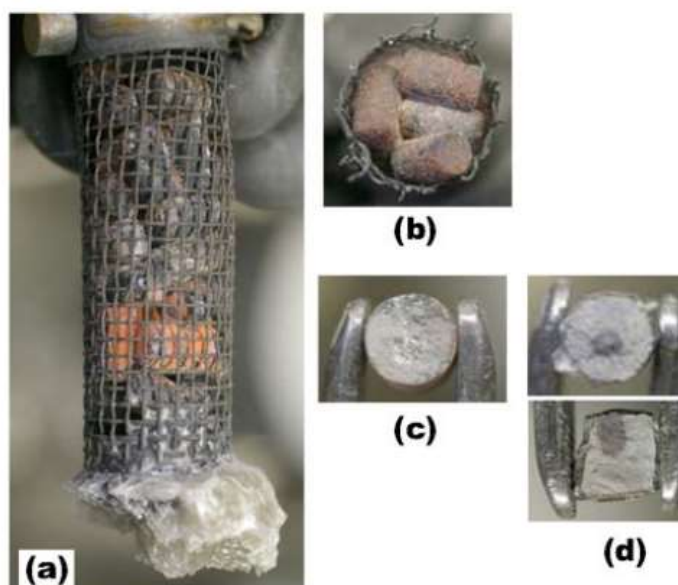


FIG. 26. Cathode product after electrolytic reduction test [59]. (a) External appearance of cathode basket; (b) Inside of cathode basket; (c) Cross section of reduced oxide pellet; (d) Cross section of partially reduced oxide pellet.

TABLE 5. MASS BALANCE IN THE ELECTROLYTIC REDUCTION.

	Porous oxide pellet ^a	Reduction product ^b	Bulk salt
Amount (adhering salt) / g	100.8	103.9	880
Elements contained / g			
U	82.600	79.600	0.060
Sr	0.890	0.020	0.870
Ce	0.890	0.850	0.130
Nd	0.890	0.860	0.007
Sm	0.890	0.740	0.060
Zr	0.890	0.800	0.004
Pd	0.890	0.910	0.000
Mo	0.890	0.700	0.000
O	12.000	0.530 ^c	(Li ₂ O:1.22 wt%)

- a. Calculated assuming that the porous oxide pellet consisted of UO₂-SrO-Ce₂O₃-Nd₂O₃-Sm₂O₃-ZrO₂ and Pd-Mo.
b. Containing elements in the adhering salt.
c. Calculated assuming that the remaining REE oxides (Ce₂O₃, Nd₂O₃ and Sm₂O₃) and the Li₂O dissolved in the adhering salt contained 0.41 and 0.12 g of oxygen, respectively.

3.3.6. Reductive extraction and verification of actinides recovery from HLLW

Reductive extraction in a LiCl-KCl/Cd or Bi system by use of lithium reductant is a potential means to separate actinides from other fission product species. The principle of the separation is shown in Fig. 27. Thermodynamic properties such as standard potentials and free energies of formation of chlorides in molten salt and activity coefficients in liquid metals, impart important knowledge for separation of actinides from other elements [67–69]. The difference of free energy of formation of chlorides, from which the separation factor between actinides and REEs is introduced, makes it possible to separate actinides. The difference of activity coefficients between actinides and REEs is more amplified in molten Bi compared to molten Cd, to which a large separation factor from REEs is attributed [67, 70, 71].

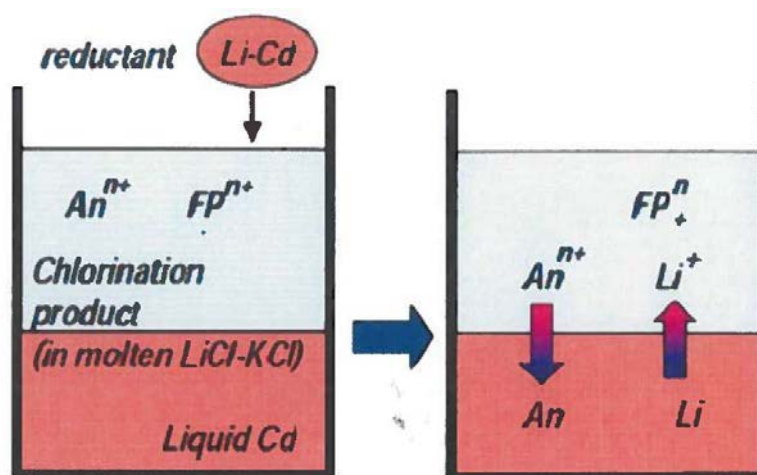


FIG. 27. Principle of reductive extraction (reproduced courtesy of CRIEPI).

For evaluating the separation behaviours of actinide elements from REEs by using the difference of distributions in molten salt/liquid metal systems, a separation factor (SF) should be defined as in Ref. [72]:

$$SF_{A/B} = \frac{(\text{mole fraction of A in salt})}{(\text{mole fraction of A in Cd})} \times \frac{(\text{mole fraction of B in Cd})}{(\text{mole fraction of B in salt})} \quad (7)$$

where $SF_{A/B}$ denotes the separation factor of element A versus element B. Among actinide elements and most of the REEs, the SF value at a certain temperature is theoretically constant, as long as their activity coefficients are assumed to be constant as these elements behave as trivalent in the salt [72]. The SF values of neptunium and REEs versus uranium in molten salt/liquid cadmium system are shown in Table 6 [70].

TABLE 6. SEPARATION FACTOR VALUES OF NEPTUNIUM AND REEs WITH RESPECT TO URANIUM IN LiCl-KCl AND LiCl-KCl/Bi SYSTEM AT 773 K (extracted from [70]).

<i>Element</i>	<i>Separation factor in LiCl-KCl/Cd</i>	<i>Separation factor in LiCl-KCl/Bi</i>
U	1	1
Np	1.9	11
Pr	42	922
Nd	45	933
Ce	49	834
La	131	2530
Gd	179	10400
Y	5320	5840

In consideration of thermodynamic properties, the reductive extraction is applied to separate actinides from spent salt accumulated FPs with trace amount of actinides produced at the electrorefining process, and from HLLW coming from current aqueous reprocessing [73]. Figure 28 shows an experimental actinide separation from a simulated HLLW salt by multistage reductive extraction together with electrorefining.

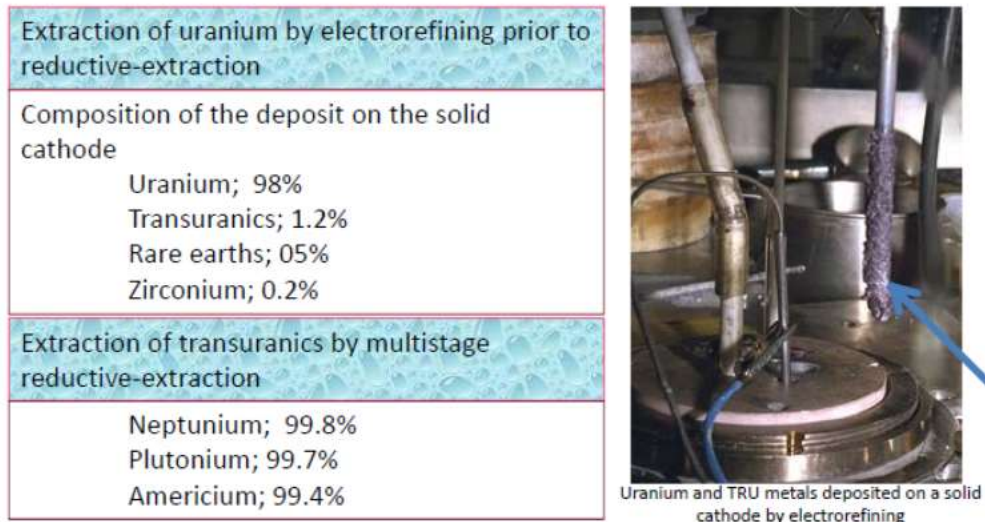


FIG. 28. TRU separations by reductive extraction by use of simulated waste composition [44].

Uranium, which represents a large proportion of the HLLW actinides, was electrochemically deposited on the solid cathode at the first stage, with the deposition including a small quantity of TRU elements. The following reductive extraction succeeded in recovering more than 99.5% of neptunium and plutonium, and 99.4% of americium into the liquid cadmium or bismuth cathode, resulting in an effective separation from the FPs, for which the concentration in the salt of the latter is 10 times greater than that of the TRU elements [66].

The experimental equipment together with uranium deposited on the cathode by electrorefining is shown in Fig. 28.

After the achievement of high decontamination in a simulated system, the reductive extraction through oxide conversion and chloride conversion of HLLW was applied to confirm the decontamination factor and distribution coefficients of actinides by using active material. Small scale experimental equipment was installed in a hot cell, and 520 g of HLLW, including Np, Am and Cm as MAs together with U and Pu, was prepared by reprocessing commercial MOX SNF [74–76]. The experimental equipment is shown in Fig. 29.



FIG. 29. TRUs recovery from HLLW prepared by SNF dissolution [44].

Mostly complete recovery of each actinide into liquid cadmium was achieved. In addition to the knowledge of thermodynamic properties of actinides and lanthanides, this experimental result verifies the technical feasibility of separation of TRU elements from HLLW by pyroprocessing. A three stage counter current reductive-extractor for engineering model development was developed for this process, for which the technological feasibility has to be explored from the perspective of operability and material flow using simulated material, in addition to determining the separation factor. Figure 30 provides a summary of this equipment.



FIG. 30. (a) Four staged counter-current extractor with $KCl-LiCl/Cd$ system for separation of actinides from lanthanides [77]; (b) The equipment of the left hand side was covered with heat-shielding in a glove-box (reproduced courtesy of CRIEPI).

3.4. PYROPROCESSING PROGRESS IN REPUBLIC OF KOREA

3.4.1. Official plan and R&D

Since the first nuclear power plant commenced operation in 1978, nuclear power has played an important role in the Korean energy supply. Republic of Korea imports most of its energy from abroad, highlighting the importance of nuclear energy generation. Currently, SNF arisings are stored at the reactor sites, but these storage facilities cannot be extended indefinitely so investigations are underway into recycling technologies. In comparison to the aqueous processes, pyroprocessing technology presents many advantages, one of which is that the pyroprocessing is able to handle relatively fresh SNF with high radioactivity and heat. This means pyroprocessing does not necessarily need a large capacity pool for storage at the plant for sufficient cooling of the SNF and it can reduce the capacity required for longer term storage of SNF. Pyroprocessing is also more favourable from a proliferation resistance perspective than aqueous processes. Based on these benefits over aqueous processes, the government of the Republic of Korea developed a long term R&D programme for pyroprocessing technology development as a potential route for SNF treatment, which connects with the SFR R&D programme. The basic research has been done for decades. Based on this R&D experience, the 10 tHM/year PRIDE facility has been constructed at KAERI to serve as a testing ground for various experiments.

3.4.2. Overview

The pyroprocess consists of two processes; a head-end process to convert the SNF assembly into a suitable feeding material for the subsequent process, and a main pyroprocess to recover uranium and TRU from SNF material. The head-end process consists of four unit processes, involving a disassembling process as the first step for the removal of the upper end fitting from SNF assembly, a cutting process of the extracted SNF rod, a decladding process for separation of SNF materials, and as a final step, a voloxidation process to fabricate the raw material required for pyroprocessing [78]. A waste treatment step in the head-end process would be considered, especially for the recovery of volatile and semi-volatile fission products. The conventional head-end processes of dismantling and chopping technologies have been developed for aqueous processing. Recently, advanced head-end processes have been developed in many countries for future nuclear fuel cycles. The objectives of an advanced head-end process are effective fuel material recovery and an increased removal of fission products that would affect downstream processes. KAERI has been developing advanced head-end process technologies based on dry processing in collaboration with INL (USA) under the International Nuclear Energy Research Initiative, 'I-NERI', programme.

3.4.3. Disassembling, rod extraction and cutting technologies

The head end process consists firstly of a mechanical process, where the spent PWR fuel assembly is dismantled⁹, the fuel rods are extracted, and are cut into shorter lengths in preparation for decladding; the dismantling equipment is dependent on the fuel assembly type (14×14, 16×16, 17×17). KAERI conducted a rod consolidation study in the 1990s, using a dummy spent PWR fuel assembly for dismantling, extracting, and cutting tests. Dismantling, extraction, and cutting operations of actual spent PWR fuel assemblies have been performed at a laboratory scale for post irradiation examination (PIE) and DUPIC (Direct Use of PWR SNF in CANDU) experiments in the PIE facility. The mechanical head-end process has been demonstrated using dummy fuel assemblies to provide the technical basis of a future pilot scale fuel recycle and rod consolidation process. The process consists of an assembly down-ender, a rod extractor, a rod cutter, a fuel decladding device, a skeleton compactor, and a gantry-mounted telescopic manipulator. Figure 31 shows the process flow for the mechanical head-end. All of the machines were designed and verified using a graphic simulator. Their performance was tested and verified by use of a dummy fuel assembly at the test facility. The rod extractor consists of a clamping table, an extraction table, an extraction rotary head, a cradle, and a side transfer. The machine unfastens the securing nuts of the bottom nozzle so that the remote manipulator can remove the bottom nozzle from the fuel assembly. The machine automatically extracts one rod at a time from a dummy 17×17 PWR fuel assembly and transfers each rod to the adjacent rod cutter. After removing all the fuel rods, the skeleton compactor is used to compact the non-fuel bearing components of the fuel assembly in preparation for disposal.

⁹ Each spent PWR fuel assembly consists of an upper structure, lower structure, spacer grids, fuel rods and guide thimble tubes.

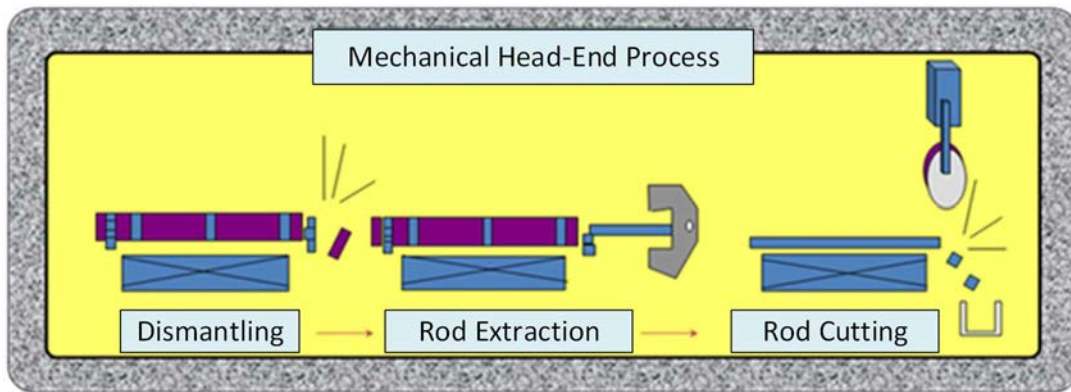


FIG. 31. Mechanical head-end process for the SNF PWR [79].

3.4.4. Decladding technology

The decladding step, where fuel material is separated from the cladding tube, of an advanced head-end process is essential in determining the efficiency of the whole recycling process. Issues that have become apparent while developing decladding technology are effective fuel material recovery and increased fission products removal, both of which can affect downstream processes. Several decladding technologies have been developed. Voloxidation treatment is a common head-end technology for SNF reprocessing. Conventional oxidative decladding technology provides an effective removal of fission gases (especially tritium), and has a good recovery efficiency from SNF with a burnup of less than 35 GWd/tHM at 500°C. KAERI has developed a mechanical decladding technology for separating fuel material from a cladding tube as a fragment type as part of the DUPIC process. Considering the current trend to extend PWR fuel burnups, the effect of the SNF burnup on the fuel recovery in the oxidative decladding technology should be investigated. The oxidative decladding efficiency of high burnup SNF was experimentally evaluated based on the results of a hot cell performance test at KAERI. It was observed that higher burnup SNF (over 50 GWd/tHM) showed around 15% low decladding efficiency due to small fuel-to-clad gap and low oxidation rate. Improved decladding efficiency for higher burnup SNF requires a longer oxidation time; over 15 h at 700°C. Compared to higher burnup SNF, lower burnup SNF (below 40 GWd/tHM) showed around 100% decladding efficiency at 500°C for 10 h with fuel lengths of less than 30 mm. However, mechanical decladding technology was effective for the recovery of pieces of SNF material.

3.4.5. Advanced voloxidation technology

Conventionally, voloxidation means oxidation and pulverization of SNF material to remove tritium at ~500°C. Recently, the concept of high temperature voloxidation has shown improvements over the conventional voloxidation process. An advanced voloxidation process, involving oxidation of SNF at high temperature using either air or oxygen, provides three important advantages. First, it may be used to separate fuel material from the cladding tube. Second, the voloxidation can control particle size, which may improve the efficiencies of downstream processes. Third, volatile and semi-volatile FPs would be removed from the fuel material prior to downstream treatment operations. KAERI has been developing an advanced voloxidation process, termed 'PRESENT' (Particle size control, REmoval of fission product, SElective gaseous Nuclide Trapping), as a head-end process for pyroprocessing technology in collaboration with INL through the I-NERI programme. The PRESENT process is planned to include functions such as particle size control to for electro-reduction feed material, FP removal (Cs, Tc, I, ³H, Kr, Xe, etc.) for downstream processes, and trapping of selective gaseous

nuclides to minimize high level waste production. KAERI showed release rates of ^{85}Kr , ^{14}C , and Cs during the Oxidation and REDuction of OXide fuel, (OREOX), step in the DUPIC fuel fabrication process. From experimental data produced by INL and KAERI, and published data, release rates of the FPs from the PRESENT process are assumed to be 98% of Cs, and 100% of Kr, Xe, ^3H , ^{14}C and ^{129}I . These data may be updated as further experimental results are gathered. KAERI is also studying an electro-reduction process to develop a feeding material form suitable for the subsequent process using SIMulated SNF (SIMFUEL).

3.4.6. Off-gas treatment technology

An off-gas treatment system for trapping fission products released from the voloxidation process is important to prevent the release of nuclides. In the mid-1990s, KAERI started research on the trapping of Caesium released from the OREOX and sintering processes in DUPIC fuel fabrication. An off-gas treatment system for trapping volatile fission gases such as ^3H , I, and ^{14}C from the OREOX process, and Cs from the sintering process has been established at the DUPIC Fuel Development Facility (DFDF). This is shown in Fig. 32. It was demonstrated that Cs released from the sintering process was completely trapped by the fly ash filter.

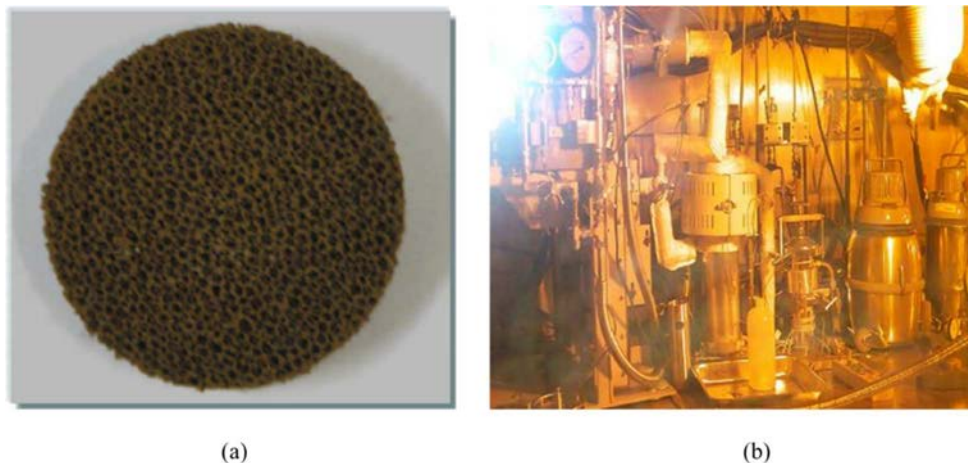


FIG. 32. Off-gas treatment system for DUPIC sintering furnace in DFDF (a) Fly-ash filter (reproduced courtesy of KAERI) (b) Off-gas trapping system ([78], reprinted with permission from Elsevier).

Based on the results of the DUPIC off-gas treatment, KAERI have been developing an off-gas trapping system for an advanced voloxidation process. Each unit process in the trapping system is arranged to effectively remove a target fission product by considering the chemical properties of the target fission products to be trapped:

- Cs is trapped on a fly ash filter at $\sim 1000^\circ\text{C}$;
- Tc is trapped on a calcium filter at $\sim 800^\circ\text{C}$;
- I is trapped on an Ag filter at $\sim 150^\circ\text{C}$;
- ^3H is trapped on a molecular sieve after conversion to high temperature oxidation by using CuO ;
- ^{85}Kr is cryogenically condensed and then trapped on solid adsorbent.

3.4.7. Solid waste treatment technology

Solid wastes generated from the head-end process consist of:

- Skeleton waste generated from SNF assembly dismantling;
- Cladding hulls generated from the decladding process;
- Spent filters generated from the off-gas treatment process;
- Other scrap waste generated from the process of chopping, decladding, and oxidation of fuel rods.

KAERI commenced a study on waste treatment technologies in 2010 for the head-end waste materials. A range of treatment technologies have been investigated based on the selected technology for pyroprocessing.

3.4.8. Oxide reduction to metal electrorefining

The electrorefining process, which is undertaken in a molten LiCl-KCl salt with a metal feed material, cannot directly accept actinide oxides as feed materials as they do not dissolve into chloride salts. In addition, materials must be electrical conductors to be used in an electrorefiner. Thus, there have been many attempts to develop an oxide reduction process to enable the metal electrorefining of commercial LWR oxide SNF. Notable technologies for the oxide reduction of SNF are metallothermic reduction and electrochemical reduction. Both technologies use molten salts as a reaction medium. A laboratory scale metallothermic reduction process, the so-called ‘Li reduction process’, that uses Li metal as a reductant for the metallization of LWR SNF has been actively studied. However, the electrochemical reduction process has drawn more attention due to its merits including simplicity, safety, and easy operability compared to the metallothermic reduction process [61, 73, 80]. After the electrolytic reduction process, the residual salt material is ~20 wt% of the cathode material. The cathode process for the removal of residual salts in the cathode basket of the electrolytic reducer can be added to ease the burden of the salt management process. The resulting metal is suitable for the direct introduction into the electrorefiner [81].

Since 2002, KAERI has adopted an electrochemical reduction technology for the oxide reduction process recent efforts have focused on the development of a laboratory scale electrochemical reduction system, the improvement and optimization of an electrolytic reduction system, the production of kinetic and physicochemical data, and the design of engineering scale electrochemical reduction system. The overall analysis on the oxide reduction of SNF has been carried out to assess the process feasibility before an engineering scale demonstration of the KAERI oxide reduction process, which consists of an electrolytic reducer for electrolytic reduction and a cathode processor for the recovery of metal (Fig. 33) [81].

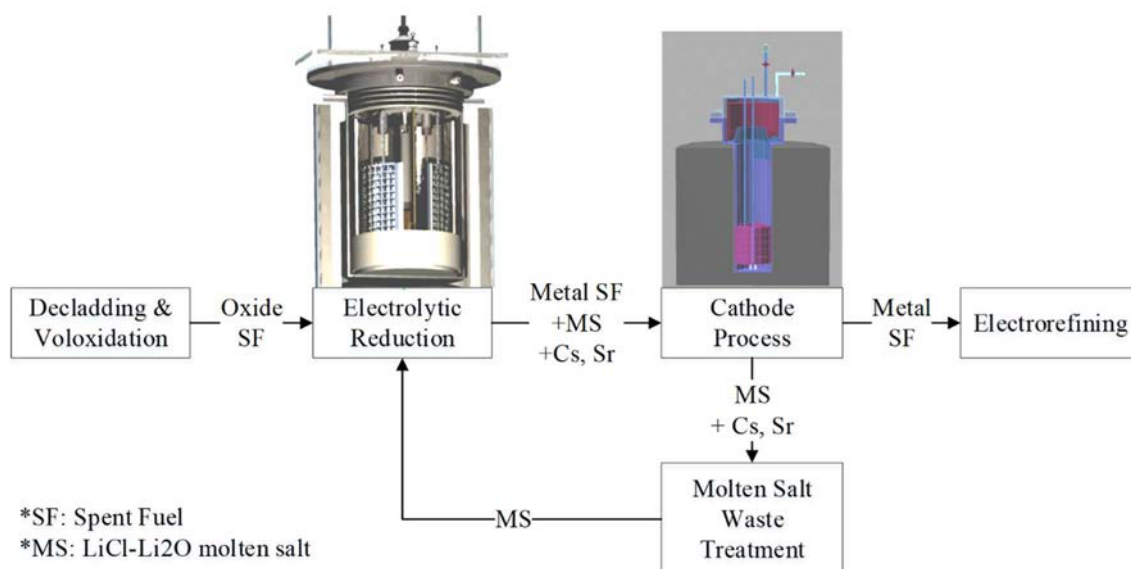


FIG. 33. Schematic description of the KAERI oxide reduction system.

3.4.8.1. Oxide reduction by metallic reductant

The application of metallic reductants that enable the reduction of spent oxide fuels at relatively lower temperatures was investigated. Mg was excluded due to handling difficulties concomitant with Mg vaporization. Although the reductive power of Ca in CaCl₂ is stronger than that of Li in LiCl, the lower melting point of LiCl (610°C, and 772°C for CaCl₂) results in less challenging operational conditions (650°C, and 850°C for CaCl₂). Additionally, it was found that during UO₂ reduction in a molten CaCl₂ bath, a dense metal skin covering the surface of the UO₂ sample due to the high operating temperature prevented the complete reduction of UO₂ [34]. A comparison of candidate processes indicated that reduction based on the reducing powder of Li metal was the most promising process for uranium oxides reduction and led KAERI to focus on this technique; KAERI's Li reduction process development programme was launched in 1997. Laboratory scale experiments characterized by using a magnesia filter were carried out until 2002. They were performed in a bath of molten LiCl at 650°C, which was saturated with Li. The process reduced oxides to metals by a chemical reaction with Li, generating Li₂O as a by-product. However, the Li reduction process needs an Li electrowinning process to recover Li from Li₂O, and there is difficulty in consolidating the metal products.

3.4.8.2. Development of electrolytic reduction process

Inspired by the recent development of electrochemical reduction technology for the metallization of oxides to valuable metals, there have been several attempts to realize the electrochemical reduction technology for the reduction of SNF. The electrochemical reduction process for SNFs operates in a bath of molten LiCl at 650°C with small quantities of dissolved Li₂O, or in CaCl₂ at about 850°C with small quantities of dissolved CaO [78]. In this electrochemical reduction process, the oxide SNF is made as a cathode. The reaction mechanism is known to proceed via direct removal of oxygen ion from the oxide cathode or chemical reaction with in-situ generated Li from Li₂O, or Ca from CaO. In the electrolytic reducer, the feed material is placed in the fuel basket. A voltage is applied between the fuel basket cathode and the anode. With the progress of electrolytic reduction reaction, the oxide ion from the oxide SNF contained in the cathode basket is evolved as a gas on the anode, leaving

the metal SNF in the cathode basket [82]. The metal SNF can then be used as the feed material for the electrorefining process. During the electrolytic reduction process, high heat load fission products, such as Cs and Sr, are dissolved into the molten salt resulting in the decrease of heat, volume, and radioactivity of the SNF. Lanthanides and metallic fission products of spent nuclear fuels are present in the cathode. The demonstration system was designed and installed in the Advanced SNF Conditioning Process Facility (ACPF) hot cell, and KAERI performed seven inactive tests with fresh U_3O_8 and SIMFUEL.

3.4.8.3. Development of cathode processing technology

After the electrolytic reduction process, the residual salt material is ~20 wt% of the cathode material. The cathode process for the removal of residual salts in the cathode basket of the electrolytic reducer can be added to ease the burden of the salt management process. The reoxidation of uranium of the metal products can occur above 945°C [83], therefore, the operation temperature of the cathode process was set lower than this. The narrow liquid region in the conditions of low pressure and temperature near the LiCl melting point enables the gas-solid separation. In the processing of cathode material from the electrolytic reduction process, the material was placed in a process crucible and was heated. After that, the salt material was boiled off and distilled for recycling. KAERI's cathode process of electrolytic reduction is characterized by the recovery of salt in powder form, which is easy to handle in a remote operation condition. The principle is the condensing of LiCl vapour as a solid in the cold region of the cathode processor. The recovered salt is sent to the waste salt regeneration process, and then recycled back to the electrolytic reduction process [78, 81, 82].

3.4.9. Metal electrorefining

3.4.9.1. High-throughput electrorefining system

The KAERI electrorefining system, which is composed of an electrorefiner, a salt distiller, and a melting furnace, recovers pure uranium from electrolytically reduced SNF. A U-chlorinator (UCl_3 making equipment) and a transportation system are also needed to operate the electrorefining system. In the electrorefiner, a uranium deposit is initiated in molten LiCl-KCl salt containing less than 10 wt% UCl_3 . Uranium dendrites are finally collected at the bottom of the reactor and transferred by a bucket-type container to a receiver. The uranium deposits are fed into a salt distiller, and the salt in the uranium deposits is distilled. The salt distilled uranium is melted and subsequently reformed to ingots for storage or for future use. The KAERI electrorefining system was designed to semi-continuously operate, and its schematic process diagram is shown in Fig. 34.

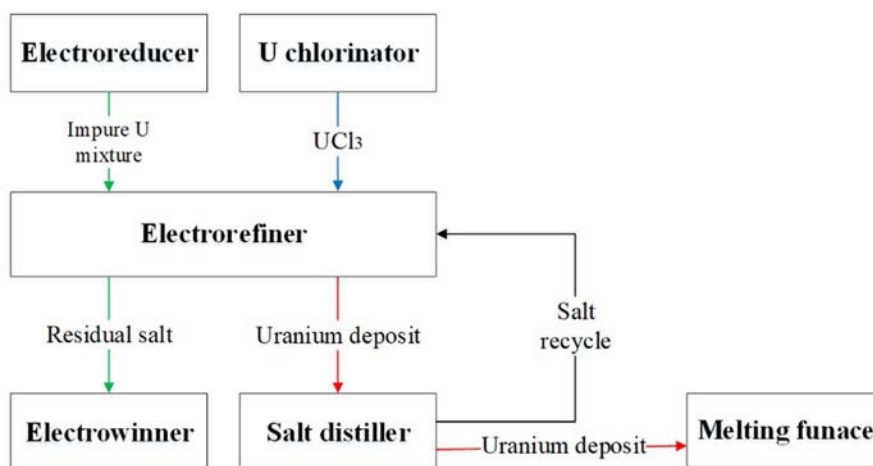


FIG. 34. Schematic description of the KAERI electrorefining system.

3.4.9.2. Electrorefiner

The role of an electrorefiner is to recover uranium from impure uranium mixture. The currently installed high throughput electrorefiner is designed to have a capacity of 20 kgU/batch [84] and is shown in Fig. 35 [85].



FIG. 35. High throughput electrorefiner equipped with graphite cathode [85].

The reduced uranium metal from the electrolytic reduction system is fed into an anode basket, which is placed at the periphery of the reactor; it rotates in order to enhance mass transfer. The cathodes, at which the uranium dendrites are deposited, are located in the core part of the reactor. At the centre of the reactor there is a scraper used to collect the uranium deposits that fall to the bottom. The LiCl-KCl eutectic solution containing UCl_3 initiates deposition of uranium onto the solid cathode. The deposited uranium at the cathodes falls spontaneously from the solid cathode at an operation condition of $500^\circ C$. It is continuously conveyed by a bucket-type container and as described above, transferred to a receiver. The remaining materials after depletion of the uranium from the feed material at the anode basket are noble metals, Fe and

Mo [81]. The salt evaporation behaviours of uranium deposits from an electrorefiner are described in Ref. [86].

3.4.9.3. Salt distiller

Uranium deposits, generated from the electrorefiner, contain about 30 wt% salt. In order to recover a pure U metal ingot, the retained salt should be removed from the uranium deposits. Salt removal from the uranium deposits should be achieved prior to the following step of uranium metal casting. A vacuum evaporation technique was applied to the removal system and the behaviour of salt evaporation from uranium deposits has been studied using a bench-scale salt distiller. The characteristics of salt evaporation depend largely on the vapor pressures of the components and the temperature [86]. The vacuum pressure and the hold temperature are the key factors of the evaporation process. A laboratory scale salt distiller with a capacity of 29 kg uranium deposit per batch has been developed [81].

3.4.9.4. Uranium melting furnace

The melting process is performed to consolidate the refined uranium deposits into a solid cylindrical metallic form to be used as raw material for SFR fuel or stored for future use. The main equipment used for the ingot casting process is a melting furnace, which consists of a vacuum chamber, a charger, a crucible, and a mould. The distilled uranium dendrite is fed to the charger where it enters the crucible, which is made of zirconia coated graphite. The vacuum chamber is first evacuated and then, using an induction coil heater, the temperature of the crucible is increased to 1300°C. The uranium dendrite is melted and then the melted uranium is poured into the mould by tilting the crucible.

3.4.9.5. Uranium chlorinator and pelletizer

The role of uranium chloride salt (UCl_3) is to stabilize the initial cell voltage between electrodes in the electrorefining reactor. The preparation process for a uranium chloride salt includes two steps: reaction of gaseous chlorine with liquid cadmium to form CdCl_2 in a Cd layer, followed by the reaction of U with CdCl_2 in LiCl-KCl eutectic salt to produce UCl_3 . The apparatus for the reaction consists of a chlorine gas generator, a chlorinator, and a wet scrubber for off-gas treatment. The prepared UCl_3 salt in LiCl-KCl eutectic salt is transferred to the electrorefiner. For the transfer of LiCl-KCl molten salt, which contains UCl_3 , to the electrorefiner, a pelletizing process has been developed. This process consists of two steps: transportation of the molten salt to a pelletizer and solidification of the molten salt in a mould. Because chlorine gas is used during the manufacture of UCl_3 , which is melted in LiCl-KCl eutectic salt, and the molten salt is strongly sensitive to moisture, the transportation of the molten salt and the pelletizer operation should be carried out under an inert gas such as Ar. The molten salt transportation is driven by pressurization of the reactor vessel while maintaining temperature above the melting point [81].

3.4.10. Salt decontamination for recycling

3.4.10.1. Salt waste from pyroprocessing

Two different types of salt waste are expected to be generated from pyroprocessing of LWR spent oxide fuels. One is LiCl salt waste containing alkali and alkaline-earth (Group I/II) FPs from the electrolytic reduction process, and the other is LiCl-KCl eutectic salt waste containing REE FPs from the electrorefining process. Since these salt wastes are both heat generating and radioactive, they must be conditioned to form durable final waste forms suitable for geological disposal. Therefore, the minimization of salt waste is one of the most important issues for the

optimization of pyroprocessing. The salt waste treatment processes carried out at KAERI are focused on two salt waste treatment technologies, the minimization of salt waste, and the fabrication of high integrity/volume reduction final waste forms. A high level flowsheet describing the salt waste treatment processes investigated by KAERI is shown in Fig. 36.

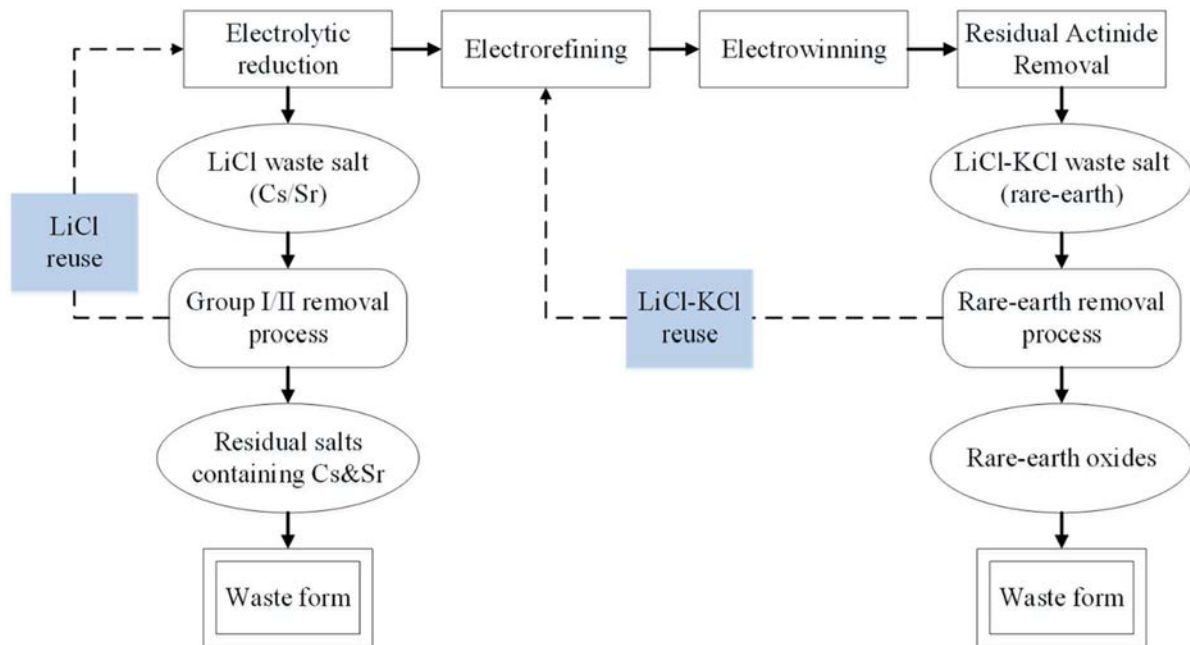


FIG. 36. Salt waste treatment process investigated by KAERI.

3.4.10.2. LiCl salt waste decontamination

To separate Group I and II fission products such as Cs and Sr, KAERI introduced a melt crystallization process, which uses the solubility difference of impurities between the crystal (solid) and the melt phase. In a melt crystallization process, the impurities prefer to remain in the melt phase and not the crystal phase. So, when LiCl salt waste containing Group I and II FPs is treated using a melt crystallization process, pure LiCl is obtained in a crystal form, while almost all Group I and II FPs are concentrated in the small amount of LiCl melt.

Since the LiCl melt contains a small amount of Group I and II FPs, it can be reused in the electrolytic reduction process. Among the many possible melt crystallization processes, based on the results of the screening-tests and an analysis on operability, the layer crystallization process was chosen as the separation method for laboratory scale Group I and II FPs separation to form LiCl salt waste [87].

Layer crystallization is a very simple process that uses cooled plates immersed in a melt for crystal formation, encouraging crystal growth as a compact crystalline layer on a cooling surface. In this process, impurities are concentrated in the melt phase and not in the crystal layer formed outer surface of crystallizer [88]. Figure 37 shows the laboratory scale layer crystallization apparatus of which the maximum batch size is 4 kg LiCl. As shown, it consists of four parts: crystallization furnace; melting furnace; crystallizer moving device; and cooling air injection system. All of the parts are located in a glove box maintained in Ar and a moisture-free atmosphere. The crystallizer, which has a cooling surface for the crystal layer growth, is a

rectangular type. In the crystallizer, a uniform temperature distribution is very important to attain even crystal growth.



FIG. 37. Laboratory scale layer crystallization apparatus [88].

3.4.10.3. Eutectic (LiCl-KCl) salt waste decontamination

In the case of rare earth FPs involved in LiCl-KCl eutectic salt waste, they are removed from eutectic salt by oxidative precipitation and the refined salt is recovered by a vacuum distillation process. REEs involved in LiCl-KCl eutectic salt wastes generated from an electrorefining process are converted to their molten salt-insoluble precipitates by reaction with oxygen in the oxidative precipitation step. After a full precipitation of these lanthanide precipitates, an eutectic salt waste is separated into two layers: upper pure (or purified) salt layer, and lower precipitate layer. The upper pure salt layer can be physically separated from the precipitate layer, where the separated pure salt layer can be reused (first pure salt recovery). Then, the adhering eutectic salt involved in the precipitate layer is separated and recovered in the distillation/condensation step (second pure salt recovery). Finally, all the remaining REE oxides or oxychlorides can be conditioned into a final waste form in the immobilization step (Fig. 38).

The residual salt can be separated and recovered as a pure salt from the lower part by a vacuum distillation process and can be recycled back to the electrorefining process. Based on the characteristics of the salt vaporization and condensation [89], the vacuum distillation system was designed, incorporating a vaporization and condensation chamber as a very simple unit. This system is subjected to the force of an inner temperature gradient of the chamber at a reduced pressure as a closed type of system. Namely, at a reduced pressure the residual salt is vaporized, with the salt vapour migrating to the condensation chamber according to the temperature gradient and is then condensed in a salt collector as a bulk phase. This makes it possible to efficiently collect the vaporized salts in the salt collector, thereby minimizing salt loss and apparatus corrosion.

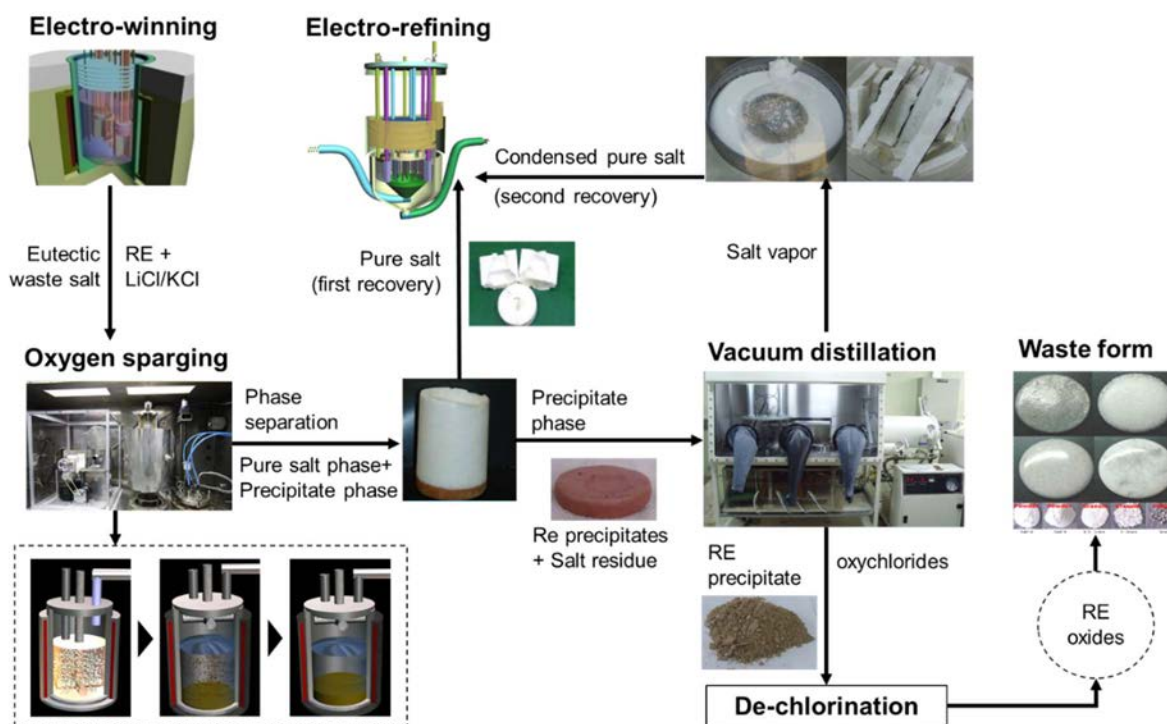


FIG. 38. Eutectic salt waste decontamination process.

3.4.11. Waste form processing

Two kinds of residual wastes can be expected to be generated by the salt waste decontamination processes; LiCl waste concentrated with Cs and Sr from LiCl decontamination, and REE precipitates from the LiCl-KCl decontamination process. It is difficult to directly apply a conventional solidification process such as vitrification or ceramization to the LiCl due to its high volatility and low compatibility with silicate glass. In order to treat salt waste for final disposal, KAERI have adopted a dechlorination approach for a non Cl containing matrix, where metal chloride is dechlorinated and thermally stabilized using a synthetic inorganic composite, $\text{SiO}_2\text{-Al}_2\text{O}_3\text{-P}_2\text{O}_5$ (SAP), and the resultant product sintered with a conventional borosilicate glass to obtain a monolithic waste form [90].

For REE wastes, a zinc titanate-based inorganic composite is applied to consolidate them using milder processing conditions, as the conventional immobilization methods such as vitrification or ceramization require more challenging processing conditions for higher waste loadings. The waste is mixed with zinc titanate-based inorganic composite, and then heat-treated to obtain a highly densified waste form.

Through use of these methods, the residual wastes produced by the two kinds of purification processes can be stabilized as a solid durable waste form for long term storage and/or disposal at a repository site.

The laboratory scale solidification equipment consists of a crushing/pulverizing stage, a mixing reaction, and a sintering step. A jaw crusher and roll mill are used for crushing and pulverizing of the salt ingot to a 100 μm powder, to minimize the dispersion of particulates. The mixing reaction is undertaken in a cone-typed vessel equipped with a two-way screwed impeller to effectively mix and react the salt, SAP, and glass. The sintering furnace has a SiC heater to elevate the temperature to 1200°C. Using this process, a highly monolithic waste form can be obtained. Based on these approaches for the two kinds of waste, an integrated

stabilization/solidification system equipped with a series of unit apparatus is under development. The qualification of the waste form is now being undertaken to determine if it meets the requirements for disposal, including evaluation of the physiochemical properties, thermal property, radiation stability, chemical durability of waste forms.

3.4.12. Metal waste processing

About 20 wt% of a LWR SNF assembly is zircaloy fuel cladding, which consists of 98 wt% Zr. Therefore, a Zr recovery process is significant opportunity for the reduction of metal waste and the overall final waste volume. In pyroprocessing, voloxidation is first used to separate the spent oxide fuel from its zircaloy cladding. If not for the fact that the zircaloy cladding is contaminated with actinides and FPs, it would qualify for disposal in low and intermediate level waste disposal sites in Republic of Korea; without decontamination, the hulls would be classified as high-level waste.

Therefore, it has been proposed that the hulls can be electrochemically decontaminated in a molten salt system. Such treatment has not been tested to date at KAERI, due to its inability to run experiments with SNF. However, there is research reported in the literature to support the concept of achieving electrochemical zircaloy decontamination in a molten salt system [91, 92]. An investigation was carried out for the zirconium recovery process using molten salt electrorefining for zircaloy cladding and channel boxes from BWR SNF. The overall concept of Zr recovery process [91] is represented in Fig. 39.

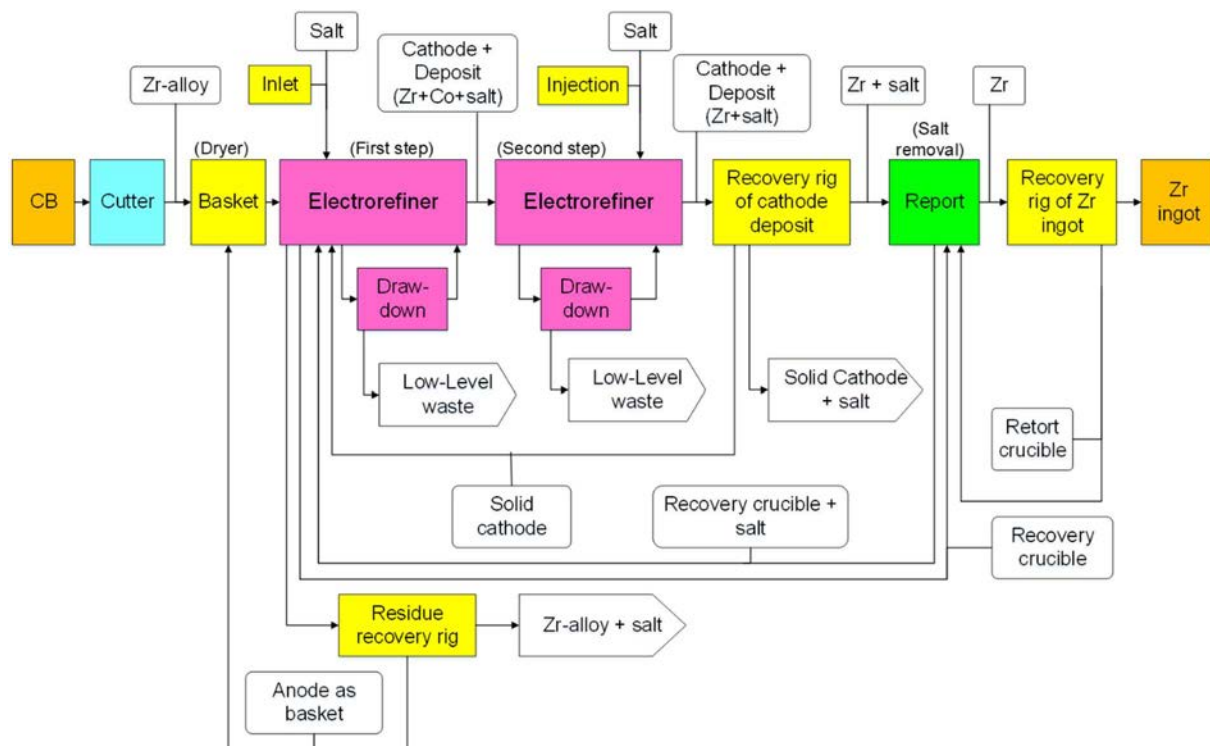


FIG. 39. Overall concept of Zr recovery process.

In this study, LiF was added to LiCl-KCl molten salt so as to prevent the disproportionate reaction $Zr^{4+} + Zr^{4+} \rightleftharpoons 2Zr$ at 923 K. When it occurs, this disproportionality interrupts the recovery of high purity zirconium. Through this approach, it was reported that Zr was deposited

on the cathode with high purity (99.9%), and the decontamination factor for Co in the deposited Zr was estimated to be 5×10^5 .

Oak Ridge National Laboratory (ORNL, USA) has developed a treatment process for SNF cladding using dry chlorination, which is a common way to produce Zr and zircaloy. It has the advantage that the zircaloy cladding surface is uniformly and effectively removed [93]. However, because of vulnerabilities related to proliferation-resistance, it is not available to countries such as Republic of Korea. In addition, a decontamination method for zircaloy cladding hulls from SNF using HF was studied by T. S. Rudisill [94], but the method is not suited to remove FPs and TRU because of their deep penetration into zircaloy cladding. Other methods such as ion-gun and dry ice spray have been developed but have some limitations such as removal speed and ineffectiveness at oxide layer removal.

3.5. DEVELOPMENTS OF SPENT NUCLEAR FUEL PYROPROCESSING TECHNOLOGY AT IDAHO NATIONAL LABORATORY

This summarizes research in SNF pyroprocessing that has been published by INL over the last decade. It includes work done both on treatment of Experimental Breeder Reactor-II and development of advanced technology for potential scale-up and commercialization. Collaborations with universities and other laboratories are included in the cited work.

3.5.1. Introduction

INL has been active in the development of pyroprocessing technology since the 1980s. This includes work done at Argonne National Laboratory – West (ANL–West) up until 2005, when it was merged with the Idaho National Engineering and Environmental Laboratory to form the INL. R&D in this area at INL has basically fallen under two missions — treatment of the SNF from EBR-II, and development of advanced technology to help close the nuclear fuel cycle and lead to commercialization.

3.5.2. Initial focus on EBR-II metal fuel treatment

The development of pyroprocessing began in the 1980s at ANL as an essential component of the IFR concept [95, 96]. EBR-II was used as the test reactor for the IFR programme, while the Fuel Cycle Facility (FCF) — now known as the Fuel Conditioning Facility — was equipped with pyroprocessing technology to perform the fuel recycle functions of the IFR. The IFR programme was terminated in 1994, but the fuel in the reactor core at the time was considered to be unsuitable for geologic disposal without some form of stabilization. Pyroprocessing technology, including the fuel fabrication steps, was deemed as the most attractive option to achieve this stabilization. HLW components of the SNF are partitioned into ceramic and metallic waste forms suitable for geologic disposal. Rather than collect Pu and other TRU elements for the fabrication of new FR fuel rods, the TRU elements could be partitioned into one or both of the waste forms. Between 1996–1999, INL (ANL-West at the time) demonstrated the feasibility of pyroprocessing the EBR-II SNF by processing 400 kgHM of driver fuel, 700 kgHM of blanket fuel, and producing a limited number of ceramic and metallic waste form samples [97]. That demonstration was judged as successful by the U.S. Department of Energy, and pyroprocessing or electrometallurgical treatment was designated as the preferred technology for treating the remaining inventory of spent EBR-II fuel [98].

In the 12 years since the completion of the EBR-II SNF treatment demonstration project, INL has continued to process SNF from EBR-II in addition to the FFTF. Table 7 shows the initial inventory of SNF and what has been processed as of 2012. In this respect, processing includes fuel chopping, electrorefining, and cathode processing. There are two electrorefiners (ER) that have been used for processing the fuel; the Mark-IV ER, and Mark-V ER. Each ER contains in excess of 500 kg of molten chloride salt containing actinides and active metal fission products (Group I, Group II, and lanthanides). Very little of this salt has yet been immobilized into ceramic waste forms, which is required for disposal. The original plan was to quickly transition from a demonstration project into production operations that would require 12 to 13 years to process the fuel. But the lack of sufficient funding to support production operations has substantially lengthened the time frame of the project. Of the original inventory, 74% of the EBR-II driver fuel and 86% of the EBR-II blanket fuel remained to be processed as of January 2012, even though the original timeframe for complete treatment had elapsed. Essentially all of the FFTF driver fuel had been treated, with a small amount set aside for fuel-related experiments. Processing of EBR-II blanket fuel was suspended with the processing focus on completing treatment of the driver fuel. It may be re-evaluated in the future whether to electrorefine the remaining blanket fuel inventory, or to separate the sodium bond and dispose of that fuel without further treatment.

TABLE 7. INVENTORY OF SNF DESIGNATED FOR PYROPROCESSING AT IDAHO NATIONAL LABORATORY (reproduced courtesy of Idaho National Laboratory).

Fuel type	EBR-II driver (tHM)	FFTF driver (tHM)	EBR-II blanket (tHM)	Total (tHM)
Initial fuel in June 1996	3.1	0.25	22.4	25.75
Fuel treated as of January 2012	0.8	0.22	3.6	4.25
Remaining untreated fuel	2.3	0.03	18.8	21.5

The slower pace of production operations has allowed R&D on the SNF treatment process to continue. Most of the unit operations that comprise the SNF treatment process have received some attention in this regard. Highlights are given in the following subsections.

3.5.2.1. Electrorefining

The electrorefiner is essentially the key unit operation in pyroprocessing. It is where the uranium is electrolytically separated from cladding hulls, bond sodium, and noble metals in the SNF. There are two engineering scale ER systems at INL that are being used concurrently for treatment of spent EBR-II fuel, referred to as the Mark-IV and Mark-V ER. Figure 40 shows drawings of these systems, which occupy a similar footprint in the FCF but have markedly different electrode designs.

Numerous aspects of the Mark-IV ER have been studied and published during the treatment campaign to date, in which approximately 830 kgHM of driver fuel has been electrorefined. Technical issues of interest have included current efficiency, U recovery efficiency, zirconium recovery, and understanding the interactions of the cadmium pool with the rest of the system [99–101].

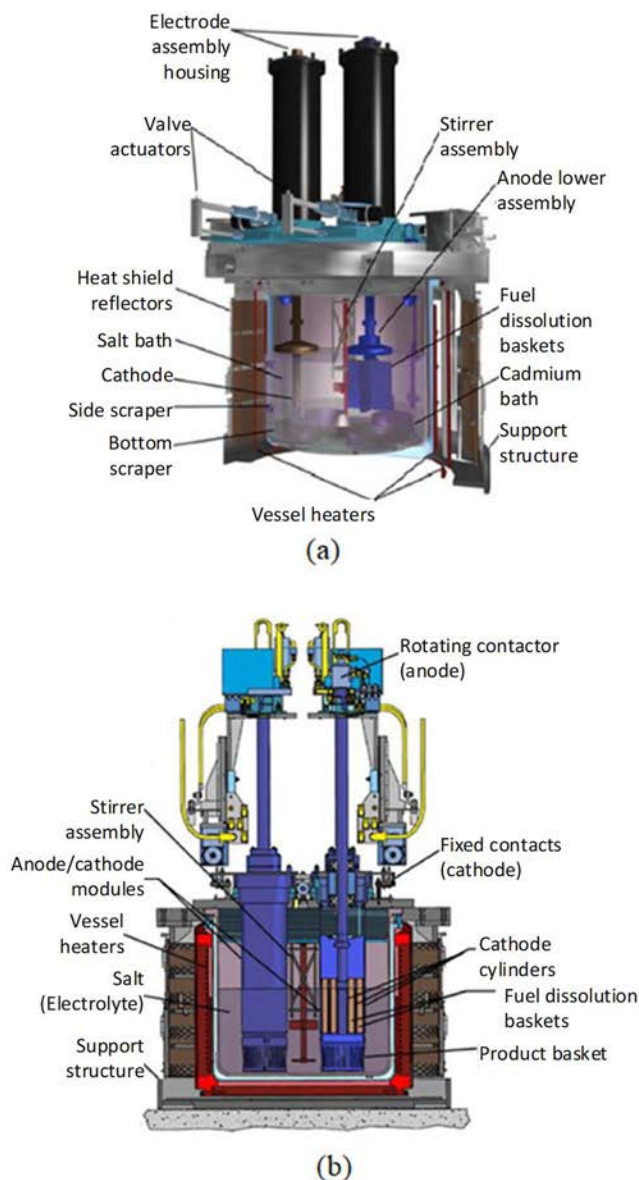


FIG. 40. Mark-IV (a) and Mark-V (b) electrorefiners from the INL fuel conditioning facility [102] (reproduced courtesy of Idaho National Laboratory).

Key goals of the electrorefining process are to dissolve as much of the uranium from the SNF as possible, while retaining zirconium and other noble metal FPs that by design should partition into the metal waste form. Li and Simpson studied the anodic dissolution process and analysed the impact on uranium dissolution and noble metal retention [100]. It was concluded that diffusion of the reactants in the porous fuel matrix was the rate-controlling step for the dissolution process, and it was found to be an inverse relationship between uranium dissolution and noble metal retention. Increasing the uranium dissolution to greater than ~98% resulted in

a significant loss of noble metals. This indicates that there is an optimal level of dissolution that can be controlled by the maximum anode potential. It was discovered that zirconium dissolution could be completely eradicated by using an interrupting current technique [99]. Under the AFCI programme, however, a stated goal was to achieve very high recycle efficiency for the actinides. Thus, a series of Mark-IV ER runs were performed with high anode potentials in order to achieve near complete oxidation of the uranium. It was reported by Li that an average of 99.7% uranium dissolution could be achieved over several runs, but that came at the cost of very high (87.8%) loss of the zirconium and moderate (23–27%) loss of the noble metal FPs [100]. In both cases, the losses are suspected to be from fine particles falling out of the basket and into the cadmium pool. The zirconium has been shown to accumulate in the cadmium pool but can be recovered to a solid cathode via co-deposition of uranium/zirconium. In this process, the cadmium pool is anodically polarized. The resulting U/Zr deposit on a steel cathode has up to 22 wt% Zr [100].

During early operations of the Mark-IV ER, the current efficiency was approximately 50%. The inefficiencies are largely due to U dendrites falling off the cathode into the cadmium pool and then having to be re-electrorefined via a deposition cycle. A deposition cycle involves anodically polarizing the cadmium pool to promote electrotransport from the cadmium pool to the cathode. It was found that improving the agitation of the salt via rotating the anode baskets resulted in significant improvements in the efficiency from 65% to 76% [100].

The cadmium pool is a unique feature of the Mark-IV ER. There is no such pool in the Mark-V ER. The motivation for including it in the system was largely to be used as a way of capturing uranium dendrites that fall off the solid steel cathode mandrel. It was reported by Li, however, that the uranium also enters the cadmium pool electrochemically [101]. It essentially acts as an intermediate electrode between the anode and cathode. U transports from the anode baskets to the nearby surface of the cadmium pool. Simultaneously, uranium transports from the cadmium pool to the nearby steel cathode. The concentration of uranium at any given time in the pool can be measured via the electric potential difference between the reference electrodes and the vessel which is in contact with the cadmium. The relation between potential and concentration was derived based on fundamental electrochemical principles and verified via comparison with experimental data. The pool is not without its drawbacks, however. The high vapour pressure of cadmium results in it condensing on various locations within the electrorefiner, which leads to electrical shorting in the ER vessel [101]. A cadmium vapour trap was installed to mitigate this problem.

To enhance the understanding of fundamental chemical and physical processes that occur in the Mark-IV ER, a project was initiated in 2007 to develop a kinetic model of the ER [103–106]. This project was in collaboration with the University of Idaho (UI), the Seoul National University (SNU), and KAERI. It was officially a part of the United States – Republic of Korea I-NERI programme. A team from UI developed a two-dimensional (2D) representation of the Mark-IV ER, while a team from SNU developed a three-dimensional (3D) representation. Amongst other objectives, it was a comparative study of the importance of complexity versus computational economy for electrorefiner modelling. The model was able to track relative dissolution of uranium and zirconium throughout the process and agreed with experimental results in showing that to minimize the dissolution of zirconium the uranium dissolution must be limited [107]. A 2D mapping of the electric potentials in the Mark-IV ER revealed interesting insight into how to optimize the ER system design. It was shown that regions far from the operating electrodes have small potential gradients and little ion movement. Thus, it is advantageous to utilize all of the space inside of the ER with cathodes and anodes.

Another insight gained from model development was that uranium concentration in the salt has a substantial effect on the electrorefining process. Increasing the uranium concentration in the salt actually reduces the rate of uranium dissolution in the fuel and increases the rate of zirconium dissolution. The model revealed the importance of the exchange current density physical property for accurately predicting electrorefining kinetics.

Unfortunately, attempts to directly measure this parameter have yielded numbers inconsistent with fits of the electrorefiner model to process data.

3.5.2.2. Cathode processing

Uranium product from the electrorefiner is in dendritic form and is coated with chloride salt (typically 20 wt% of the product) from the ER electrolyte. After it has been harvested from the cathode mandrel (Mark-IV ER) or product collector (Mark-V ER), it is loaded into a crucible and inserted into the cathode processor (CP). In the CP, the temperature is raised to 1200°C under a vacuum ranging from atmospheric to 27 Pa. A drawing of the CP is shown in Fig. 41 [107].

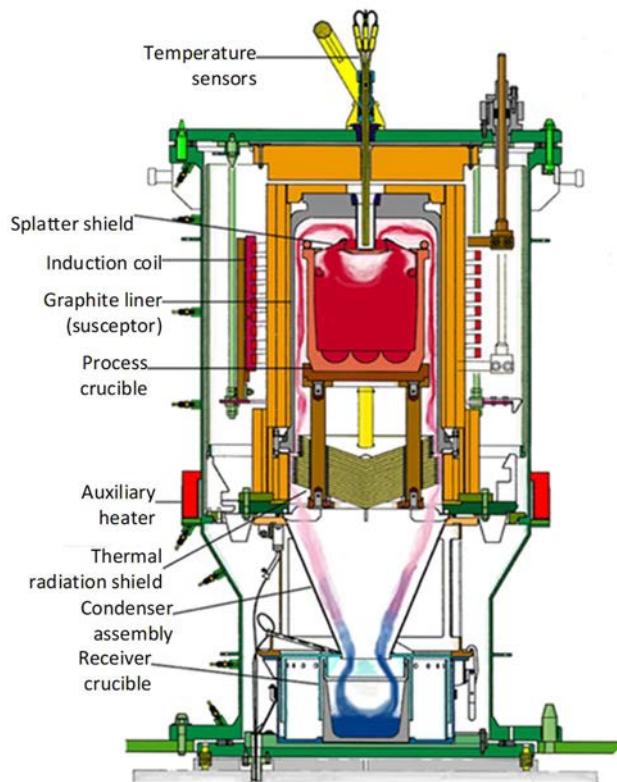


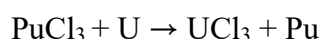
FIG. 41. Cathode processor located in the INL fuel conditioning facility (reproduced courtesy of Idaho National Laboratory).

Research related to the CP has been primarily focused on determining distillation efficiencies, minimizing uranium product contamination, and investigating different crucible options.

Distillation efficiency for active metal chlorides by design should be as close to 100% as possible. That is because these salts should be recycled to the electrorefiner or sent to the

ceramic waste process. Over numerous runs during treatment of EBR-II driver fuel, it was found that the distillation efficiency for these active metals ranged from ~98.6–99.96% [97]. Interestingly, there was a linear correlation observed between mole fraction of any salt compound in the molten mixture and that compound's distillation efficiency.

As for the issue of product purity, the main objective is to ensure that the uranium product from blanket electrorefining is suitably pure so that it can be disposed of as a low-level waste. Plutonium contamination, in particular, is an obstacle to such a waste management plan and has been observed routinely in the blanket uranium product. Experiments were performed that revealed the CP operation as the source of this plutonium contamination [107]. In other words, the plutonium is not initially in the metal deposit phase on the cathode; it goes into that phase during actual CP operations. As the salt is distilled, the following reaction becomes thermodynamically more favourable:



It was shown that plutonium levels in the uranium product can be reduced by as much as 90% by adding cupric chloride to the salt, effectively generating UCl_3 and shifting the chemical equilibrium in the above equation to the left [107].

An investigation of different CP crucible materials was carried out. Initial operations utilized a graphite mould coated by a zirconia wash [107]. These crucibles are problematic with respect to the time required to clean and re-coat them. Also, the coating reacts with the salt/metal charge to form oxide dross. Two alternative crucible materials have been investigated — castable zirconia and hafnium nitride coated niobium [107, 108]. The castable crucible also has the dross problem but significantly reduces the preparation time needed for each crucible and, thus, improves process throughput rate. The coated niobium crucible results in no dross formation and requires no preparation in between runs. However, it will chemically react with any zirconium in the cathode product and it was found that the coating process developed more imperfections as the crucible size was increased to production scale (15 litres). The coated niobium crucible is also very expensive compared to the coated graphite and castable options. Thus, current production operations in the CP utilize the castable zirconia crucible.

3.5.2.3. *Ceramic waste processing*

The reference process for preparing waste salt from the electrorefiners for permanent disposal is known as the ceramic waste process (CWP). The CWP consists of several unit operations, including zeolite size-reduction, zeolite drying, salt/zeolite blending, and pressureless consolidation [109–111]. Figure 42 shows a detailed flowsheet for the CWP featuring photographs of the engineering-scale equipment.

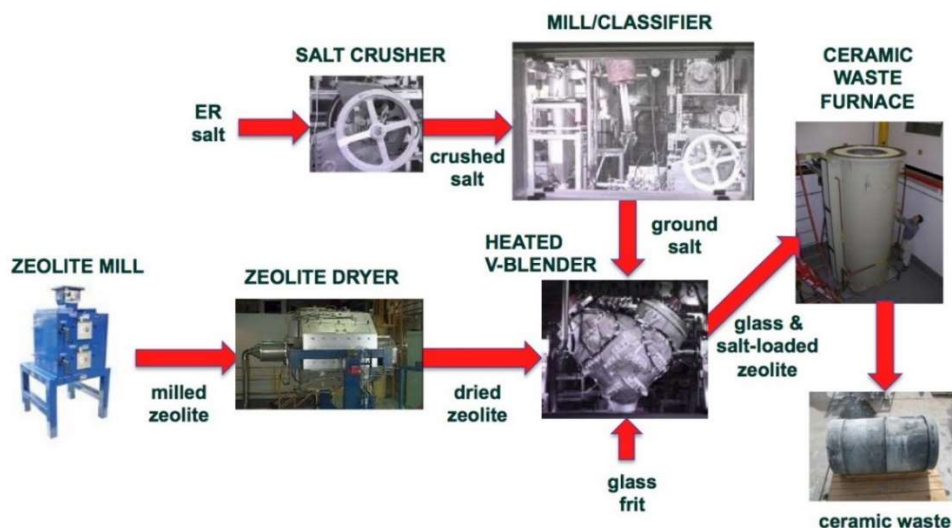


FIG. 42. EBR-II SNF treatment ceramic waste process [102] (reproduced courtesy of Idaho National Laboratory).

The objective of the CWP is to immobilize the salt containing LiCl-KCl and active metal chlorides into glass-bonded sodalite ingots with a nominal mass of 400 kg. It has been estimated that at least 33 tonnes of ceramic waste forms will be needed to immobilize all of the salt that will eventually be generated from EBR-II SFT, corresponding to 82 waste forms of this size. Those waste estimates were based on a calculation that was performed in 2007 and may need to be updated based on current safety basis limitations in the INL hot cell facilities. Early development of this process used a hot isostatic press (HIP) for the final conversion of zeolite and glass powder into the waste form. But it was found that a higher temperature sintering process could achieve nearly the same result with only a slight decrease in density of the final waste form. The HIP process operated at a pressure of 1.72×10^7 MPa (25 000 psi) and 850°C, while the pressureless consolidation (PC) process operates at atmospheric pressure and 925°C. Operation of a PC furnace in a hot cell was evaluated to be considerably more practical than utilizing a HIP. The weight of the equipment compared to the maximum load on the hot cell floor was a major issue of concern.

During initial stages of the development of the CWP, there was no standard established for dryness of the zeolite. Zeolite-4A, which has high aluminium content, is extremely hygroscopic and will quickly absorb greater than 20 wt% water into its pores. It was known that this water must be removed prior to blending with the salt to avoid a large release of steam in the closed V-blender. That steam would likely over pressurize the vessel and combine with the salt to cause widespread corrosion of the equipment. Furthermore, any residual water left in the zeolite could compete with the salt for absorption sites and, thus, reduce the capacity of the zeolite to immobilize salt. The approach taken with zeolite drying was to determine the level of dryness that could be practically obtained without overheating the zeolite or using an excessively long drying cycle. The moisture level that was selected as the process target was 0.3 wt%. There are a variety of methods that can be used to analyse the moisture content in the zeolite, all of which require careful handling of the zeolite in a dry atmosphere to prevent re-absorption of water. The most reliable method was determined to be Karl-Fisher titration coupled with a tube furnace operating at 600°C. Zeolite samples of approximately 10 mg are slid into the hot zone of the furnace with flowing dry gas. The gas carries any moisture thermally released into the titration cell. A custom dryer was developed to dry zeolite batches up to about 100 kg. This system,

referred to as a Mechanically Fluidized Dryer (MFD) involves a retort that continually rotates inside of fixed heaters. The motion of the retort does not effectively mix the zeolite powder but does promote heat and mass transfer via fluidization of the powder. Off-gas from the retort can either be released to the atmosphere or sent through a vacuum system. During initial heat up of the zeolite when most of the moisture is released, the steam is vented directly to the atmosphere. Once the temperature reaches 500°C, the system is sealed, and off-gas is directed through a vacuum system. Drying tests performed in non-vacuum conditions indicated that the vacuum conditions result in lower residual moisture levels in the zeolite with all other conditions essentially the same. The standard heating cycle with the MFD system is to hold the zeolite at 500°C for 12 h under vacuum. Moisture levels as low as 0.15 wt% has been obtained in this system under these conditions.

To immobilize the waste salt, it is blended with dehydrated zeolite-4A in a high temperature V-blender. The V-blender is one of only three systems in the CWP that have been tested in a hot cell with real waste from SNF. Unlike the MFD, its geometric design does facilitate powder mixing, which is important due to the need to distribute salt powder evenly through the batch of dried zeolite. With each rotation of the V-blender, the powder is divided into two volumes and then recombined. The off-set geometric design ensures that each rotation splits the powder differently. The operating conditions for the blending were established using both a laboratory-scale and an engineering-scale V-blender. Free chloride measurements were used to quantify the effectiveness of each blending run. It was found that minimizing the quantity of large particles in the milled salt is important for achieving a low free chloride value. Holding the temperature at 500°C for 15 h is typically sufficient to minimize the free chloride. Frequently, it was observed that salt/zeolite cakes on some regions of the inner V-blender wall. Strategies have been proposed to minimize this caking but have not yet been tested. Final optimization of the V-blender process should address this caking issue, which has been observed in both laboratory-scale and engineering-scale V-blender experiments.

Recent developments in pressureless consolidation have been attained via full-scale testing with surrogate salts. A multi-section container was designed, built, and tested to contain the ceramic material during consolidation. The volume is reduced approximately 60% as a result of consolidation, leaving much excess length in the container that would otherwise need to be cut off and discarded. The design of the multi-section container is such that the upper half is removed after consolidation and then used as the lower half of the next container. For the 400 kg sized waste forms, the temperature cycle involves a 40 h hold at 500°C followed by a 75 h hold at 925°C [111]. A forced cool-down can minimize the overall cycle time, but it has been found that cracking of the ceramic occurs during this cool down. During one full-scale waste form run, 14 cracking events were detected using a microphone placed outside of the furnace and audio recording software. Solidification stress is believed to be the cause of the cracking, not thermal stress. Solidification stress theory and its comparison to the pressureless consolidation data was presented by Solbrig et al. [112].

3.5.2.4. *Metal waste processing*

After each fuel batch is electrorefined, the cladding hulls remain in the anode baskets along with unreacted actinides, zirconium, and noble metals. It has been shown that zirconium and noble metal retention is a function of the extent of actinide removal. But most of these elements tend to be retained with the cladding hulls. When the anode baskets are pulled from the salt, a significant coating of salt remains on the surface of the hulls. This salt is separated via distillation in the metal waste furnace [113] as shown in Fig. 43. The metal waste furnace also

serves to consolidate the cladding hulls and residual fuel constituents into a metallic ingot that is suitable to be disposed of as a high level waste form.

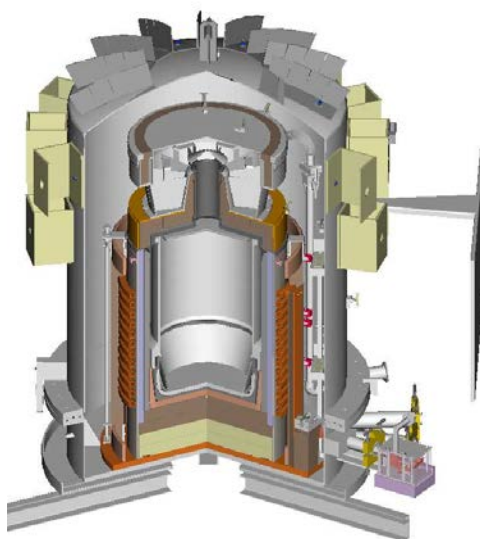


FIG. 43. Metal waste furnace designed to process cladding hulls from the electrorefining of spent EBR-II fuel (reproduced courtesy of Idaho National Laboratory).

In addition to cladding hulls, plenums containing sodium metal are also processed in the metal waste furnace [113]. Iron chloride is added to the process crucible and heated to 800°C for 75 minutes to convert the sodium to sodium chloride. Salt distillation and melting of the metal alloy ingot is accomplished via heating the process crucible to 1560°C for 3 h under vacuum. The metal waste furnace is inductively heated and capable of reaching 1700°C under a vacuum of 26.7 Pa (200 mTorr).

Zirconium is added to the process crucible in the form of 1.5 mm diameter wire. This is necessary to bring the metal waste form composition to a target value of 15 wt% zirconium with a minimum of 5 wt% and maximum of 20 wt%. The metal waste form is primarily composed of two metallographic phases, a ferrite solid solution, and a FeZr₂-type intermetallic. Actinides are exclusively bound in the FeZr₂ intermetallic. The noble metal fission products are also found in the intermetallic, though cobalt, molybdenum, manganese, tin, and technetium also have some solubility in the ferrite solid solution. Zirconium contents less than 5 wt% are unable to encapsulate FPs and actinides [114–117]. Alloys with greater than 20 wt% zirconium have increased the brittleness.

Crucible material selection was found to be the key, due to the high reactivity of uranium trichloride in the salt with some oxides and the reactivity of sodium metal with graphite. Alumina refractory lined graphite was selected with the plenums placed inside of a thin-walled steel liner to prevent sodium metal reaction with graphite. The sodium is oxidized to sodium chloride via reaction with iron chloride during the metal waste furnace run.

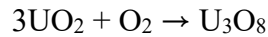
3.5.3. Conditioning oxide fuel for pyroprocessing treatment

While the U.S. Department of Energy envisions pyroprocessing as being used ideally for the recycle of metallic FR fuel, research at INL has been performed in support of LWR oxide fuel conditioning to make it compatible with electrorefining. In recent years, this has been primarily

motivated via collaboration with the Republic of Korea under the I-NERI programme and more recently the United States – Republic of Korea Joint Fuel Cycle Study programme.

3.5.3.1. Voloxidation

Voloxidation is the high temperature process by which oxygen or air reacts with oxide SNF. The primary oxidation reaction is as follows:

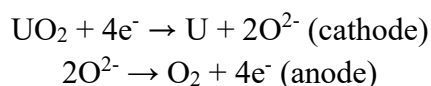


This can be the head-end step for either pyroprocessing or aqueous processing of SNF. Benefits to its use include removal of volatile fission products, separation of fuel from cladding, and particle size reduction to promote fast reaction kinetics for the oxide reduction process or fast dissolution rates for aqueous processing. INL collaborated with KAERI and ORNL on development of this process. In 2008, results of voloxidation tests using spent BR-3 fuel with different process parameters were summarized [117]. Oxidation temperatures ranged from 500 to 700°C. The effect of vacuum at high temperature (950°C) after lower temperature oxidation was examined. The effect of air versus O₂ as the oxidant was examined. And the effect of cladding versus no cladding was examined on removal of various FPs. Analyses included particle size, percent fuel removal from the cladding, and removal of various FPs. Six FPs were found to be significantly depleted from the fuel due to the voloxidation experiments, including rhodium, ruthenium, technetium, molybdenum, tellurium, and caesium. Complete removal of the fuel from the cladding was achieved with an oxidation temperature of only 500°C for 2 h. Increasing the temperature, however, resulted in fewer fines in the oxidized powder product. Increasing the oxidation temperature also tended to increase the removal of fission products. Applying vacuum at 950°C after the fuel oxidation was also found to assist in the removal of fission products.

An off-gas treatment system (OTS) has been developed with the objective to trap key volatile fission products — iodine, technetium, and caesium [118]. The OTS consists of three zones, each containing a different solid absorbent and maintained at a different temperature. Zone 1 contained AgX zeolite and was held at 150°C with the objective of collecting the iodine. Zone 2 contained CaO/fly-ash (Si/Al = 2) at 600°C for collecting technetium. Zone 3 contained fly-ashes at 1000°C and was used for collecting caesium. Three samples of SNF were run in the voloxidation system with oxidation of the fuel at 500°C. After an initial run in which incomplete fuel oxidation was observed, the next two runs yielded data that demonstrated the effectiveness of these filters. The iodine trapping was particularly efficient with 84–100% collection based on initial iodine content in the fuel estimated using ORIGEN. Optimal technetium collection of 72% was observed in Zone 2 based on initial technetium concentration determined via fuel sampling. And up to 66% of the caesium was found to collect in Zone 3, also based on sampling of the initial fuel. The only unexpected result was the detection of equimolar concentrations of caesium and technetium in the tubing connecting the zones. This has been hypothesized to be due to the formation of CsTcO₄.

3.5.3.2. Oxide reduction

Whether oxide fuel is first voloxidized or not, it must be reduced completely to metallic form prior to processing in an electrorefiner. While early research into an oxide reduction process focused on chemical reduction using lithium metal dissolved in LiCl [119], focus in the last decade has been on electrolytic reduction using LiCl-Li₂O as the electrolyte. The reactions at each electrode are the following:



The electrolytic reactions keep the lithium oxide concentration from increasing and simplify the process to only a single furnace and vessel.

All electrolytic reduction experiments performed at INL have involved lab scale molten salt furnaces with maximum fuel batches of about 50 g. Experiments with SNF were performed in the Hot Fuel Dissolution Apparatus (HFDA), a lab scale molten salt furnace installed in the Hot Fuel Examination Facility (HFEF) hot cell. The fuel was either mechanically crushed or voloxidized to achieve small particles prior to loading in the cathode baskets. SNF samples used in these studies included fuel from the Belgian LWR, BR-3 [120–122] and MOX fuel that had been irradiated in EBR-II [123].

In studies with spent BR-3 fuel, current efficiency was observed to vary from 21% to 45% [120]. Fission products caesium, barium, strontium, and iodine partitioned into the salt phase with very low concentrations of uranium and plutonium detected. Up to 99.7% reduction of UO_2 to uranium metal and 97.8% reduction of PuO_2 to plutonium metal was observed [120]. Meanwhile, REE reduction was less with an upper value of about 80%. In some cases, batches of BR-3 fuel that had been electrolytically reduced were then subjected to electrorefining [122]. In these runs, no effort was made to remove the adhering salt from the oxide reduction process. Uranium metal deposits were successfully obtained, and REE FPs were found to accumulate in the LiCl-KCl salt as expected. There were some interface issues discovered between the oxide reduction and electrorefining steps. Salt carryover resulted in higher than normal depletion of uranium from the salt, in part from reaction with lithium oxide to make uranium oxide.

In addition to reducing crushed BR-3 fuel, some batches of this fuel were first decladed via voloxidation, which resulted in particle size reduction and loss of volatile fission products. The voloxidized fuel has a chemical state of U_3O_8 , which was found to readily convert to uranium metal in the oxide reduction process [121]. Voloxidation results in a fraction of the fuel having a particle size of less than 45 μm , and those particles were separated from the rest of the material via sieving prior to running in the oxide reduction process. Either sintered metal or porous magnesia baskets were used to contain fine fuel particles.

MOX fuel that had been irradiated in EBR-II was also used in oxide reduction tests [123]. A wide range of reduction efficiencies were observed with the MOX fuel, but the efficiency appeared to improve with each of the five runs completed. This appeared to be partially due to varying levels of unintentional re-oxidation of samples during storage. Elevated concentrations of iodine and tellurium were observed in the salt from reducing MOX fuel, and that appeared to lead to significant chemical attack on the platinum anode. Examination of the anode after testing indicated about 20% loss of the platinum. Anode potentials progressively increased during the MOX fuel treatment, significantly more than had been observed with LWR fuel treatment. Electrorefining was also performed on the reduced MOX fuel. This resulted in higher than normal concentrations of TRU in the solid cathode deposits (1.7% to 15%), which may be attributed to a drop in UCl_3 concentration in the salt from reaction with the TRU elements. One liquid cadmium cathode run was performed for the purpose of U/TRU recovery that resulted in a Pu/U ratio of 4.2 in the metal deposit.

Some kinetic testing and modelling have also been done on oxide reduction as a part of collaboration with KAERI. As part of I-NERI project, a series of laboratory-scale uranium oxide samples were reduced in a molten salt furnace installed in an inert atmosphere glove box

at INL [124]. Additional data was collected at KAERI in their laboratory-scale systems [125]. These experiments involved runs with both stainless steel mesh and sintered stainless steel baskets in an attempt to understand the effect of the basket on the kinetics. Higher retention of lithium oxide was measured in the sintered stainless steel baskets, indicating that diffusion of the lithium oxide out of the fuel was effectively restricted with the sintered metal baskets. Partial reduction tests were attempted to obtain data useful for kinetic modelling. Much of the data was suspect, however, as there was not always a consistent relationship between applied charge and extent of reduction. The kinetic model developed by University of Idaho for oxide reduction was focused on the processes occurring at the cathode and assumed the kinetics were limited by charge transfer and diffusion [126]. Validation of the model was hindered by the inconsistent kinetic data.

3.5.3.3. Oxide reduction salt treatment

One of the technical challenges associated with development of an oxide reduction process is how to manage the waste salt generated. The molten LiCl-Li₂O electrolyte, as previously discussed, is contaminated by a number of FPs including caesium, strontium, barium, and iodine [120]. Concentration limits have not yet been established for these elements in the salt, but it is certain that they will have to be regulated. The negative impact of FP accumulation was observed during the previously mentioned reduction of irradiated MOX fuel [123]. One option is to carryover salt from oxide reduction to electrorefining and replaces the salt with clean LiCl-Li₂O. This would result in significant conversion of UCl₃ in the salt to UO₂ from reaction with the lithium oxide, and that UO₂ would need to be collected and recycled to the oxide reduction step. Alternatively, the salt can be distilled from the reduced fuel and recycled to the oxide reduction system. That leaves two options for dealing with FP accumulation; throw-away of the salt (as in the ceramic waste process), or selective chemical separation. The latter option was investigated by Sachdev et al. [127]. In this study, the ability of zeolite-4A to selectively absorb or exchange Cs⁺ and Sr²⁺ cations out of LiCl was examined. Both molten salt and solidified powder salt were studied. The molten salt contacts were done at 650°C, and it was found that the zeolite degraded at that temperature and was ineffective at removing the FPs from the salt. The solid state contact tests with the powders were done in a small scale V-blender at 500°C and 550°C. In those tests, the zeolite retained its crystalline structure and removed as much as 99.6% of the Cs and 99.5% of the Sr from the salt. This solid state ion exchange process with zeolite-4A, thus has potential for cleaning up the oxide reduction salt.

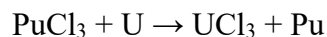
3.5.4. Technology development to support commercialization of pyroprocessing

Key objectives to commercializing pyroprocessing are recovering actinides for recycle to new fuel and minimizing the volume of high level waste generated by the process. The latter issue is largely contingent upon effectively handling the contaminated salt from the electrorefiner. The ceramic waste process previously mentioned is effective at immobilizing the ER salt into a robust waste form. However, it is non-selective in nature and involves the loss of useful LiCl, KCl and actinides from the process. Thus, research in recent years has been funded at INL to examine both actinide recovery and salt waste minimization. This technology is not intended to be applied to the processing of SNF from EBR-II. Rather, it is to support future application of the technology in scaled up and perhaps commercialized installations.

3.5.4.1. Actinide recovery

While standard electrorefining onto a steel cathode typically results in a high purity uranium metal and very little co-deposition of TRU elements, a liquid cadmium cathode (LCC) has been shown to be effective at simultaneously collecting both U and TRU elements [118]. The LCC

is effective due to the stabilization of plutonium metal in the cadmium phase. It has a very low activity coefficient in the cadmium phase compared to uranium, which shifts the equilibrium for the following reaction to the right:



Without the cadmium phase present, the reaction proceeds in the opposite direction and results in oxidation of any plutonium metal back into the salt phase.

INL has performed a number of LCC experiments using both the engineering-scale Mark-V ER and the lab scale HFDA [119–121, 128]. Engineering scale tests were reported by Vaden et al. [119]. In these tests, 26 kg of cadmium metal was loaded into a beryllium oxide crucible and lowered into the salt. Three tests were performed, each resulting in 1–2 kg of heavy metal collected. The Pu/U ratio in the salt was initially 10.8 but dropped to 3.7 as a result of the LCC tests. With decreasing Pu/U in the salt, the Pu/U in the LCC product also decreased. Current efficiency was found to range from 76–99% with dendrite formation being a probable source of inefficiency. A pounder was used to minimize formation of these dendrites but was only successful in one of the three runs. Technically, it was a paddle that rotated and oscillated up and down during the experiments. Its range of motion extended to just above the cadmium surface to avoid displacement of cadmium from the crucible. The beryllium oxide crucibles were found to be easily damaged and do not appear to be a viable option for long term, reusable crucibles.

One of the primary objectives of running laboratory scale LCC tests was to collect data to support calculation of separation factors of both actinides and rare earths between the salt and cadmium phases. In the engineering scale LCC tests, separation factors for REEs could not be calculated due to the fact that they are present in very low concentrations in the Mark-V ER. In the laboratory-scale HFDA system, it is possible to spike REE chlorides into the salt to run tests capable of generating such separation factors.

Li et al. reported two series of experiments, one with equilibrium conditions and one with non-equilibrium conditions. In one set of tests, Mark-IV salt with 2 wt% REEs was used. In the other set of tests, REEs were spiked into a mixture of Mark-IV and Mark-V salt to a level of 5 wt%. In the equilibrium tests, the LCC was allowed to sit in the salt for a period of time after the electric potential was shut off. In the non-equilibrium tests, the cathodes were immediately pulled out of the salt after the potential was shut off. Over both series of experiments, the Pu/U ratio in the salt varied from 0.8 up to 3.6. Plutonium recovery was measured over this entire range, but the ratio of Pu/U in the LCC product was found to be a linear function of the ratio in the salt. REE contamination in the LCC product was measured to be as high as 6.7 wt%. Separation factors were measured for REEs, and they were found to be strongly dependent on the cathode potential, i.e., the more cathodic the potential, the higher concentration of REEs in the LCC. Cathode potential did not have a significant effect on MA separation factors, which has a benefit with respect to proliferation.

A detailed analysis of the laboratory scale LCC test results was published in 2010. Measured separation factors relative to U were shown to be smaller than published in the literature and it was concluded that an LCC should be operated as close to its open circuit potential as possible to minimize REE contamination. It was recommended to use an LCC with a large surface to volume ratio which would then minimize the current density at the interface and make the cathode potential less negative.

Another approach to recovering actinides from electrorefiner salt is referred to as drawdown. Drawdown can be an electrochemical or chemical process that extracts U and TRU from the salt. Unlike the LCC electrorefining process, it can be used to achieve very low concentrations of actinides in the salt. At INL, drawdown using lithium reduction has been investigated [129]. In this work to date, REE chlorides have been used as surrogates for actinide chlorides. The objective of the experiments has been to understand the selectivity of drawdown using lithium as a function of thermodynamic properties. To understand how well actinides may be removed from the salt while leaving REEs unreduced, REE pairs with different free energy of formation values were reacted with lithium. Given free energy differences comparable to those between actinides and REEs, it was found that there is relatively poor selectivity. Using lithium to reduce a large fraction of the plutonium chloride from the salt is expected to also result in substantial reduction of REEs. Thus, other drawdown methods are currently being investigated.

3.5.4.2. Salt waste minimization

In order to minimize the generation of salt-related waste from pyroprocessing, research emphasis has been focused on selectively removing fission products from the LiCl-KCl salt. The most thoroughly investigated technology for this purpose is salt-zeolite ion exchange. In this process, ions from the molten salt replace ions initially in the zeolite. If the zeolite is pre-loaded with Li⁺ or K⁺ ions, the effective outcome is to clean up the salt from the ER. Early investigation of this process by researchers at ANL showed that there was favourable selectivity for fission products in the zeolite [130]. This motivated a series of experimental studies in which molten salt solutions were contacted with dehydrated zeolite-4A for 24 h or longer to achieve ion exchange equilibrium [131–133]. Each fission product was investigated separately by preparing chloride salt mixtures containing LiCl, KCl and a select FP chloride. By this approach, it was possible to develop uptake curves as a function of final concentration in the salt. And this led to the development of equilibrium models. The first model proposed by INL was based on the concept that there are two active sites for exchange in the zeolite: framework sites and occluded sites [133]. The framework sites are where cations balance the negative charge of the Al-O tetrahedra. Initially, zeolite-4A contains Na⁺ cations to serve this purpose. The other site originates from the diffusion of salt molecules into the zeolite pores. Approximately 12 Cl⁻ ions can absorb into the zeolite per pseudo unit cell based on the following formula, where M is a generic metal cation with a +1 charge. The M⁺ cations are effectively the second site for ion exchange, as they can be replaced by FP cations from the salt:



Phongikaroon et al. later expanded the model to include divalent and trivalent FPs with data to support fitting of the model [134]. A study on the ion exchange model included the ability to predict the moles of salt occlusion per unit cell of the zeolite and expanded the data fit to include more experimental data [135]. The FPs that are now included in the fully predictive equilibrium model include Cs⁺, Rb⁺, Sr²⁺, Nd³⁺, Ce³⁺, Ba²⁺, La³⁺, Pr³⁺ and Y³⁺. U³⁺ is also included in the model as well as the base salt components (Li⁺, K⁺ and Na⁺).

Most recently, study of salt-zeolite ion exchange has expanded into kinetic investigations. Equilibrium is typically achieved in 24–72 h, but that might be considered too long for a scaled up, commercial process. Shaltry et al. used ternary and quaternary salt experiments, similar to those used for the equilibrium tests, with focus on rate of uptake of Cs⁺ and Sr²⁺ [136]. A novel experimental method was introduced in this study to maximize the useful data from each experiment. The volume of salt to volume of zeolite was high enough that the salt composition did not change significantly during each test. But the zeolite composition did change substantially with uptake of the Cs or Sr. To obtain kinetic data over a wide time range with

each experiment, a few pellets of zeolite were removed every hour or two followed by re-immersion of the basket into the salt. Then each set of pellets were washed, dissolved, and analysed to determine uptake of the FP of interest at the time of the sample. Several models were considered with the best fit to a diffusion-limited model. Time to complete exchange was about 30 minutes for Cs and 100 min for Sr, but that was using a standard bead size of 2 mm diameter. Based on the conclusion that the exchange was diffusion limited in the beads, smaller particles should result in faster uptake of the FPs. Allensworth et al. combined molten salt contacts and solid-state powder contacts to investigate the mechanism of salt transport into the zeolite particles [137]. It was shown in this study that a molten state for the salt is not required to achieve absorption of the FPs into the zeolite. This opens the door for different approaches to removing FPs from molten salts, especially for salt systems such as LiCl-Li₂O that have very high melting points. It also shows that it is possible to absorb concentrated FPs into the zeolite after LiCl-KCl has been separated and recycled to the ER. This is important for connecting the zeolite-based ceramic waste process to a zone freezing method (which selectively removes LiCl-KCl from the salt) for minimizing salt waste from the ER.

3.5.5. Conclusions

Over the last decade, INL has been a leader in the development of pyroprocessing technology in the U.S. via processing of EBR-II fuel and study of advanced technology to support potential scale-up of the process. In the process of treating 16% of the original inventory of EBR-II fuel, much has been learned about pyroprocessing at INL. Advancements have been made in electrorefining, cathode processing, and waste processing as a direct result of the EBR-II fuel treatment project. Tremendous amounts of data have been collected, and models for various unit operations have been developed and validated against data. While the technology was originally developed for metal fuel such as EBR-II driver and blanket fuel, significant progress has been made towards developing the unit operations needed to efficiently treat oxide fuel using pyroprocessing and to recover actinides for application to a closed nuclear fuel cycle. Key current challenges for process development include achieving high efficiency for actinide recovery, minimizing high-level waste generated by the process, and demonstrating the ability to effectively safeguard nuclear materials in a pyroprocessing facility. Work continues on these challenges, utilizing the INL's unique processing facilities and expertise while leveraging partnerships with other laboratories and universities.

3.6. ELECTROREFINING IN MOLTEN LiCl-KCl USING SOLID ALUMINIUM CATHODES AT JRC-KARLSRUHE

The pyrochemical reprocessing of spent nuclear fuel developed at JRC-Karlsruhe is based on electrorefining in molten LiCl-KCl bath using reactive solid aluminium cathodes [138–141] because a major focus is on the separation of all actinides (An) from FPs. In this process, electroseparation of An from FPs is carried out in a LiCl-KCl molten salt at 450°C by applying a constant current between the metallic fuel contained in a tantalum basket and an aluminium cathode. During the electrolysis, actinide cations arising from the anodic oxidation of the fuel are electro-transported and deposited on to the aluminium cathode where they form An-Al alloys. The principle of the electrorefining process is illustrated in Fig. 44. Alkali, alkaline earth metals, and REE FPs are also dissolved into the melt during the process, but they are not reduced thanks to the controlled deposition potential. Theoretically, zirconium and more noble metal FPs should not be oxidised and remain in the anodic basket. However, in practice, the extent of their co-oxidation depends on the required portion of recovered actinides.

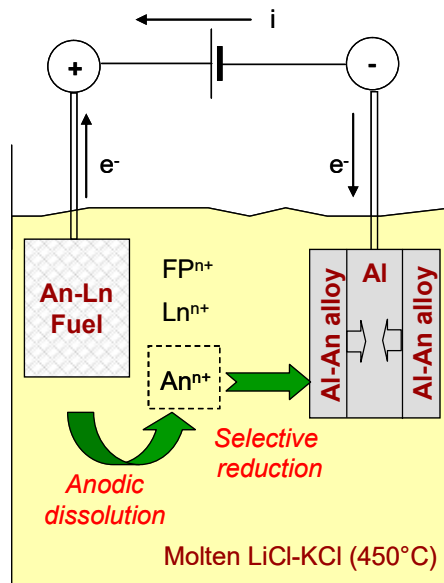


FIG. 44. Principle of electrorefining process of metallic An-Ln fuel [139].

3.7. DEVELOPMENT OF PYROCHEMICAL TECHNOLOGIES FOR SNF REPROCESSING IN RUSSIAN FEDERATION

3.7.1. Introduction

Currently, uranium and mixed uranium-plutonium fuel from the existing power reactors is reprocessed at the ‘Mayak’ Combine. The Mining and Chemical Complex in Zheleznogorsk has capacities for SNF dry storage and reprocessing of mixed uranium-plutonium fuel; sites for the SNF reprocessing and HLW final geological disposal are being arranged. The Federal Target Programme “Nuclear Power Technologies of New Generation for the Period 2010–2015 and until 2020s” [142] has been established to develop innovative nuclear power technologies based on FRs with a closed fuel cycle. The programme emphasizes that fuel is to be recycled to maximise resource utilization. Within this framework, FRs and closed fuel cycle enterprises will be set up to develop the corresponding areas of nuclear power engineering, in addition to the construction of thermal NPPs.

Due to the possibility of having a breeding factor greater than one, FRs can breed fissile materials. The quantity of fissile materials extracted through FR SNF reprocessing is sufficient to fabricate fuel for the next refuelling, with no requirement for additional enriched uranium; the charging is done using only natural or depleted uranium. The regenerated uranium is neither extracted out of the cycle nor accumulated. It should be mentioned that a transition to the closed fuel cycle with FRs allows a significant simplification of the production structure, as no mining and enrichment of uranium is needed, nor long term storage of SNF. A further advantage of FRs is a possibility to utilize minor actinides such as neptunium and americium.

The majority of FRs with liquid metal coolant (lead-cooled reactor BREST) [143] and with sodium coolant BN reactors [144, 145] use either MNUP or MOX fuel. Two technologies described below were tested with irradiated fuel in 2010-2015. Now an alternative pyrochemical technology is under development [146]. The hydrometallurgy part of combined technology was not changed.

The above-said Federal Target Programme covers the activities on the closed fuel cycle with FRs (the first results have been obtained) as well as design and development of demo facilities for the FR SNF reprocessing.

3.7.2. Fuel cycle of lead-cooled fast reactors

The scheduled duration of the FR external fuel cycle should not exceed two years, with the average burnup achieving 10 at %¹⁰. A technology of carbothermal synthesis has been selected as a basic process to fabricate MNUP powder, while a pellet technology is used to fabricate fuel. The facilities for BREST MNUP SNF reprocessing should provide for reprocessing of one year cooled fuel containing 10–15% of fissile materials with a burnup of ~10 at % as well enabling fabrication of a mixture of actinides with a purification factor about 10⁶. To reprocess MNUP SNF, a process containing both pyrochemical operations (including lead pyroelectrochemical processes) and hydro-metallurgical operations was proposed to refine target products (U-Pu-Np-Am) and treat radioactive waste [147, 148]. Figure 45 presents the schematic flowsheet of the Pyro-Hydro (PH) process.

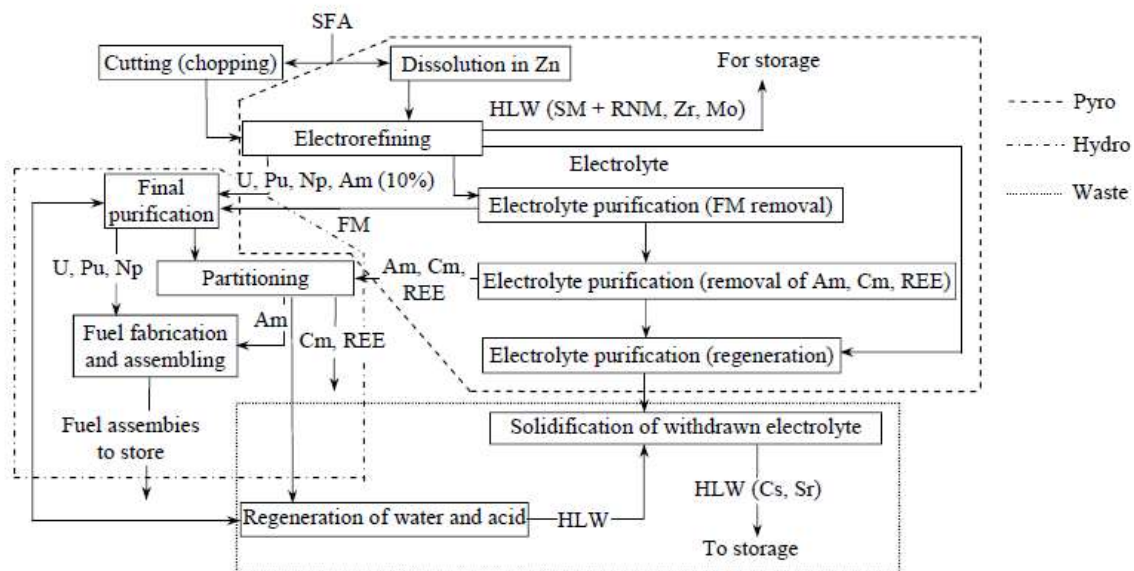


FIG. 45. Schematic flowsheet of the PH process [149].

The following process operations have been tested in laboratory conditions using real products: removal of a stainless cladding in zinc melt; extraction refining of uranium, plutonium and neptunium; separation of REEs and trans-plutonium elements.

¹⁰ at%: atom percent fission. This is another unit to measure burnup. Burnup is measured as the fraction of fuel atoms that underwent fission in %FIMA (fissions per initial metal atom) or %FIFA (fissions per initial fissile atom) as well as, preferably, the actual energy released per mass of initial fuel in gigawatt-days/metric ton of heavy metal (GWd/tHM), or similar units. Nuclear engineers often roughly approximate 10% burnup as just less than 100 GWd/t.

The following procedures are components of the pyrochemical part of combined reprocessing of MNUP from lead-cooled FR:

- Removal of cladding in Zn;
- Electrorefining of nitride SNF to produce anode and cathode products;
- Treatment of anode products and cleaning of anode cage;
- Sublimation of salt and cadmium from different products;
- Extraction purification of salt from actinides in the systems ‘molten salt – liquid metal’;
- Sorption purification of salt on zeolites from FPs and return of the purified salt back to the SNF reprocessing;
- Local gaseous purification during pyrochemical operations (Cs, Sb, Te, Se, radioactive noble gases, tritium).

The hydro-metallurgical part of combined reprocessing of MNUP from lead-cooled FR contains:

- Dissolution of all products containing U, Pu, Np, Am, Cm;
- Cleaning of solutions;
- Extraction-crystallization refinement of non-separated uranium-plutonium-neptunium mixture;
- Extraction of TPE fraction from raffinate of extraction-crystallized affinage of U, Pu and Np;
- Separation of Am-Cm pair;
- Vaporization of liquid medium and high level waste;
- Production of U, Pu, Np and Am oxides;
- Production of curium oxides for a long term storage;
- Treatment of medium and high level waste.

3.7.3. Fuel cycle of sodium-cooled fast reactors

Research reactors with sodium coolant (BOR-60, MBIR) and power reactors of BN type (BN-600, BN-800 and BN-1200) can operate using MOX fuel. The process under consideration for MOX fuel reprocessing is chemical oxidation with further electrochemical cathode deposition in molten salt chlorides.

In 1964, RIAR started developing technologies for the SNF reprocessing using a pyrochemical method in molten alkali metal chlorides. During 50 years of research, a large array of work has been covered regarding the chemistry of uranium and plutonium in salt systems and the development of process equipment [150–155]. A pilot facility was put into operation to produce granulated MOX fuel; this facility provides BOR-60 with nuclear fuel [156, 157]. A concept of pyroelectrochemical process in the fuel cycle was proposed [158]. To promote this concept, a facility was designed and installed in the hot cell for pilot reprocessing of SNF from BN-350 [159] and BOR-60 [160] FRs. In particular, MOX fuel to MOX fuel reprocessing was trialled and technologically implemented [161]. Figure 46 presents one of the concepts for on-site FR closed fuel cycle [162].

Once the fuel pins are unsealed and the fuel is ground, the following process stages are undertaken:

- (a) Dissolution of fuel by chlorination is done in molten alkali metal chlorides with gaseous chlorine. After chlorination, uranium comes into the melt as uranyl ions UO_2^{2+} , plutonium as Pu^{3+} and Pu^{4+} , and neptunium as both oxygen-free ions (Np^{3+} and Np^{4+}) and oxidized ions (NpO^{2+} and NpO_2^{2+}) in a comparable relation. Practically all FPs and MA come to the melt as oxygen-free ions;
- (b) Electrolytical deposition of U, PuO_2 (oxidized melt) on the cathode is performed by flowing through a melt of gaseous mixture $\text{Cl}_2 + \text{O}_2 + \text{N}_2$. Oxidation of the Pu-containing solution with a gaseous mixture containing oxygen and chlorine is used to control the rate of plutonium dioxide deposition on the cathode. Cations of plutonium oxychloride compounds PuO^{2+} and PuO_2^{2+} resulted from melt oxidation taking part in the cathode process of MOX fuel generation. FPs such as caesium, strontium, lanthanides, and the majority of americium and practically all curium remain in the melt. Prior to fabrication of fuel pins using vibropacking, the mixed granulate of MOX fuel is transferred to washing from captured salts and their further vacuum sublimation;
- (c) Phosphate (carbonate) purification of melt is completed by using sodium orthophosphate (sodium carbonate). The purification is based on the fact that the majority of FPs with an oxidation level of ≥ 2 make low-soluble complex orthophosphates (or oxides in case of carbonate deposition) in molten salt and they are quantitatively deposited. Thus, the phosphate (oxide) deposit contains strontium, with most of REEs, americium and curium remaining in the melt. However, the deposition purification of melt does not prevent the release of radioactive caesium, and so, the melt activity increases with time. After multiple uses, the melt becomes one of the radioactive wastes produced.

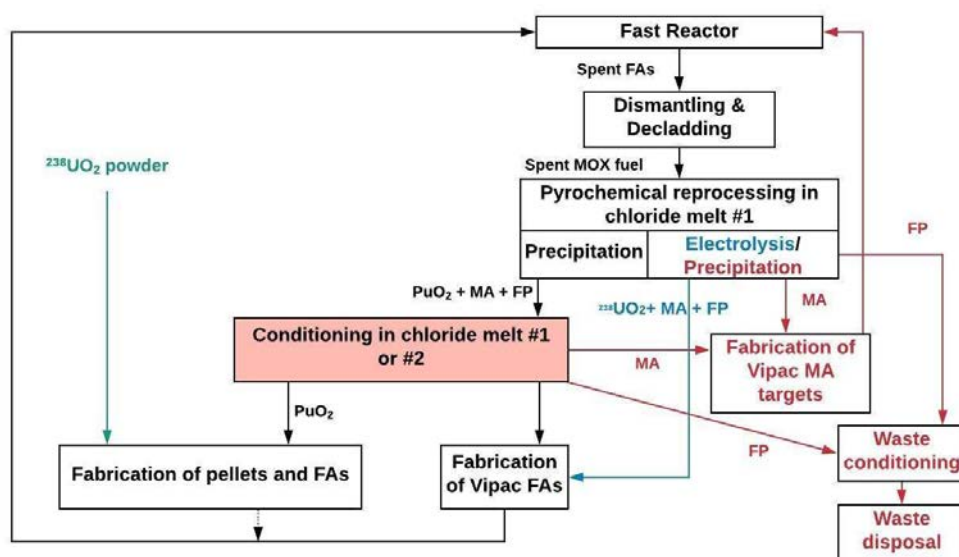


FIG. 46. Concept for FR closed fuel cycle.

Low level purification of MOX fuel after the pyrochemical reprocessing is compensated by a remote fabrication of fuel pins by vibropacking.

3.7.4. Conclusion

Two promising reprocessing procedures are considered in the Russian Federation to be industrially applied for the closed fuel cycle of FRs: pyrochemical reprocessing of MOX fuel

for sodium-cooled reactors, and combined reprocessing of dense spent MNUP for lead-cooled reactors. At present, research is undertaken to justify the selected reprocessing procedures; equipment is developed for specific stages of chemical reprocessing of irradiated fuel to extract nuclear materials and treat MA and radioactive waste; a pilot module is designed and planned for operation for an on-site SNF reprocessing module.

3.8. PYROCHEMICAL TECHNOLOGY BASED ON FLUORIDE VOLATILITY PROCESS IN CZECH REPUBLIC

The separation techniques known as ‘volatilization’ or ‘fluoride volatility’ are typical dry processes. They involve the fluorination of SNF with fluorine gas and the subsequent separation of resultant volatile compounds (represented mainly by uranium hexafluoride) from non-volatile fluorides, in the first instance from PuF₄. The volatilization technique based on heterogeneous reaction between fluorine gas and powdered SNF oxides is known as Fluoride Volatility Method (FVM). In Czech Republic, this method uses a flame fluorinator for the conversion of oxides to fluorides. The principle of FVM resides in fluorination of a mixture of elements forming fluorides with different volatility. The fluorides, which are volatile under reaction conditions, escape from the mixture, whilst the others form a mixture of solid products. There are two main methods of undertaking the fluorination reaction — either direct flame fluorination, or reaction in a fluid bed. In the Czech Republic Nuclear Research Institute, the former process is examined at a semi pilot plant scale with the aim of verifying its applicability for the reprocessing of SNF. The list of SNF components forming volatile and non-volatile fluorides at working conditions under study is given in Table 8.

TABLE 8. THE LIST OF VOLATILE AND NON-VOLATILE FLUORIDES OF SELECTED ELEMENTS IN SPENT NUCLEAR FUEL.

Volatile fluorides	Non-volatile fluorides	
UF ₆ ^a	PuF ₄ ^a	YF ₃
NpF ₆ ^a	CsF	InF ₃
IF ₅	PrF ₃	AmF ₃
TcF ₆	SmF ₃	CmF ₃
RuF ₅	ZrF ₄	CdF ₂
MoF ₆	EuF ₃	PmF ₃
SeF ₆	GdF ₃	RbF
TeF ₆	LaF ₃	AgF
NbF ₅	PrF ₃	BaF ₂
Kr, Xe	SnF ₄	ZnF ₂

^a Important elements forming both volatile and non-volatile fluorides depending on their oxidation state.

The process first involves de-cladding the SNF pins and converting the oxide fuel into granulated powder either by grinding, or by oxidation of UO₂ into higher oxides by voloxidation. The powdered oxides are then subjected to direct fluorination in a flame fluorinator, the ignition temperature of which is ~250°C. As the reaction between oxide fuel

powder and fluorine gas is spontaneous and highly exothermic, the temperature immediately reaches 1500–1700°C. The main purpose of the fluorination process is the separation of actinides from most of the fission products. The separation efficiencies of selected SNF components by using the FVM within the frame of MSTR (Molten Salt Transmutation Reactor) are shown in Table 9. The fluorination reactions of uranium, plutonium, minor actinides, and lanthanides are given in Table 10.

TABLE 9. ACHIEVED SEPARATION EFFICIENCIES OF SELECTED SNF COMPONENT BY USING THE FLUORIDE VOLATILITY PROCESS [163].

Chemical elements	Achieved separation efficiency (%)
U	95–99.5
Pu	~ 98–99.5
Np	~ 60–70
Nb, Ru	~ 95–99
Am, Cm	Individually inseparable (in non-volatile fluoride stream)
FP forming solid fluorides	Individually inseparable (in non-volatile fluoride stream)

TABLE 10. FLUORINATION REACTION OF URANIUM, PLUTONIUM AND LANTHANIDES [163].

Uranium:	$\text{UO}_2 (\text{s}) + 3\text{F}_2 (\text{g}) \rightarrow \text{UF}_6 (\text{g}) + \text{O}_2 (\text{g}),$
	$\Delta_r H^\circ_{298.15} = -1062.4 \text{ kJ/mol U}$
	or
	$\text{U}_3\text{O}_8 (\text{s}) + 3\text{F}_2 (\text{g}) \rightarrow 3\text{UF}_6 (\text{g}) + 4\text{O}_2 (\text{g}),$
	$\Delta_r H^\circ_{298.15} = -955.8 \text{ kJ/mol U}$
Plutonium:	$\text{PuO}_2 (\text{s}) + 2\text{F}_2 (\text{g}) \rightarrow \text{PuF}_4 (\text{s}) + \text{O}_2 (\text{g}),$
	$\Delta_r H^\circ_{298.15} = -722.4 \text{ kJ/mol Pu}$
	or
	$\text{PuO}_2 (\text{s}) + 3\text{F}_2 (\text{g}) \rightarrow \text{PuF}_6 (\text{g}) + \text{O}_2 (\text{g}),$
	$\Delta_r H^\circ_{298.15} = -693.1 \text{ kJ/mol Pu}$
	$\text{PuF}_4 (\text{s}) + \text{F}_2 (\text{g}) \leftrightarrow \text{PuF}_6 (\text{g}), K_p = [\text{PuF}_6]/[\text{F}_2]$
Lanthanides:	$2\text{Ln}_2\text{O}_3 (\text{s}) + 6\text{F}_2 (\text{g}) \rightarrow 4\text{LnF}_3 (\text{s}) + 3\text{O}_2 (\text{g})$

Note: Reaction enthalpies were obtained from the thermochemical data of pure substances.

This method has potential for processing short cooled FR SNFs because of the stability of inorganic fluorides under high radiation.

4. OUTSTANDING ISSUES FOR INDUSTRIAL APPLICATION

4.1. ENGINEERING SCALE DEVELOPMENT

In order to demonstrate the technical feasibility of pyroprocessing and to commercialize the process, studies for scaling-up technologies of unit equipment are required. In addition to the engineering scale equipment design, studies for remote operability and maintainability of process or equipment are also important to realize pyroprocessing at an engineering scale. Increasing remote operability and maintainability is advantageous for equipment operation and safe facility maintenance.

For this reason, KAERI's PRIDE engineering scale demonstration facility for pyroprocessing was developed. The purpose of PRIDE is to support integrated pyroprocessing demonstration and equipment improvement, essential to realize pyroprocessing. PRIDE operates with a 50 kgHM/batch capacity and will use depleted uranium with surrogate materials to show integrated performance and scale-up technologies of full-spectrum pyroprocessing.

The PRIDE cell consists of a large scale argon atmosphere cell (40.3 m length, 4.8 m width, 6.4 m height) equipped with cell operation equipment (e.g. transfer locks, in-cell crane, windows, cell lights, feed-through), remote operation devices (Master Slave Manipulators (MSMs), Bridge-transported Dual arm Servo-Manipulator), utilities.

The major process equipment installed in the argon cell include an electrolytic reducer, cathode processor, electrorefiner, salt transfer system, salt distiller, liquid cadmium cathode (LCC) electrowinner, residual actinide recovery apparatus, cadmium distiller, waste molten salt treatment apparatus. There are also several pieces of process equipment installed within the first floor of PRIDE, namely a voloxidizer, salt waste form fabrication system, UCl_3 fabrication system, and uranium ingot melting furnace.

In addition to the collection of scale-up data of a unit process, the facility enables engineering-scale studies and a test of the material transfers between the adjacent equipment and processes. The cell equipment such as in-cell crane and transfer lock systems have been developed to be able to handle the process equipment, transportation of process materials, and for efficient maintenance. The utility systems for supplying coolant and electricity and high vacuum (HVAC) system were designed to have sufficient capacity.

To transfer the large equipment and materials in and out of the cell, a large equipment transfer system was installed (2.6 m in diameter and 2.2 m in height, up to 2.8 tonnes). This system is equipped with a purging system for exchanging gases (air to argon, or argon to air) so that the inert atmosphere of the cell can be maintained. Within the PRIDE cell, equipment is handled by an in-cell crane with a 3 tonne capacity. To operate the process equipment in the cell, several remote tools were designed and fabricated. MSMs were set up for remote operation and maintenance of the equipment. A bridge-transported dual arm servo-manipulator with six cameras and two robotic arms was developed and installed to handle detailed operations outside of the reach of the MSMs and to provide the operator with a rear view of the equipment.

The PRIDE argon system was developed to control the concentration of impurities (oxygen <50 ppm, moisture <50 ppm) and the temperature (~28–40°C) within the argon cell. A feed-through system for supplying utilities and control signal into the cell was designed to ensure

maintainability of equipment. A sensor system was developed to monitor the temperature, the concentration of oxygen and moisture, as well as the pressure in the argon cell.

4.1.1. Head-end process

An engineering-scale rotary voloxidizer has been developed to fabricate a granular feed for the PRIDE electrolytic reduction process. The batch-type rotary voloxidizer consists of: a voloxidation chamber; a driving system and rollers for rotation of chamber and tilting system; indirect heating unit; gas inlet and outlet ports; special rotary joints. The voloxidation chamber is of horizontally cylindrical type, with a conical frustum made of INCONEL alloy 601 (melting range 1360–1411°C). The thermal treatment temperature for fabrication of granules is limited to 1200°C, in consideration of the melting range of voloxidation chamber material. The tilting system was installed to charge U_3O_8 powder or UO_2 pellets into voloxidation chamber, and to discharge UO_2 particles and granules from voloxidation chamber. The tilting system is driven by hydraulic cylinders. The special rotary joint enables the connection of the rotary voloxidation chamber to non-rotary parts, such as the gas inlet and outlet ports. Thermal granulation is used to fabricate UO_{2+x} granules from tumbling U_3O_8 powder in the rotating voloxidation chamber. UO_2 particles of less than 1 mm are recycled for thermal granulation.

4.1.2. Electrolytic reduction

In 2012, the engineering scale electrolytic reduction system (50 kgHM/batch) was installed within PRIDE and consists of an electrolytic reducer and an electrolytic reduction cathode processor. Prior to the installation of this equipment, only gram scale hot tests of electrolytic reduction had been completed. The purpose of the system was to test scale up of the electrolytic reduction technology using depleted uranium oxides and simulated fuels. The electrolytic reducer produces metals by supplying electrical energy between a cathode basket containing solid oxides and six platinum anodes. The oxygen ion from the cathode basket moves to anodes via a high temperature $LiCl-Li_2O$ molten salt medium and evolves as oxygen gas. Following the reaction, high purity metal including uranium and some non-reduced rare earth oxides remain in the cathode basket. During the electrolytic reduction, Sr and Ba from the simulated fuels are dissolved into the molten salts as chloride forms, and thus separated from the metal products. Around 15–20 wt% residual salts are present in the metal products produced by the electrolytic reducer. The 100 kgHM/batch scale cathode processor can remove these residual salts by distillation, enabling the supply of pure metal to the electrorefiner. The equipment can also separate the metal products from the cathode basket and recover salts in the powder form, which is beneficial for salt transportation. For the practical application of electrolytic reduction technology to the treatment of LWR SNF, engineering scale hot tests using SNF are essential. In addition, efforts such as the optimization of electrolysis cell design and development of alternative anodes should be made to increase throughput and improve economics.

4.1.3. Electrorefiner

The engineering scale electrorefiner installed at PRIDE was developed to deposit uranium only with a graphite cathode. The cylindrical electrorefiner has 25 graphite cathode electrodes arranged in a double layered array in the core part, and a rotating mesh type anode basket (consisting of 4 cartridges) at the periphery of the electrorefiner. The graphite cathode minimizes the sticking of the uranium deposit on cathode surface, so requires no stripping operation [164]. During the electrorefining process, uranium deposits as a uranium-graphite intercalation compound at the outermost layer and a dendritic uranium deposit is then self-scraped, falls down, and is collected at the bottom of the electrorefiner [165]. The fallen deposits

are drawn out by a bucket-type deposit retriever, as follows: a bucket with many small holes is located at the lower part of the transfer pipe, which is opened and connected to the bottom of the electrorefiner. A rotating scraper, which is placed at the bottom of the electrorefiner, turns around and collects the dendritic uranium deposit, and then puts them in the bucket. As the bucket filled with uranium deposit moves up, the molten salt is displaced of the bucket. As the bucket arrives at the upper position, the bottom of the bucket opens, and the deposit pours out.

4.1.4. Salt transport

As the pyrometallurgical separation is carried out using two processes (a uranium deposit process (electrorefining) with a solid cathode, and electrowinning to co-deposit TRU and REEs with LCC), the transport of molten salt from the electrorefiner to the electrowinner is one of the key issues in the Korean pyroprocessing method. Considering the volume difference between electrorefiner and electrowinner, a transportation of salt ingot followed by suction and filling molten salt up mould has been developed.

An engineering scale salt transport system installed in PRIDE has six ingot moulds (mould capacity of 10 kg LiCl-KCl salt) on a turntable. When the TRU surrogate and REEs are accumulated following a electrorefining operation, the salt transport system is connected to the electrorefiner by the upper flange of the latter. A 10 kg molten salt ingot mould is filled by suction using a vacuum system. This is repeated to fill six moulds, and then the moulds are allowed to cool to room temperature. The cooled and solidified salt ingot is separated from the mould by heating the mould's outer surface. Finally, the salt ingots are placed in a storage container and transported.

Preliminary experiments of the suction-based lab-scale molten salt transport system showed 99.5% transport rate (ratio of transported salt to total salt) under a vacuum range of 13.3–1333.2 Pa (0.1–10 torr) at 500°C.

4.1.5. Electrowinning

The electrowinning process is one step of pyroprocessing enabling the simultaneous recovery of uranium and TRUs from the remaining salt using a LCC and follows the electrorefining process. The essential technologies have been developed to enhance the throughput of electrowinning process. In order to demonstrate these technologies, the PRIDE engineering scale electrowinning system was established. It consists of the LCC electrowinning equipment, the residual actinides recovery (RAR) equipment, and the cadmium distiller. The equipment design was based on trials using laboratory scale experimental apparatus and introduced the concepts of remote operation. A 3D test was conducted to review the feasibility of remote operation, with the initial design modified based on the results gathered; the electrowinning equipment installed in the PRIDE argon cell was manufactured based on those results.

During the electrowinning process, uranium and TRU elements are electrochemically co-deposited at an LCC. To increase uranium recovery, a mesh-type LCC structure was installed. The RAR scheme, which combines electrolysis using an LCC and oxidation of REE FPs using a CdCl₂ oxidant, has been established by KAERI. The RAR process equipment allows recovery of residual uranium in the salt transferred from the LCC electrowinning equipment, resulting in the recycle of actinides and the minimization of waste volume. In the RAR scheme, LiCl-KCl salt is used as electrolyte. Chlorine gas evolves from the anode since it is made of glassy carbon and graphite. The LCC electrowinning and RAR equipment have a capacity of 80 kg of salt and 10 kg of cadmium per batch. Using selective distillation, Cd is recovered to recycle as a cathode material in the LCC electrowinning equipment, and the residual U is transferred to an ingot

casting furnace to produce a metal fuel ingot. The capacity of the Cd distiller is 10 kg of cadmium per batch.

4.1.6. Remote handling and automation

Due to the nature of the process characteristics, pyroprocessing should be conducted within a completely sealed argon cell or shielded hot-cell. As all the equipment has to be operated and maintained remotely out of cell, development of remote handling is an important part of pyroprocessing scale-up. A conventional remote handling system consists of several mechanical MSMs, a master-slave servo-manipulator, a power manipulator, radiation-hardened industrial robots, cranes, etc; these components can be selectively chosen for a given task. The ability to maintain this equipment remotely has top priority. One common approach is to duplicate the same module for the redundant use; the spare module can be utilized while a failed module is repaired in a maintenance area. Another approach is to replace the failed module with a new one remotely. All equipment and devices have been designed as an assembly of modules, taking into consideration easy attachment/detachment for replacement.

In order to achieve higher throughputs in pyroprocessing, automation is required. Automation is a proven technology and widely used in the industrial field. However, sensors and electrical motors are not durable under radiation, and it is still restrictively implemented in nuclear facilities, normally only in areas of low radiation or low complexity. For pyroprocessing, there is no commercialized facility, and all current operations and maintenance are performed through either manual operation or master-slave operation. Therefore, automation technologies should be developed simultaneously with process equipment. The development of radiation-hardened components to an integrated control system is an area of further study.

4.1.7. Safeguard technology development in Republic of Korea

In contrast with conventional aqueous reprocessing, pyroprocessing has higher proliferation resistance as pure uranium and pure plutonium are not separated. This is one of the major considerations for the inclusion of pyroprocessing as part of future nuclear energy systems. Safeguardability of pyroprocessing is one of the advantages of pyroprocessing technology. High performance nuclear material accounting technologies and the effective safeguards system are very important and should be established as part of its commercialization.

Conventional nuclear material accounting technologies used in aqueous reprocessing facilities cannot directly be applied as there are many types of process materials, including heterogeneous plutonium and uranium, and a high radiation field from the FPs.

Nuclear fuel cycle facilities such as DFDF, the ACPF, and PRIDE have been built with their safeguards systems developed by KAERI. A non-destructive neutron measurement device, the DUPIC safeguards Neutron Counter (DSNC) was developed by KAERI through a joint collaboration with Los Alamos National Laboratory (LANL) [166]. It was authorized by IAEA and it has been operated since 2000 (Fig. 47). KAERI also developed the ACP Safeguards Neutron Counter (ASNC) for nuclear material accounting in the ACPF [167] that is presented in Fig. 48. The measurement principle of the ASNC is similar to the DSNC, but has a higher detection efficiency, and it is designed for remote repair and maintenance within high-radiation hot cells. C/S systems for the DFDF and the ACPF were also developed to collect and analyse the radiation and the image information using the neutron monitor and the survey cameras, and the undeclared movement of the nuclear material could be detected in real time. A unified NDA, in which three independent signals, such as neutron counting, gamma-ray spectroscopy, and

weighing, are collected simultaneously from the process materials has been developed for the PRIDE nuclear material accountancy system. An integrated safeguards information system for PRIDE is being developed to collect and display the survey images, nuclear material accounting data, process monitoring data, and safeguards information.

KAERI and the Korea Institute of Nuclear Non-proliferation and Control (KINAC) has conducted a Member State Support Programme (MSSP) entitled “Support for Development of a Safeguards Approach for a Pyroprocessing Plant” since 2008. A reference engineering-scale pyroprocessing facility (REPF) was designed. It was designed with a process batch size of 50 kgHM, campaign throughput of 500 kgHM, and annual throughput of 10 tHM. A material balance area (MBA) and key measurement point (KMP) of the REPF were identified, and possible nuclear material accounting methods for each KMP were proposed. A simulation programme called Pyroprocessing Material flow and Material unaccounted for Uncertainty Simulation (PYMUS) was developed to analyze the nuclear material flow and to calculate the material unaccounted for uncertainty of the REPF.

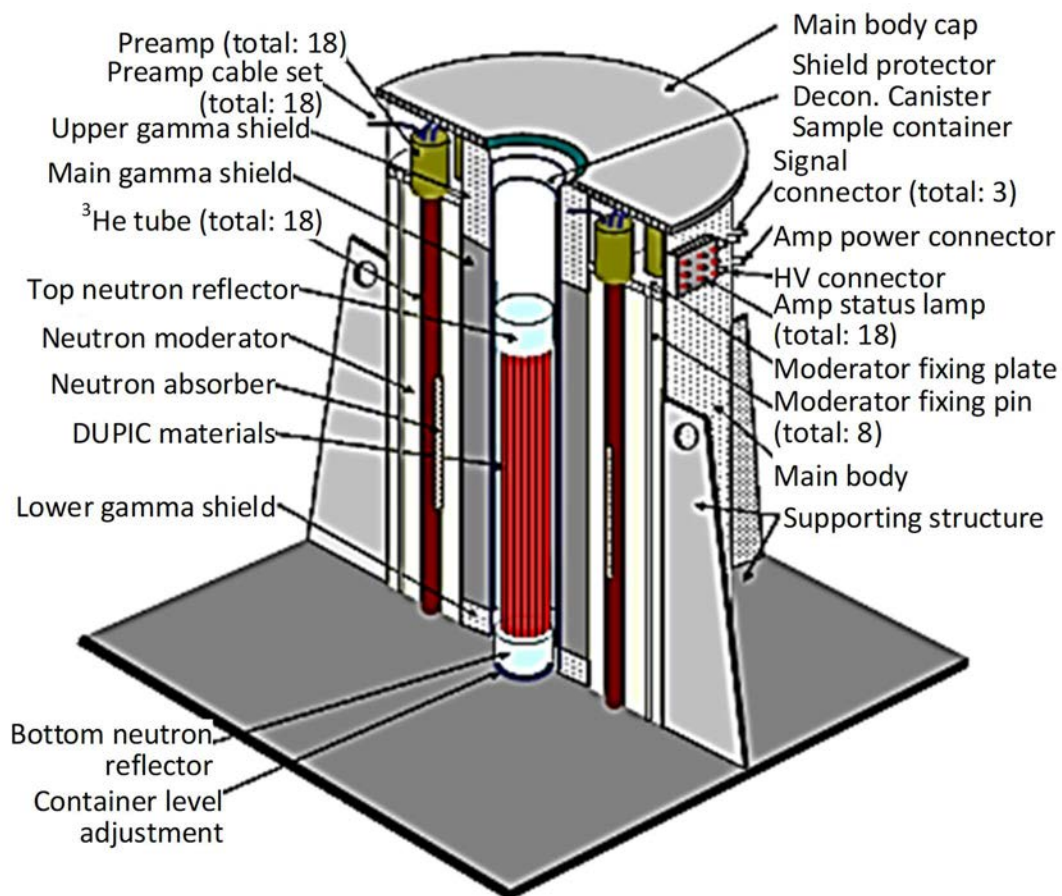


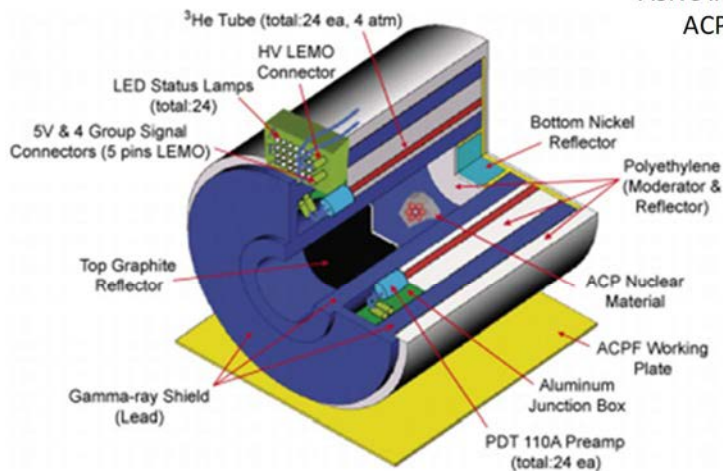
FIG. 47. DUPIC Safeguards Neutron Counter (reproduced courtesy of KAERI).

ACP Safeguards Neutron Counter (ASNC)

- A passive neutron coincidence counter
- **Gamma-ray shield:** 6 cm lead
- Sample cavity: Φ 21 cm x 33 cm
- **Neutron detection efficiency:** 21%
- **Full remote maintenance** capability (LEMO connectors)
- Developed in cooperation with LANL
- Deployed at the ACPF in 2005



ASNC installed in the ACPF hot cell



3D MCNPX model of the ASNC

FIG. 48. ACP Safeguards Neutron Counter (reproduced courtesy of KAERI).

A Joint Fuel Cycle Study (JFCS) between Republic of Korea and USA to explore the technical, economical, and non-proliferation acceptability of pyroprocessing technology was agreed. Collaborations on safeguards have been completed, including seven technically focused areas: safeguards technical direction and analysis; safeguards testing with irradiated material; technology for nuclear material accountancy; technology for containment and surveillance; safeguards for dry storage and repositories; modelling and simulation; and safeguards and security by design.

The application of conventional safeguards technologies used for accountancy of nuclear materials should be investigated and new safeguards technologies should be further developed to establish and improve the safeguardability of pyroprocessing. The Republic of Korea has experience in the development and implementation of nuclear material accounting instruments and safeguards systems for the nuclear fuel cycle facilities. R&D efforts are ongoing through close international collaboration to achieve the safeguards approach for the pyroprocessing.

4.2. PRODUCT PURITY IN PYROPROCESSING WITH METAL ELECTROREFINING

4.2.1. Benefit of increased product purity

4.2.1.1. Uranium product purity

Pyroprocessing of spent oxide fuels from nuclear power plants is designed to recover most of the uranium to be used in FRs. Electrorefining of chloridized spent nuclear fuel in LiCl-KCl salt leads to the deposition of the majority of uranium metal in the melt onto the solid cathode. Impurities in the uranium metal product may include TRU elements and other transition metals, as well as trapped salts. The majority of the recovered uranium is expected to be stored for an extended period of time prior to FR utilization. The inclusion of excessive amount of radioactive species will force uranium deposits be stored as either intermediate level waste or high level waste, which incur higher storage costs.

The contamination of uranium deposits with an excessive amount of TRU elements can raise more serious issues relating to accountancy of sensitive nuclear materials, particularly plutonium. As the deposition of plutonium starts near the end of electrorefining process, there can be a significant concentration gradient within the uranium metal near the surface. The uranium salt distillation process will facilitate plutonium removal, making materials accountancy more complicated. Therefore, it is more desirable to terminate the uranium electrorefining process at a point ensuring an adequate margin against the initiation of plutonium deposition.

If an excessive amount of uranium is left behind following electrorefining, the electrowinning process can be utilized for its recovery. An LCC will dissolve uranium and TRU elements, while limiting the entry of REEs. A subsequent distillation of the LCC produces a mixture of uranium and TRU elements. If the product is to be used for producing critical FR uranium based fuels, the quantity of uranium in the distillates does not present any disadvantage. More often than not, additional uranium will be required to achieve the desired uranium composition in the fuel. In this case, the only disadvantage of carrying excessive uranium into electrowinning process will be the increased volume of liquid cadmium cathode to balance the actinide composition.

If a subcritical FR is to be used, the effectiveness of using the double strata approach should be examined. As the subcritical system with its inherent neutronic safety features can burn fuels consisting of TRU or MA elements only, the inclusion of uranium can degrade the support ratio of the transmutation system.

4.2.1.2. Fuel product purity

Pyroprocessing has a limited separation capability for actinides against REEs, this feature provides a 'dirty fuel standard', with the resulting product containing a significant amount of radioactive FPs, providing an intense radiation barrier to theft. An excessive quantity of REEs can cause fuel fabrication difficulties.

For metallic fuels, REEs can introduce regions of low melting point and hence, can aggravate fuel-cladding chemical interactions. The immiscibility of REEs produces intermetallic precipitates; the introduction of intermetallic compound can affect the homogeneity of the fuel composition during casting process [168].

For oxide fuels, sintering of fuels particles requires fine control of the metal to oxygen atom stoichiometry. An inclusion of an excessive amount of trivalent REEs can cause oxygen deficiency, potentially decreasing the melting point. A mismatch in the oxide crystal structure between actinides and REEs may limit the structural stability of fuel pellets.

The inclusion of REE impurities present greater issues for nitride fuels. A large difference in the lattice parameters of actinide nitrides and lanthanide nitrides are reported [169], resulting in a miscibility gap. Therefore, REE impurity limits are more restrictive for nitride fuels.

4.2.1.3. Fission product target product purity

Iodine and technetium are two long-lived FPs that require particular consideration. Where a waste repository is to be sited in a reducing environment (such as granite bedrock), iodine garners particular attention due to its high solubility and migration behaviour.

The transmutation of iodine requires no isotopic separation, but high purity compounds are required for thermal and radiation resistance, and it has been found that sodium iodide is the most stable compound for the target. In order to produce a stoichiometric composition, impurities have to be minimized. Often, silver has been used to recover iodine from gaseous releases during head-end processes; the voloxidation process is demonstrated to recover over 99% of the iodine inventory of spent oxide fuels [170]. Contamination of silver iodide during the production of NaI should be minimized.

Tc is a noble metal with good miscibility with several metallic elements and has thermal and radiation resistance. Tc can be captured from the volatile release of Tc_2O_3 during the voloxidation process [170]. Its purification is needed in the production of metallic target materials and no isotopic separation is necessary.

4.2.1.4. Caesium and Strontium product purity

Caesium and strontium represent the majority of heat source in the final wastes. The higher the heat sources, the greater potential for leaching and migration of radioactive species due to their thermal driving forces. Using voloxidation, up to 98% of caesium can be recovered during the vaporization process. The remaining caesium is dissolved in molten salt, and additional recovery can be achieved by undertaking a zone refining process of the molten salt. Strontium can be recovered from molten salt by a precipitation process [171].

In many countries, it is planned that caesium and strontium will be stored within surface stores for a period of about 10 half-lives, after which they can be disposed of as low level wastes. If they can be sufficiently purified, they have potential in other applications. Caesium can be used as a radioactive (gamma) sources within irradiation facilities including sterilization and environmental remediation. Purified strontium can be used for beta sources with moderate shielding. Due to its high power density and long half-life, some applications may warrant an investment in purification capability.

4.2.2. Material flow and product purity

The electrorefining with metal electrorefining produces a mixture of actinides in a liquid metal cathode, in which the uranium content should be adjustable by collecting uranium in a solid cathode. An example calculated material flow for spent oxide fuel treatment is shown in Fig. 49, along with estimated material losses after rinsing of the cladding hulls and scrubbing of the waste salt.

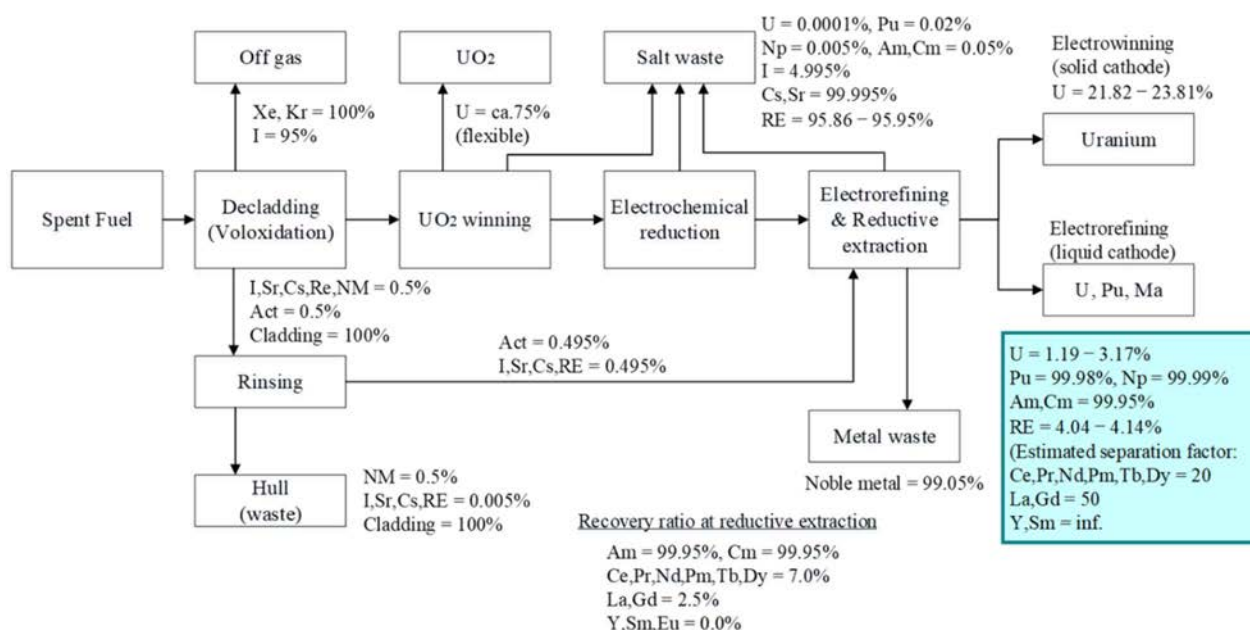


FIG. 49. Material flow on spent oxide fuel treatment.

The estimated composition at a liquid cadmium cathode in this process is given in Table 11, based on treatment of LWR spent oxide fuel.

TABLE 11. ESTIMATED COMPOSITION AT LIQUID CADMIUM CATHODE.

	SNF			
	UO ₂ , 45 GWd/t	UO ₂ , 60 GWd/t	MOX, 45 GWd/t	MOX, 60 GWd/t
Uranium (wt%)	46.5	45.7	47.0	46.4
Plutonium (wt%)	46.5	45.7	47.0	46.4
MA (wt%)	4.6	5.9	5.2	6.0
REEs (wt%)	2.3	2.7	0.8	1.2

4.2.3. Characterization of the product

The product given in Table 11 has the radiation properties shown in Table 12. This table compares the properties of plutonium recovered by PUREX type reprocessing of LWR SNF, weapon grade plutonium, and TRU recovered from pyroprocessing.

TABLE 12. RADIATION PROPERTIES OF PRODUCTS.

	Radiation type				
	Alpha-activity (Ci)	N-activity (n/s)	Photons/s (Gamma radiation)	MeV/s	Decay heat (W)
Per g of TRU pyrochemically produced	1.53E+00	8.80E+04	1.10E+10	2.30E+08	5.20E-02
Per g of LWR Pu	8.50E-01	1.40E+03	5.00E+09	5.10E+07	2.70E-02
Per gram of weapon-grade Pu	9.00E-02	1.30E+02	2.90E+08	3.10E+06	3.00E-03

Moreover, due to similarities in electrochemical potential, there will be REE impurities present in the pyrochemical product.

The TRU product has a lethal dose with high neutron activity and high energy gamma radiation, thus requiring a heavily shielded hot cell facility for handling. In addition to radiation, the high heat production of the product also requires consideration for operations.

4.2.4. Reduction of process losses

Voloxidation, hull electrorefining, and PyroRedsox (Pyrochemical reductive extraction and selective oxidation) processes all play an important role in enhancing separation efficiency and reducing the final waste volume.

The voloxidation process is the preceding step to the electrolytic reduction process and is a combination of volatilization and oxidation reactions [172]. To enhance the efficiency of electrolytic reduction, the voloxidation process oxidizes SNF from UO_2 to U_3O_8 ; the subsequent volume expansion splits and separates SNF from the Zr-4 cladding. In this process, a small amount of volatile fission products including iodine and technetium are generated as gases that can be trapped by filters. The solid pieces of uranium, TRUs, and FPs are oxidized at the operating temperature of 1200°C [173]. Noble metals, caesium, technetium from the SNF are filtered in the off-gas treatment system [174, 175]. Caesium is transferred to storage, and technetium and iodine are fabricated into transmutation targets for use in a nuclear transmutation system.

The separated cladding hulls (containing small amounts of uranium and TRUs from voloxidation process) and uranium and noble metals from the electrorefiner anode are introduced to the hull electrorefining. PWR cladding (irradiated Zircaloy-4) would be classed as high level waste without further treatment. If zirconium can be efficiently separated from actinides and FPs, it can be inexpensively disposed of in low and intermediate level waste sites. Electrorefining can be used to achieve this decontamination. This process has been tested using a Zr-2 BWR channel box in Japan, rather than fuel cladding due to various restrictions on performing separations processes on active fuels. Therefore, the ability to numerically simulate the Zr electrorefining process and validate against available data is, thus, viewed as critical for development of this technology.

Waste salts containing trace amounts of actinides are normally managed as HLW. PyroRedsox — a combined process of pyrochemical reductive extraction and selective oxidation — is designed to further decontaminate salts of actinides. Salts that will be subjected to PyroRedsox include the used molten salt from electrorefining and electrowinning processes, and contaminated bismuth resulting from the molten salt purification process after hull electrorefining process. PyroRedsox uses bismuth liquid metal in order to obtain high separation efficiency between the molten salt and the liquid metal.

In the PyroRedsox process, molten salt from electrorefining and electrowinning process contacts bismuth liquid metal. REEs of bismuth are selectively oxidized by BiCl_3 to molten salt, leaving the actinides in the liquid bismuth. Oxidized REEs can be obtained in the form of precipitated solid oxides by providing oxygen gas into the molten salt. Because of the difficulty in achieving complete separation of actinides and REEs, actinides in the bismuth are oxidized to the molten salt that is then recycled to electrorefining. Clean bismuth is transferred to the PyroRedsox process. As a final waste stream, precipitated REEs are treated as a ceramic waste form that includes a small quantity of actinides.

4.3. PROCESS MODELLING

4.3.1. Overview of process modelling development

The application of computational methods in pyrochemical reprocessing studies has made a valuable input towards the fundamental understanding of various issues in the flowsheet. Johnson proposed thermochemical modelling of the electrorefining process based on the equilibria among pairs of elements and their respective chlorides, which could be envisaged to exist at the interface between the anode and the electrolyte, as well as that between the cathode and the salt [176, 177]. A mass tracking code ‘PYRO’, or pyroprocess, was developed by Ackerman [178–180]. The results of the model for uranium, plutonium and REEs were validated by the experiments of Tomczuk et al. [181]. Kobayashi et al. developed a code ‘TRAIL’ (Transportation of Actinides in Electrorefiner) based on the diffusion layer theory [182], which was validated by several experiments using different sizes of electrorefiners. A code called ‘DEVON’ (Detailed Evaluation of Potential Distribution) has been developed on the basis of the Laplace equation to estimate the effect of polarization on cell resistance as well as on ion current distribution, which are solved by finite element methods [183–186]. A similar code ‘PALEO’ (Program for Analyzing Electrorefining Operation) by Kobayashi et al. [187] was developed to model the recovery of uranium at the solid cathode from the spent molten salt using a cadmium-lithium anode. Li et al. have developed the ‘FIDAP’ computation code for the electrical field distribution in the Mark-IV electrorefiner and potential gradients near the cathode [188–192]. A computational model for the Mark-IV electrorefiner by Hoover et al. [104] has been developed for modelling the dissolution of the SNF at the anode taking into account uranium, plutonium, and zirconium. Ahluwalia et al. modelled the electrotransport of uranium from a liquid cadmium anode to a solid cathode based on surface overpotential and Butler-Volmer kinetics called ‘GPEC’ (General Purpose Electrochemical Code). The model predicts the current structure at the liquid cadmium anode and also explains the bell shape of the deposit observed with this mode of electrotransport on the basis of multinodal simulations [193–196]. A more complicated time dependent model has also been given by Bae et al. known as ‘REFIN’ which employs both convective and diffusive mass transport [197, 198]. The results of the model match with that of the previous model TRAIL and those of the experiments carried out by Tomczuk et al. Modelling of the electrorefining process has also been carried out as a part of a private sector initiative between United States and Japan [199–206] and the PYROREP

project [207]. Nawada et al. have earlier reported a model which was also based on the lines of thermodynamic equilibria discussed by Johnson. It used fractional mass transport coefficient (FMTC) and relative fractional mass transport coefficient (RFMTC) [208–210].

Ghosh et al. [211] have developed ‘PRAGAMAN’ code, based on equilibrium thermodynamic considerations similar to Nawada et al. and Johnson et al., and is considered more robust and versatile in terms of its ability of giving unique solutions to many of the different conditions arising in the electrorefiner which was not possible in the one by Nawada et al.

Multi-physics based electrochemical modelling within the framework of computational fluid dynamics to simulate the electrotransport behaviour in the molten salt has been carried out by Kim et al. [212]. The numerical assessment of high throughput electrorefiner using computational fluid dynamics code CFX has been recently carried out by Lee et al. [84, 85].

4.3.2. Process modelling at KAERI

KAERI’s modelling architecture consists of three-tiered models: unit process; operation; and the plant-level model.

The unit process model can be addressed using governing equations and empirical equations as a continuous system. This level model focuses on the SNF element behaviour by chemical reaction or electrochemical reaction in molten salt. Well known governing equations, such as Nernst and Butler-Volmer equations, are applied with empirical parameter adjustments based on the experiment. A unit process model is being developed throughout the overall process: voloxidation, oxide reduction, electrorefining, electrowinning, waste salt treatment, metal waste treatment and off-gas treatment. Some process modelling has completed its first version. Things to be considered in numerical calculation are to use an efficient algorithm to solve differential equations or optimization problems.

In contrast to the unit process model, the operation model describes operational behaviour as a discrete event system. Operational issues can be set up by modelling the transferring, storing, withdrawing, and feeding of various forms of material as material flows. This model can interface unit process models to make an integrated process model. Rigorous modelling is based on the acquisition of operational data: utilization of resources such as machines, human operators and transportation vessels, and operation time, procedure, and change of material forms.

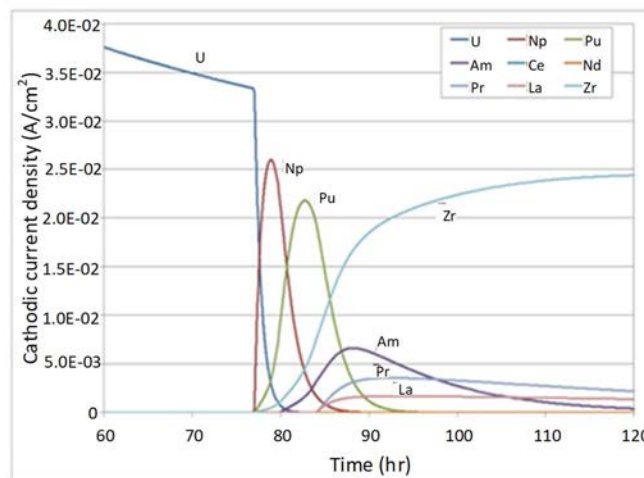
A plant-level model is an integrated model of unit process and operation model based on a framework of dynamic material flow and database connection. At this level, various analysis modules can be added in the model enabling us to analyse safeguards issues, recommend pyroprocessing technology development, evaluate cost and support license, permits and approvals relevant to engineering scale or commercialized facility in the future.

4.3.3. Modelling of electrorefining process

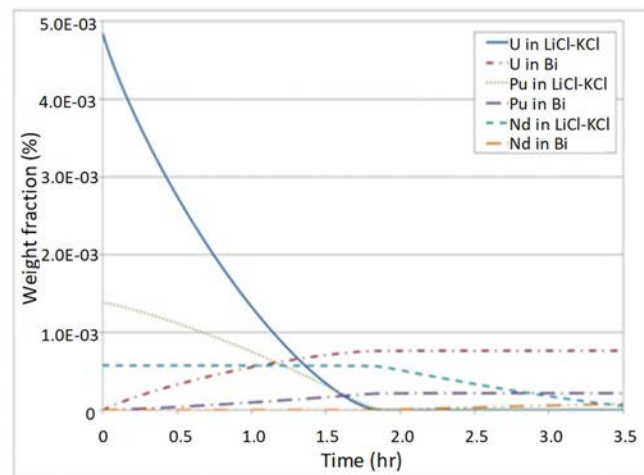
In order to optimize each recovery process of pyroprocessing with low-cost and reduced experimental trial and error, a design approach using computational models is necessary. Therefore, various groups have developed a number of computational models including REFIN [213], PYRO [214], TRAIL [182], and GPEC [193]. Despite significant improvements in experimental and modelling studies, there is still inconsistency and uncertainty between experiments and simulations. One of the main reasons may be the irregularity of effective anode

area variation with complex dendrite growth at the cathode surface, which is definitely required to be considered in computational design and analysis [215–217].

Seoul National University (SNU) has developed REFIN, a one-dimensional electrochemical reaction code, and simulated nuclide behaviour in electrorefining, reductive extraction and selective oxidation. Figure 50(a) represents the cathodic current densities for each element during electrorefining and Fig. 50(b) indicates variation of weight fraction of each element in molten salt and liquid bismuth during reductive extraction. Using results such as these from computational models, the deposition behaviour of the cathode, electrorefining operational time to achieve high purity uranium recovery, and the separation factor of reductive extraction and selective oxidation can be predicted.



(a)



(b)

FIG. 50. Modelling results for (a) electrorefining and (b) reductive extraction by REFIN [218].

SNU has also developed a 3D electrochemo-hydrodynamic model to design and evaluate an electrorefiner for spent nuclear fuels treatment in pyrochemical partitioning. The developed model was utilized for the benchmark of applied cell potential as a function of time during

Mark-IV electrorefiner experiments conducted by INL [219]. The results have shown that the three-dimensional model predictions were in good agreement with experimental results. In addition, the model was used for predicting local TRU contamination on the cathode during electrorefining based on the applied current, rotational speed of electrodes, and weight fraction of nuclides in molten salt.

These computational models can be effectively deployed for system design and determination of operating conditions for each process in pyroprocessing. However, due to uncertainties in modelling, in addition to experimental variation such as anode dissolution and cathode deposition behaviour during electrorefining, the formation of inter-metallic compounds during reductive extraction using liquid metal, and limitations of current models, greater effort is required in obtaining experimental data sets for developing numerical model and benchmarking studies.

For this reason, a benchmark using the developed 3D model has been carried out against data obtained from a rotating hull cell experiment. The rotating hull cell experiment has been widely used as a proven technology for investigating electrochemical behaviours as it enables generation of a single experiment to utilise a wide range current density along the working electrode and a change in the hydrodynamic conditions such as diffusion boundary layer thickness, according to the rotational speed of the cylindrical working electrode [220].

The experiment was conducted with a solution containing $50 \text{ mmol/dm}^3 \text{ Cu}^{2+}$ ions under various applied currents and electrode rotational speeds. The applied current densities selected were below the limiting current density for each rotational speed. Figure 51 shows the overpotential distribution at the cathode according to various rotational speeds. There are minor discrepancies between the simulated results and experimental data, but the tendency of distributions showing that non-uniformity increases as applied current density rises show good agreement with the experimental results. Therefore, these results reveal that the 3D modelling approach is appropriate for electrochemo-hydrodynamic simulation.

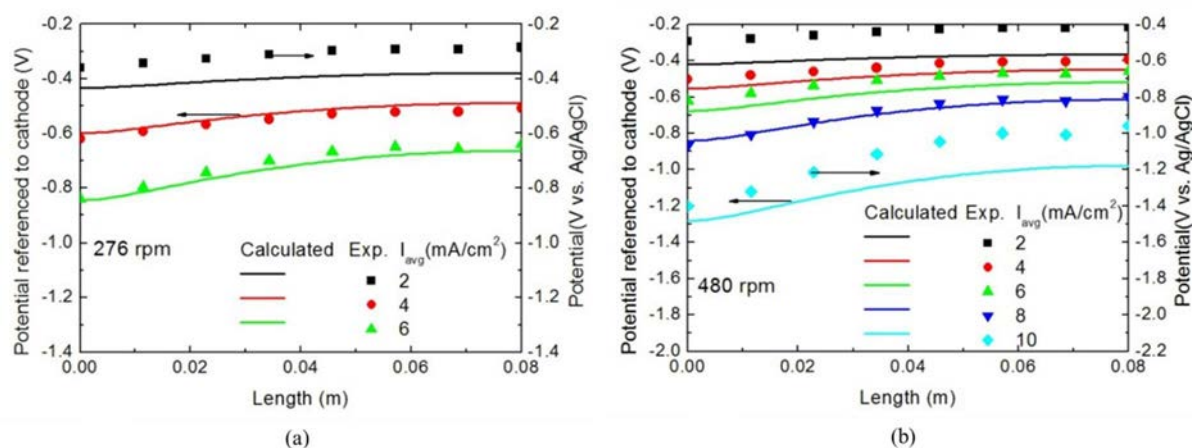


FIG. 51. Comparison of simulated results and experimental data on overpotential distribution along the working electrode (working electrode rotational speeds are (a) 276 rpm and (b) 480 rpm (reproduced courtesy of KAERI)).

Until now, multi-element electrochemical reaction simulations have been mainly conducted using one-dimensional computational code, and three-dimensional simulation has been performed by using current density correlations generated by one-dimensional electrochemical reaction codes. However, in order to reflect the hydrodynamic effects resulting from the complicated electrorefiner geometry and electrochemical effects from the multi-element reaction in modelling, a 3D multi-element electrochemo-hydrodynamic model should be developed in the future. In addition, the experimental and modelling studies on anode dissolution behaviour and cathode deposition morphology for various operating conditions are also required so as to reduce the uncertainties and discrepancies between modelling and experimental results.

4.3.4. Anodic dissolution model of metallic fuel

4.3.4.1. Anode dissolution model

The anodic dissolution of U-Zr or U-Pu-Zr fuels is the most influential factor in determining the process rate and dissolution rate, both of which directly affect the design and specification of the pyroprocessing facility. Since zirconium has a high standard redox potential next to that of uranium, some zirconium dissolution will occur along with the actinides if the uranium in the fuel is completely removed by the anodic dissolution. Dissolved zirconium in the electrorefiner is reduced again by a chemical reaction or cell circuit formation on the electrorefiner, which returns actinides to the electrolyte again. A considerable part of such reduced zirconium would form minute particles of poor adhesion, fall onto the electrolyte, and finally accumulate in the electrorefiner. It is also predicted that high dissolution ratio of zirconium has a negative influence on the decontamination against noble metal FPs, since zirconium in the anode residue is considered to collect these FPs in its fibrous structure [46, 47, 221]. Iizuka et al. developed the anodic dissolution model with a layer formation model in the electrorefining stage, based on the assumption that dissolution of actinides and zirconium is a diffusion-controlled process [213]. Figure 52 shows the schematic presentation of anodic dissolution along the anodic alloy. In this model, the surface layer consists of the anode residue and a diffusion layer at the molten salt electrolyte side of the anode surface. Undissolved alloy and porous zirconium layers are located at the central and outer regions of the anodic residue, respectively.

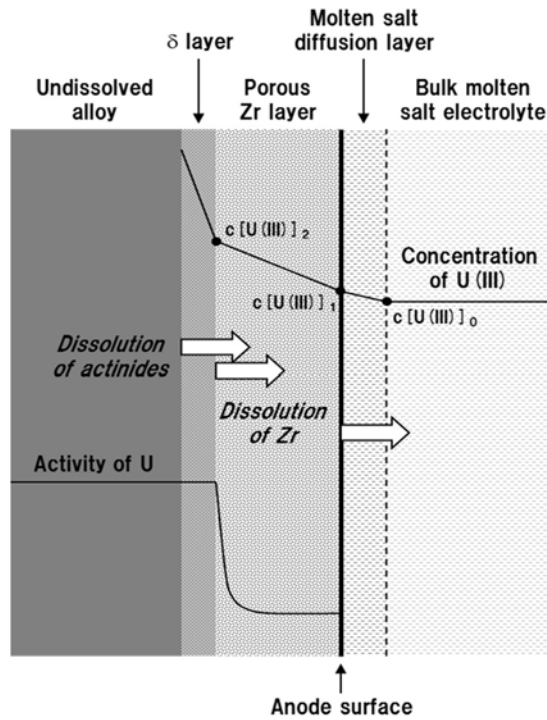


FIG. 52. Schematic presentation of anodic dissolution along anodic alloy [221].

The presence of an intermediate layer in between the diffusion layer and surface layer with a composition corresponding to the δ phase (layer) has been proposed based on experimental observations. The δ layer, the porous zirconium layer, and the molten salt diffusion layer act as diffusion barriers to the dissolved actinides species. The δ layer is formed as an intermediate state of the anodic dissolution of the actinides from the undissolved metal fuel alloys. Fine cracks were observed in the δ layer by the decrease in the volume due to the dissolution of some part of actinides. These cracks with a narrow width act as a path for the diffusion of the dissolved actinides from the undissolved alloy layer. The effective diffusion coefficients of dissolved actinide species in this layer were defined as the rate to migrate to the outer region through these cracks, which are considered to be significantly lower than that the migration rate in the bulk molten salt electrolyte.

The porous zirconium layer is formed by the further dissolution of the actinides from the δ layer. The outer diameter of this layer was the same as that of the alloy before the anodic dissolution while most zirconium was left undissolved. A small amount uranium was observed analytically, even following an electrorefining operation for a few days.

Based on this model, the anode potential was assumed to be determined by the local equilibrium in a redox reaction between uranium species at the surface of this layer. As it was assumed that the actinides were supplied from the undissolved alloy, or from the surrounding layer through the diffusion layer after the actinides was anodically dissolved, the Nernst diffusion model was adopted. Regarding plutonium, as it does not come into contact with the electrolyte until the coexisting uranium starts to dissolve due to the lower standard redox potential of plutonium, this model assumes that the plutonium anodic dissolution rate is proportional to that of uranium, according to their existing ratio in the undissolved alloy.

The parameters to be assumed or measured for calculation using this model are as follows:

- Diffusion coefficients of U(III), Pu(III) and Zr(IV) in LiCl-KCl at operating temperature;
- Diffusion coefficients of U(III), Pu(III) and Zr(IV) in porous zirconium layer at operating temperature;
- Diffusion coefficients of U(III), Pu(III) and Zr(IV) in δ layer at operating temperature;
- Solubility of actinides and zirconium chlorides, UCl_3 , $PuCl_3$ and $ZrCl_4$ in LiCl-KCl;
- Thickness of molten salt diffusion layer;
- Composition and density of U-Zr and U-Pu-Zr alloys;
- Composition and density of δ layer;
- Composition and density of porous zirconium layer;
- Standard electrode potentials of U(III)/U(0), Pu(III)/Pu(0) and Zr(IV)/Zr(0);
- Cell resistance in electrorefining test;
- Phase segregation in irradiated or annealed alloy.

These parameters (assumed or measured) are listed in Table 13.

TABLE 13. PARAMETERS AND PROPERTIES USED IN ANALYSIS OF ANODE BEHAVIOUR [221].

	U(III)	Pu(III)	Zr(IV)
In bulk LiCl-KCl	1.0×10^{-5}	1.13×10^{-5}	
Diffusion coefficient in porous Zr layer (cm^2/s , at 773K)	0.7×10^{-5}		
Diffusion coefficient in δ layer (cm^2/s , at 773K)	1.0×10^{-8}		
Solubility in LiCl-KCl (mol frac., at 773K)	0.15 in total	0.013	
Standard redox potential at 773K	-1.25	-1.55	-0.85
	U-Zr	U-Pu-Zr	
Density (g/cm^3)	15.9 [202]	15.9	
Composition (wt.%)	Zr: 9 wt% U: balance	Pu: 19 wt% Zr: 10 wt% U: balance	
Diameter (cm)	0.29	0.24	
Cladding	Stainless-steel	-	
Molar density (mol/cm^2)	U: 0.0616 Zr: 0.0136	U: 0.0474 Pu: 0.0126 Zr: 0.0174	
Molar volume (cm^3/mol)	33.7		
Thickness of diffusion layer (cm)	Engineering scale test using U-Zr		0.025 [193]
	Small scale test using U-Pu-Zr		0.050

4.3.4.2. Calculation results and discussion

The anodic dissolution model was applied to the engineering-scale electrorefining test with several kilograms of U-Zr-FP alloy loaded in the anode in an initial concentration of 2.05 wt% uranium in LiCl-KCl eutectic salt [47]. The calculation results using the layer formation model are given in Fig. 53. Because the current applied in the early stage of this test was high, 450 A, and then reduced down to 5 A, the results reflect that dissolution of zirconium would start at the early stage and that 55.1% of the zirconium loaded in the anode would be dissolved at the end of the calculation. The experimental test in this condition confirmed the dissolution of zirconium with 45.8 %, indicating the model assumption that dissolution occurs only at the chopped section of SNF (i.e. planar-type model), reproducing the anode behaviour. In case of the clad U-Zr alloy pins chopped to various lengths, the effect of the ratio of the side face area to the chopped face appears. The calculation results reveal that the anodic dissolution of the clad U-Zr alloy pin progresses preferentially in the axial direction and that the anode behaviour estimated by the planar-type model is in good agreement with the experimental

results. However, it was found that the discrepancy between the calculated and experimental results became significant for longer pins due to the cylindrical surface of the alloy against the cladding tube working as an anode surface, in addition to the chopped section. It is also expected that the undissolved region in the anode residue becomes round in shape as the solution comes close to completion, while it is simply assumed to become thinner in the planar-type model. Therefore, an extension of the anode dissolution model to three dimensions is required in parallel with the observation of the irradiated fuels during the anode dissolution to improve the precision in the calculation.

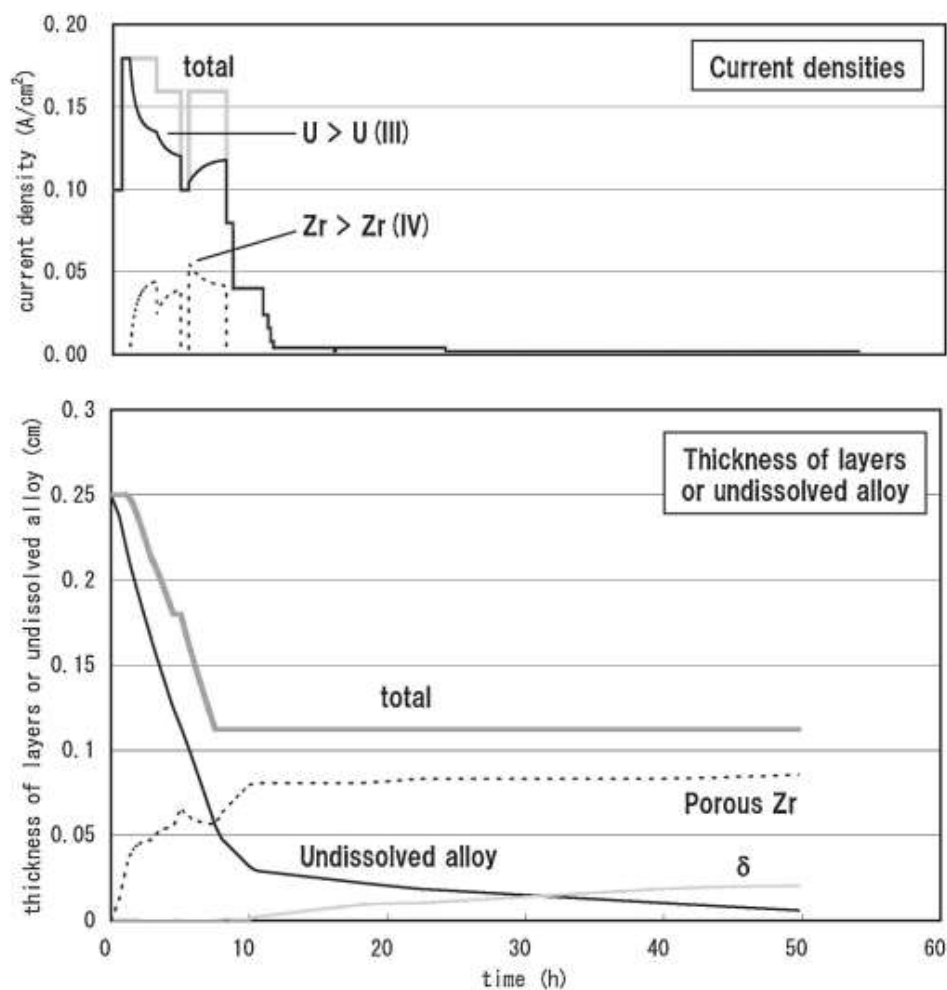


FIG. 53. Change in partial current densities and thickness of layers in anode residue Run E-5 calculated by planar type anode model [221].

Calculation of the anode potential using the anode model was conducted using small-scale electrorefining tests of 10 g of U-Pu-Zr. The calculated anode potentials and current density vs. electric charge are given in Fig. 54 with the experimental data. The electric charge passed between the electrodes and the thickness of the layers in the radial direction of the pins, which are taken as the X and Y axes, respectively.

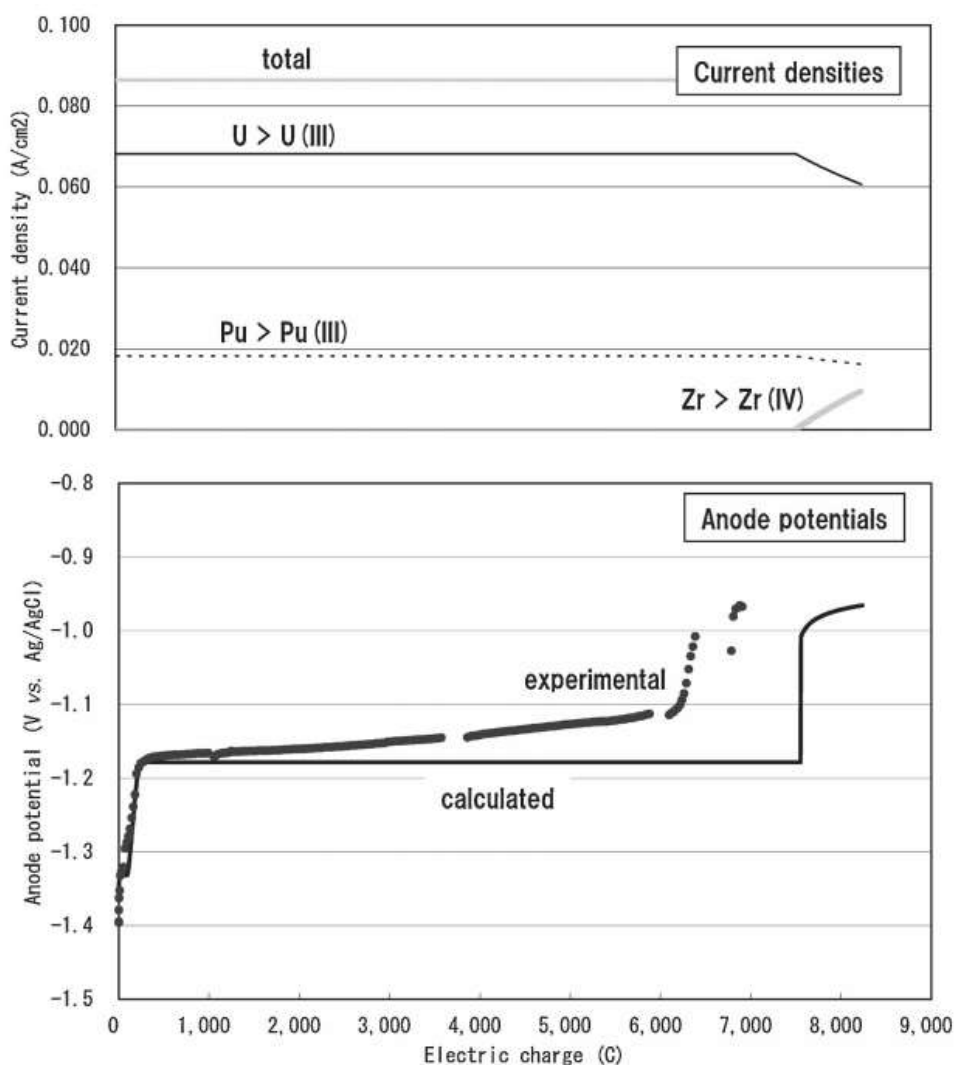


FIG. 54. Change in partial current densities and anode potential during electrorefining tests using U-Pu-Zr ternary alloy calculated using the cylindrical-type anode model [221].

The calculated result reproduces the anode potential observed, such as the rapid rise at the beginning and near the end, and the plateau in between. The rise of potential at the beginning of the test is caused by the growth of the δ and porous zirconium layers. While the thickness of the porous zirconium layer continues to increase even after the initial anode potential rise, the uranium activity approaches its lower limit (ca. 2.0×10^{-4} assumed in this model) and its influence on the anode potential quickly becomes moderate. The second rapid increase in the anode potential is due to the fact that the concentration of U(III) in the porous zirconium layer reaches its solubility and that this layer is dissolved to maintain the anode current density.

Differences were observed between the calculated and experimental results. The anode potential in the experimental data continued to increase slowly in the period between two rapid rises, while the calculated anode potential remains constant over the same period. There are some hypotheses for this difference in appearance. One is that there was some inhomogeneity or distribution of the porous zirconium layer thickness at the anode surface. The actual anode potential is considered to be determined by a statistically representative value of this thickness distribution that should gradually increase until zirconium begins to dissolve. Another

possibility is the change of the uranium activity dissolved in the solid alpha-zirconium phase. The concentration of uranium allowed in this phase seems low, so its diffusion coefficient must also be very low. However, its concentration at the surface, which determines the electrochemical potential, might possibly be decreased by long term anodic dissolution.

Moreover, the following information or parameters are required to improve the precision of the calculation; such as, exact estimation of the solubility of actinides in molten salt electrolyte and the diffusion coefficients in the porous zirconium layer, observation of the irradiated fuels during the anodic dissolution, and extension of the anode model to a 3D system.

4.3.5. Computational model for the Mark-IV electrorefiner

4.3.5.1. Motivation and approach

A pair of computational models for INL's Mark-IV ER have been developed as a joint project between INL, KAERI, SNU, and UI [219]. The Mark-IV ER has been used at INL to separate uranium from spent EBR-II driver fuel. KAERI and SNU developed a rigorous 3D model [222], while INL and UI focused on a less computationally intensive 2D model [103-105, 223]. These two computational models were derived based on fundamental electrochemical, thermodynamic, and kinetic theories. The 2D model is based on the interfaces within the Mark-IV ER across which mass transfer and electrochemical reactions occur, with the primary focus on the anode/molten salt and molten salt/cathode interfaces. To further reduce complexity, only three species have been investigated: uranium, plutonium, and zirconium, which constitute greater than 90% by mass of the spent EBR-II driver fuel [99].

4.3.5.2. Model development

The developed 2D model is based on fundamental electrochemical theory for both the cathode and anodes, as shown by the equations in Fig. 55 [104, 222]. With a combination of the three constraints shown, it is possible to develop a system of three equations to solve the problem. For N species, these three equations result in N , N , and 1 total equations, respectively, creating a system of $2N+1$ equations and $2N+1$ unknowns (I_i , $\eta_{i,s}$, and E_t). This system can be solved using any number of optimization routines. This new method allows the user to alter any of the 'known' variables (e.g. exchange current density, initial salt composition, mass transfer coefficients, interfacial surface area.) without affecting the overall solving scheme. It also enables the investigation of different studies for each interface, while not altering the solving scheme of the other interfaces.

$$\begin{aligned}
E_{ij} &= E_i^0 + \frac{RT}{z_i F} \ln(\gamma_{i,s} X_{i,sj}) & I_{ij} &= i_0 A_{tj} \left(e^{\frac{z_i \alpha F}{RT} \eta_{i,sj}} - e^{-\frac{z_i (1-\alpha) F}{RT} \eta_{i,sj}} \right) \\
C_{i,sj} &= C_{salt} X_{i,sj} & \sum_i I_{ij} &= I_{cell} \\
N_{ij} &= k_{ij} A_{tj} (C_{i,sj} - C_{i,salt}) & E_{tj} &= E_{ij} + \eta_{i,sj} \\
I_{ij} &= z_i F N_{ij}
\end{aligned}$$

In red: guessing variables|

In blue: variables known from thermodynamic data and/or operating conditions

Constraints:

- (1) $I_{ij}(E_{ij}) = I_{ij}(\eta_{i,sj})$
- (2) $E_{tj} = E_{ij} + \eta_{i,sj}$
- (3) $\sum I_{ij} = I_{cell}$

FIG. 55. Modelling approach organization, where subscript i represents the species and subscript j represents the interface. E_{ij} is the equilibrium potential, $X_{i,sj}$ is the mole fraction at the electrode surface, $C_{i,sj}$ is the concentration at the electrode surface, C_{salt} is the total bulk salt concentration, N_{ij} is the molar mass transfer, I_{ij} is the partial current, $\eta_{i,sj}$ is the overpotential at the electrode surface, E_{tj} is the total electrode potential and all other variables are defined in Table 14.

4.3.5.3. Computational procedure

The commercial software ‘Matlab’ has been used to execute the aforementioned numerical scheme. To limit computational complexity, currently only U(III), Pu(III) and Zr(IV) have been considered. However, more species may be included with sufficient thermodynamic data. The selection of these three specific species is not arbitrary. First, uranium is the principle element of interest, as the purpose of the electrorefining process is to separate the uranium from the SNF and because it is the most prevalent species [183]. Second, plutonium is also an important constituent in these calculations because its behaviour in previous experimental work involving U-Pu-Zr alloys has been difficult to determine [183]. Third, zirconium is the most active of the noble metals present in the SNF; therefore, the separation of uranium and zirconium is of great interest and is one of the primary goals of the anodic process in the ER. It should also be noted that zirconium is the second most prevalent species in the SNF [223]. As there are three species in the present study, N is three and both the anode and cathode systems to be solved consist of seven equations and seven unknowns.

4.3.5.4. Important parameters

Many parameters can be obtained directly from system thermodynamics. However, there are other parameters that must be determined from directly specified conditions. Parameters used in the model and equations illustrated in Fig. 55 are summarized in Table 14.

TABLE 14. PARAMETERS USED IN THE MODEL AND EQUATIONS [216].

	U/UCl ₃	Zr/ZrCl ₄	Pu/PuCl ₃	LiCl/ KCl	Total/ mixture
A _{i,a} , Initial anodic surface area (m ²)	0.476	0.257	0.013	-	0.746
C _{i,salt} , Initial bulk salt concentration (mol/m ³)	557	0	16.9	27974	28547
E _i ⁰ , Standard reduction potential (V vs. Ag/AgCl)	-1.274	-1.088	-1.555	-	-
F, Faraday constant (C/eq)			96485		
i ₀ , Exchange current density (A/m ²)			0.5		
I _{cell} , Applied cell current (A)			40–100 (see Fig. 58)		
k _{i,a} ⁰ , Initial anodic mass transfer coefficient (m/s)	4.70×10 ⁻⁶	4.00×10 ⁻⁶	3.89×10 ⁻⁶	-	-
R, Ideal gas constant(J/molK)			8.314		
T, Operating temperature (K)			773		
z _i , Valence (eq/mol)	3	4	3	1	-
α, Anodic transfer coefficient			0.4		
γ _{i,s} , Activity coefficient	0.00139	0.00448	0.0041	-	-

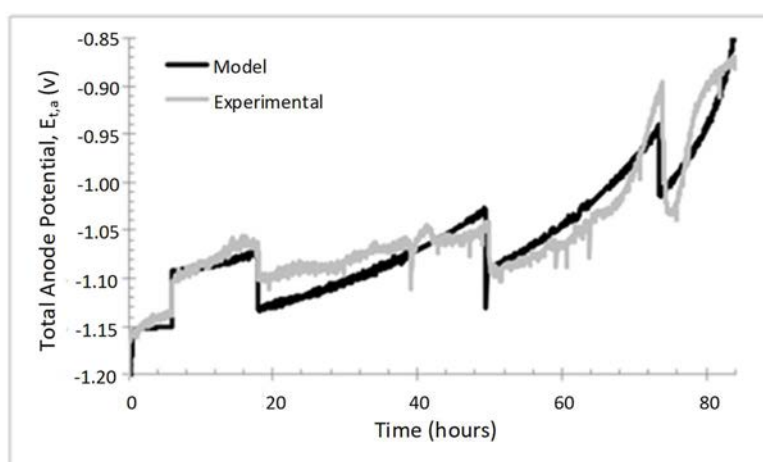
Data from a set of electrorefining experiments run in the Mark-IV ER have been used to facilitate the modelling process. The experiment was run with two anodes and one cathode, which was exchanged for a fresh one approximately 39 hours into the run. The modelled experiments were run in a controlled current mode with an applied current, I_{cell}, changing periodically as shown in Fig. 56.

Accurate modelling of the interfacial surface areas at both electrodes is incredibly important as the electrochemical reactions of most interest take place across these interfaces. The total anodic surface area is modelled as decreasing with each individual species' available surface area as a fraction of the total. The cathode surface area increases as the electrorefining process progresses and material is deposited onto the cathode. The cathode has been modelled as a smooth cylinder growing as current is passed.

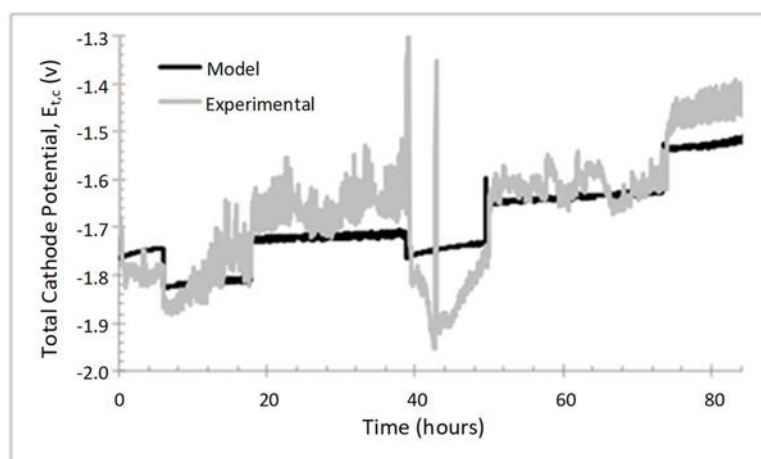
The mass transfer coefficients at both the anode and cathode, k_{i,a} and k_{i,c}, are a measure of how well species *i* can move through the boundary layer separating the electrode surface and the bulk electrolyte. The initial values are calculated for both electrodes using a Sherwood correlation for a rotating cylinder. Anodic mass transfer coefficients are assumed to decrease as the SNF is dissolved as discussed in previous work.

4.3.5.5. Results and discussion

The calculated anode and cathode potentials as compared with the experimental potentials in the Mark-IV ER can be seen in Fig. 56. The modelled total potential trends are seen to match well with the experimental trends throughout the electrorefining process. The values calculated for the anode match the experimental results with an RMS error of 1.83% [104], while those calculated for the cathode have an RMS error of 3.79%. The large oscillations in the cathodic experimental data are likely due to the rough and uneven growth of deposits on the cathode. As previously mentioned, the cathode is modelled as a smooth cylinder, which results in a relatively smooth potential plot.



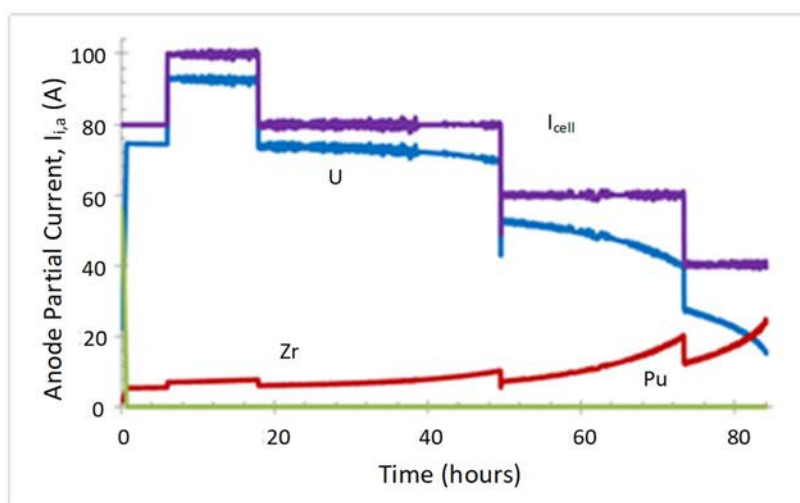
(a)



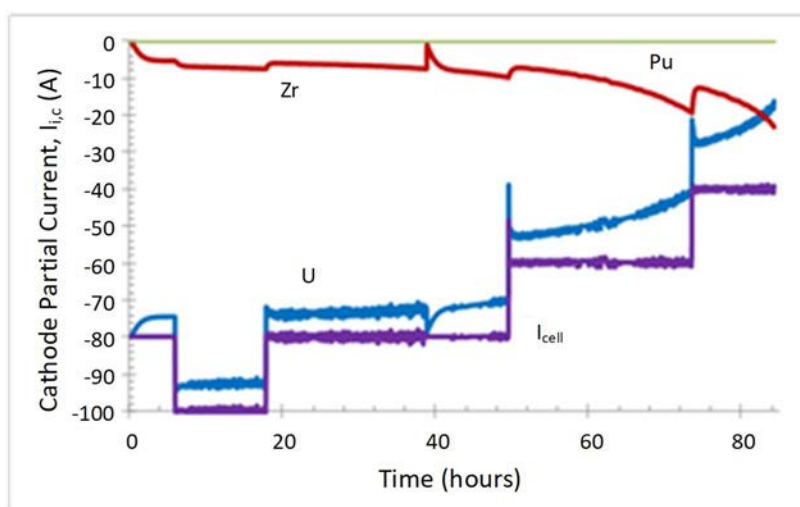
(b)

FIG. 56. (a) Anode and (b) cathode potential comparisons [216].

The partial currents at both electrodes are another important parameter to analyse. The partial current can be used to calculate the rate at which each species is being either dissolved from the anode or deposited onto the cathode using Faraday's Law. The calculated partial currents can be seen in Fig. 57.



(a)



(b)

FIG. 57. (a) Anode and (b) cathode partial currents [216].

Figure 57 shows that the majority of the current is involved in uranium dissolution at the anode. However, as the electrorefining process proceeds, more zirconium is electrochemically dissolved. At the cathode, the majority of the deposited product is, as desired, uranium. As the amount of zirconium being dissolved from the anode into the electrolyte increases, more zirconium ions are available in the bulk electrolyte to be deposited along with uranium at the cathode.

4.3.5.6. Two-dimensional distributions

The 2D potential and current distributions within the Mark-IV ER are essential in determining the mass balance and location of the different species within the ER. A material balance can be performed within the Mark-IV ER and simplified to show that the Laplace equation, $\nabla^2 \phi = 0$, can be used to describe the potential distribution within the molten salt electrolyte. This equation is solved with a Neumann boundary condition, $\nabla \phi = 0$, at the ER wall and the anode/cathode potentials, $E_{t,a}/E_{t,c}$, from the model at the respective electrode surfaces to find

the potential distribution. From the solution and a version of Ohm's law, $i = -\kappa\nabla\phi$, the current distribution can be solved.

Matlab is used to calculate the potential and current distributions within the electrolyte because it has a partial differential equation solver using the finite element method. In the modelled run, the ER was operated with two anodes and one solid steel cathode as shown in Fig. 58. For simplicity, the rotating cruciform anodes and dendritically growing cathode have been considered cylindrical. The radius of the cathode increases throughout the electrorefining process as a function of the amount of deposited material as described previously.

To calculate the current distribution, the electrical conductivity, κ , of the bulk electrolyte needs to be calculated. For the modelled system containing Li^+ , K^+ , U^{3+} , Zr^{4+} , Pu^{3+} , and Cl^- ions, the total conductivity is found to be almost constant throughout the electrorefining process at 205 S/m [105].

The total potential and current distributions at ten hours into the experiment are plotted in Fig. 58(a) and 58(b) respectively. From both distributions, the majority of the current is seen to flow directly between the two anodes and the cathode. The distributions throughout the electrorefining process appear similar with the potential gradients tending to increase as the cathode grows and the process proceeds [105]. The potential gradient in the lower region of Fig. 58(a) is small with little current (Fig. 58(b)), and therefore there are few moving ions in this area of the ER. Hence, a possible second cathode could be placed in this region to better use the available space within the ER.

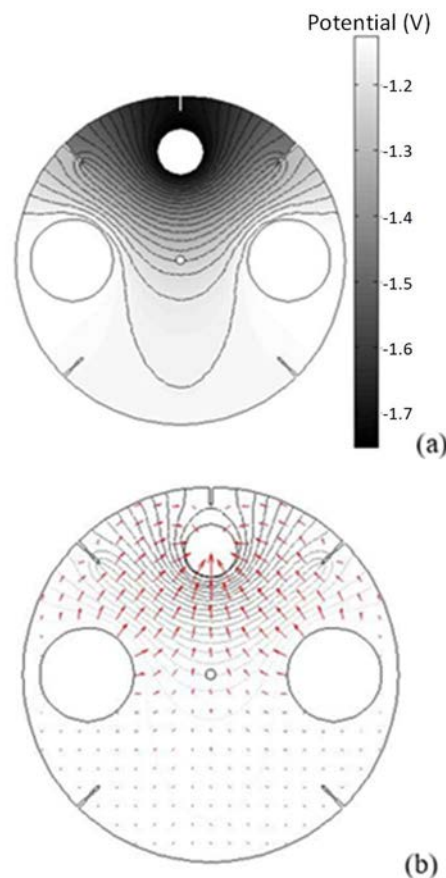


FIG. 58. (a) Potential distribution and (b) current distribution at 10 hours into the experimental run [105].

4.3.5.7. *Summary*

A simplistic optimization routine has been developed and applied to the electrochemical reactions occurring at both the anode and cathode of an ER utilized for the electrochemical processing of SNF. This routine has been incorporated into a computational model of the Mark-IV ER, currently operational at INL. Results from the modelling process reveal that plutonium is rapidly exhausted from the anode fuel baskets. Throughout the remainder of the electrorefining process uranium is the main species being both dissolved from the anode and deposited on the cathode. However, as time progresses, zirconium dissolution and deposition start to become important processes. The total electrode potentials as calculated by the model were compared with potentials from a set of experiments run in the Mark-IV. The calculated and experimental potentials are shown to match with RMS errors of 1.83% and 3.79% for the anode and cathode, respectively.

The 2D potential and current distributions within the bulk electrolyte of the Mark-IV ER have also been examined. The total electrical conductivity of the molten salt electrolyte depends upon composition and is shown to be ~ 205 S/m. The potential distributions show the highest potential gradients exist directly between the anodes and cathode. The regions furthest from the operating electrodes have small potential gradients and little ion movement.

Future work on the ER model development will include increasing the number of species being examined. The model currently includes species making up greater than 90% of the mass of the SNF and the inclusion of additional species should increase the accuracy of modelling the process. The dendritic deposition of uranium at the solid cathode will be further investigated to include this uneven, somewhat random, growth pattern. These studies will involve more accurately determining the actual exchange current density within the Mark-IV ER from experiments.

5. ECONOMIC ASPECTS OF PYROPROCESSING

5.1. BACKGROUND

Ko et. al. [224] has performed economics analysis in various nuclear fuel cycle options including pyroprocessing option linked to SFRs. They chose four nuclear fuel cycle options considerable in a foreseeable future under the nuclear power situation of the Republic of Korea: once-through cycle, DUPIC recycling (DUPIC), thermal recycling by using MOX fuel in PWR (PWR-MOX) and SFR recycling employing pyroprocessing (Pyro-SFR). This chapter summarizes the results of Ko's paper which is a systematic cost comparison among these nuclear fuel cycles.

5.2. MATERIAL FLOW OF NUCLEAR FUEL CYCLE OPTIONS

Four fuel cycle options considered in this study are specified by the breakdown structures consisted by series of components, as shown in Fig. 59, respectively.

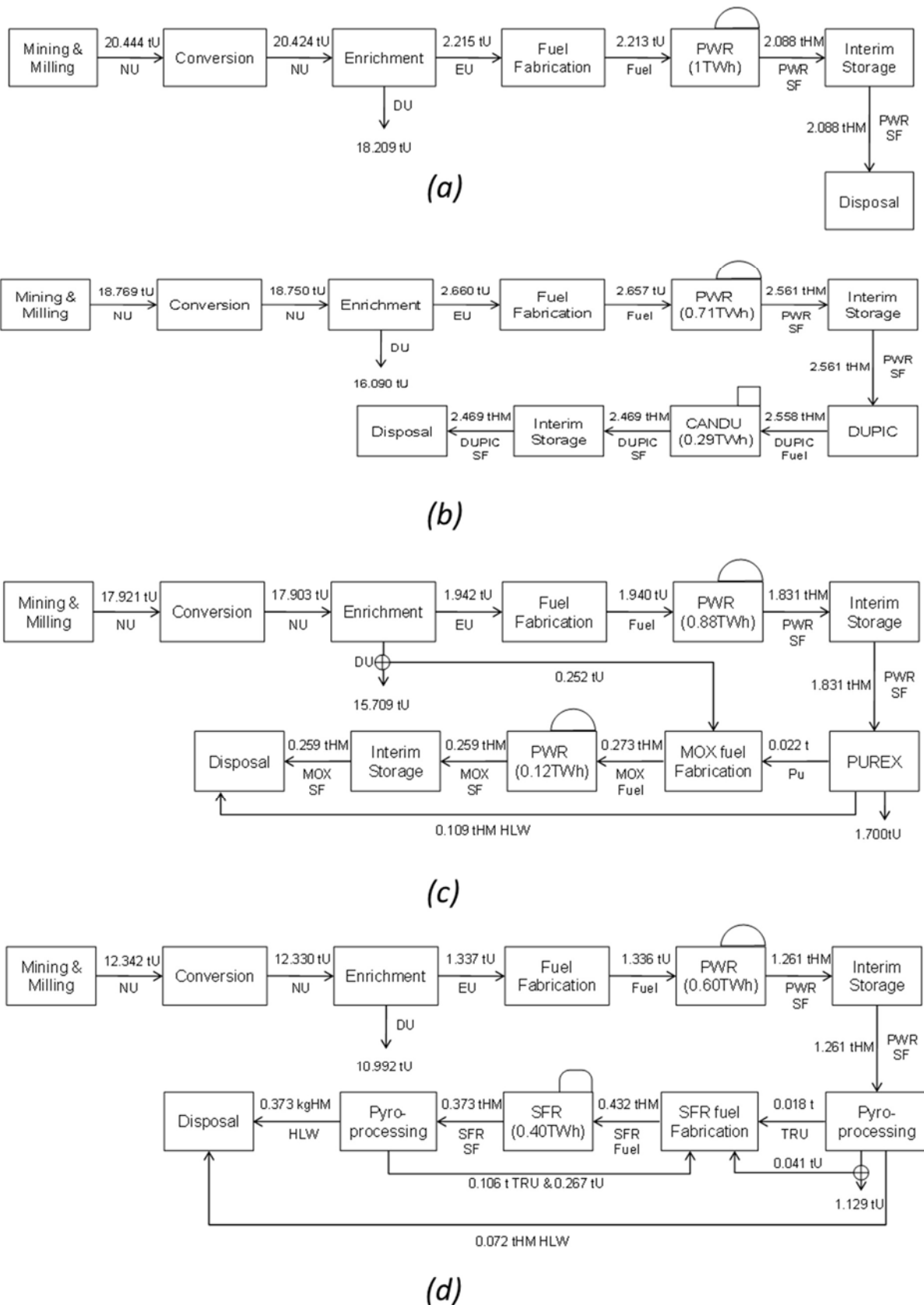


FIG. 59. Main components in nuclear fuel cycles (a) Once-through cycle (b) DUPIC recycling (c) PWR-MOX recycling (d) Pyro-SFR recycling [224].

A FR utilizes fast neutrons of which higher energy can burn both ^{235}U and TRU elements. This aspect makes it possible to transmute the TRUs and extract energy at the same time. In Pyro-SFR recycling, shown as Fig. 59(d), the PWR SNF would be reprocessed to obtain TRU-bearing fuels for the FRs, while the remaining uranium partitioned from the PWR SNF would be disposed of as low and intermediate level radioactive wastes. In this cycle, an SFR with a conversion ratio of 0.6067 is considered as the reference FR. Pyroprocessing has been developed to reprocess the oxide fuels discharged from PWRs and to fabricate metallic fuels containing TRU for future SFRs. The metal fuelled SFR using alloys of Actinides-Zirconium (AcZr) has a high potential for recycling actinides by being integrated with the pyroprocessing. The TRU fuel after burning in SFR would be repeatedly reprocessed by pyroprocessing and the recovered TRUs would be recycled into SFR to close the fuel cycle.

The material flow values in Fig. 59 were calculated using the equilibrium model based on 1 TW/h electricity output [224].

5.3. ECONOMICS OF NUCLEAR FUEL CYCLE OPTIONS

The results from Monte Carlo simulation are shown in Table 15 and Fig. 60. With the assumption that each of the unit cost is triangular distribution, a total of 50,000 extractions of Latin Hyper curve were performed. The standard deviation (SD) for the low fuel cycle cost (LFCC) ranges between 1.16~1.69 mills/kWh (1 mill = 0.1 cents) as shown in Table 15. The difference between the LFCC of Pyro-SFR and once-through is 0.04 mills/kWh concerning the mean data, which is much smaller than the SD for the once-through option, 1.69 mills/kWh. This means the cost of Pyro-SFR fuel recycle lies within the error bound of the Direct Disposal option. The cost of DUPIC and PWR-MOX also have the possibility to fall into the error bound of once-through, respectively, but their possibilities are relatively smaller.

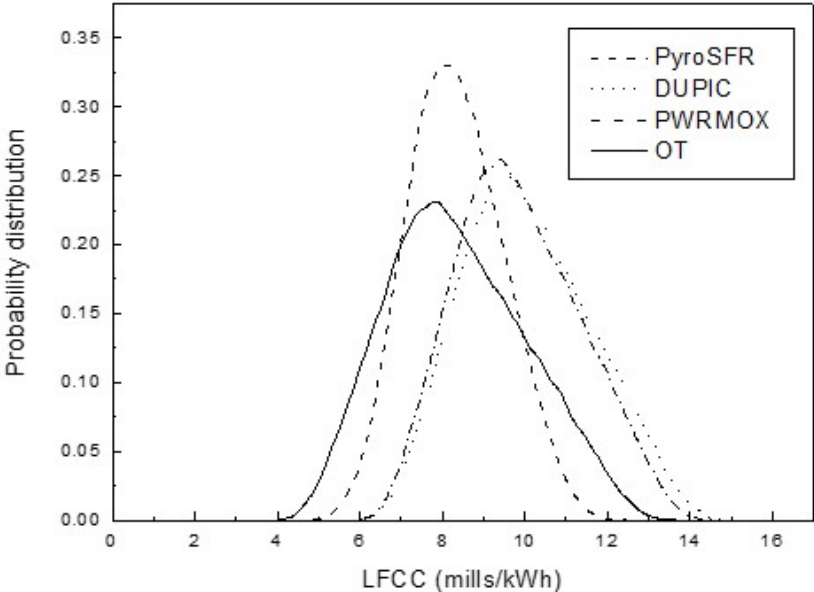


FIG. 60. Comparisons of the probabilistic density function of LFCCs using a triangular distribution [224].

TABLE 15. RESULTS OF THE MONTE CARLO SIMULATION FOR THE UNCERTAINTY ANALYSIS OF LFCCS [224].

	Once-through	DUPIC	PWR-MOX	Pyro-SFR
Min	3.99	5.68	5.74	4.51
Max	13.79	15.30	14.77	12.64
Mean	8.35	10.06	9.83	8.31
SD	1.69	1.57	1.55	1.16

In conclusion, even though the means value of the Pyro-SFR is a little lower than that of the once-through fuel cycle, the difference in the fuel cycle cost between the Pyro-SFR and once-through fuel cycle is negligible, considering the uncertainty associated with the unit cost of the fuel cycle components. Therefore, other factors such as technological and political risk, environmental effects, public acceptability, and non-proliferation, could play important roles in determining a future nuclear fuel cycle option [224].

6. SUMMARY AND CONCLUSIONS

Pyrochemical processes have been the subject of active research during the last decade in respect of the advantages in chemical and nuclear compatibility, and proliferation-resistance when applied to partitioning and transmutation of radionuclides present in spent nuclear fuels. Some Member States and International Organizations are involved in the development of advanced nuclear fuel cycles that could effectively incorporate actinide recycling to reduce inventories of plutonium and minor actinides. In particular advanced partitioning methods based on pyroprocesses are being developed and investigated, keeping in mind the immense role of pyrochemical processing of spent metallic, oxide and nitride fuels in actinide recycling that reduces long term radio-toxicity considerably.

Pyroprocessing technology has not yet been proven as a mature technology for commercial implementation. China and India, requiring a large energy increment, have initiated studies on pyroprocessing of metal FR fuel for attaining high breeding ratios. Some countries, such as France, Japan, Republic of Korea, and Russian Federation, that have historically used nuclear energy are exploring this fuel cycle technology for advanced Generation IV nuclear systems. Some programmes are in the stage of developing an engineering scale device for the electrorefiner and others, such as the fuel treatment programme of EBR-II spent metal fuel with the MARK-IV and MARK-V electrorefiners in INL, USA and the verification of spent oxides fuel treatment with oxide electrorefining in CRIEPI, Japan, KAERI, Republic of Korea, and RIAR, Russia are promising developments of engineering scale installation.

Meanwhile, significant effort is still required to implement pyroprocessing at a commercial scale. Development areas for achievement of the implementation goal that have been discussed in this publication are summarized below:

Establishment of flowsheets

Comprehensive flowsheet studies are required in order to minimize the process losses with residual actinides recovery from waste salt. The salt cleaning makes an inevitable role to significantly reduce the waste volume. An off-gas treatment system with/without high temperature salt fume is also required.

Specification of product composition with rare earth impurities

The concentrations of the various fission products in the cathode deposit depends on several factors such as their concentrations in the molten salt electrolyte, current, anode and cathode potentials. The composition of the product from the cathode deposit, especially with respect to REE FPs, could pose problems during fuel re-fabrication due to their solubilities in U-Zr alloys. Hence studies are required to optimise the process parameters to achieve a product of desired composition. The product composition effectively influences the fabrication of homogeneous fuel. Minimizing the amount of REEs should be beneficial for fuel fabrication (e.g. large immiscibility of rare earth in U-Zr alloy, i.e., less than 1% solubility).

Treatment of bonded sodium

Part of the bonded sodium in the metal fuel pin would form sodium iodide with the FP iodine and it may partly remain as sodium metal. During electrorefining, metallic sodium would form sodium chloride, and after a few batches of electrorefining, it could increase the liquidus temperature of electrolyte above 500°C. Its removal from the electrolyte is also difficult. Hence, it is desirable to remove the bonded sodium before loading the chopped pin segments into the

electrorefiner and methods have to be developed for its effective removal, or studies on the influence of bond sodium during electrorefining will be required.

Physico-chemical characterization of multi-components molten salts

An assessment of the physico-chemical properties that may impact the behaviour of multi-components molten salts (i.e. solubility, volatility, influence of oxygen ingress, heat capacity, viscosity, achievement of phase diagrams, etc.) is urgently required both in chloride and in fluoride media. Experimental programmes should specifically address the gaps in knowledge for molten salt systems of interest in order to evaluate different aspects of the processes. Special attention should be given to so far non-available properties of An and FP in molten chlorides or molten fluorides salts. In addition, modelling should be further developed in order to build tools that would be able to predict these physico-chemical data and then, help to optimize the experimental programs.

High volatility of americium

One of the advantages of pyroprocessing is MA recycling. However, the high volatility of americium present along with U and Pu would be a problem during injection casting. The lower thermodynamic activity of americium when present as an alloy with U-Pu-Zr would reduce its vapour pressure. Nevertheless, its behaviour during injection casting needs to be studied.

Fuel casting requires more than 1200°C. The vaporization of americium has a high rate with increasing temperature. Though the activity of americium in molten metal with U-Pu-Zr largely decreases, the americium behaviour should be evaluated at the casting stage for fuel fabrication.

Waste treatment/solidification and long term durability

This applies to not only waste salt, but also other different kinds of wastes, such as alpha contaminated solid waste, and filters containing captured salt/metal should be treated to make a stable form. The long term durability, i.e., soundness and leachability of such waste forms should be evaluated.

Engineering installation, engineering-scale equipment

The pyroprocessing consists of several steps, decladding, voloxidation electrorefining, cathode processing, fuel casting, waste treatment/solidification, and off-gas treatment, the engineering design of each requires a handling device that has to be fully operated remotely in an inert atmosphere; this aspect is quite important to enable commercial deployment. This extends to transport and remote maintenance of all devices from the outside of the hot cell. This system largely affects the operational capability of the facility.

Process monitoring and analytical techniques for salt and metal media

Analytical control methods used for pyroprocesses generally requires sampling and further dissolutions in aqueous media. Such methods are time consuming in term of samples preparation and results interpretation and may delay important choices or decisions while operational. Moreover, they lead to the production of aqueous waste that needs to be processed.

Thus, the development of on-line monitoring systems for molten salt processes is of a primary importance for a future industrial process implementation and routine controls. Some techniques already identified, i.e. Raman spectrometry, LIBS (Laser Induced Breakdown Spectroscopy) should be investigated and further developed for reliable qualitative and quantitative analysis.

Modelling and computational simulation

Although several developments on process modelling and computational simulation have been reported for the electrorefining process and the electrorefiners, the need exists for enhancing the efforts in this area to optimize flowsheets and for optimising the design of the equipment such as electrorefiner, cathode processor etc. An integrated model incorporating all the process steps needs to be developed.

Safeguardability

The ease of safeguards applications to aqueous processes depends on the sampling of the solution from the dissolver which provides information on the inventory of fissile material in the facility. Meanwhile, the pyroprocessing has no capability to receive the uniform material to validate the total fissile material in the process. The complete difference system has to be developed, in which how to get the shipper-receiver difference should be established, and in which position the key measuring points (KMP) should be implemented. The containment and surveillance (C&S) and the near-real time nuclear material accountancy (NRTA) will be effectively deployed. The ICT gravimetric method gives potential information for the shipper-receiver difference. In the case of processing blanket fuels, new credibility of non-proliferation has to be regulated.

Finally, it may be concluded that P&T is a multidisciplinary approach, where a closer collaboration and a better integration of the different disciplines involved would improve the chances of a successful implementation. P&T deployment can be foreseen in a few decades from now in the best case. This means a mandatory need to preserve knowhow through consistent P&T programmes. The rationale and the motivation to develop a P&T scenario are very similar in the different countries. The priorities in the implementation process might sometimes differ. P&T implementation means remote fabrication of the fuel, i.e. increased costs for the deployment of more complex processes. A general principle for the development of any process in a P&T scenario should be simple and robust.

REFERENCES

- [1] WORLD NUCLEAR ASSOCIATION, Nuclear Power in France, <http://www.world-nuclear.org/info/Country-Profiles/Countries-A-F/France/>.
- [2] BASAK, U., Thorium Fuel Cycle Activities in IAEA presented at International Thorium Energy Conference, Oct 28–31, Geneva, Switzerland (2010).
- [3] INTERNATIONAL ATOMIC ENERGY AGENCY, Spent Fuel Reprocessing Options, IAEA-TECDOC-1587 (2008).
- [4] WATTAL, P.K., BASU, S., Radioactive waste management practices in India: achievements and challenges, *Sci. Cult.* **79** 1-2 (2013) 45–51.
- [5] RAJ, K., PRASAD, K.K., BANSAL, N.K., Radioactive waste management practices in India, *Nucl. Eng. Des.* **236** 7–8 (2006) 914–930.
- [6] NUCLEAR REGULATION AUTHORITY, Enforcement of the New Regulatory Requirements for Commercial Nuclear Power Reactors (2013).
- [7] <http://www.aec.go.jp/jicst/NC/iinkai/teirei/siry02015/siry039/siry01-1.pdf> (available in Japanese).
- [8] WORLD NUCLEAR ASSOCIATION, Japan Nuclear Fuel Cycle (accessed April 2019), <http://www.world-nuclear.org/information-library/country-profiles/countries-g-n/japan-nuclear-fuel-cycle.aspx>.
- [9] Strategic Energy Plan (2018), available at: https://www.enecho.meti.go.jp/en/category/others/basic_plan/5th/pdf/strategic_energy_plan.pdf.
- [10] WORLD NUCLEAR ASSOCIATION, Nuclear Power in South Korea (accessed April 2019), <http://www.world-nuclear.org/information-library/country-profiles/countries-o-s/south-korea.aspx>.
- [11] NUCLEAR ENERGY AGENCY OECD, Review of Operating and Forthcoming Experimental Facilities Opened to International R&D Co-operation in the Field of Advanced Fuel Cycles, available at: [http://www.oecd.org/officialdocuments/publicdisplaydocumentpdf/?cote=NEA/NSC/R\(2018\)4&docLanguage=En](http://www.oecd.org/officialdocuments/publicdisplaydocumentpdf/?cote=NEA/NSC/R(2018)4&docLanguage=En).
- [12] ADAMOV, E.O., The White Book of Nuclear Power. Closed NFC with fast reactors (in Russian), JSC NIKIET Publishing House, Moscow, ISBN 978-5-98706-129-91a, (2020) 498.
- [13] KHAPERSKAYA, A., et al., Spent Nuclear Fuel Management System in the Russian Federation, Proc. International Conference on the Management of Spent Fuel from Nuclear Power Reactors: An Integrated Approach to the Back End of the Fuel Cycle, Vienna, Austria, 15 June 2015 (2019).
- [14] ADAMOV, E.O., et al., Conceptual framework of a strategy for the development of nuclear power in Russia to 2100, *At. Energy* **112** 6 (2012) 391–403.
- [15] SHADRIN, A.Y., et al., Hydrometallurgical Reprocessing of BREST-OD-300 Mixed Uranium-plutonium Nuclear Fuel, *Procedia Chem.* **21** (2016) 148–155.
- [16] SHADRIN, A.Y., et al., Fast reactor SNF reprocessing for closed nuclear fuel cycle Proc. International Conference on the Management of Spent Fuel from Nuclear Power Reactors: Learning from the Past, Enabling the Future, Vienna, 23-28 June 2019 (2020).
- [17] LEBEDEV, V.A., Selectivity of liquid Metal Electrodes in molten Halides, Chelyabinsk, Metallurgiya (in Russian) (1993).
- [18] JOHNSON, I., CHASANOV, M., YONCO, R.M., Pu-Cd System: Partial Phase Diagram, *Trans. Met. Soc. of AIME* **233** (1965) 1408.

- [19] ELLINGER, F.H., LAND, C.C., STRUEBING, V.O., The Plutonium – Gallium System, *J. Nucl. Mater.* **12** (1964) 226–236.
- [20] LAMBERTIN, D., CHEDHOMME, S., BOURGES, G., SANCHEZ, S., PICARD, G.S., Activity coefficients of plutonium and cerium in liquid gallium at 1073 K: Application to a molten salt/solvent metal separation concept, *J. Nucl. Mater.* **341** (2005) 131–140.
- [21] KURATA, M., SAKAMUARA, Y., MATSUI, T., Thermodynamic quantities of actinides and rare earth elements in liquid bismuth and cadmium, *J. Alloys and Comp.* **234** (1996) 83.
- [22] DELPECH, S., et al., Electrochemical Determination of Gadolinium and Plutonium Solvation Properties in Liquid Gallium at High Temperature, *Nucl. Technol* **163** 3 (2008) 373–381.
- [23] LAPLACE, A., et al., Liquid metallic solvents classification for actinide/ lanthanide separation, Actinide and Fission Product Partitioning and Transmutation, Ninth Information Exchange Meeting, Nîmes, France, 25–29 September 2006, OECD NUCLEAR ENERGY AGENCY, (2007).
- [24] CONOCAR, O., DOUYÈRE, N., LACQUEMENT, J., Distribution of actinides and lanthanides in a molten fluoride/liquid aluminum alloy system, *J. Alloys Compd.* **389** 1 (2005) 29–33.
- [25] GRANDJEAN, A., Feasibility of immobilizing fluorinated pyrochemical reprocessing salts in a glass-ceramic matrix, *MRS Proceedings* **848** (2004) 9–32.
- [26] RAULT, L., et al., Test of Actinide-Lanthanide Separation in an Aluminum-Based Pyrochemical System, *Nucl. Technol* **139** 2 (2002) 167–174.
- [27] LACQUEMENT, J., BOUSSIER, H., LAPLACE, A., CONOCAR, O., GRANDJEAN, A., Potentialities of fluoride-based salts for specific nuclear reprocessing: Overview of the R&D program at CEA, *J. Fluor. Chem* **130** 1 (2009) 18–21.
- [28] VIGIER, J.-F., RENARD, C., HENRY, N., LAPLACE, A., ABRAHAM, F., Molten Salt Synthesis of a Mixed-Valent Lanthanide(III/IV) Oxychloride with an Unprecedented Sillen X24 Structure: $Ce_{1.3}Nd_{0.7}O_3Cl$, *Inorg. Chem.* **51** 7 (2012) 4352–4358.
- [29] USAMI, T., et al., Pyrochemical reduction of uranium dioxide and plutonium dioxide by lithium metal, *J. Nucl. Mater.* **300** 1 (2002) 15–26.
- [30] HUR, J.-M., HONG, S.-S., LEE, H., Reduction of U_3O_8 to U by a metallic reductant, Li, *J. Radioanal. Nucl. Chem.* **284** 1 (2010) 7–11.
- [31] BYCHKOV, A.V., ISHUNIN, V.S., KORMILITSYN, M.V., Reduction of uranium oxides with lithium in a lithium chloride melt, *Radiochemistry* **51** 5 (2009) 464.
- [32] USAMI, T., et al., Lithium reduction of americium dioxide to generate americium metal, *J. Nucl. Mater.* **304** (2002) 50–55.
- [33] KURATA, M., INOUE, T., SERP, J., OUGIER, M., GLATZ, J.-P., Electro-chemical reduction of MOX in LiCl, *J. Nucl. Mater.* **328** 2 (2004) 97–102.
- [34] SAKAMURA, Y., KURATA, M., INOUE, T., Electrochemical Reduction of UO_2 in Molten $CaCl_2$ or LiCl, *J. Electrochem. Soc.* **153** 3 (2006) D31.
- [35] IIZUKA, M., INOUE, T., OUGIER, M., GLATZ, J.-P., Electrochemical Reduction of (U, Pu) O_2 in Molten LiCl and $CaCl_2$ Electrolytes, *J. Nucl. Sci. Technol.* **44** 5 (2007) 801–813.
- [36] HERRMANN, S.D., LI, S.X., SIMPSON, M.F., PHONGIKAROON, S., Electrolytic Reduction of Spent Nuclear Oxide Fuel as Part of an Integral Process to Separate and Recover Actinides from Fission Products, *Sep Sci Technol* **41** 10 (2006) 1965–1983.
- [37] LEBEDEV, V., SALNIKOV, V., SIZIKOV, I., RYMKEVICH, D., Mechanism and kinetics of processes occurring at TiO_2 cathode in $CaCl_2$ -CaO melt, *Russian Journal of Applied Chemistry – Russ. J. Appl. Chem-Eng. Tr.* **80** (2007) 1503–1508.

- [38] KAWAMURA, H., ITO, Y., Electrodeposition of cohesive carbon films on aluminum in a LiCl–KCl–K₂CO₃ melt, *J. Appl. Electrochem* **30** (2000) 571–574.
- [39] ITO, Y., Electrochemical Formation of Thin Carbon Film from Molten Chloride System, *ECS Proceedings Volumes 1992-16* 1 (1992) 574–585.
- [40] MASSOT, L., CASSAYRE, L., CHAMELOT, P., TAXIL, P., On the use of electrochemical techniques to monitor free oxide content in molten fluoride media, *J. Electroanal. Chem.* **606** 1 (2007) 17–23.
- [41] GIBILARO, M., et al., Direct electrochemical reduction of solid uranium oxide in molten fluoride salts, *J. Nucl. Mater.* **414** 2 (2011) 169–173.
- [42] CHIDAMBARAM, R., GANGULY, C., Plutonium and thorium in the Indian nuclear programme, *Curr. Sci.* **70** 1 (1996) 21–35.
- [43] RAJ, B., KAMATH, H.S., NATARAJAN, R., VASUDEVA RAO, P.R., A perspective on fast reactor fuel cycle in India, *Prog. Nucl. Eng.* **47** 1 (2005) 369–379.
- [44] INOUE, T., KOYAMA, T., ARAI, Y., State of the Art of Pyroprocessing Technology in Japan, *Energy Procedia* **7** (2011) 405–413.
- [45] INOUE, T., KOCH, L., Development of pyroprocessing and its future direction, *Nucl. Eng. Technol.* **40** (2008).
- [46] IIZUKA, M., UOZUMI, K., OGATA, T., OMORI, T., TSUKADA, T., Development of an Innovative Electrefiner for High Uranium Recovery Rate from Metal Fast Reactor Fuels, *J. Nucl. Sci. Technol.* **46** 7 (2009) 699–716.
- [47] IIZUKA, M., OMORI, T., TSUKADA, T., Behavior of U-Zr Alloy Containing Simulated Fission Products during Anodic Dissolution in Molten Chloride Electrolyte, *J. Nucl. Sci. Technol.* **47** (2010) 244–254.
- [48] CARLS, E., BLASKOVITZ, R., JOHNSON, T., OGATA, T., Tests of prototype salt stripper system for IFR fuel cycle (1993).
- [49] HANSON, B., HOPKINS, P., DONALDSON, N., Pyrochemistry: A program for industrialization, *Proc. GLOBAL 2003*, New Orleans, United States, November 16–20, 2003.
- [50] HUNTLEY, W.R., SILVERMAN, M.D., System design description of forced-convection molten-salt corrosion loops MSR-FCL-3 and MSR-FCL-4, *ORNL/TM-5540* (1976).
- [51] BARTH, D., PACHECO, J., KOLB, W., RUSH, E., Development of a High-Temperature, Long-Shafted, Molten-Salt Pump for Power Tower Applications, *ASME J. Sol. Energy Eng.* **124** (2002) 170–175.
- [52] WATANBE, H., HASHIMOTO, H., KATAGIRI, I.K., TANG, B., Improvement of performance of vibration pump for molten salt at high temperature, *Trans. Japan. Soc. Mech. Eng.* **602** (1996) 3649–3653.
- [53] KOYAMA, T., HIJIKATA, T., YOKOO, T., INOUE, T., Development of engineering technology basis for industrialization of pyrometallurgical reprocessing, *Proc. GLOBAL 2007*, Boise, Idaho, 2007.
- [54] HIJIKATA, T., KOYAMA, T., Development of High-Temperature Transport Technologies for Liquid Cadmium in Pyrometallurgical Reprocessing, *J. Eng. Gas Turb Power* **131** 4 (2009).
- [55] HIJIKATA, T., KIONOSHITA, K., UOZUMI, K., KOYAMA, T., Development of Transport Technologies for High-temperature Fluid in Pyrometallurgical Reprocessing, *Energy Procedia* **39** (2013) 127–140.
- [56] HIJIKATA, T., MURAKAMI, T., KOYAMA, T., Development of high-temperature transport technologies for liquid Cd cathode of pyro-reprocessing, *Proc. International conference on fast reactors and related fuel cycles (FR09): Challenges and opportunities International Atomic Energy Agency (IAEA)*, Kyoto, Japan, 2012.

- [57] JOHNSON, I., Solubilities in liquid metals, ANL-HMF-SL-1747, Argonne National Laboratory, Lemont, IL (1960).
- [58] SHUNK, F.A., Constitution of binary alloys. 2nd Supplement 2nd Supplement, McGraw-Hill, New York, NY (1969).
- [59] SAKAMURA, Y., AKAGI, M., Pyrochemical Reprocessing Tests to Collect Uranium Metal from Simulated Spent Oxide Fuel, Nucl. Technol **179** 2 (2012) 220–233.
- [60] IIZUKA, M., SAKAMURA, Y., INOUE, T., Electrochemical reduction of (U–40Pu–5Np)O₂ in molten LiCl electrolyte, J. Nucl. Mater. **359** 1 (2006) 102–113.
- [61] HERRMANN, S., LI, S., SIMPSON, M., Electrolytic Reduction of Spent Oxide Fuel–Bench-Scale Test Results, Proc. Int. Conf. Nuclear Energy Systems for Future Generation and Global Sustainability (GLOBAL2005), Tsukuba, Japan, Oct. 9–13, 2005.
- [62] JEONG, S.M., Scale-up effect in an electrochemical reduction of U₃O₈ in a LiCl–Li₂O molten salt system, Proc. Int. Conf. Nuclear Energy Systems for Future Generation and Global Sustainability (GLOBAL2005), Tsukuba, Japan, Oct.9–13, 2005.
- [63] SAKAMURA, Y., OMORI, T., Electrolytic Reduction and Electrorefining of Uranium to Develop Pyrochemical Reprocessing of Oxide Fuels, Nucl. Technol **171** 3 (2010) 266–275.
- [64] MASSALSKI, T.B., MURRAY, J.L., BENNETT, L.H., BAKER, H., Binary alloy phase diagrams, American Society for Metals, Metals Park, OH (1986).
- [65] GOURISHANKAR, K.V., JOHNSON, G.K., JOHNSON, I., Thermodynamics of mixed oxide compounds, Li₂O Ln₂O₃ (Ln=Nd or Ce), Metall. Mater. Trans. B **28** 6 (1997) 1103–1110.
- [66] KATO, T., SAKAMURA, Y., IWAI, T., ARAI, Y., Solubility of Pu and rare-earths in LiCl–Li₂O melt, Radiochimica Acta **97** 4–5 (2009) 183–186.
- [67] SAKAMURA, Y., et al., Measurement of standard potentials of actinides (U,Np,Pu,Am) in LiCl–KCl eutectic salt and separation of actinides from rare earths by electrorefining, J. Alloys Compd. **271–273** (1998) 592–596.
- [68] SAKAMURA, Y., INOUE, T., STORVIC, T.S., GRANTHEM, L.F., Development of Pyropartitioning Process. Separation of Transuranium Elements from Rare Earth Elements in Molten Chlorides Solution: Electrorefining Experiments and Estimation by Using the Thermodynamic Properties, Proc. International Conference on Evaluation of Emerging Nuclear Fuel Cycle Systems (GLOBAL '95), Versailles, France, 1995.
- [69] INOUE, T., et al., Development of Partitioning and Transmutation Technology for Long-Lived Nuclides, Nucl. Technol **93** 2 (1991) 206–220.
- [70] KURATA, M., SAKAMURA, Y., HIJIKATA, T., KINOSHITA, K., Distribution behavior of uranium, neptunium, rare-earth elements (Y, La, Ce, Nd, Sm, Eu, Gd) and alkaline-earth metals (Sr,Ba) between molten LiCl–KCl eutectic salt and liquid cadmium or bismuth, J. Nucl. Mater. **227** 1 (1995) 110–121.
- [71] KINOSHITA, K., et al., Separation of Uranium and Transuranic Elements from Rare Earth Elements by Means of Multistage Extraction in LiCl–KCl/Bi System, J. Nucl. Sci. Technol. **36** 2 (1999) 189–197.
- [72] KOYAMA, T., JOHNSON, T.R., FISCHER, D.F., Distribution of actinides in molten chloride salt/cadmium metal systems, J. Alloys Compd. **189** 1 (1992) 37–44.
- [73] INOUE, T., Actinide recycling by pyro-process with metal fuel FBR for future nuclear fuel cycle system, Prog. Nucl. Eng. **40** 3 (2002) 547–554.
- [74] UOZUMI, K., IIZUKA, M., KURATA, M., INOUE, T., Demonstration of pyropartitioning technology by denitration and chlorination experiment using real high-level liquid waste, Proc. International Workshop for Asian Nuclear Prospect Kobe, Japan (2008).

- [75] UOZUMI, K., et al., Demonstration of pyro-partitioning process to recover TRUs from genuine high-level liquid waste, Proc. Proceedings of the GLOBAL 2009 congress - The Nuclear Fuel Cycle: Sustainable Options and Industrial Perspectives, France, 2009.
- [76] UOZUMI, K., et al., Recovery of Transuranium Elements from Real High-Level Liquid Waste by Pyropartitioning Process, *J. Nucl. Sci. Technol.* **48** 2 (2011) 303-314.
- [77] KOYAMA, T., HIJIKATA, T., KINOSHITA, K., YOKOO, T., INOUE, T., Development of engineering technology basis for pyrometallurgical reprocessing: development of transport technology and pyroprocess equipments in “Actinide and Fission Product Partitioning and Transmutation - Ninth Information Exchange Meeting, 25–29 September 2006”, OECD Nuclear Energy Agency, Paris (2007).
- [78] LEE, H., et al., Pyroprocessing technology development at KAERI, *Nucl. Eng. Technol.* **43** (2011).
- [79] NUCLEAR ENERGY AGENCY OECD, State-of-the-Art Report on the Progress of Nuclear Fuel Cycle Chemistry, OECD-NEA, Paris (2018).
- [80] KARELL, E.J., GOURISHANKAR, K.V., SMITH, J.L., CHOW, L.S., REDEY, L., Separation of Actinides from LWR Spent Fuel Using Molten-Salt-Based Electrochemical Processes, *Nucl. Technol* **136** 3 (2001) 342–353.
- [81] SONG, K.-C., et al., Status of pyroprocessing technology development in Korea, *Nucl. Eng. Technol.* **42** (2010) 131–144.
- [82] LEE, H., et al., Current Status of Pyroprocessing Development at KAERI, *Sci. Technol. Nucl. Install.* **2013** (2013) 343492.
- [83] HUR, J.-M., CHOI, I.-K., CHO, S., JEONG, S.M., SEO, C.-S., Preparation and melting of uranium from U₃O₈, *J. Alloys Compd.* **452** (2008) 23–26.
- [84] LEE, J.H., et al., Assessment of a High-Throughput Electrorefining Concept for a Spent Metallic Nuclear Fuel—I: Computational Fluid Dynamics Analysis, *Nucl. Technol* **162** 1 (2008) 107–116.
- [85] LEE, J.H., et al., Assessment of a High-Throughput Electrorefining Concept for a Spent Metallic Nuclear Fuel—II: Electrohydrodynamic Analysis and Validation, *Nucl. Technol* **165** (2009) 370–379.
- [86] PARK, S., et al., Salt evaporation behaviors of uranium deposits from an electrorefiner, *J. Radioanal. Nucl. Chem. - J Radioanal. Nucl. Chem.* **283** (2010) 171–176.
- [87] KIM, E.-H., PARK, G.-I., CHO, Y.-Z., YANG, H.-C., A New Approach to Minimize Pyroprocessing Waste Salts Through a Series of Fission Product Removal Process, *Nucl. Technol* **162** 2 (2008) 208–218.
- [88] CHO, Y.-Z., AHN, B.-G., EUN, H.-C., JUNG, J.-S., LEE, H.-S., Melt Crystallization Process Treatment of LiCl Salt Waste Generated from Electrolytic Reduction Process of Spent Oxide Fuel, *Energy Procedia* **7** (2011) 525–528.
- [89] YANG, H.-C., EUN, H.-C., CHO, Y.-Z., LEE, H.-S., KIM, I.-T., Fundamental Study on a Salt Distillation from Mixtures of Rare Earth Precipitates and LiCl-KCl Eutectic Salt, *Nucl. Technol* **171** 3 (2010) 300–305.
- [90] KIM, I.-T., PARK, H.-S., PARK, S.-W., KIM, E.-H., Alternative Technology for the Treatment of Waste LiCl Salt by Using Gelation with a Si-P-Al Material System and a Subsequent Thermal Conditioning Method, *Nucl. Technol* **162** 2 (2008) 219–228.
- [91] FUJITA, R., NAKAMURA, H., HARUGUCHI, Y., Development of Zirconium Recovery Process for Zircaloy Claddings and Channel Boxes from Boiling Water Reactors by Electrorefining in Molten Salts, Proc. ICAPP’05, Seoul, Republic of Korea, May 15–19, 2005, ID 5686, 2005.
- [92] GOTO, T., NOHIRA, T., HAGIWARA, R., ITO, Y., Selected topics of molten fluorides in the field of nuclear engineering, *J. Fluor. Chem* **130** 1 (2009) 102-107.

- [93] DELCUL, G.D., Possible Recycle of Most Components from LWR Spent Fuel including Uranium, Cladding and Transuranium Elements, *Trans. Am. Nucl. Soc.* **97** (2007) 77–78.
- [94] RUDISILL, T.S., Decontamination of Zircaloy cladding hulls from spent nuclear fuel, *J. Nucl. Mater.* **385** 1 (2009) 193–195.
- [95] CHANG, Y.I., The Integral Fast Reactor, *Nucl. Technol* **88** 2 (1989) 129–138.
- [96] TILL, C.E., CHANG, Y.I., HANNUM, W.H., The intergral fast reactor-an overview, *Prog. Nucl. Eng.* **31** 1 (1997) 3–11.
- [97] BENEDICT, R.W., HENSLEE, S.P., EBR-II spent fuel treatment demonstration project, *Trans Am Nucl Soc* **77** (1997) 75–76.
- [98] U.S. DEPARTMENT OF ENERGY, Record of Decision for the Treatment and Management of Sodium-Bonded Spent Nuclear Fuel, *Federal Register* **65** 182 (2000) 565654–556570.
- [99] LI, S.X., SIMPSON, M.F., Anodic process of electrorefining spent driver fuel in molten LiCl-KCl-UCl₃/Cd system, *Mining Metall. Explor.* **22** 4 (2005) 192–198.
- [100] LI, S.X., JOHNSON, T.A., WESTPHAL, B.R., GOFF, K.M., BENEDICT, R.W., Electrorefining Experience For Pyrochemical Reprocessing of Spent EBR-II Driver Fuel, *Proc. GLOBAL 2005*, Tsukuba, Japan, 2005.
- [101] LI, S.X., Experimental Observations on the Roles of the Cadmium Pool in the Mark-IV Electrorefiner, *Nucl. Technol* **162** 2 (2008) 144–152.
- [102] SIMPSON, M., Developments of Spent Nuclear Fuel Pyroprocessing Technology at Idaho National Laboratory, INL/EXT-12-25124 (2012).
- [103] HOOVER, R., PHONGIKAROON, S., LI, S., SIMPSON, M., YOO, T.-S., A Computational Model of the Mark-IV Electrorefiner: Phase I—Fuel Basket/Salt Interface, *J. Eng. Gas Turb Power* **131** 5 (2009).
- [104] HOOVER, R.O., PHONGIKAROON, S., SIMPSON, M.F., LI, S.X., YOO, T.-S., Development of Computational Models for the Mark-IV Electrorefiner—Effect of Uranium, Plutonium, and Zirconium Dissolution at the Fuel Basket-Salt Interface, *Nucl. Technol* **171** 3 (2010) 276–284.
- [105] HOOVER, R., PHONGIKAROON, S., SIMPSON, M., YOO, T.-S., LI, S., Computational Model of the Mark-IV Electrorefiner: Two-Dimensional Potential and Current Distributions, *Nucl. Technol* **173** (2011) 176–182.
- [106] CHOI, I., SERRANO, B.E., LI, S.X., HERMANN, S., PHONGIKAROON, S., Determination of Exchange Current Density of U³⁺/U Couple in LiCl-KCl Eutectic Mixture, *Proc. GLOBAL 2009 - The Nuclear Fuel Cycle: Sustainable Options and Industrial Perspectives*, France, 2009.
- [107] WESTPHAL, B., MARSDEN, K., PRICE, J., LAUG, D., On the Development of a Distillation Process for the Electrometallurgical Treatment of Irradiated Spent Nuclear Fuel, *Nucl. Eng. Technol.* **40** (2008).
- [108] WESTPHAL, B.R., MARSDEN, K.C., PRICE, J.C., Development of a Ceramic-Lined Crucible for the Separation of Salt from Uranium, *Metall. Mater. Trans. A* **40** 12 (2009) 2861.
- [109] SIMPSON, M.F., et al., A Description of the Ceramic Waste Form Production Process from the Demonstration Phase of the Electrometallurgical Treatment of EBR-II Spent Fuel, *Nucl. Technol* **134** 3 (2001) 263–277.
- [110] SIMPSON, M., SACHDEV, P., Development of electrorefiner waste salt disposal process for the EBR-II spent fuel treatment project, *Nucl. Eng. Technol.* **40** (2008).
- [111] MORRISON, M.C., BATEMAN, K.J., SIMPSON, M.F., Scale up of ceramic waste forms for the EBR-II spent fuel treatment process, *Proc. International Pyroprocess Research Conference*, Idaho National Laboratory, United States, INL/CON--10-19439 (2010).

- [112] SOLBRIG, C.W., MORRISON, M.C., SIMPSON, M.F., BATEMAN, K., Experimental Verification of Solidification Stress Theory, INL/CON-10-19439, Proc. International Pyroprocessing Research Conference, Idaho National Laboratory, United States, November, 2010.
- [113] MARSDEN, K., KNIGHT, C., BATEMAN, K., WESTPHAL, B., LIND, P., Process and equipment qualification of the ceramic and metal waste forms for spent fuel treatment, Proc. GLOBAL 2005: Proceedings of the international conference on nuclear energy systems for future generation and global sustainability, Atomic Energy Society of Japan, Japan, 2005.
- [114] ABRAHAM, D.P., MCDEAVITT, S.M., PARK, J., Microstructure and phase identification in type 304 stainless steel-zirconium alloys, *Metall. Mater. Trans. A* **27** 8 (1996) 2151–2159.
- [115] MCDEAVITT, S.M., ABRAHAM, D.P., PARK, J.Y., Evaluation of stainless steel–zirconium alloys as high-level nuclear waste forms, *J. Nucl. Mater.* **257** 1 (1998) 21–34.
- [116] KEISER, D.D., JR., WESTPHAL, B.R., Consolidation of Cladding Hulls from the Electrometallurgical Treatment of Spent Fuel, University of North Texas Libraries, UNT Digital Library, <https://digital.library.unt.edu>; crediting UNT Libraries Government Documents Department. (1998).
- [117] KEISER, D.D., ABRAHAM, D.P., SINKLER, W., RICHARDSON, J.W., MCDEAVITT, S.M., Actinide distribution in a stainless steel–15 wt% zirconium high-level nuclear waste form, *J. Nucl. Mater.* **279** 2 (2000) 234–244.
- [118] BATTLES, J.E., MILLER, W.E., GAY, E.C., Pyrometallurgical processing of Integral Fast Reactor metal fuels, Proc. International Conference on Nuclear Fuel Reprocessing and Waste Management, Japan, ANL/CP—70796 (1991).
- [119] VADEN, D., et al., Engineering-Scale Liquid Cadmium Cathode Experiments, *Nucl. Technol* **162** 2 (2008) 124–128.
- [120] LI, S.X., HERMANN, S.D., SIMPSON, M.F., Experimental Investigations into U/TRU Recovery Using a Liquid Cadmium Cathode and Salt Containing High Rare Earth Concentrations, Proc. GLOBAL 2009, Paris, France, September 6–11, 2009.
- [121] LI, S.X., HERRMANN, S.D., GOFF, K.M., SIMPSON, M.F., BENEDICT, R.W., Actinide Recovery Experiments with Bench-Scale Liquid Cadmium Cathode in Real Fission Product-Laden Molten Salt, *Nucl. Technol* **165** 2 (2009) 190–199.
- [122] HERRMANN, S.D., LI, S.X., Separation and Recovery of Uranium Metal from Spent Light Water Reactor Fuel Via Electrolytic Reduction and Electrorefining, *Nucl. Technol* **171** 3 (2010) 247–265.
- [123] HERRMANN, S.D., LI, S.X., WESTPHAL, B.R., Separation and Recovery of Uranium and Group Actinide Products From Irradiated Fast Reactor MOX Fuel via Electrolytic Reduction and Electrorefining, *Sep Sci Technol* **47** 14–15 (2012) 2044–2059.
- [124] HERRMANN, S., LI, S., SERRANO-RODRIGUEZ, B., Observations of Oxygen Ion Behavior in the Lithium-Based Electrolytic Reduction of Uranium Oxide, Proc. Global 2009, Paris, France, September 6–11, 2009.
- [125] PARK, B.H., LEE, I.W., SEO, C.S., Electrolytic reduction behavior of U₃O₈ in a molten LiCl–Li₂O salt, *Chem. Eng. Sci.* **63** (2008) 3485–3492.
- [126] PHONGIKAROON, S., HERRMANN, S.D., SIMPSON, M.F., Diffusion Model for Electrolytic Reduction of Uranium Oxides in a Molten LiCl–Li₂O Salt, *Nucl. Technol* **174** 1 (2011) 85–93.
- [127] SACHDEV, P., SIMPSON, M.F., FRANK, S.M., YANO, K., UTGIKAR, V., Selective Separation of Cs and Sr from LiCl-Based Salt for Electrochemical Processing of Oxide Spent Nuclear Fuel, *Sep Sci Technol* **43** 9–10 (2008) 2709–2721.

- [128] LI, S.X., HERRMANN, S.D., SIMPSON, M.F., Electrochemical Analysis of Actinides and Rare Earth Constituents in Liquid Cadmium Cathode Product from Spent Fuel Electrowinning, *Nucl. Technol* **171** 3 (2010) 292–299.
- [129] SIMPSON, M.F., et al., Selective Reduction of Active Metal Chlorides from Molten LiCl-KCl using Lithium Drawdown, *Nucl. Eng. Technol.* **44** 7 (2012) 767–772.
- [130] AHLUWALIA, R.K., GEYER, H.K., PEREIRA, C., ACKERMAN, J.P., Modeling of a Zeolite Column for the Removal of Fission Products from Molten Salt, *Ind. Eng. Chem. Res.* **37** 1 (1998) 145–153.
- [131] LEXA, D., JOHNSON, I., Occlusion and ion exchange in the molten (lithium chloride-potassium chloride-alkali metal chloride) salt + zeolite 4A system with alkali metal chlorides of sodium, rubidium, and cesium, *Metall. Mater. Trans. B* **32** 3 (2001) 429–435.
- [132] LEXA, D., Occlusion and ion exchange in the molten (lithium chloride+potassium chloride+alkaline-earth chloride) salt+zeolite 4A system with alkaline-earth chlorides of calcium and strontium and in the molten (lithium chloride+potassium chloride+actinide chloride) salt+zeolite 4A system with the actinide chloride of uranium, *Metall. Mater. Trans. B* **34** 2 (2003) 201–208.
- [133] SIMPSON, M., GOUGAR, M., Two-Site Equilibrium Model for Ion Exchange between Monovalent Cations and Zeolite-A in a Molten Salt, *Ind. Eng. Chem. Res.* **42** (2003) 4208–4212.
- [134] PHONGIKAROON, S., SIMPSON, M., Equilibrium model for ion exchange between multivalent cations and zeolite-A in a molten salt, *AIChE Journal* **52** (2006) 1736–1743.
- [135] YOO, T.-S., et al., Salt-Zeolite Ion-Exchange Equilibrium Studies for a Complete Set of Fission Products in Molten LiCl-KCl, *Nucl. Technol* **171** 3 (2010) 306–315.
- [136] SHALTRY, M., PHONGIKAROON, S., SIMPSON, M.F., Ion exchange kinetics of fission products between molten salt and zeolite-A, *Microporous and Mesoporous Materials* **152** (2012) 185–189.
- [137] ALLENSWORTH, J.R., SIMPSON, M.F., YIM, M.-S., PHONGIKAROON, S., Investigation of Fission Product Transport into Zeolite-A for Pyroprocessing Waste Minimization, *Nucl. Technol* **181** 2 (2013) 337–348.
- [138] SERP, J., et al., Electroseparation of Actinides from Lanthanides on Solid Aluminum Electrode in LiCl-KCl Eutectic Melts, *J. Electrochem. Soc.* **152** (2005) C167–C172.
- [139] SOUČEK, P., MALMBECK, R., NOURRY, C., GLATZ, J.P., Pyrochemical Reprocessing of Spent Fuel by Electrochemical Techniques Using Solid Aluminium Cathodes, *Energy Procedia* **7** (2011) 396–404.
- [140] SOUCEK, P., Recovery of actinides from spent nuclear fuel by pyrochemical reprocessing, *Proc. Global 2009, Paris, France, September 6–11, 2009.*
- [141] SOUCEK, P., et al., Electrowinning of U-Pu-Zr-alloy fuel onto solid Aluminium cathodes in molten LiCl-KCl, *Radiochimica Acta* **96** (2008) 315–322.
- [142] FEDERAL TARGET PROGRAM, Nuclear Power Technologies of New Generation for the Period 2010-2015 and until 2020 (FTP NPNG), Decree of the Government of the Russian Federation.
- [143] ORLOV, V.V., et al., The closed on-site fuel cycle of the brest reactors, *Prog. Nucl. Eng.* **47** 1 (2005) 171–177.
- [144] POPLAVSKII, V.M., CHEBESKOV, A.N., MATVEEV, V.I., BN-800 as a New Stage in the Development of Fast Sodium-Cooled Reactors, *At. Energy* **96** 6 (2004) 386–390.
- [145] KOCHETKOV, L.A., KIRYUSHIN, A.I., OSHKANOV, N.N., Sodium-cooled fast reactors in Russia: Looking beyond the year 2000, *At. Energy* **74** 4 (1993) 265–267.
- [146] ZAIKOV, Y.P., et al., Research and development of the pyrochemical processing for the mixed nitride uranium-plutonium fuel, *Journal of Physics: Conference Series* **1475** (2020) 012027.

- [147] SHADRIN, A., et al., Fuel fabrication and reprocessing for nuclear fuel cycle with inherent safety demands, *Radiochimica Acta* **103** (2015) 163–173.
- [148] SHADRIN, A., Plutonium Use in Nuclear Fuel Cycle – Options for Russia, Proc. Global 2015, Paris, France, September 20–24, 2015.
- [149] SHADRIN, A.Y., et al., PH process as a technology for reprocessing mixed uranium–plutonium fuel from BREST-OD-300 reactor, *Radiochemistry* **58** 3 (2016) 271–279.
- [150] SKIBA, O.V., VOROBAY, M.P., KAPSHUKOV, I.I., Investigation of NaCl - KCl – UO₂Cl₂. Salt Systems, *Nucl. Energy* **2** (1969) 121–124.
- [151] VOROBAY, M.P., SKIBA, O.V., BLOKHIN, N., Products of plutonium dioxide chlorination in alkali metal molten chlorides, *Nucl. Energy* **3** (1972) 553–556.
- [152] VOROBAY, M.P., BEVZ, A.S., SKIBA, O.V., Chlorination of uranium oxides in alkali metal molten chlorides and their mixtures, *Zh Neorg Khim* **3** (1978) 1618–1622 (in Russian).
- [153] VAVILOV, S.K., Thermodynamics and kinetics of reduction-oxidation and electrode reactions of plutonium in the melt of eutectic mixture NaCl – CsCl, *Radiochemistry* **27** 1 (1985) 116–121.
- [154] SAVOCHKIN, Y.P., Interaction of plutonium with oxygen in chloride melts, Preprint RIAR-5 (1990) 788.
- [155] TSYKANOV, V.A., SKIBA, O.V., PORODNOV, P.T., Developments in the field of FR fuel cycle, Preprint RIAR-4 (1987) 715.
- [156] STEINKOPF, H., KROMPASS, R., TZYKANOV, V.A., Characteristics and performance of the Plant for refabrication of vibrocompacted fuel elements for the BOR-60 reactor, *Kerntechnik* (1990).
- [157] SKIBA, O.V., MAYORSHIN, A.A., MAKAROV, V.A., PORODNOV, P.T., Development and operation experience of the pilot plant for fuel pin and assembly production based on vibropac uranium- plutonium fuel, report 15-4, Proc. Int. Conf. Fast reactors and related fuel cycles, Kyoto, Japan, Oct. 28–Nov.1, 1991.
- [158] SKIBA, O.V., BYCHKOV, A.V., IVANOV, V.B., Pyroelectrochemical process to reprocess irradiated oxide uranium - plutonium fuel in a short-term FR fuel cycle, Proc. Concept for Nuclear Engineering Development, Risk Analysis, 1991.
- [159] BYCHKOV, A.V., Pyroelectrochemical Reprocessing of Irradiated FBR MOX Fuel. Experiment on Irradiated Fuel of the BN-350 Reactor, Proc. Int. Conf. Evaluation of Emerging Nuclear Fuel Cycle Systems, GLOBAL '95, Versailles, France, Sept. 11–14, 1995.
- [160] BYCHKOV, A.V., et al., Pyroelectrochemical reprocessing of irradiated FBR MOX fuel 3 Experiment on high burn-up fuel of the BOR-60 reactor, Proc. Int. Conf. Future Nuclear Systems. GLOBAL '97, Atomic Energy Society of Japan, Pacifico Yokohama, Yokohama, Japan, 1997.
- [161] KORMILITSYN, M.V., BYCHKOV, A.V., ISHUNIN, V.S., Pyroelectrochemical reprocessing of irradiated fuel of fast reactors, Generalization of experience on BOR-60 spent nuclear fuel reprocessing using approacher “UO₂→UO₂” “MOX→PuO₂ and MOX→MOX”, Proc. Int. Conf. Global 2003, New Orleans, USA, November 16–20, 2003.
- [162] BYCHKOV, A.V., et al., Experimental checking and justification of pyrochemical origin plutonium dioxide application for pellet MOX-fuel fabrication, Joint ICTP/IAEA School on Physics and Technology of Fast Reactors Systems (2009).
- [163] UHLÍŘ, J., MARECEK, M., Fluoride volatility method for reprocessing of LWR and FR fuels, *J. Fluor. Chem* **130** (2009) 89–93.
- [164] KIM, J.-G., LEE, S.-J., PARK, S.-B., HWANG, S.-C., LEE, H., High-throughput Electrorefining System with Graphite Cathodes and a Bucket-type Deposit Retriever, *Procedia Chem.* **7** (2012) 754–757.

- [165] KANG, Y., et al., Electrodeposition characteristics of uranium by using a graphite cathode, *Carbon* **44** (2006) 3142–3145.
- [166] LEE, Y.G., CHA, H.R., KIM, H.D., HONG, J.S., KANG, H.Y., Development of DUPIC safeguards neutron counter, Korea, Republic of (1999).
- [167] KIM, H., SHIN, H.S., AHN, S.K., Status and Prospect of Safeguards By Design for the Pyroprocessing Facility, IAEA-CN-184/71, Symposium on International Safeguards, International Atomic Energy Agency (IAEA) (2010).
- [168] INOUE, T., Characterization of fuel alloys with minor actinides, *Trans. Am. Nucl. Soc.* **64** (1991) 552.
- [169] AKABORI, M., SHIRASU, Y., TAKANO, M., MINATO, K., Fabrication and property measurements of MA nitride fuels and LLFP targets Proc. 7th Information Exchange Meeting on Actinide and Fission Product Partitioning and Transmutation, Jeju, Korea, Oct.14–16, 2002.
- [170] WESTPHAL, B.R., et al., Effect of Process Variables During the Head-end Treatment of Spent Oxide Fuel, Proc. International Pyroprocessing Research Conference, Idaho National Laboratory, Idaho Falls, United States, Aug. 8–10, 2006.
- [171] NUCLEAR ENERGY AGENCY OECD, Spent Nuclear Fuel Reprocessing Flowsheet NEA/NSC/WPFC/DOC (2012).
- [172] PARK, B., SEO, C.-S., A semi-empirical model for the air oxidation kinetics of UO₂, *Korean Journal of Chemical Engineering - Korean J. Chem. Eng.* **25** (2008) 59–63.
- [173] YOO, J.-H., SEO, C.-S., KIM, E.-H., LEE, H., A conceptual study of pyroprocessing for recovering actinides from spent oxide fuels, *Nucl. Eng. Technol.* **40** (2008).
- [174] WESTPHAL, B.R., et al., Selective Trapping of Volatile Fission Products with an Off-Gas Treatment System, *Sep Sci Technol* **43** 9-10 (2008) 2695–2708.
- [175] KOREA ATOMIC ENERGY RESEARCH INSTITUTE, Development of Voloxidation Process for Treatment of LWR Spent Fuel, KAERI/RR-2840/2006, (2006).
- [176] JOHNSON, I., The thermodynamics of pyrochemical processes for liquid metal reactor fuel cycles, *J. Nucl. Mater.* **154** 1 (1988) 169–180.
- [177] JOHNSON, I., An introduction to pyrochemistry with emphasis on nuclear applications, ANL Report, ANL-01/16, Argonne National Laboratory, Lemont, IL (2001).
- [178] ACKERMAN, J.P., PYRO, A system for modelling for reprocessing, *Trans. Am. Nucl. Soc.* **60** (1989) 168.
- [179] ACKERMAN, J.P., PYRO: New capability for isotopic mass tracking in pyroprocess simulation, Proc. International Conference on the physics of reactors: operation, design and computation, Marseille, France, 23–26 Apr 1990.
- [180] ACKERMAN, J.P., JOHNSON, T.R., Partitioning of actinides and fission products between metal and molten salt phases: Theory, measurement, and application to IFR pyroprocess development, ANL Report, ANL/CMT/CP-79275, Argonne National Laboratory, Lemont, IL (1993).
- [181] TOMCZUK, Z., Uranium Transport to Solid Electrodes in Pyrochemical Reprocessing of Nuclear Fuel, *J. Electrochem. Soc.* **139** 12 (1992) 3523.
- [182] KOBAYASHI, T., TOKIWAI, M., Development of TRAIL, a simulation code for the molten salt electrorefining of spent nuclear fuel, *J. Alloys Compd.* **197** 1 (1993) 7–16.
- [183] KOBAYASHI, T., FUJITA, R., FUJIE, M., KOYAMA, T., Polarization Effects in the Molten Salt Electrorefining of Spent Nuclear Fuel, *J. Nucl. Sci. Technol.* **32** 7 (1995) 653–663.
- [184] KOYAMA, T., FUJITA, R., HZUKA, M., SUMIDA, Y., Pyrometallurgical Reprocessing of Fast Reactor Metallic Fuel—Development of a New Electrorefiner with a Ceramic Partition, *Nucl. Technol* **110** 3 (1995) 357–368.

- [185] KOBAYASHI, T., FUJITA, R., NAKAMURA, H., KOYAMA, T., Evaluation of Cadmium Pool Potential in a Electrorefiner with Ceramic Part it ion for Spent Metallic Fuel, *J. Nucl. Sci. Technol.* **34** 1 (1997) 50–57.
- [186] KOBAYASHI, T., TOKIWAI, M., GAY, E.C., Investigation of Cell Resistance for Molten Salt Electrorefining of Spent Nuclear Fuel, *J. Nucl. Sci. Technol.* **32** 1 (1995) 68-74.
- [187] KOBAYASHI, T., FUJITA, R., NAKAMURA, H., KOYAMA, T., IIZUKA, M., Electrorefining Experiments to Recover Uranium with a Cadmium-Lithium Anode and Their Theoretical Evaluation, *J. Nucl. Sci. Technol.* **36** 3 (1999) 288–296.
- [188] LI, S.X., Anodic process of electrorefining spent nuclear fuel in molten LiCl-KCL-UC13/Cd system, ANL Report, ANL/ENT/CP-108124, Argonne National Laboratory, Lemont, IL.
- [189] LI, S.X., Experimental observations to the electrical field for electrorefining of spent nuclear fuel in the Mark-IV electrorefiner, ANL Report, ANL/TD/CP-96452, Argonne National Laboratory, Lemont, IL (1998).
- [190] LI, S.X., Initial results for electrochemical dissolution of spent EBR-II fuel, ANL Report, ANL/TD/CP-96338, Argonne National Laboratory, Lemont, IL (1998).
- [191] JOHNSON, T.A., LAUG, D.V., LI, S.X., SOFU, T., Experimental observations on electrorefining spent nuclear fuel in molten LiCl-KCl/liquid cadmium system, ANL Report, ANL/NT/CP-98226, Argonne National Laboratory, Lemont, IL (1999).
- [192] LI, S.X., VADEN, D., MARIANI, R.D., JOHNSON, T.A., Experimental observations on the role of the cadmium pool in Mark-IV ER, ANL Report, ANL/NT/CP-101394, Argonne National Laboratory, Lemont, IL (2000).
- [193] AHLUWALIA, R.K., HUA, T.Q., Electrotransport of Uranium from a Liquid Cadmium Anode to a Solid Cathode, *Nucl. Technol* **140** 1 (2002) 41–50.
- [194] AHLUWALIA, R.K., GEYER, H.K., The GC Computer Code for Flow Sheet Simulation of Pyrochemical Processing of Spent Nuclear Fuels, *Nucl. Technol* **116** 2 (1996) 180–195.
- [195] AHLUWALIA, R., HUA, T.Q., GEYER, H.K., Behavior of Uranium and Zirconium in Direct Transport Tests with Irradiated EBR-II Fuel, *Nucl. Technol* **126** 3 (1999) 289–302.
- [196] AHLUWALIA, R.K., HUA, T.Q., GEYER, H.K., Removal of Zirconium in Electrometallurgical Treatment of Experimental Breeder Reactor II Spent Fuel, *Nucl. Technol* **133** 1 (2001) 103–118.
- [197] BAE, J., YI, K.-W., PARK, B.G., HWANG, I., A time-dependent electrochemical model of pyrochemical partitioning for waste transmutation, *Proc. Global 2003: Atoms for Prosperity: Updating Eisenhowers Global Vision for Nuclear Energy*, New Orleans, United States, 16–20 November, 2003.
- [198] BAE, J., YI, K.W., PARK, B.G., HWANG, I.S., LEE, H.Y., Development of electrochemical-hydrodynamic model for electrorefining process, *Proc. GLOBAL 2005*, Tsukuba, Japan, 9–13 October, 2005.
- [199] ROY, J.J., Modelling of electroseparation of actinides and rare earths in molten salt, *Proc. International Conference OMEGA/OECD/NEA Partitioning/Transmutation*, 1991.
- [200] TECHNICAL PROGRESS REPORT. Private sector initiatives between the United States and Japan July-1988-December 1988, AI-DOE-13567, United States (1988).
- [201] TECHNICAL PROGRESS REPORT. Private sector initiatives between the United States and Japan July-1987-December 1987, AI-DOE-13565, United States (1988).
- [202] TECHNICAL PROGRESS REPORT. Private sector initiatives between the United States and Japan July-1989-December 1989, RI/RD92-116 United States (1990).

- [203] TECHNICAL PROGRESS REPORT. Private sector initiatives between the United States and Japan July-1992-December 1992, RI/RD93-167 ROCKWELL INTERNATIONAL, United States (1993).
- [204] TECHNICAL PROGRESS REPORT. Private sector initiatives between the United States and Japan July-1991-December 1991, RI/RD159 United States (1993).
- [205] TECHNICAL PROGRESS REPORT. Private sector initiatives between the United States and Japan July-1990-December 1990, RI/RD93-150 United States (1993).
- [206] TECHNICAL PROGRESS REPORT. Private Sector Initiative Between the United States and Japan, January 1993-September 1998 RD98-372 THE BOEING COMPANY (1998).
- [207] BOUSSIER, H., MALMBECK, R., MARUCCI, G., Pyrometallurgical processing research programme (PYROREP), Final technical report, co-funded by the European Commission (2003).
- [208] NAWADA, H.P., BHAT, N.P., Thermochemical modelling of electrotransport of uranium and plutonium in an electrorefiner, *Nucl. Eng. Des.* **179** 1 (1998) 75–99.
- [209] NAWADA, H.P., BHAT, N.P., BALASUBRAMANIAN, G.R., Thermochemical Modeling of Electrorefining Process for Reprocessing Spent Metallic Fuel, *J. Nucl. Sci. Technol.* **32** 11 (1995) 1127–1137.
- [210] NAWADA, H.P., BHAT, N.P., BALASUBRAMANIAN, G.R., Some Computations in Planning Reconstitution of a 500-MW(electric) Fast Breeder Reactor (Metallic) Fuel by Electrorefining, *Nucl. Technol* **114** 1 (1996) 97–110.
- [211] GHOSH, S., REDDY, B.P., NAGARAJAN, K., RAO, P.R.V., PRAGAMAN: A Computer Code for Simulation of Electrotransport during Molten Salt Electrorefining, *Nucl. Technol* **170** 3 (2010) 430–443.
- [212] KIM, K.R., et al., Multi physics modeling of a molten-salt electrolytic process for nuclear waste treatment, *IOP Conference Series: Materials Science and Engineering* **9** (2010) 012002.
- [213] PARK, B.G., HWANG, I.S., Simulation of Electrorefining Process Using Time-dependent Multi-component Electrochemical Model: REFIN, Proceeding of the Korean Nuclear Society Autumn Meeting, Department of Nuclear Engineering, Seoul National University, Republic of Korea (1999).
- [214] ACKERMAN, J.P., Chemical basis for pyrochemical reprocessing of nuclear fuel, *Ind. Eng. Chem. Res.* **30** 1 (1991) 141–145.
- [215] IIZUKA, M., KINOSHITA, K., KOYAMA, T., Modeling of anodic dissolution of U–Pu–Zr ternary alloy in the molten LiCl–KCl electrolyte, *J. Phys Chem Solids* **66** 2 (2005) 427–432.
- [216] HOOVER, R.O., Development of a Computational Model for the Mark-IV Electrorefiner (Master Thesis), University of Idaho, Idaho Falls, United States, (2010)
- [217] CHOI, S., et al., Three-dimensional multispecies current density simulation of molten-salt electrorefining, *J. Alloys Compd.* **503** 1 (2010) 177–185.
- [218] PARK, J., CHOI, S., KIM, K., AHN, D., HWANG, I.S., Kinetic Modeling of Pyrochemical Reductive Extraction Process, presented at Workshop on Computational Model for Pyroprocess of Spent Nuclear Fuels, Jeju National University, Feb. 1st, 2010, Jeju, Republic of Korea (2010).
- [219] CHOI, S., et al., Uncertainty studies of real anode surface area in computational analysis for molten salt electrorefining, *J. Nucl. Mater.* **416** 3 (2011) 318–326.
- [220] LOW, C.T.J., ROBERTS, E.P.L., WALSH, F.C., Numerical simulation of the current, potential and concentration distributions along the cathode of a rotating cylinder Hull cell, *Electrochim. Acta* **52** 11 (2007) 3831–3840.

- [221] IIZUKA, M., MORIYAMA, H., Analyses of Anodic Behavior of Metallic Fast Reactor Fuel Using a Multidiffusion Layer Model, *J. Nucl. Sci. Technol.* **47** 12 (2010) 1140–1154.
- [222] KIM, K., et al., Computational analysis of a molten-salt electrochemical system for nuclear waste treatment, *J. Radioanal. Nucl. Chem.* **282** (2009) 449–453.
- [223] CUMBERLAND, R., HOOVER, R., PHONGIKAROO, S., YIM, M.-S., Analysis of Equilibrium Methods for the Computational Model of the Mark-IV Electrorefiner, *Nucl. Eng. Technol.* **43** (2011) 547–556.
- [224] KO, W.I., GAO, F., Economic Analysis of Different Nuclear Fuel Cycle Options, *Sci. Technol. Nucl. Install.* **2012** (2012) 293467.

ABBREVIATIONS

ACPF	Advanced SNF Conditioning Process Facility
ACSEPT	actinide separation for partitioning and transmutation
ADS	accelerator driven system
AFCI	advanced fuel cycle initiative
AHWR	advanced heavy water reactor
AmEX	Americium alone EXtraction
ANL	Argonne National Laboratory
ASNC	ACP safeguards neutron counter
ASTRID	Advanced Sodium Technological Reactor for Industrial Demonstration
BARC	Bhabha Atomic Research Centre
BN	Beloyarsk Nuclear
BRC	Blue Ribbon Commission
BREST	lead cooled fast reactor
CANDU	Canadian-deuterium uranium
CEA	Commissariat à l'Énergie Atomique (Commission for Atomic Energy)
COEX	co- extraction process
CORAL	Compact Facility for Reprocessing of Advanced Fuels in Lead Cells
CP	cathode processor
CV	cyclic voltammetry
CWP	ceramic waste process
DEVON	detailed evaluation of potential distribution
DFDF	DUPIC Fuel Development Facility
DFRP	Demonstration Fast Reactor Fuel Reprocessing Plant
DIAMEX	DIAMide EXtraction process
DOVITA	dry reprocessing, oxide fuel, vibro-pack, integral, transmutation of actinides
DSNC	DUPIC safeguard neutron counter
DUPIC	Direct Use of PWR SNF in CANDU
EBR	experimental breeder reactor
EDEC	Experimental and Demonstration Energy Complex
ER	electrorefiner
FACT	Fast Reactor Fuel Cycle Technology
FBR	fast breeder reactor
FBTR	fast breeder test reactor

FCF	fuel cycle facility
FCR&D	fuel cycle research & development
FFTF	Fast Flux Test Facility
FMTC	fractional mass transport coefficient
FP	fission product
FRFCF	Fast Reactor Fuel Cycle Facility
FRM	Fabrication/Refabrication Module
FVM	fluoride volatility method
GANEX	group extraction of actinides
GNEP	Global Nuclear Energy Partnership
GPEC	General Purpose Electrochemical Code
HFDA	hot fuel dissolution apparatus
HFEF	Hot Fuel Examination Facility
HIP	hot isostatic process
HLLW	high level liquid waste
HLW	high level waste
HM	heavy metal
HTO	hydrogen tri-oxide
IFR	integral fast reactor
IGCAR	Indira Gandhi Centre for Atomic Research
I-NERI	International Nuclear Energy Research Initiative
INL	Idaho National Laboratory
ITU	Institute of Transuranium Elements
JFCS	Joint Fuel Cycle Study
JNFL	Japan Nuclear Fuel Ltd
JRC	Joint Research Center
KAERI	Korea Atomic Energy Research Institute
KARP	Kalpakkam Reprocessing Plant
KEPCO	Korea Electric Power Company
KINAC	Korea Institute of Nuclear Non-Proliferation and Control
KMP	key measurement point
LCC	liquid cadmium cathode
LFCC	low fuel cycle cost
LIBS	laser induced breakdown spectroscopy
LWR	light water cooled reactor

MA	minor actinides
MBA	material balance area
MBIR	Multipurpose Fast Research Reactor
MCC	Mining and Chemical Complex
METI	Ministry of Economy, Trade and Industry (in Japan)
MFBR	metal based fast breeder reactor
MFD	mechanically fluidized dryer
MNUP	mixed nitride uranium-plutonium fuel
MOX	mixed oxide
MSM	master slave manipulator
MSR	molten salt reactor
MSTR	molten salt transmutation reactor
NFBC	non-fuel bearing components
NPP	nuclear power plant
NRA	Nuclear Regulation Authority
OFBR	oxide based fast breeder reactor
OREOX	oxidation and reduction of oxide fuel
OT	Once Through
OTS	off-gas treatment system
P&T	partitioning and transmutation
PALEO	Program for Analyzing Electrorefining Operation
PC	pressureless consolidation
PDC	Pilot Demonstration Centre
PDE	Partial Differential Equation
PFBR	prototype fast breeder reactor
PFBR	prototype fast breeder reactor
PHWR	pressurized heavy water reactor
PIE	post irradiation examination
PIEF	Post Irradiation Examination Facility
PRC	Polyfunctional Radiochemical Complex
PREFRE	Power Reactor Fuel Reprocessing
PRESENT	Particle size control, REMoval of fission product, SElective gaseous Nuclide Trapping
PRIDE	PyRoprocess integrated Inactive DEmonstration
PUREX	plutonium uranium recovery by extraction
R&D	research and development

RAR	residual actinide recovery
REE	rare earths elements
REPF	Reference Engineering-scale Pyroprocessing Facility
RepU	reprocessed uranium
RFMTC	relative fractional mass transport coefficient
RHC	rotating hull cell
RIAR	Research Institute of Atomic Reactor
RM	reprocessing module
SANEX	Selective ActiNide EXtraction
SAP	SiO ₂ -Al ₂ O ₃ -P ₂ O ₅
SCC	Siberian Chemical Combine
SEM-EDX	scanning electron microscope-energy dispersion x X ray
SFR	sodium cooled fast reactor
SIMFUEL	SiMulated SNF
SNF	spent nuclear fuel
SNU	Seoul National University
SVBR	svintsovo vismutny bystryi reactor - lead-bismuth fast reactor
TBP	tri-butyl phosphate
TODGA	Tetra-Octyl DiGlycol Amide
TPE	transplutonium elements
TRAIL	transportation of actinides in electrorefiner
TRU	TRansUranic
UREX	URanium Extraction Process
VVWVER	water water energetic reactor (From the Russian VVER – vodo vodyanoi energetichesky reactor)
WDS	wave length dispersive spectrometry
XRD	X ray diffraction

CONTRIBUTORS TO DRAFTING AND REVIEW

Basak, U.	International Atomic Energy Agency
Bourg, S.	Commission for Atomic Energy, France
Constantin, A.	International Atomic Energy Agency
González-Espartero, A.	International Atomic Energy Agency
Hwang, I. S.	Seoul National University, Republic of Korea
Inoue, T.	Central Research Institute of Electrical Power Industries, Japan
Khaperskaya, A.	Rosatom, Russian Federation
Kormilitsyn, M.	Kurchatov Institute, Russian Federation
Lee, H. S.	Korea Atomic Energy Research Institute, Republic of Korea
Li, S. X.	Idaho National Laboratory, USA
Lizin, A. A.	Rosatom, Russian Federation
McManniman, L.	International Atomic Energy Agency
Marsden, K.	Idaho National Laboratory, USA
Mendes, E.	Commission for Atomic Energy, France
Nagrajan, K.	Indira Gandhi Centre for Atomic Research, India
Osipenko, A. G.	Rosatom, Russian Federation
Shadrin, A. Y.	Rosatom, Russian Federation
Simpson, M.	University of Utah, USA
Uhlir, J.	Nuclear Research Institute, Czech Republic

Technical Meetings

Vienna, Austria: 28–30 June 2011; 18–20 November 2013

Consultancy Meetings

Marcoule, France: 25–27 July 2012

Vienna, Austria: 27–29 May 2015



IAEA

International Atomic Energy Agency

No. 26

ORDERING LOCALLY

IAEA priced publications may be purchased from the sources listed below or from major local booksellers.

Orders for unpriced publications should be made directly to the IAEA. The contact details are given at the end of this list.

NORTH AMERICA

Bernan / Rowman & Littlefield

15250 NBN Way, Blue Ridge Summit, PA 17214, USA

Telephone: +1 800 462 6420 • Fax: +1 800 338 4550

Email: orders@rowman.com • Web site: www.rowman.com/bernan

REST OF WORLD

Please contact your preferred local supplier, or our lead distributor:

Eurospan Group

Gray's Inn House
127 Clerkenwell Road
London EC1R 5DB
United Kingdom

Trade orders and enquiries:

Telephone: +44 (0)176 760 4972 • Fax: +44 (0)176 760 1640

Email: eurospan@turpin-distribution.com

Individual orders:

www.eurospanbookstore.com/iaea

For further information:

Telephone: +44 (0)207 240 0856 • Fax: +44 (0)207 379 0609

Email: info@eurospangroup.com • Web site: www.eurospangroup.com

Orders for both priced and unpriced publications may be addressed directly to:

Marketing and Sales Unit

International Atomic Energy Agency

Vienna International Centre, PO Box 100, 1400 Vienna, Austria

Telephone: +43 1 2600 22529 or 22530 • Fax: +43 1 26007 22529

Email: sales.publications@iaea.org • Web site: www.iaea.org/publications

**International Atomic Energy Agency
Vienna**